NICKEL-CATALYZED SUZUKI-MIYAURA CROSS-COUPLINGS TO SET BENZYLIC, DIARYL AND TRIARYL ALL-CARBON QUATERNARY STEREOCENTERS IN HIGH ENANTIOPURITY

by

Tianyu Tan

A thesis submitted to the Faculty of the University of Delaware in partial fulfillment of the requirements for the degree of Master of Science in Chemistry and Biochemistry

Spring 2017

NICKEL-CATALYZED SUZUKI-MIYAURA CROSS-COUPLINGS TO SET BENZYLIC, DIARYL AND TRIARYL ALL-CARBON QUATERNARY STEREOCENTERS IN HIGH ENANTIOPURITY

by

Tianyu Tan

Approved: _____
Mary P. Watson, Ph.D.
Professor in charge of thesis on behalf of the Advisory Committee

Approved: _____
Murray V. Johnston, Ph.D.
Chair of the Department of Chemistry and Biochemistry

Approved: _____
George H. Watson, Ph.D.
Dean of the College of Arts and Sciences

Approved: _____
Ann L. Ardis, Ph.D.
Senior Vice Provost for Graduate and Professional Education

ACKNOWLEDGMENTS

It's always my sincere privilege to study and work with my academic advisor, Prof. Mary P. Watson. I learned a lot under your mentorship, not only the knowledge from books, but also ideas and experience working in the lab. I have trained my scientific thinking abilities and developed problem-solving skills within the three-year period. I feel blessed to have you as my mentor.

I would also like to thank all the M.P.Watson group members. You all feel like family members to me. My special thanks go to Dr. Qi Zhou and Dr. Bibaswan Biswas for your guidance on my research. I also thank Dr. Jixin Liu for your kindness and selflessness. I benefit a lot from you in all aspects. I will always remember those days studying and working together with Jennie Liao and Javon Rabb-Lynch. It's my pleasure to be with you guys.

I also send my sincere gratitude to Prof. Donald Watson, Prof. Neal Zondlo, Prof. Joseph Fox, Prof. Joel Rosenthal, Prof. Catherine Grimes, and Prof. Klaus Theopold. I am grateful for what I have learned from you both in and out of the classes. Dr. Geoffery Sametz, thank you for being my teaching assistant advisor. I enjoy working with you to help students learn both knowledge and skills in the lab.

Then I would like to thank Dr. Shi Bai for his NMR service, Dr. Stephan Chan and Dr. PapaNii Asare-Okai for the help with Mass Spectroscopy, and Dr. Glenn Yap for his help with X-ray crystallography. I am grateful to the chemistry department staff, Susan Cheadle, Sue James, Pat McMahon, John Famiglietti, Douglas Nixon, Brandon Calitree and Gary Lance. I feel so warm whenever I need help from you.

Last but never the least, I wish I can acknowledge my gratitude to my parents for their endless love and selfless support. With your care and love, I don't feel lonely when I am studying abroad. Finally, I would also like to thank Tingting Luo for her accompany in the first two years, and my dear friends Long Chen, Rujin Cheng, Weijun Gui, Siqi Shen and Jingjing Li.

TABLE OF CONTENTS

LIST OF TABLES

LIST OF SCHEMES

LIST OF FIGURES

ABSTRACT

Over the decades, chemists have been dedicated to building quaternary carbon centers via various methods. Transition metal-catalyzed asymmetric cross-couplings have been proven to be highly efficient in synthesizing the targeted structure in high enantiomeric purity. In particular, the use of allylic electrophiles is conspicuous in this kind of reaction; however, the lack of such chemistry for non-allylic electrophiles limits the scope.

In the first chapter, prior work in the preparation of all-carbon quaternary centers via catalytic reactions is discussed. Methods like enantioselective alkylation, arylation, allylation, aldol reaction, conjugate addition, and cycloaddition are introduced.

The second chapter tells the contribution of our group in synthesizing all-carbon quaternary stereogenic centers in both high yields and excellent levels of stereochemical fidelity. This stereospecific, nickel-catalyzed Suzuki-Miyaura arylation of tertiary benzylic acetates with organoboron nucleophiles has been developed to deliver diaryl- and triarylalkanes with an economically and environmentally friendly catalytic system. Great tolerance of a variety of functional groups also stressed the mildness of the reaction conditions.

Overall, this thesis describes the first example of synthesizing diaryl and triaryl benzylic all-carbon quaternary stereocenters in a stereospecific fashion, which is a very significant finding and provides a highly attractive entry to enantioriched benzylic quaternary centers.

Chapter 1

PRIOR ART IN THE SYNTHESIS OF ALL-CARBON QUATERNARY STEREOCENTERS

1.1 Introduction

Many bioactive, natural and pharmaceutical products contain all-carbon quaternary centers (Figure 1.1).[1] This importance attracts the great interest of synthetic chemists to synthesize these structures accordingly. However, over the past few decades, it has proven great challenging to synthesize chiral quaternary centers in good enantiomeric purity due to steric repulsion between the carbon substituents.[2] Many methods have been applied to complete all-carbon quaternary center constructions with high enantiomeric excess, and these can be divided into two groups, catalytic and non-catalytic reactions.

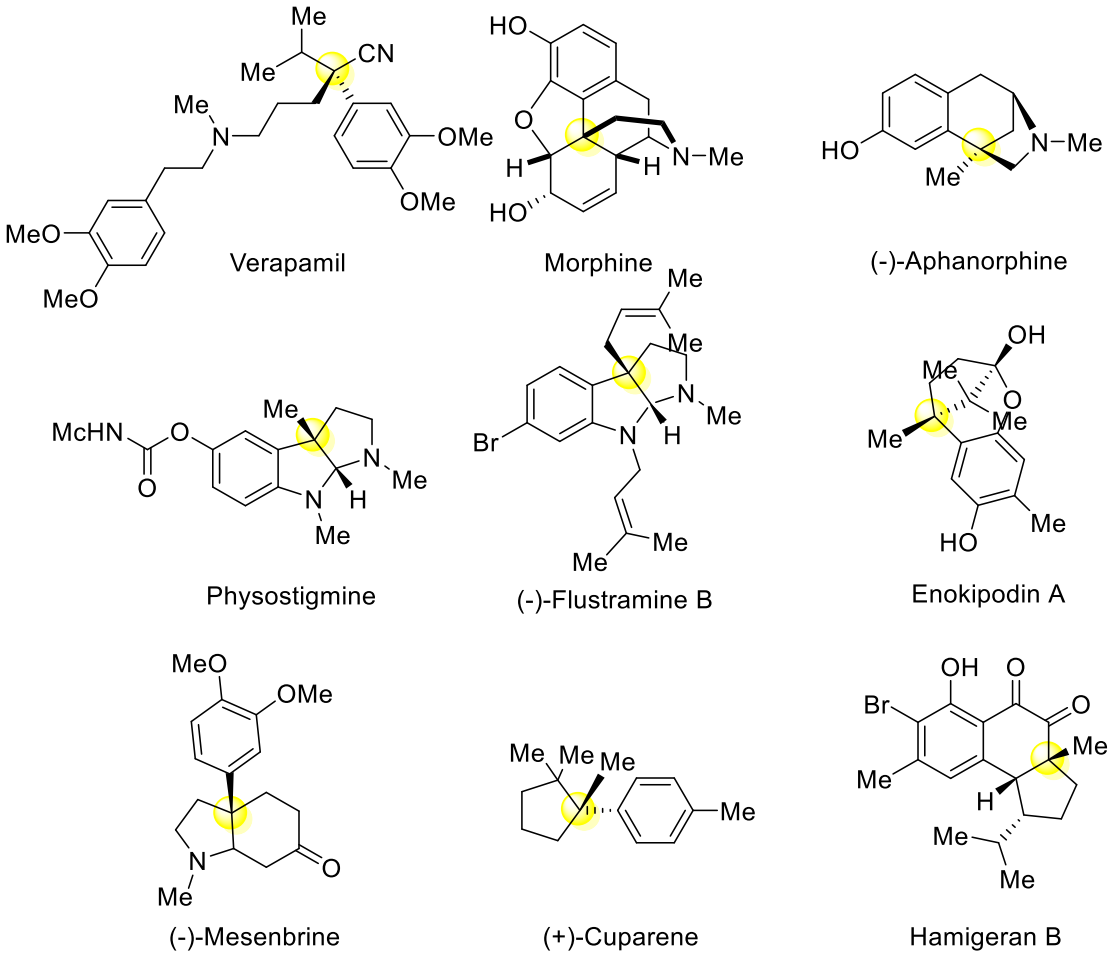

Figure 1.1: Bioactive Molecules Containing All-Carbon Quaternary Centers

1.2 Non-Catalytic Methods

Aggarwal has contributed a great deal in the field of synthesis of all-carbon quaternary centers. He and his co-workers reported a method to construct the quaternary stereogenic centers in high enantiospecificity (Scheme 1.1). They first built tertiary boronic ester **1.1** by lithiation/borylation of a secondary carbamate,[3] and then transformed boronate **1.1** into a variety of products with all-carbon quaternary stereogenic centers. High enantiospecificity is observed for all these reactions.[4]

Scheme 1.1: Stereospecific Lithiation/Borylation to Set All-Carbon Quaternary Centers (Aggarwal)

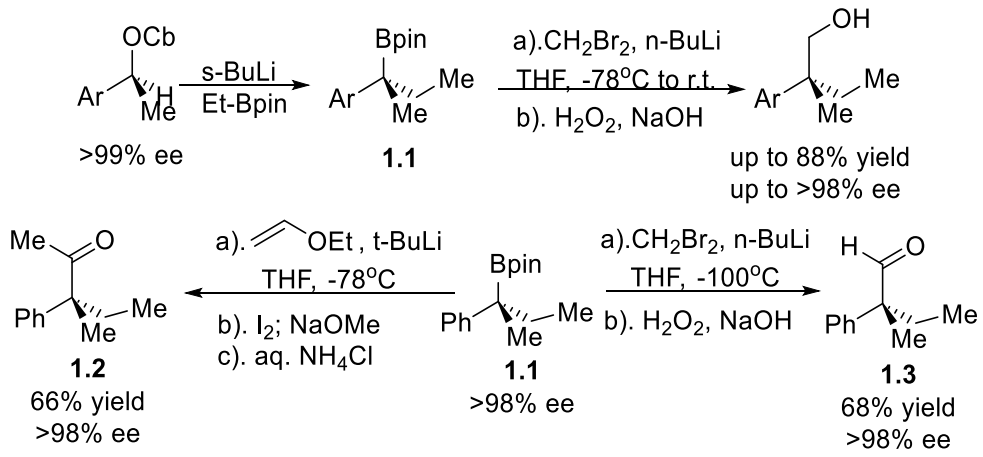

Similar enantiospecific couplings have been reported to reach heteroaromatic compounds with all-carbon quaternary centers from secondary or tertiary pinacol boronic esters (Scheme 1.2).[5] However, a limitation of these reactions is that the functional groups of the substrates cannot be basic due to the use of organolithium reagents.

Scheme 1.2: Stereospecific Lithiation/Borylation to Set Hetereoatom-Contained All-Carbon Quaternary Centers (Aggarwal)

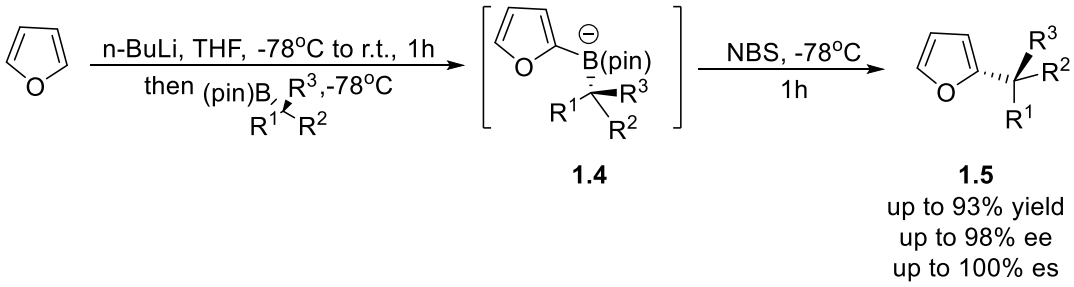

1.3 Catalytic Methods

Among all the methods that have been applied to complete asymmetric synthesis of all-carbon quaternary centers, asymmetric catalysis proves to be a great solution.[6] Such methods have been demonstrated for cyclic substrates, as well as more difficult acyclic substrates, which have an increased number of degrees of freedom.[7] Different methods including enantioselective conjugate additions, allylic substitutions, arylations, aldol reactions, Diels-Alder reactions, intra- and intermolecular Heck reactions will be briefly discussed.

1.3.1 Enantioselective Allylic Substitution

Enantioselective allylic substitution reactions have obtained significant attention recently for accessing optically active building blocks in total synthesis, however this field remains to be further developed to obtain all-carbon quaternary stereocenters in an enantioselective fashion. A prochiral allylic electrophile is cross-coupled with nucleophile to deliver the desired structure (Scheme 1.3).

Scheme 1.3: General Enantioselective Allylic Substitution

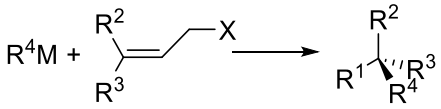

The Hoveyda group reported an asymmetric allylic substitution reaction to form an allene-bearing all-carbon quaternary center catalyzed by a chiral copper(I)-*N*-Heterocyclic Carbene (NHC) system (Scheme 1.4).[8] Enantioselectivity of this reaction could be as high as 98% with high yields as well. An S_N2' mechanism to form the allenyl addition product was preferred to the propargyl addition one.

Scheme 1.4: Cu(I)-NHC Ligand Catalyzed Allylic Substitution Using Phosphate as Leaving Group (Hoveyda)

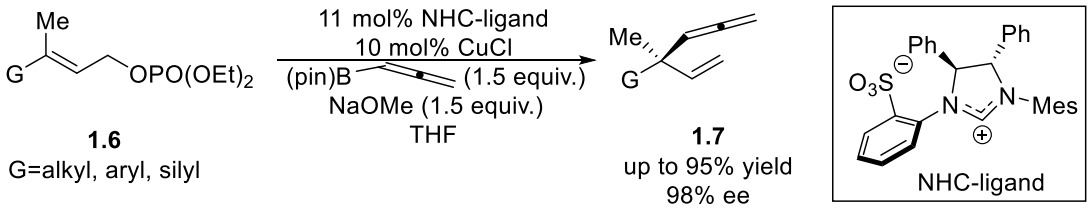

Reported by Alexakis group, the NHC ligand can also be applied in a copper-free reaction, where bromide acts as the leaving group instead of phosphoric or carboxylic ester (Scheme 1.5).[9]

Scheme 1.5: Copper-Free Allylic Substitution Using Bromide as Leaving Group (Alexakis)

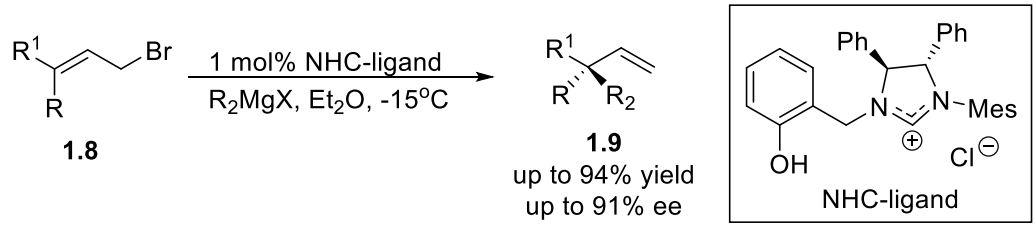

Stoltz and co-workers reported the first enantioselective allylation of a β-ketoester catalyzed by the Ir-*N*-aryl-phosphoramidite catalyst to set a quaternary center as well as an adjacent tertiary one (Scheme 1.6).[10] High yields and ee's have been achieved, as well as good to excellent regio- and diastereoselectivity. A variety of allyl electrophiles and β-ketoesters were well tolerated.

Scheme 1.6: Ir-Catalyzed Enantioselective Allylation Using Carboxylic Ester as Leaving Group (Stoltz)

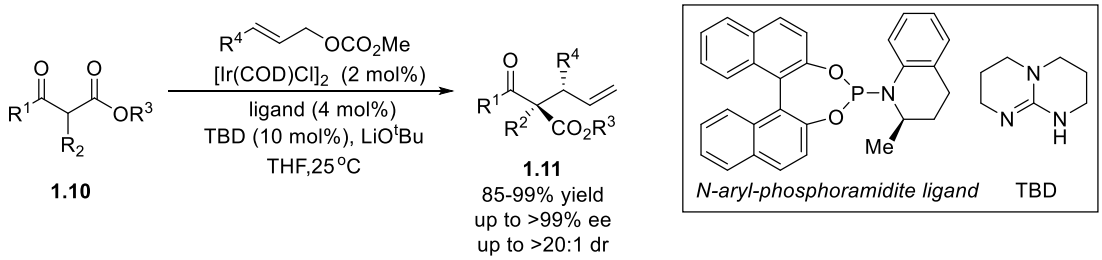

Trost developed his asymmetric Tsuji-Trost reaction, which is also known as asymmetric allylic alkylation (AAA) during the total synthesis of (+)-alllocyathin B_2 (Scheme 1.7).[11] By protecting one side of the ketone, the other α-position can be allylated to construct the quaternary stereocenter in good yield and excellent enantiopurity using a chiral palladium catalyst.

Scheme 1.7: Pd-Catalyzed Asymmetric Allylic Alkylation (Trost)

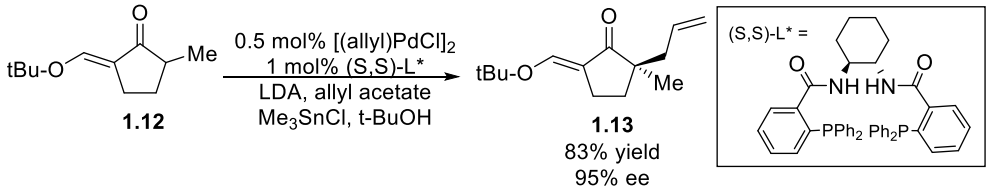

Recently the Carreira group reported an enantio- and diastereodivergent dual catalysis to set two quaternary stereocenters in one product (Scheme 1.8).[12] Starting with allylic alcohol **1.14** and the α-branched aldehyde **1.15**, they can control the diastereoselectivity by selective pairing of a chiral iridium catalyst and an amine catalyst. These catalysts work together to form the carbon-carbon bond with the formation of two quaternary stereocenters. Excellent enantioselectivity can be achieved. In this case, all possible diastereoisomers can be accessed in enantiomerically pure forms.

Scheme 1.8: Dual-Catalysis: α-Allylation of Branched Aldehydes (Carreira)

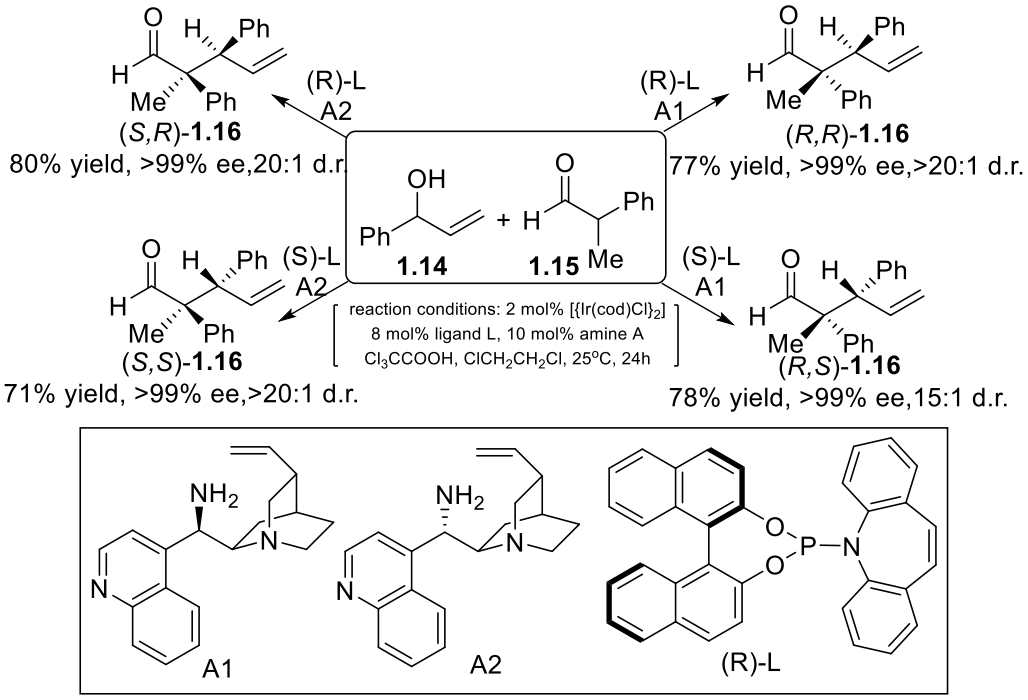

The Krische group reported the first catalytic enantioselective C-C couplings of methanol to set the all-carbon quaternary centers (Scheme 1.9). 2-Substituted dienes have been inserted into the C-H bond of methanol regioselectively.[13] High enantioselectivity has been achieved by the using of the chiral Ir-PhanePhos catalyst.

Scheme 1.9: Ir-Catalyzed Insertion of Diene to Methanol (Krische)

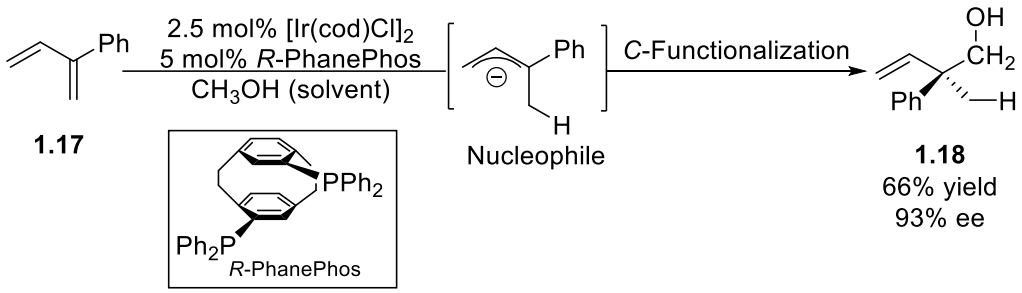

When the nucleophile is activated as either a carbanion or organometallic intermediate, carbon-carbon bond formation can be achieved by cross-coupling with a

carbon electrophile (Scheme 1.10). By using chiral counter-cations, people have developed catalytic asymmetric phase-transfer alkylation reactions. Quaternary ammonium salts or metals can be used as the chiral counter-cations $(Y^*)^+$.[14]

Scheme 1.10: Asymmetric Alkylation Using Chiral Counter-Cation $(Y^*)^+$

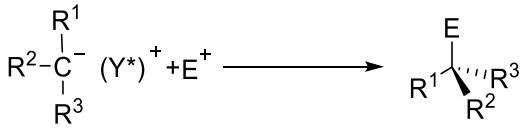

$(Y^*)^+$ = R_4N, Al, Co, Cu, K, Li, Na/La, Ni, Pd, Rh, Cl_3Si*

For example, Weinstock and co-workers reported an enantioselective Robinson annulation via phase-transfer catalysis using a quaternary ammonium catalyst (Scheme 1.11). In their proposed tight ion pairs,[15] a π-π interaction, π-allyl/alkyl interaction, and hydrogen bond between the enolate and the *N*-benzylcinchonidinium help to reach the desired enantioselectivity.

Scheme 1.11: Enantioselective Robinson Annulation via Phase-Transfer Catalysis (Weinstock)

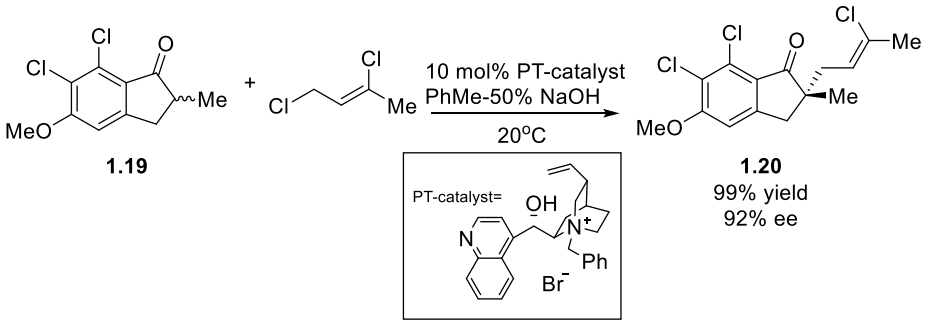

The Morken group has recently reported sequential Suzuki-Miyaura cross-coupling reactions to construct quaternary all-carbon stereocenters (Scheme 1.12).[16] Simple starting materials of geminal bis(boronates), alkenyl halides and C(sp^2) electrophiles were used. A γ,γ'-disubstituted allylboronate **1.22** was obtained in the first

step using a palladium-bidentate phosphine ligand catalytic system, which acted as an allylic nucleophile in the following step. Then a stereospecific S_E2' transmetalation with the palladium-C(sp^2) specie followed by a rapid reductive elimination delivered the allylic all-carbon quaternary center **1.23** at the γ-position in high yield and both excellent enantiospecificity and regioselectivity.

Scheme 1.12: Umpolung Approach to the Asymmetric Construction of Quaternary All-Carbon Stereocenters (Morken)

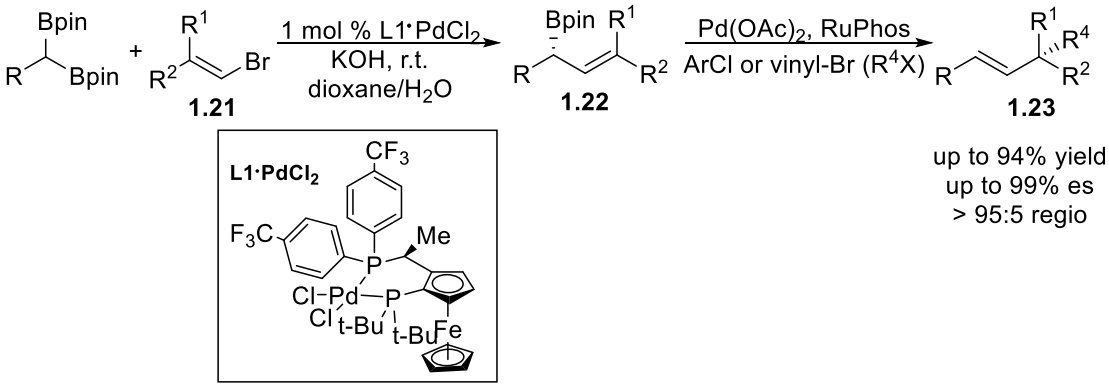

Another example to construct the quaternary stereocenters using substitution of γ,γ'-disubstituted secondary allylic picolinates **1.24** with stoichiometric alkylcopper reagents was reported by Kobayashi (Scheme 1.13).[17] In their work, a 1:1 ratio of stoichiometric alkylcopper reagent to ZnX_2 was used and high levels of regioselectivity (rs), yield and chirality transfer (CT) were achieved. The absolute configuration of the chiral quaternary carbon could be controlled by the geometry of the olefin in the picolinates.

Scheme 1.13: ZnI_2-Promoted Regio- and Stereoselective Substitution of γ,γ'-Disubstituted Secondary Allylic Picolinates to Construct Quaternary All-Carbon Centers (Kobayashi)

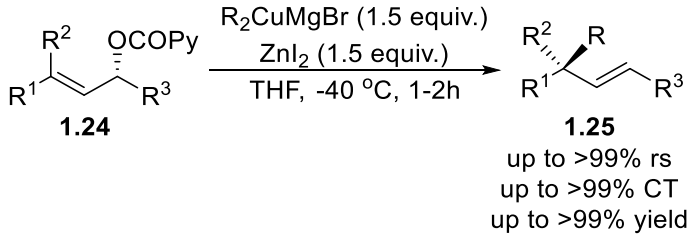

1.3.2 Enantioselective Conjugate Addition

Conjugate addition plays an important role in building new carbon-carbon bonds. And as for the construction of all-carbon quaternary stereocenters, enantioselective conjugate addition involving carbon nucleophiles can be widely developed in the field of chemical synthesis.

Scheme 1.14: General Enantioselective Conjugate Addition

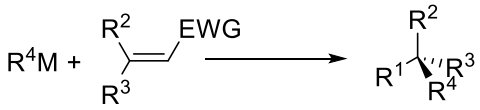

The Christoffers group constructed the quaternary stereocenters via a nickel-catalyzed asymmetric Michael addition (Scheme 1.15).[18] They generated the chiral catalyst in situ. Although low in yields and only one entry exceeded 90 % ee, their reactions conditions were easily operated in lab.

Scheme 1.15: Asymmetric Michael Addition with Chiral Catalyst Generated In-Situ (Christoffers)

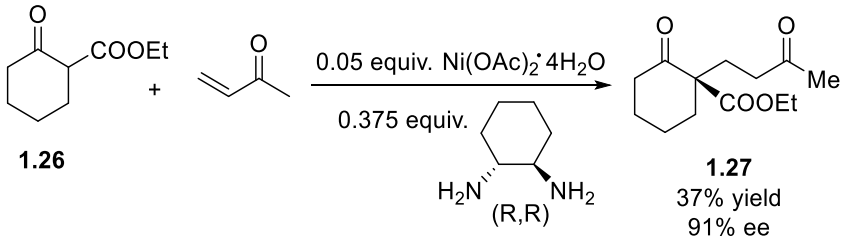

The Jacobsen group reported an enantioselective conjugate additions of electron-deficient nitriles to the α,β-unsaturated imides catalyzed by a chiral salen-Al complex to generate all-carbon **1.29** or heteroatom-substituted **1.30** quaternary centers (Scheme 1.16).[19]

Scheme 1.16: Enantioselective Conjugate Addition Using Chiral Salen-Al Complex (Jacobsen)

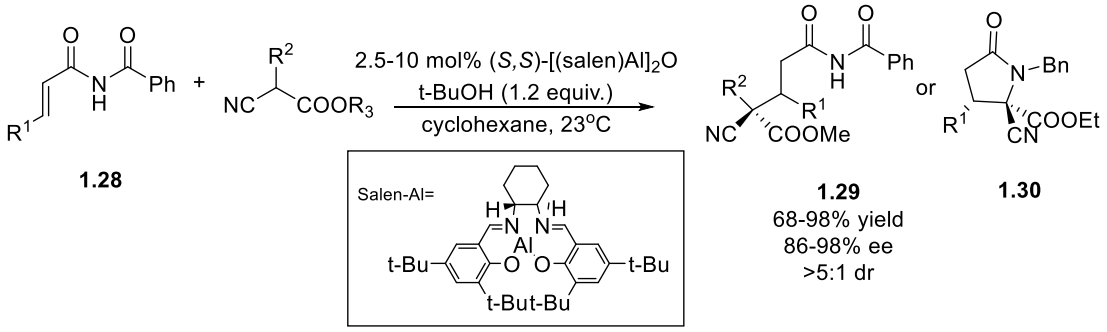

The Stoltz group reported the first Pd-catalyzed Michael addition of commercially available aryl boronic acids to β-substituted cyclic enones **1.31** to set all-carbon quaternary centers (Scheme 1.17).[20] Reaction conditions are friendly to air and moisture, which makes this reaction easy to operate in lab.

Scheme 1.17: Pd-Catalyzed Michael Addition of Aryl Boronic Acids to β-substituted Cyclic Enones (Stoltz)

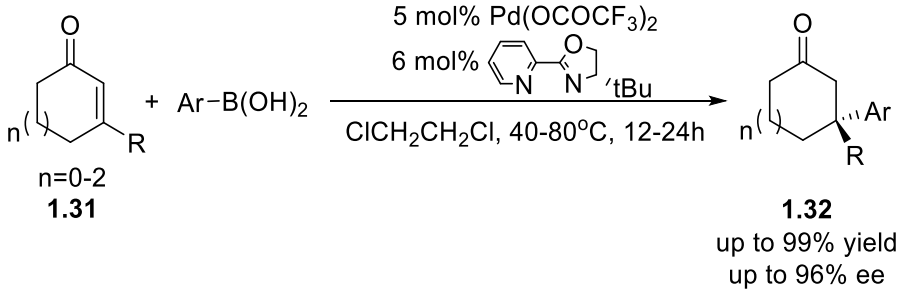

1.3.3 Enantioselective Arylation

α-Arylation of ketones and related compounds can also be used to construct quaternary stereocenters. The Buchwald group described the use of a nickel(0)-BINAP catalytic system to set quaternary stereocenters in synthetic useful yields and good ee's from α-substituted lactones **1.33** (Scheme 1.18).[21] In their case, zinc(II) salts have been found to have accelerating effects on the α-quaternization.

Scheme 1.18: Enantioselective Ni(0)-Catalyzed Arylation of α-Substituted Lactones (Buchwald)

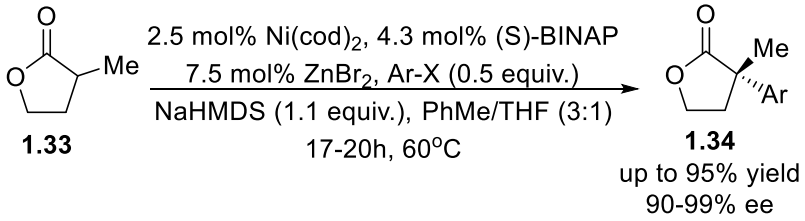

1.3.4 Enantioselective Aldol Reaction

Scheme 1.19: Diastereoselectivity Issues in Aldol Reaction to Set Quaternary Centers

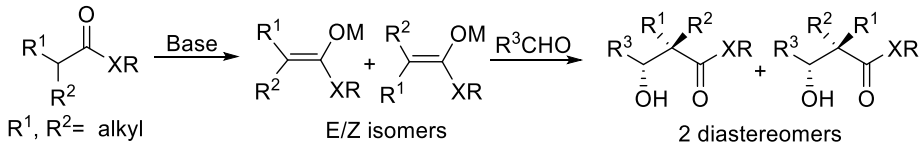

The aldol reaction is widely used and very convenient in forming carbon-carbon bonds. In order to construct quaternary centers, it requires α,α-disubstituted carbonyl compounds. However, due to difficulties in selective enolization of α,α-disubstituted carbonyl compounds, both E- and Z-enolates can be generated, resulting in two diastereomers of aldol products (Scheme 1.19).[22] The issue can be solved by using an oxazolidinone chiral auxiliary (Scheme 1.20).[23] The benzyl group blocks one face to control the aldol-type reaction enantioselectively. The stereochemistry of this major product can be well-explained by the Zimmerman-Traxler transition state.

Scheme 1.20: Blocking One Fase with Benzyl Group to Achieve Enantioselectivity

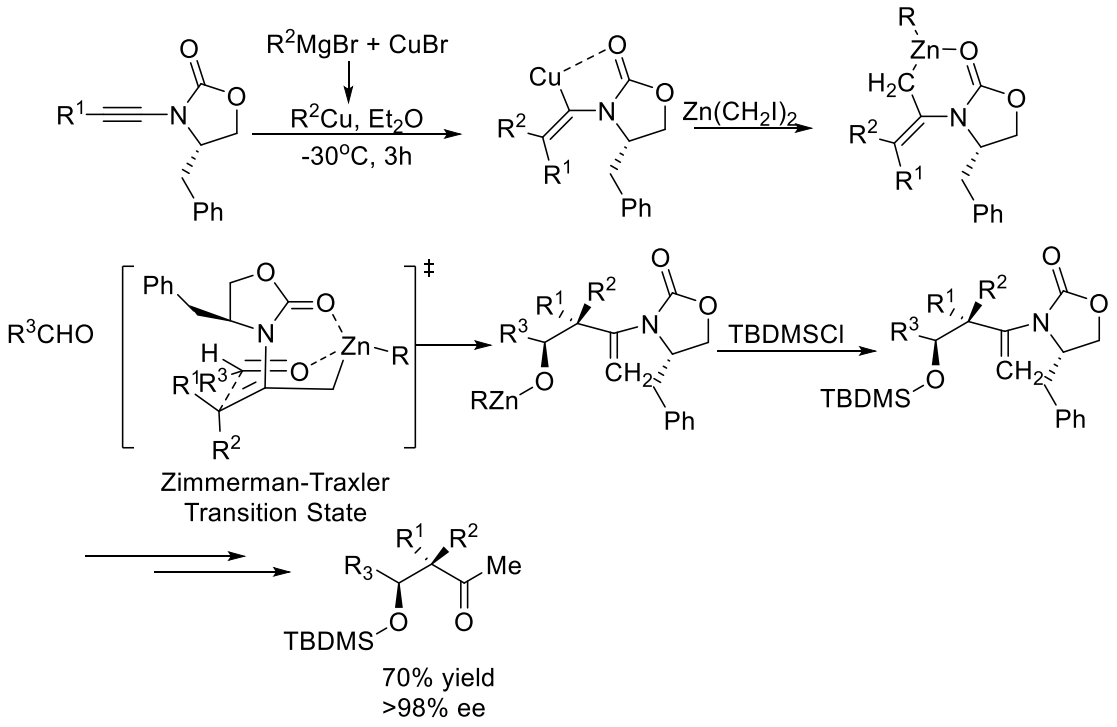

1.3.5 Heck Reaction

1.3.5.1 Intramolecular Heck Reaction

This type of reaction has been commonly applied in the synthesis of natural products. During their total synthesis of furaquinocin E, Trost and co-workers applied an intramolecular reductive Heck cyclization and subsequent acetylation to obtain the acetate in good regio-, enantio-, and diastereoselectivity, as well as good yield (Scheme 1.21).[24]

Scheme 1.21: Intramolecular Heck Reaction Used in the Total Synthesis of Furaquinocin E (Trost)

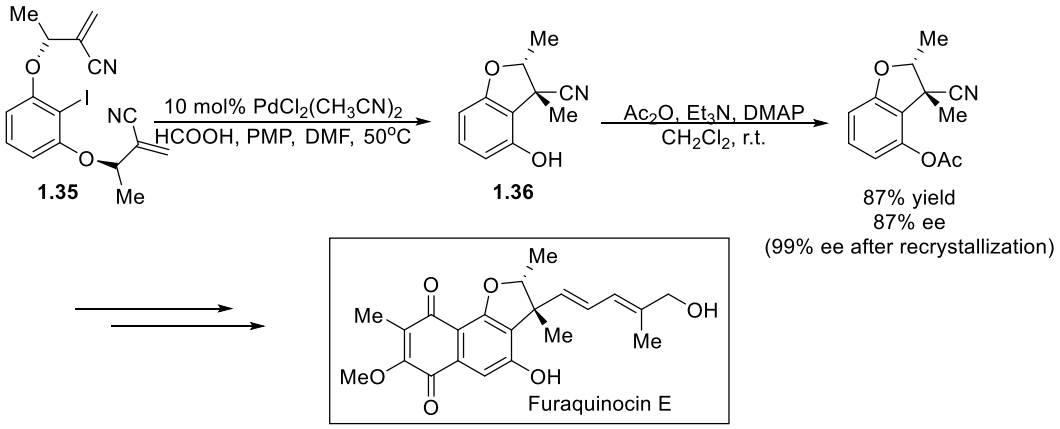

Other similiar examples can also be seen in the total syntheses of xestiqyunone and quadrigemine C.[25]

1.3.5.2 Intermolecular Heck Reaction

The Sigman group recently published a palladium-catalyzed enantioselective intermolecular Heck-type reaction to construct quaternary stereocenters from trisubstituted alkenyl alcohols and aryl boronic acids (Scheme 1.22).[26] The absolute configuration and enantioselectivity of the stereocenter are determined by the geometry of the starting alkenyl alcohol, or to be more specific, the orientation of the alkene when the palladium-ligand complex has been bound to it. The proposed chain-walking mechanism of this Heck-type reaction has been supported by an isotope labeling experiment.

Scheme 1.22: Pd-Catalyzed Enantioselective Intermolecular Heck Reaction (Sigman)

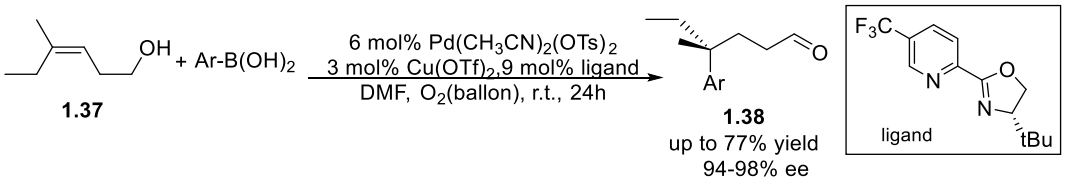

1.37

1.38
up to 77% yield
94-98% ee

1.3.6 Asymmetric Diels-Alder Reaction

Scheme 1.23: Asymmetric Diels-Alder Reaction Using Prochiral Dienophile

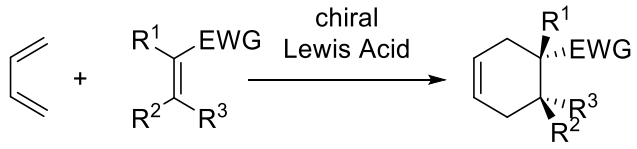

Two approaches to set quaternary centers via a Diels-Alder reaction have been provided. The first one uses prochiral dienophiles, in which chiral Lewis acids can be B, Al, Ti, Cr, Fe, Cu, Ru, Sm, or Gd possessing chiral ligands (Scheme 1.23).[27] For example, Rawal and his co-workers optimized the following enantioselective Diels-Alder reaction using prochiral dienophile **1.39** on a multigram-scale to obtain both good yields and high ee's (Scheme 1.24).[28]

Scheme 1.24: Enantioselective Diels-Alder Reaction Using Prochiral Dienophile (Rawal)

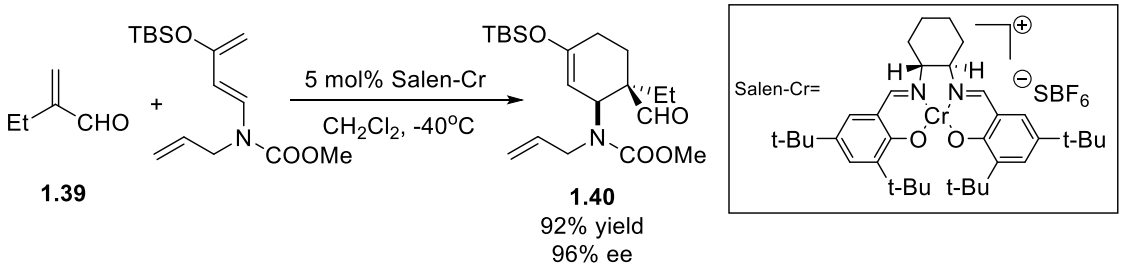

Scheme 1.25: Asymmetric Diels-Alder Reaction Using Prochiral Diene

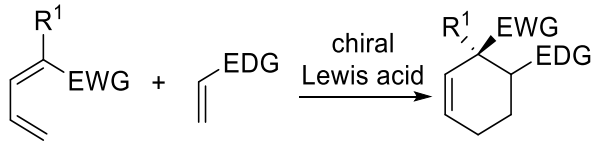

The other type is a less developed strategy, where people use prochiral dienes in inverse electron-demand Diels-Alder reactions (Scheme 1.25). In 1994, the Evans group reported a catalytic, enantioselective, inverse electron-demand Diels-Alder (IEDDA) reaction. High ee was achieved in the cycloaddition of 3-carboxylmethyl-2-pyrone with thiophenylethylene which was catalyzed by a 2,2'-dihydroxyl-1,1'-binaphthyl-Yb complex (Scheme 1.26).[29]

Scheme 1.26: Catalytic, Enantioselective Inverse Electron-Demand Diels-Alder (IEDDA) Reaction Using Prochiral Diene (Evans)

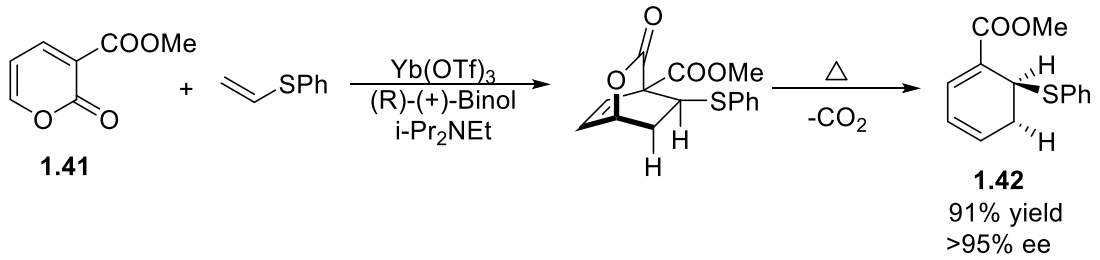

1.4 Conclusion

Other methods to synthesize all-carbon quaternary stereogenic centers that were not discussed in the context include Mannich reaction,[30] catalytic C-H insertion with metal carbenoid species,[31] rearrangement reactions.[32] Most of the methods to create all-carbon quaternary stereogenic centers were developed over the past decade. However even for those most developed methods that are discussed in this chapter, limitations exist in their substrate scope. In addition, only a few transition metals other than palladium have been applied in the catalytic asymmetric reactions. Thus, there are still more aspects to be discovered and further developed in this field of research, which inspire the direction of our research described in Chapter 2.

REFERENCES

(1) (a) Zhang, Y.; Trost, B. M. *J. Am. Chem. Soc*. **2006**, *128*, 4590. (b) Mermerian, A. H.; Fu, G. C. *Angew. Chem. Int. Ed.* **2005**, *44*, 949. (c) Bartoli, G. *Angew. Chem. Int. Ed.* **2006**, *45*, 4966. (d) Hawner, C.; Alexakis, A. *Chem. Commun.* **2010**, *46*, 7295. (e) Burtoloso, A. C. B. *Synlett.* **2009**, *2009*, 320. (f) Wang. J.; Clive, D. L. J. *J. Org. Chem.* **2004**, *69*, 2773.

(2) (a) Douglas C. J.; Overman, L. E. *Proc. Natl. Acad. Sci.* **2004**, *101*, 5363. (b) Carreira, E. M.; Kvaerno, L. *Classics in Stereoselective Synthesis*; Wiley-VCH: Weinheim, **2009**. (c) Guzman-Perez, A.; Corey, E. J. *Angew. Chem., Int. Ed.* **1998**, *37*, 388. (d) Mann, A.; Christoffers, J. *Angew. Chem., Int. Ed.* **2001**, *40*, 4591.

(3) (a) Stymiest, J. L.; Bagutski, V.; French, R. M.; Aggarwal, V. K. *Nature*, **2008**, *456*, 778. (b) Bagutski, V.; French, R. M.; Aggarwal, V. K. *Angew. Chem*. **2010**, *122*, 5268. (c) Bagutski, V.; Ros, A.; Aggarwal, V. K. *Tetrahedron* **2009**, *65*, 9956.

(4) Sonawane, R. P.; Jheengut, V.; Rabalakos, C.; Larouche-Gauthier, R.; Scott, H. K.; Aggarwal, V. K. *Angew. Chem. Int. Ed.* **2011**, *50*, 3760.

(5) (a) Bonet, A.; Odachowski, M.; Leonori, D.; Essafi, S.; Aggarwal, V. K. *Nat. Chem.* **2014**, *6*, 584. (b) Llaveria, J.; Leonori, D.; Aggarwal, V. K. *J. Am. Chem. Soc*. **2015**, *137*, 10958.

(6) (a) *Comprehensive Asymmetric Catalysis*, Vols. *1-3;* Jacobsen, E. N.; Pfaltz, A.; Yamamoto, H., Eds.; Springer: Berlin, **1999**. (b) *Catalytic Asymmetric Synthesis*; Ojima, I., Ed; Wiley-VCH: Weinheim, **2004**. (c) Noyori, R. *Asymmetric Catalysis in Organic Synthesis*; Wiley-VCH: Weinheim, **1994**. (d) *Fundamental of Asymmetric Catalysis*; Walsh, P. J.; Kozlowski, M. C., Eds.; University Science Books: Sausalito, CA, **2009**.

(7) (a) Das, J. P.; Marek, I. *Chem. Commun*. **2011**, *47*, 4593. (b) Marek, I.; Sklute, G. *Chem. Commun*. **2007**, *43*, 1683.

(8) Jung, B.; Hoveyda, A. H. *J. Am. Chem. Soc.* **2012**, *134*, 1490.

(9) Jackowski, O.; Alexakis, A. *Angew. Chem. Int. Ed*. **2010**, *49*, 3346.

(10) Liu, W.-B.; Reeves, C. M.; Stoltz, B. M. *J. Am. Chem. Soc.* **2013**, *135*, 17298.

(11) (a) Schroeder, G. M.; Trost, B. M. *J. Am. Chem. Soc.* **1999**, *121*, 6759. (b) Pissot-Soldermann, C.; Chen, I.; Schroeder, G. M.; Trost, B. M. *J. Am. Chem. Soc.* **2004**, *126*, 4480. (c) Dong, L.; Schroeder, G. M.; Trost, B. M. *J. Am. Chem. Soc.* **2005**, *127*, 2844.

(12) Krautwald, S.; Sarlah, D.; Scharfroth, M.; Carreira, E. M. *Science*, **2013**, *340*, 1065.

(13) Nguyen, K. D.; Herkommer. D.; Krische, M. J. *J. Am. Soc. Chem.* **2016**, *138*, 14210.

(14) (a) *Catalytic Asymmetric Synthesis.* O'Donnell, M. J., Ojima, I., Eds.; Wiley-VCH: New York, **2000**. (b) Nelson, A. *Angew. Chem. Int. Ed*. **1999**, *38*, 1583.

(15) Bhattacharya, A.; Dolling, U.-H.; Grabowski, E. J. J.; Karady, S.; Ryan, K.M.; Weinstock, L. *Angew. Chem. Int. Ed*. **1986**, *25*, 476.

(16) Potter, B.; Edelstein, E. K.; Morken, J. P. *Organic Letters.* **2016**, *18*, 3286.

(17) Feng, C.; Kaneko, Y.; Kobayashi, Y. *Tetrahedron Lett.*, **2013**, *54*, 4629.

(18) Robler, U.; Werner, T.; Christoffers, J. *Eur. J. Org. Chem.* **2000**, 701.

(19) Taylor, M. S.; Jacobsen, E. N. *J. Am. Chem. Soc.* **2003**, *125*, 11204.

(20) Kikushima, K.; Holder, J. C.; Gatti, M.; Stoltz, B. M. *J. Am. Chem. Soc.* **2011**, *13*, 6902.

(21) Spielvogel, D. J.; Buchwald, S. L. *J. Am. Chem. Soc*. **2002**, *124*, 3500.

(22) Minko, Y.; Pasco, M.; Mejuch, T.; Gilboa, N.; Chechik, H.; Das, J. P.; Marek, I. *J. Am. Chem. Soc.* **2014**, *136*, 2682.

(23) Das, J. P.; Chechik, H.; Marek, I. *Nature Chem*, **2009**, *1*, 128.

(24) Thiel, O. R.; Tsui, H.-C.; Trost, B. M. *J. Am. Chem. Soc*. **2003**, *125*, 13155.

(25) (a) Maddaford, S. P.; Andersen, N. G.; Cristofoli, W. A.; Keay, B. A. *J. Am. Chem. Soc*. **1996**, *118*, 10766. (b) Lebsack, A. D.; Link, J. T.; Overman, L. E.; Stearns, B. A. *J. Am. Chem. Soc*. **2002**, *124*, 9008.

(26) Mei, T.-S.; Patel, H. H.;Sigman, M. S. *Nature*, **2014**, *508*, 340.

(27) Corey, E. J. *Angew. Chem. Int. Ed.* **2002**, *41*, 1650.

(28) Wang, K.; Bungard, C. J.; Nelson, S. G. *Org. Lett*. **2007**, *9*, 2325.

(29) Marko, I. E.; Evans, G. R. *Tetrahedron Lett.* **1994**, *35*, 2771.

(30) (a) Tiong E. A.; Gleason, J. L. *Org. Lett.*, **2009**, *11*, 1725. (b) Mase, N.; Tanaka, F.; Barbas III, C. F. *Org. Lett.*, **2003**, *5*, 4369. (c) Mase, N.; Tanaka, F.; Barbas III, C. F. *Angew. Chem. Int. Ed.*, **2004**, *43*, 2420. (d) Chowdari, N. S.; Suri, J. T.; Barbas III, C. F. *Org. Lett.*, **2004**, *6*, 2507.

(31) (a) Davies, H.M.L.; Manning, J.R. *Nature*, **2008**, *451*, 417. (b) Davies, H.M.L.; Dick, A.R. *Top. Curr. Chem*. **2010**, *292*, 303. (c) Davies H.M.L. *Angew. Chem. Int. Ed.* **2006**, *45*, 6422. (d) Davies H. M. L.; Beckwith, R. E. J. *Chem. Rev.* **2003**, *103*, 2861. (e) Kalinin, A. V.; Ene, D. G.; Doyle, M. P. *J. Am. Chem. Soc.* **1996,** *118*, 8837. (f) Wu, C.; Ye, F.; Wang, C.; Zhao, Y.; Wang, J. *J, Org. Chem.* **2015**, *80*, 8748.

(32) (a) Ziegler, F. E. *Chem. Rev.*, **1988**, *88*, 1423. (b) Martin-Castro, A. M. *Chem. Rev.*, **2004**, *104*, 2939.

Chapter 2

STEREOSPECIFIC NICKEL-CATALYZED SUZUKI-MIYAURA ARYLATION OF BENZYLIC ACETATES TO SET DIARYL AND TRIARYL ALKANES

Portions of this chapter have been published in [*J. Am. Chem. Soc*. **2016**, *138*, 12057] and are reproduced with permission.

2.1 Introduction

As discussed in Chapter 1, all-carbon quaternary stereocenters are important. However, they are hard to make when they are isolated from functional groups. Transition metal-catalyzed cross-couplings should be possible, but has not yet been developed for non-allylic electrophiles with high ee. Stereospecific cross-couplings of allylic electrophiles have been developed to deliver all-carbon quaternary centers in high ee. Specifically, Kobayashi reported using allylic electrophiles with Grignard or zinc reagents (Scheme 2.1).[1a, 1b] However, these nucleophiles limit the substrate scope. The umpolung approach has also been demonstrated by the Morken group where an allylic electrophile has been transferred to an allylic boronate as the nucleophile in the subsequent Suzuki-Miyaura cross-coupling reaction (Scheme 1.12).[1c]

Scheme 2.1: Stereospecific Cross-Coupling Using Allylic Electrophiles and Grignard Reagents (Kobayashi)

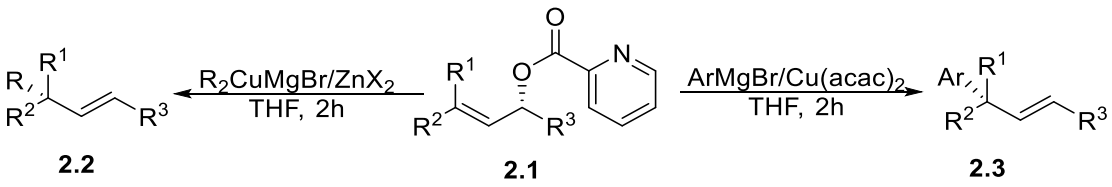

With respect to non-allylic substrates, benzylic all-carbon quaternary centers can be obtained in non-asymmetric fashion, like Biscoe's nickel-catalyzed Kumada cross-

coupling reactions, Fu's nickel-catalyzed Suzuki alkylations and Doyle's nickel-catalyzed Negishi cross-couplings (Scheme 2.2). [2] Notably, in a single example in Doyle's work, a promising 27% ee was given to form the enantioenriched quaternary stereocenter.[2c]

Scheme 2.2: Ni-Catalyzed Non-Asymmetric Cross-Coupling to Set Benzylic Quaternary Centers

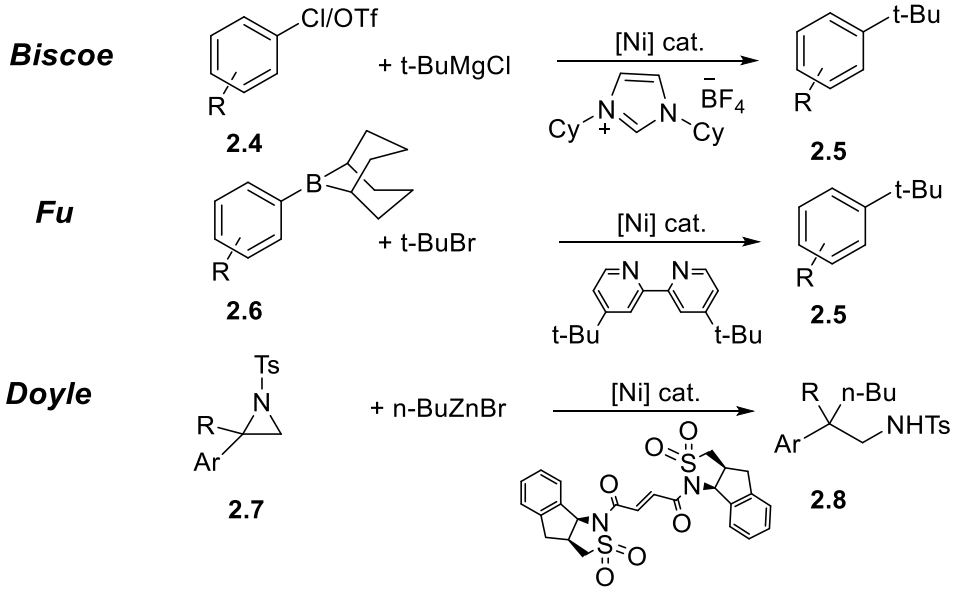

Insipired by the previous work on building tertiary stereocenters in our group (Scheme 2.3), the stereospecific nickel-catalyzed arylation of benzylic pivalates and ammonium salts, [3] my colleague Dr. Qi Zhou came up with the idea to apply this method to form all-carbon benzylic quaternary stereocenters. He proposed a stereospecific Suzuki-Miyaura arylation of tertiary benzylic carboxylates to deliver diaryl and triaryl all-carbon quaternary stereocenters (Scheme 2.4).

Scheme 2.3: Ni-Catalyzed Suzuki Arylation of Secondary Benzylic Electrophiles (Watson)

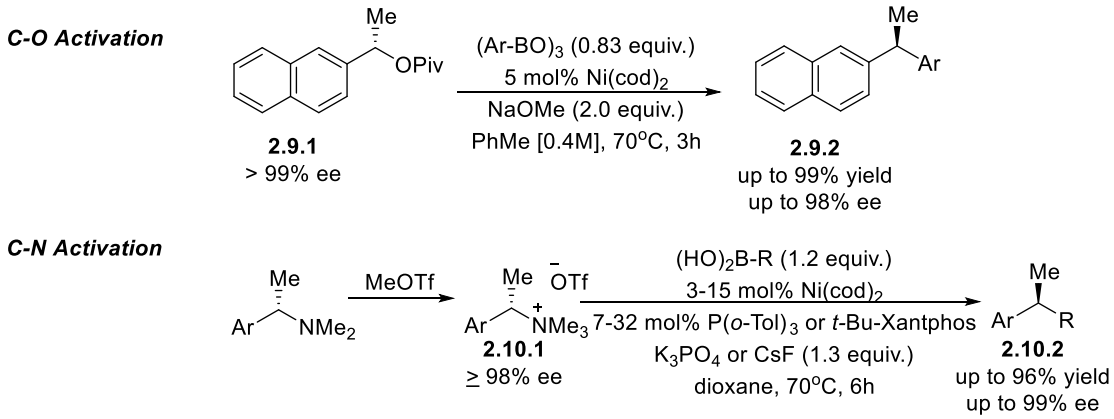

In considering this reaction, we anticipated several potential challenges. Due to the increased steric hindrance of the tertiary electrophiles, the oxidative addition step in the catalytic process may be deaccelerated. β-Hydride elimination can be much more competitive due to the existance of the β-hydrogen on the alkyl groups. High stereochemical fidelity could also be a challenge. All these challenges and concerns will be discussed and solved with optimization of the reaction.

Scheme 2.4: Proposed Ni-Catalyzed Suzuki-Coupling to Set Diaryl and Triaryl All-Carbon Quaternary Centers

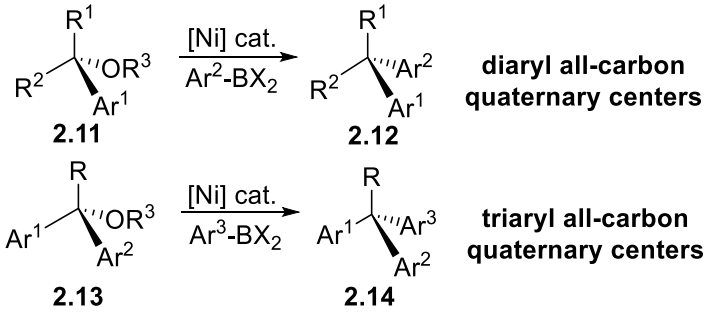

2.2 Results and Discussion

To start with, we need to have the enantiomeric excess (ee) of the starting material as high as possible. Following the enantioselective strategy to deliver tertiary benzylic alcohols reported by Walsh's group,[4] a solvent-free ethyl addition to 2-acetonaphthone under the catalysis of titanium tetraisoproxide and a chiral bis(sulfonamide) diol ligand gave the tertiary benzylic alcohol in 75% yield and 97% ee (Scheme 2.6). This chiral ligand can be synthesized easily by the coupling of (*R*,*R*)-cyclohexyldiamine and camphorsulfonyl chloride and the reduction of the ketone to the corresponding alcohol (Scheme 2.5).[5] Subsequent acylation then gives acetate **2.19**.

Scheme 2.5: Synthesis of the Chiral Bis(sulfonamide) Diol Ligand **2.16** (Walsh)

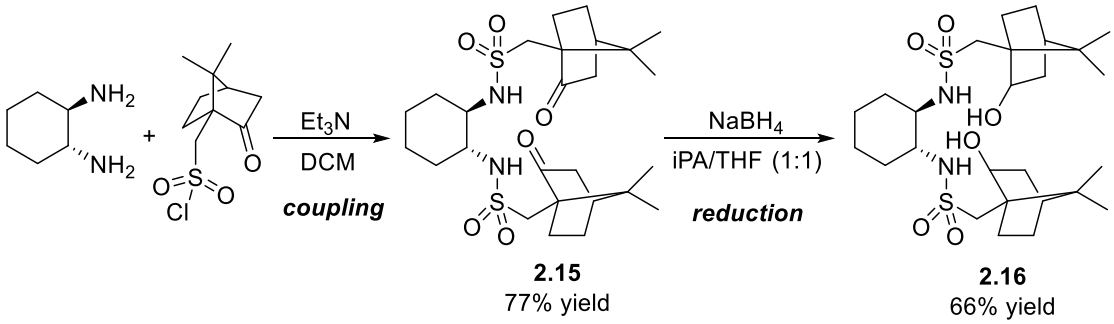

Scheme 2.6: Preparation of the Tertiary Benzylic Alcohol **2.18** and Acetylation

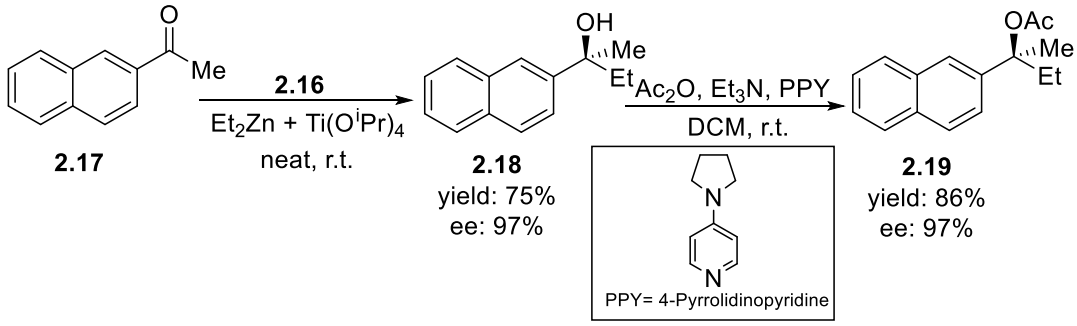

With the enantioriched model substrate **2.19** in hand, Dr. Zhou optimized the reaction. Under the best conditions for arylation of secondary benzylic pivalates, he was delighted to notice that the target diarylalkane was formed in high yield (74%), but low stereochemical fidelity (20% ee) as well as trace amount of olefins **2.23** (entry 1, Table 2.1). The olefin byproducts likely come from β-hydride elimination, but E2 elimination is also possible.

Table 2.1: Optimization of Reaction Parameters[a]

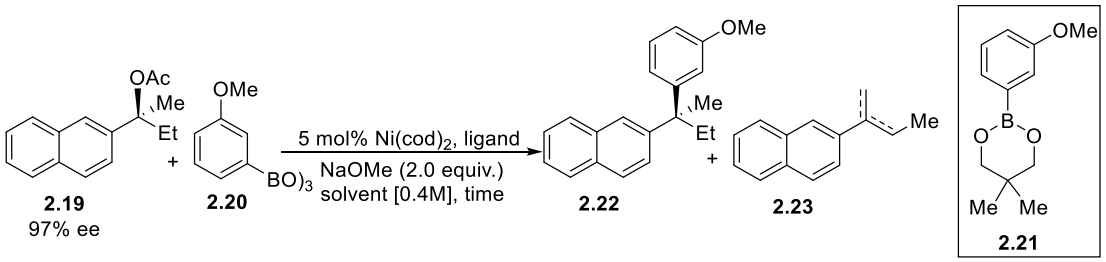

entry	ligand (mol %)	temp. (^oC)	solvent	time (h)	yield (%)[b] **2.22**	yield (%)[b] **2.23**	ee (%)[c]	es (%)[d]
1	none	80	PhMe	2	93	2	20	21
2	PCy_2Ph (11)	80	PhMe	2	74	22	87	90
3	PCy_2Ph (11)	60	PhMe	5	72	25	90	93
4	PCy_2Ph (11)	60	THF	5	63	24	93	96
5	CyJohnPhos (11)	40	THF	16	57	9	96	99
6	CyJohnPhos (5)	40	THF	16	81	6	96	99
7	CyJohnPhos (5)	40	2-Me-THF	22	92	8	96	99
8[e,f]	**CyJohnPhos (5)**	**40**	**2-Me-THF**	**22**	**99**	**≤3**	**97**	**>99**

[a] Conditions: **2.19** (0.10mmol), **2.20** (1.0 equiv.), $Ni(cod)_2$ (5 mol%), ligand, NaOMe (2.0 equiv.) and solvent (0.4 M, 0.25 mL) in a one-drum vial, unless otherwise noted. [b] Determined by ^1H NMR using an internal standard. Total yields over 100% reflect the error of ^1H NMR yields, particularly for minor products. [c] Determined by HPLC using a chiral stationary phase. [d] es = enantiospecificity = $(ee_{product})/(ee_{starting\ material})$. [e] $NiCl_2 \cdot DME$ in place of $Ni(cod)_2$. [f] **2.21** in place of **2.20**.

Starting at this point, Dr. Zhou optimized the reaction by adjusting the reaction parameters. The presence of dicyclohexylphenyl phosphine ligand (PCy_2Ph) increased the ee from 20% to 87% (entry 2, Table 2.1). The ee can be increased all the way to 90% by lowering the temperature from 80 ^oC to 60 ^oC, extending the time from 2 to 5 hours (entry 3, Table 2.1), and switching to a polar solvent, THF instead of toluene (entry 4, Table 2.1). However the yield of the byproduct alkene increased as well, from trace amount (2%) all the way to 24% (entry 4, Table 2.1). Dr. Zhou successfully controlled

the formation of these alkenes by using Buchwald ligands, which were efficient in decreasing the β-hydride elimination likely due to blocking the open coordination site needed for β-hydride elimination.[6] Finally by screening a set of Buchwald-type biphenyl phosphine ligands at a lower temperature of 40 ^{o}C for 22 hours, he was glad to find that the use of (2-biphenyl)dicyclohexylphosphine (CyJohnPhos) resulted in <10% yield of the olefin byproducts and 96% ee of the desired product, although with a slightly low yield of 57% (entry 5, Table 2.1). With a 1:1 ratio of $Ni(cod)_2$: CyJohnPhos, 81% yield of the desired product was achieved with good ee of 96% (entry 6, Table 2.1). Finally the best condition was found when an air-stable Ni(II) pre-catalyst was used instead of $Ni(cod)_2$ and a 'greener' solvent, 2-methyltetrahydrofuran (2-Me-THF), was used. Further improvement was realized by replacing the aryl boroxine with the aryl boronic acid neopentylglycol esters (entry 8, Table 2.1). All these added up to deliver desired diarylalkane **2.22** with nearly quantitative yield (99%) and high stereochemical fidelity (97% ee). The formation of β-hydride elimination product has been well contolled with less than 3% yield.

At this point, I joined this project, together with another collegue, Dr. Kelsey Cobb, to help Dr. Zhou with the substrate scope by trying a series of organoboron reagents to see how well this methodology can be applied. To our delight, good yields and high levels of stereochemical fidelity can be achieved under these optimized conditions (entry 10, Table 2.1) with a variety of aryl boronate esters to deliver diarylalkanes. Different kinds of functional groups on the aryl ring of the boronate esters are well tolerated, including electron-rich substituents like dimethylamine (**2.25**) and methoxyl groups (**2.22**, **2.26**), electron-poor ones such as amide (**2.29**), ester (**2.28**), trifluoromethyl (**2.30**), fluoride (**2.31**) and chloride (**2.27**). An increasingly steric allyl

hindered 2,4-dimethylphenyl boronic acid neopentylglycol ester can also be successsfully cross-coupled (**2.32**) to give good yield and excellent ee (95%) which indicates how powerful our catalytic system is. However there are some limitations in this reaction. When arenes with heteroatoms (**2.34** – **2.38**) or vinyl groups (**2.39**) are involved, the reaction did not succeed in giving the desired final products probably due to the nickel catalysts being poisoned by coordination of heteroatoms or double bonds.

Figure 2.1: Unsuccessful Aryl Boronate Esters

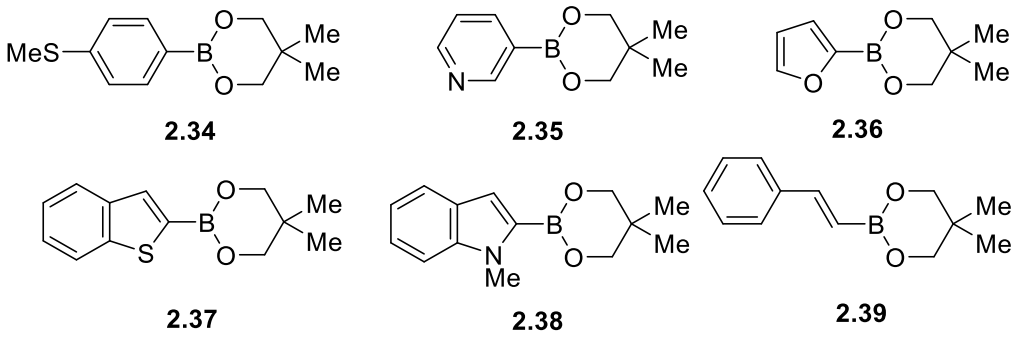

Scheme 2.7: Scope of Aryl Boronate Esters[a]

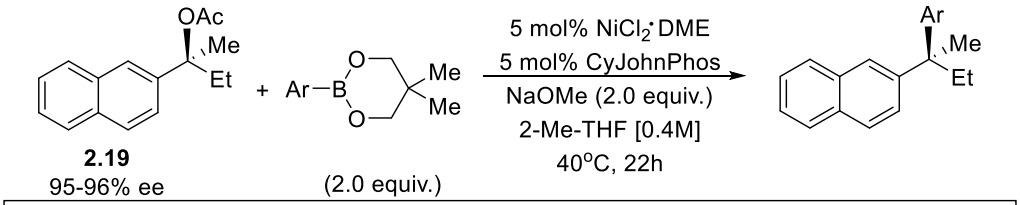

2.19
95-96% ee

(2.0 equiv.)

2.22
89% yield
93% ee
98% es

2.24
95% yield
95% ee
99% es

2.25
82% yield
96% ee
>99% es[b]

2.26
93% yield
96% ee
>99% es

2.27
57% yield
92% ee
97% es

2.28
87% yield
96% ee
>99% es[c,d]

2.29
86% yield
94% ee
98% es[c]

2.30
81% yield
96% ee
>99% es

2.31
95% yield
94% ee
98% es

2.32
89% yield
95% ee
99% es

2.33
86% yield
92% ee
97% es

[a] Conditions: **2.19** (0.40 mmol), aryl boronate ester (2.0 equiv.), $NiCl_2$·DME (5 mol %), CyJohnPhos (5 mol %), NaOMe (2.0 equiv.), 2-Me-THF (0.4 M, 1 mL), 40 °C, 22h, unless noted. Average isolated yield (±9%) and ee's (±1%, determined by HPLC or SFC using a chiral stationary phase) or duplicate reactions, unless otherwise noted. [b] Single experiment. [c] 60 °C, 12 h. [d] 3.0 equiv. of aryl boronate esters.

Meanwhile Dr. Zhou developed the substrate scope of the tertiary acetate side successfully by changing the aryl and alkyl substituents. As for the aryl substituent, electron-rich 6-methoxyl-naphthyl group (**2.34**), increasingly steric hindered 1-naphthyl group (**2.35**), and a heteroaryl one which is 3-quinolinyl group (**2.36**) are used to give the final products in good to excellent yields with also terrific more than 98% enantiospecificities. Many choices are available for the alkyl substituent R^1, such as silyl ether (**2.37**), phenethyl (**2.38**) and allyl (**2.39**) groups. When switching from methyl to ethyl group at R^2 position (**2.40**), the product can also be formed with 77% yield and 98% es. More importantly, all-carbon triarylmethanes can also be formed with this strategy in good yield and excellent ee (**2.41**, **2.42**), which can be further developed to broaden the application of this cataytic cross-coupling. I will discuss this in detail later.

Scheme 2.8: Scope of Tertiary Acetates[a]

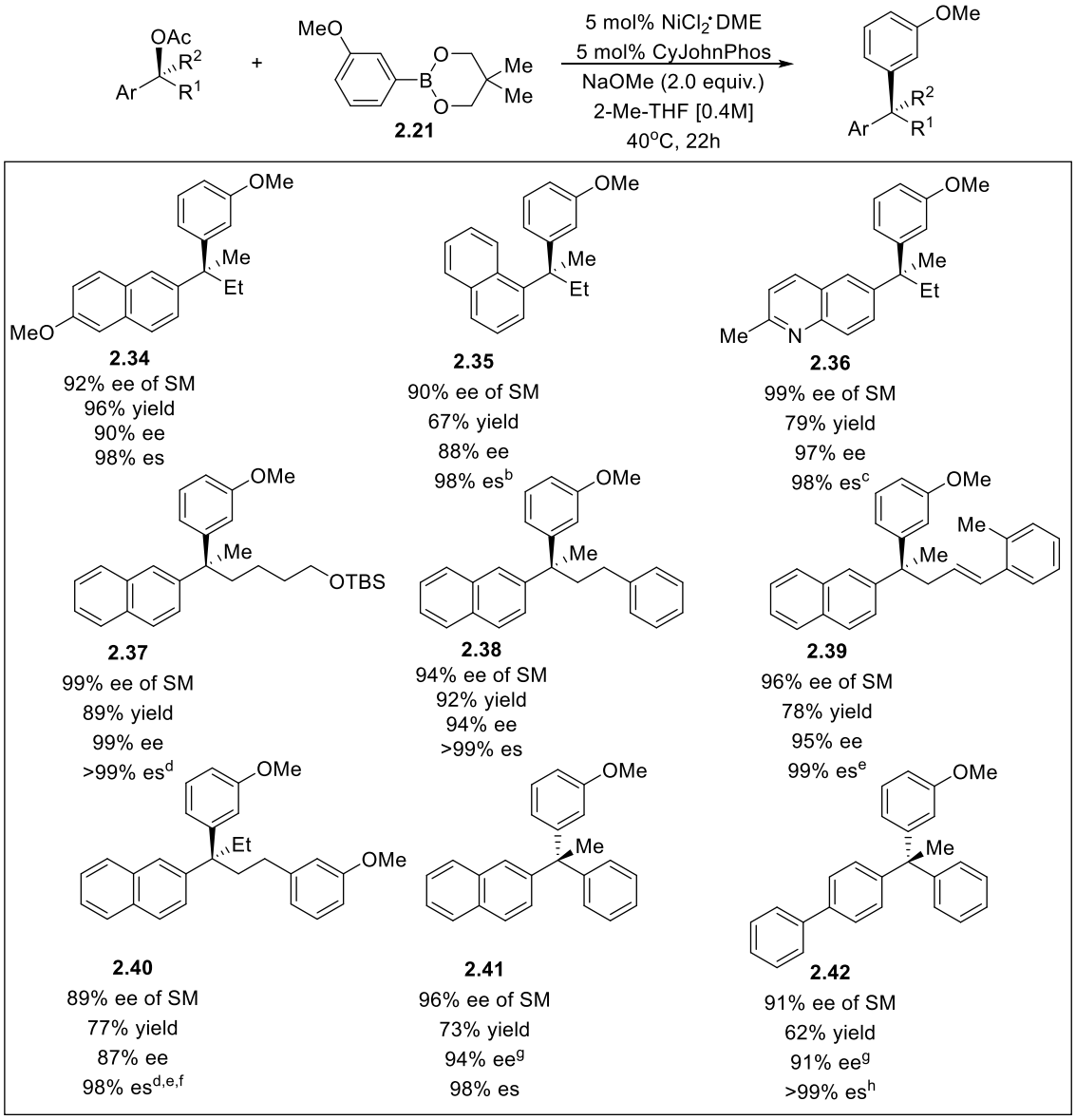

[a] Conditions: see Scheme 2.7. Average isolated yields (±7%) and ee's (±1%). [b] A second run gave **2.35** in 78% yield, 83% ee, 99% es using 84% ee of SM. [c] 60 °C, 24 h. [d] Single experiment. [e] **2.20** (0.83 equiv.) in place of **2.21**. [f] A second run gave **2.40** in 63% yield, 86% ee, 99% es using 87% ee of acetate. [g] Opposite enantiomer of starting material used. [h] 10 mol % $NiCl_2$·DME, 10 mol % CyJohnPhos, 60 °C, 48h.

I also helped in confirmation of the absolute configuration of the starting materials to support our hypothesis on the reaction mechanism. Enantioriched starting

material acetate **2.19** is an oil after column chromotography. After extensive experimentation, such as making an over-saturated solution, diffusion, adding a seed crystal, the acetate still remained an oil without crystallization. However, I was able to grow a crystal by putting the pure acetate in the freezer, which helped its solidification. The absolute configuration of the acetate was proved to be *S* by X-ray crystallography. With the absolute configuration of product **2.29** confirmed to be *R* via X-Ray crystallography using Cu *K*α radiation, [7] we are confident that this reaction proceeds with overall retention of absolute configuration. In this case, the mechanism is consistent with the one proposed for the stereoretentive cross couplings of secondary benzylic and allylic pivalates, a directed S_N2' oxidative addition directed by the leaving group, in which the nickel catalyst is bound by the acetate to add in an S_N2' fashion (**A**, Scheme 2.9). This mode of oxidative addition results in the net retention of stereochemistry.

Figure 2.2: Evidence of Net Retention in the Ni(II)-Catalyzed Suzuki-Miyaura Arylation of Tertiary Benzylic Carboxylates

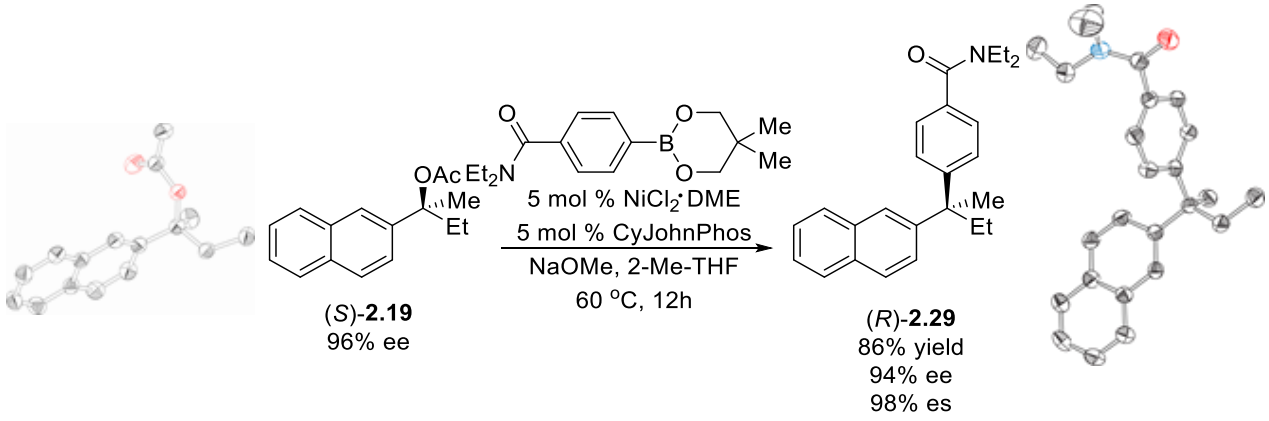

Scheme 2.9: Putative Catalytic Cycle

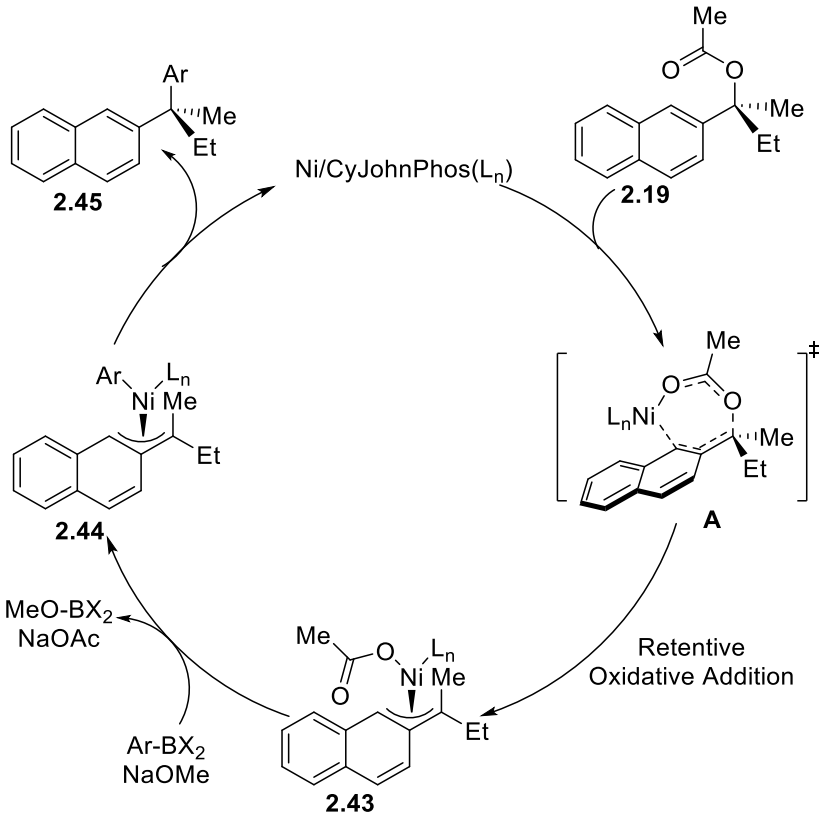

As shown in Scheme 2.7, triaryl alkanes with quaternary stereocenters can be formed using this strategy. This method represents the only stereoselective or stereospecific route to these products. In addition, the substitution of dibenzylic acetates did not require a naphthyl substituent, biphenyl product **2.33** was formed in good yield under only slightly modified reaction conditions. To further develop this catalytic system to the delivery of triaryl benzylic all-carbon quaternary centers, I continued to optimize the reaction condition based on the result of **2.42** by Dr. Zhou. First a group of Buchwald ligands have been tested, which did not work as well as the earlier best ligand CyJohnPhos. Then I did a systematically screening of increasing the aromacity of the phosphine ligands and was happy to find out that the ligand

dicyclohexylphenylphosphine (PCy_2Ph) worked out better than others with a yield of 42%. Adding only one methyl substituent on the phosphine ligand phenyl group increased and the yield by 30%. With this in hand, the best ligand so far would be $PCy_2(o\text{-}MeC_6H_4)$ which delivered a higher yield of 69% than the preliminary result reported in the paper.

Scheme 2.10: Ligand Screening Using Racemic Acetate **2.46** Catalyzed by $NiCl_2 \cdot DME$[a]

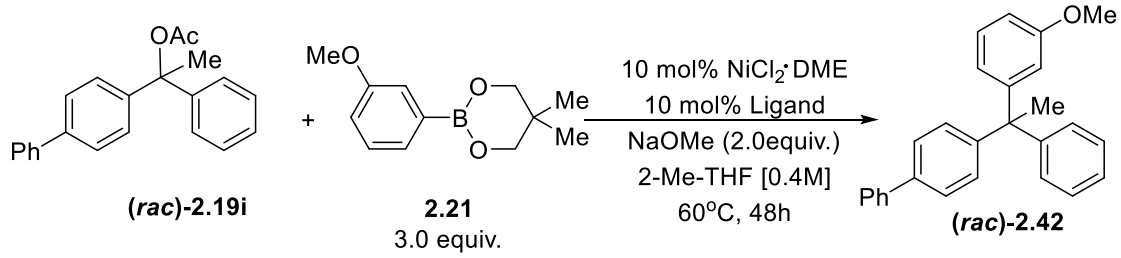

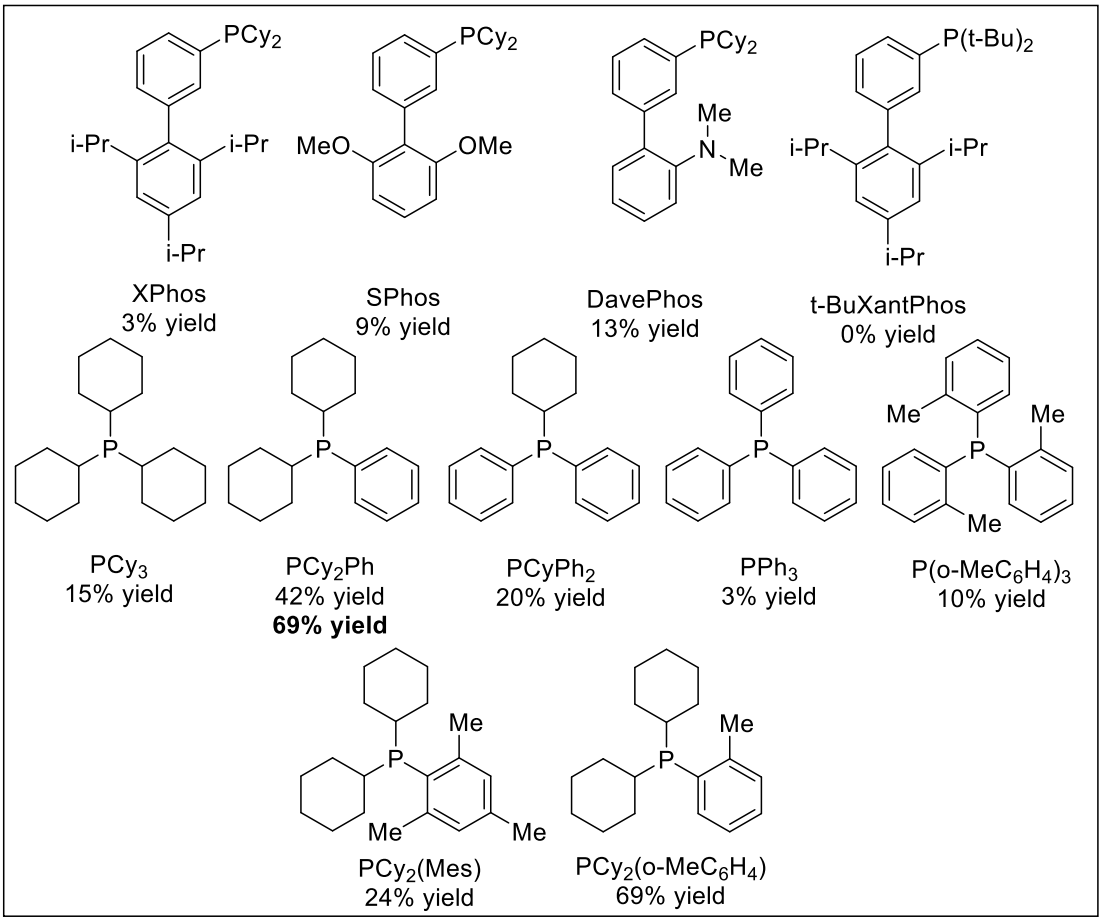

[a] Conditions: ***(rac)*-2.19i** (0.10 mmol), **2.21** (3.0 equiv.), $NiCl_2 \cdot DME$ (10 mol %), Ligand (10 mol %), NaOMe (2.0 equiv.), 2-Me-THF (0.4 M, 0.25 mL), 60 °C, 48h, unless noted. Yields determined by ^1H NMR using an internal standard.

Meanwhile, my colleague Dr. Bibaswan Biswas noticed that when using $Ni(cod)_2$ and PCy_2Ph, the yield was increased to 69%. Then I conducted another ligand investigation using $Ni(cod)_2$ as the nickel source. The use of $Ni(cod)_2$ turned out to

increase the yield with the ligand $PCy_2(o\text{-}MeC_6H_4)$ still as the best one. The yield of the reaction increased to 78% with no starting material left. However, 13% elimination and 15% hydrolysis byproducts did exist. To our delight, the stereospecificity of this new catalytic system was still outstanding. The product **2.42** was obtained in 94% ee and 99% es (Scheme 2.12).

Scheme 2.11: Ligand Screening Using Racemic Acetate **2.19i** Catalyzed by $Ni(cod)_2$[a]

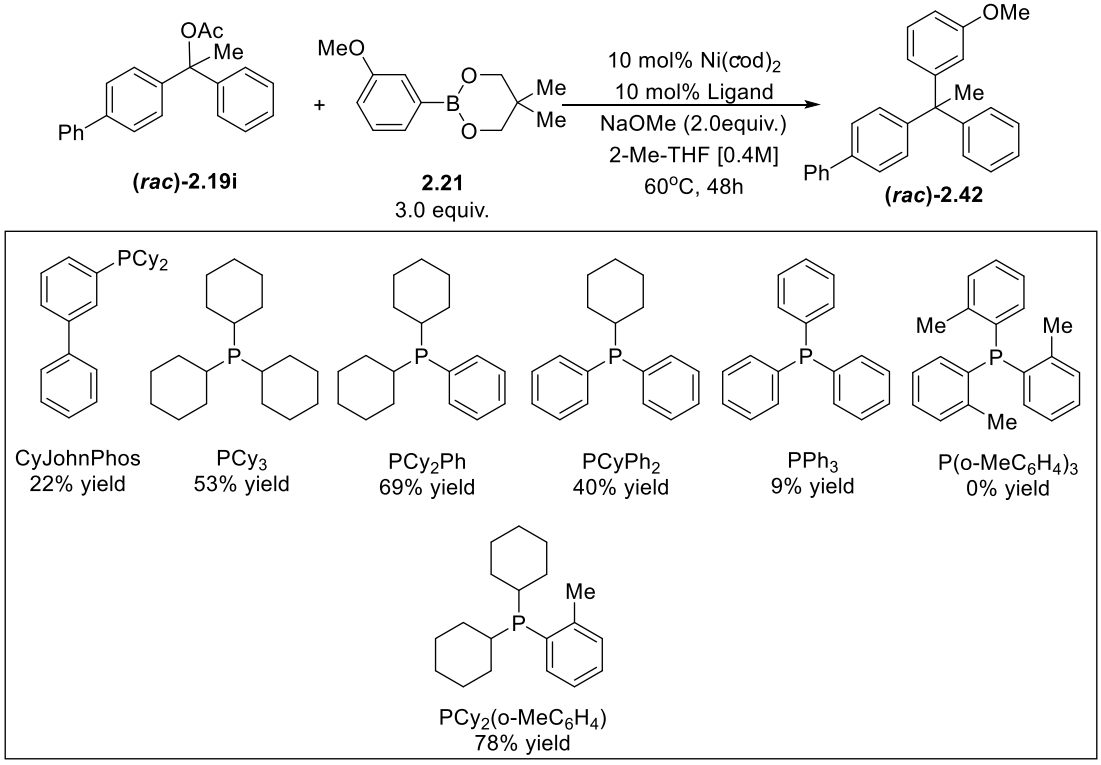

[a] Conditions: **(*rac*)-2.19i** (0.10 mmol), **2.21** (3.0 equiv.), $Ni(cod)_2$ (10 mol %), Ligand (10 mol %), NaOMe (2.0 equiv.), 2-Me-THF (0.4 M, 0.25 mL), 60 °C, 48h, unless noted. Yields determined by ^1H NMR using an internal standard.

Scheme 2.12: New Catalytic System Used in the Stereospecific Suzuki-Miyaura Arylation to Set Triaryl Quaternary Centers[a]

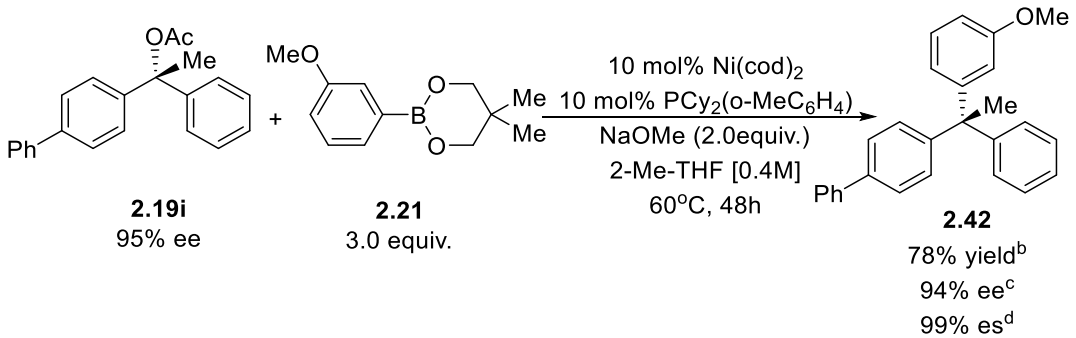

Conditions: [a] **2.19i** (0.10 mmol), **2.21** (3.0 equiv.), $Ni(cod)_2$ (10 mol %), $PCy_2(o\text{-}MeC_6H_4)$ (10 mol %), NaOMe (2.0 equiv.), 2-Me-THF (0.4 M, 0.25 mL), 60 °C, 48h. [b] Determined by ^1H NMR using an internal standard. [c] Determined by HPLC using a chiral stationary phase. [d] es = enantiospecificity = $(ee_{product})/(ee_{starting\ material})$.

Having shown increased yield for diphenyl-substituted **2-19i**, I wanted to investigate an acetate with an even simpler aryl substituent. In this case, a less conjugated tertiary alcohol has been synthesized using Walsh's procedure with a high yield of 95% and a high ee of 90%. The corresponding acetate **2.19j** was generated in 86% yield, while maintaining the same ee. First I used racemic acetate **2.19j** with both Ni(II) and Ni(0) catalysts and the three best ligands, CyJohnPhos, PCy_2Ph and $PCy_2(o\text{-}MeC_6H_4)$ to see the yields. $PCy_2(o\text{-}MeC_6H_4)$ turned out to be the best among these three ligands. Notably when I doubled the amount of nickel catalyst and ligand (entry 7, Table 2.2), the yield increased significantly to 69%, with neither starting material nor hydrolysis byproduct observed. Only 24% β-hydride elimination byproduct was found. This result gave me the idea that the amount of ligand matters in this reaction, which led me to systematic screening of the ratio of nickel to ligand.

Table 2.2: Further Optimization Between Nickel Catalysts and Phosphine Ligands in Less Conjugated π-System[a]

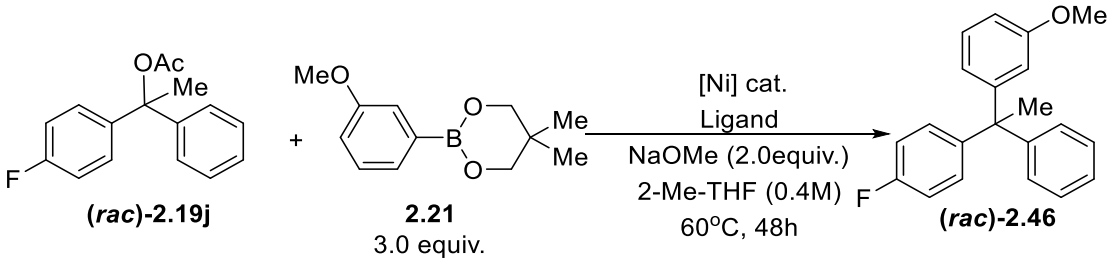

entry	[Ni] (mol %)	Ligand (mol %)	yield (%)
1	$Ni(cod)_2$（10）	CyJohnPhos（10）	30
2	$Ni(cod)_2$（10）	PCy_2Ph（10）	44
3	$Ni(cod)_2$（10）	$PCy_2(o\text{-}MeC_6H_4)$ (10)	48
4	$NiCl_2$·DME (10)	CyJohnPhos (10)	27
5	$NiCl_2$·DME (10)	PCy_2Ph (10)	11
6	$NiCl_2$·DME (10)	$PCy_2(o\text{-}MeC_6H_4)$ (10)	45
7	$NiCl_2$·DME (20)	$PCy_2(o\text{-}MeC_6H_4)$ (20)	69

[a] Conditions: **(*rac*)-2.19j** (0.10 mmol), **2.21** (3.0 equiv.), [Ni] catalyst (10 mol %), Ligand (10 mol %), NaOMe (2.0 equiv.), 2-Me-THF (0.4 M, 0.25 mL), 60 °C, 48h, unless noted. Yields determined by ^1H NMR using an internal standard.

Given the fact that $Ni(cod)_2$ is less stable to air and moisture, I performed the following investigation with Ni(II) pre-catalyst and the best ligand $PCy_2(o\text{-}MeC_6H_4)$. Enantioenriched **2.19j** was used, so that stereospecificity could also be evaluated. Lower loading of the catalyst resulted in low yield (entries 1 and 2, Table 2.3) and did not help in achieving high ee's. The best ratio of nickel to ligand is 1:2.5 (entry 4) to give the best yield of 73% with an enantiospecifity of 87%. After that, increasing the catalyst loading does not help to improve the yield or ee.

Table 2.3: Systematic Screening of Nickel Catalyst to Phosphine Ligand Ratio in the Stereospecific Suzuki-Miyaura Arylation of Less Conjugated π-System[a]

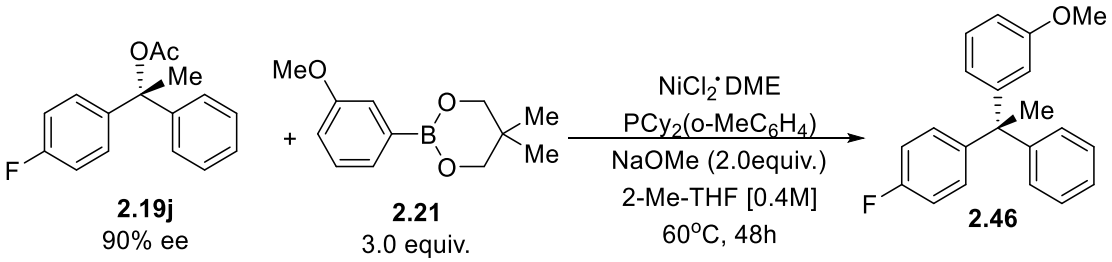

entry	$NiCl_2$·DME (mol %)	$PCy_2(o\text{-}MeC_6H_4)$ (mol %)	yield[b] (%)	ee[c] (%)	es[d] (%)
1	3	6	9	-	-
2	5	10	18	73	81
3	10	20	54	78	87
4	10	25	73	78	87
5	10	30	61	76	84
6	10	40	57	78	87
7	10	50	60	77	86

[a] Conditions: **2.19j** (0.10 mmol), **2.21** (3.0 equiv.), $NiCl_2$·DME, $PCy_2(o\text{-}MeC_6H_4)$, NaOMe (2.0 equiv.), 2-Me-THF (0.4 M, 0.25 mL), 60 °C, 48h, unless noted. [b] Determined by ^1H NMR using an internal standard. [c] Determined by HPLC using a chiral stationary phase. [d] es = enantiospecificity = $(ee_{product})/(ee_{starting\ material})$.

2.3 Conclusion

To sum up, we have developed a nickel-catalyzed Suzuki-Miyaura arylation of tertiary benzylic acetates to set diaryl and triaryl all-carbon quaternary centers in high yield and excellent stereochemical fidelity, which was also the first example of such reactions to our knowledge.[8] In our reaction, cheap, air-stable $NiCl_2$·DME has been used with commercially available phosphine ligand, as well as easily synthesized neopentylglycol boronic esters and highly enantioenriched tertiary acetates as the starting materials. For acetates with naphthyl-like subsituents, the enantiospecifity of

the product can be as high as ≥ 99%. And I also modified this catalytic system to apply it to acetates with a less conjugated π-substituent where synthetically useful yield and good enantiospecifity can be obtained. An S_N2' mechanism has been proposed to support on our observation of net retention of configuration from starting material to final product.

2.4 Experimental Section

2.4.1 General Information

Reactions were performed in oven-dried vials with Teflon-lined caps or in oven-dried round-bottomed flasks unless otherwise noted. On occasions when a viscous mixture formed in the reaction vials, a higher speed of stirring or shaking was performed to guarantee sufficient mixing. Flasks were fitted with rubber septa, and reactions were conducted under a positive pressure of N_2. Stainless steel syringes or cannulae were used to transfer air- and moisture-sensitive liquids. Flash chromatography was performed on silica gel 60 (40-63 μm, or 5-20 μm 60Å) unless otherwise noted. Commercial reagents were purchased from Sigma Aldrich, Acros, Fisher, Strem, TCI, Combi Blocks, Alfa Aesar, or Cambridge Isotopes Laboratories and used as received with the following exceptions: sodium methoxide, anhydrous 2-methyltetrahydrofuran, diethyl zinc, dimethyl zinc (1.0 M in PhMe) were purchased from vendors and immediately placed in a N_2-atmosphere glovebox for storage. Acetic anhydride and Ti(O-*i*Pr)$_4$ were distilled before use and stored under N_2. Toluene, CH_2Cl_2, and THF were dried by passing through drying columns and stored over activated 4Å MS in a N_2-atmosphere glovebox.[9] (*R,R*)-Bis(sulfonamide) diol ligand **2.16** was prepared according to reported literature procedure.[10] Bis(4-((*tert*-

butyldimethylsilyl)oxy)butyl)zinc was prepared according to reported literature procedure and used immediately.[11] Oven-dried potassium carbonate was added into $CDCl_3$ to remove trace amount of acid. Proton nuclear magnetic resonance (^1H NMR) spectra and carbon nuclear magnetic resonance (^{13}C NMR) spectra were recorded on both 400 MHz and 600 MHz spectrometers. Chemical shifts for protons are reported in parts per million downfield from tetramethylsilane and are referenced to residual protium in the NMR solvent ($CHCl_3$ = δ 7.26). Chemical shifts for carbon are reported in parts per million downfield from tetramethylsilane and are referenced to the carbon resonances of the solvent ($CDCl_3$ = δ 77.2). Data are represented as follows: chemical shift, multiplicity (br = broad, s = singlet, d = doublet, t = triplet, q = quartet, p = pentet, m = multiplet, dd = doublet of doublets, h = heptet), coupling constants in Hertz (Hz), integration. Infrared (IR) spectra were obtained using FTIR spectrophotometers with material loaded onto a NaCl plate. The mass spectral and X-ray crystallography data were obtained at the University of Delaware facilities. Optical rotations were measured using a 2.5 mL cell with a 0.1 dm path length. Melting points were taken on a Stuart SMP10 instrument. Enantiomeric excess (ee) was determined using chiral HPLC analysis at the University of Delaware or chiral SFC analysis at Lotus Separations, Inc.

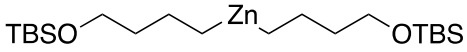

bis(4-((*tert*-butyldimethylsilyl)oxy)butyl)zinc

2.4.2 Stereospecific Arylation to Prepare Diaryl and Triaryl Alkanes

2.4.2.1 General Procedure A: Streospecific Arylation of Tertiary Benzylic Acetates

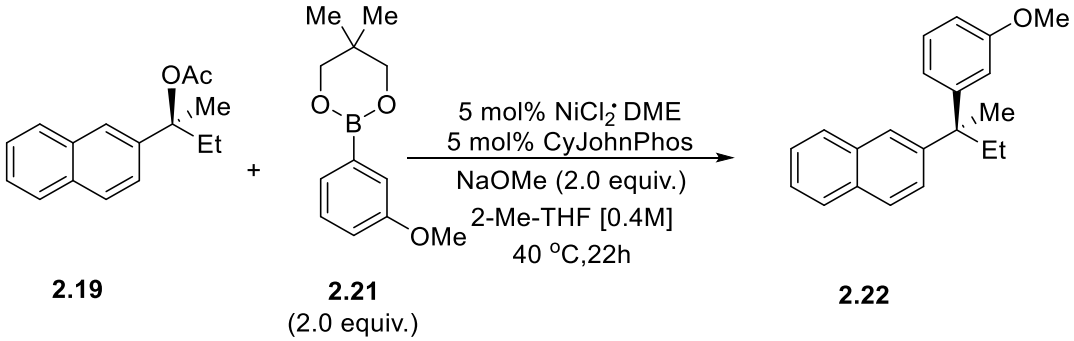

2.19 **2.21** (2.0 equiv.) **2.22**

(*S*)-2-(2-(3-Methoxyphenyl)butan-2-yl)naphthalene ((*S*)-2.22). In a N_2-atmosphere glovebox, $NiCl_2$·DME (4.4 mg, 0.020 mmol, 5 mol %), CyJohnPhos (7.0 mg, 0.020 mmol, 5 mol %) and NaOMe (44 mg, 0.80 mmol, 2.0 equiv) were weighed into a 1-dram vial fitted with a magnetic stir bar. 2-(3-Methoxyphenyl)-5,5-dimethyl-1,3,2-dioxaborinane (**2.21**, 176 mg, 0.800 mmol, 2.0 equiv) and (*S*)-2-(naphthalen-2-yl)butan-2-yl acetate (**2.19**, prepared in 95% ee, 97 mg, 0.40 mmol, 1.0 equiv) were added, followed by 2-Me-THF (1.0 mL, 0.4 M). The vial was capped with a Teflon-lined cap and removed from the glovebox. The mixture was stirred at 40 °C for 22 h. The reaction mixture was then diluted with Et_2O (5 mL) and filtered through a plug of silica gel and Celite®, which was then rinsed with Et_2O (~ 15 mL). The filtrate was concentrated and then purified by silica gel chromatography (0−2% Et_2O/hexanes) to give the compound **2.22** (run 1: 100.3 mg, 86%; run 2: 105.7 mg, 91%) as a colorless sticky oil. The enantiomeric excess was determined to be 93% (run 1: 93% ee; run 2: 92% ee) by chiral HPLC analysis (CHIRALPAK IB, 0.6 mL/min, 0.1% *i*-PrOH/hexane, λ=254 nm); t_R(major) = 12.058 min, t_R(minor) = 14.930 min. $[\alpha]_D^{24} = -10.2°$ (c 4.25, $CHCl_3$): ^{1}H NMR (600 MHz, $CDCl_3$) δ 7.85 – 7.81 (m, 1H), 7.81 – 7.77 (m, 2H), 7.69

(d, J = 8.7 Hz, 1H), 7.49 – 7.42 (m, 2H), 7.21 – 7.16 (m, 2H), 6.83 – 6.79 (m, 2H), 6.76 – 6.69 (m, 1H), 3.75 (s, 3H), 2.31– 2.20 (m, 2H), 1.70 (s, 3H), 0.77 (t, J = 7.3 Hz, 3H); ^{13}C NMR (151 MHz, $CDCl_3$) δ 159.4, 151.5, 146.9, 133.3, 131.9, 128.9, 128.1, 127.6, 127.5, 127.2, 125.9, 125.5, 124.9, 120.4, 114.3, 110.3, 55.3, 46.8, 33.9, 26.9, 9.4; FTIR (NaCl/thin film) 3054, 2967, 2934, 2877, 1599, 1582, 1485, 1457, 1430, 1290, 1254, 1053, 819, 749, 703, 477 cm^{-1}; HRMS (CI+) $[M+H]^+$ calculated for $C_{21}H_{23}O$: 291.1749, found: 291.1773.

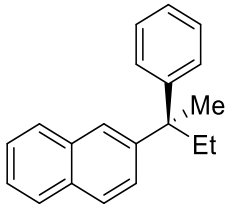

(*R*)-2-(2-Phenylbutan-2-yl)naphthalene ((*R*)-2.24). Prepared via General Procedure A using **2.19** (prepared in 96% ee) as a colorless oil (run 1: 100 mg, 96%; run 2: 96.8 mg, 93%). The enantiomeric excess was determined to be 95% (run 1: 95% ee; run 2: 95% ee) by chiral SFC analysis (CHIRALCEL OJ-H (25 x 0.46 cm), 3.0 mL/min, 15% EtOH(0.1% diethylamine)/CO_2 (100 bar), λ=220 nm); t_R(major) = 6.25 min, t_R(minor) = 7.32 min. $[\alpha]_D^{24}$ = +13.3° (c 1.02, $CHCl_3$): ^{1}H NMR (400 MHz, $CDCl_3$) δ 7.88 – 7.78 (m, 3H), 7.71 (d, J = 8.7 Hz, 1H), 7.53 – 7.43 (m, 2H), 7.33 – 7.18 (m, 6H), 2.36 – 2.22 (m, 2H), 1.73 (s, 3H), 0.79 (t, J = 7.4 Hz, 3H); ^{13}C NMR (101 MHz, $CDCl_3$) δ 149.7, 147.0, 133.2, 131.8, 128.10, 128.07, 127.63, 127.61, 127.5, 127.3, 126.0, 125.7, 125.6, 124.9, 46.8, 33.8, 26.9, 9.4; FTIR (NaCl/thin film) 3055, 2968, 2934, 2876, 1599, 1494, 1444, 1380, 1273, 1131, 1029, 948, 897, 770 cm^{-1}; HRMS (EI+) [M]+ calculated for $C_{20}H_{20}$: 260.1565, found: 260.1558.

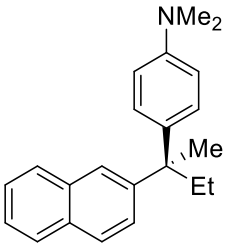

(*R*)-*N*,*N*-Dimethyl-4-(2-(naphthalen-2-yl)butan-2-yl)aniline ((*R*)-2.25). Prepared via General Procedure A using **2.19** (prepared in 96% ee) as a white solid (mp 64–66 °C; 99 mg, 82%). The enantiomeric excess was determined to be 96% by chiral SFC analysis (CHIRALCEL OJ-H (25 x 0.46 cm), 3.5 mL/min, 55% MeOH(0.1% diethylamine)/CO_2 (100 bar), λ=220 nm); t_R(major) = 11.68 min, t_R(minor) = 17.76 min. $[\alpha]_D^{24}$ = +22.6° (c 3.8, $CHCl_3$): ^{1}H NMR (600 MHz, $CDCl_3$) δ 7.81 (dd, *J* = 8.0, 1.3 Hz, 1H), 7.79 – 7.74 (m, 2H), 7.67 (d, *J* = 8.7 Hz, 1H), 7.48 – 7.38 (m, 2H), 7.21 (dd, *J* = 8.7, 1.9 Hz, 1H), 7.11 – 7.05 (m, 2H), 6.68 – 6.63 (m, 2H), 2.91 (s, 6H), 2.28 – 2.15 (m, 2H), 1.67 (s, 3H), 0.76 (t, *J* = 7.3 Hz, 3H); ^{13}C NMR (151 MHz, $CDCl_3$) δ 148.6, 147.6, 137.8, 133.3, 131.8, 128.2, 128.1, 127.50, 127.46, 127.4, 125.8, 125.4, 124.8, 112.3, 45.9, 40.8, 34.0, 27.0, 9.4; FTIR (NaCl/thin film) 3431, 3054, 2966, 2934, 2876, 1613, 1519, 1444, 1348, 1201, 1166, 948, 818, 746, 569, 476 cm^{-1}; HRMS (LIFDI) [M]+ calculated for $C_{22}H_{25}N$: 303.1987, found: 303.1966.

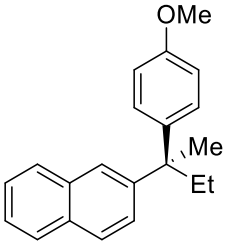

(*R*)-2-(2-(4-Methoxyphenyl)butan-2-yl)naphthalene ((*R*)-2.26). Prepared via General Procedure A using **2.19** (prepared in 96% ee) as a colorless oil (run 1: 110 mg, 95%; run 2: 105.7 mg, 91%). The enantiomeric excess was determined to be 96% (run 1: 96% ee; run 2: 96% ee) by chiral SFC analysis (CHIRALCEL OJ-H (25 x 0.46 cm),

3.0 mL/min, 25% *i*-PrOH(0.1% diethylamine)/CO_2 (100 bar), λ=220 nm); t_R(major) = 4.89 min, t_R(minor) = 6.27 min. $[\alpha]_D^{24}$ = +12.4° (c 0.98, $CHCl_3$): ^{1}H NMR (400 MHz, $CDCl_3$) δ 7.89 – 7.83 (m, 1H), 7.83 – 7.77 (m, 2H), 7.71 (d, *J* = 8.7 Hz, 1H), 7.54 – 7.43 (m, 2H), 7.23 – 7.13 (m, 3H), 6.87 – 6.80 (m, 2H), 3.81 (s, 3H), 2.35 – 2.16 (m, 2H), 1.71 (s, 3H), 0.79 (t, *J* = 7.3 Hz, 3H); ^{13}C NMR (101 MHz, $CDCl_3$) δ 157.5, 147.2, 141.8, 133.2, 131.8, 128.6, 128.1, 127.6, 127.5, 127.3, 125.9, 125.5, 124.8, 113.3, 55.3, 46.1, 34.0, 27.1, 9.4; FTIR (NaCl/thin film) 3055, 2967, 2932, 2876, 1511, 1463, 1441, 1298, 1248, 1182, 1034, 852, 745 cm^{-1}; HRMS (CI+) $[M+H]^+$ calculated for $C_{21}H_{23}O$: 291.1749, found: 291.1768.

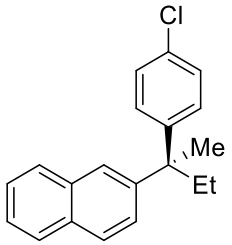

(*R*)-2-(2-(4-Chlorophenyl)butan-2-yl)naphthalene ((*R*)-2.27). Prepared via General Procedure A using **2.19** (prepared in 95% ee) as a colorless oil (run 1: 62.1 mg, 53%; run 2: 70.4 mg, 60%). The enantiomeric excess was determined to be 92% (run 1: 92% ee; run 2: 92% ee) by chiral SFC analysis (CHIRALCEL OJ-H (25 x 0.46 cm), 3.0 mL/min, 15% EtOH(0.1% diethylamine)/CO_2 (100 bar), λ=220 nm); t_R(major) = 6.18 min, t_R(minor) = 6.97 min. $[\alpha]_D^{24}$ = +10.8° (c 1.66, $CHCl_3$): ^{1}H NMR (600 MHz, $CDCl_3$) δ 7.86 (d, *J* = 8.0 Hz, 1H), 7.85 – 7.79 (m, 2H), 7.73 (d, *J* = 8.7 Hz, 1H), 7.55 – 7.45 (m, 2H), 7.31 – 7.25 (m, 2H), 7.20 – 7.13 (m, 3H), 2.35 – 2.19 (m, 2H), 1.72 (s, 3H), 0.80 (t, *J* = 7.4 Hz, 3H); ^{13}C NMR (151 MHz, $CDCl_3$) δ 148.3, 146.4, 133.3, 131.9, 131.6, 129.1, 128.2, 128.1, 127.8, 127.5, 127.0, 126.1, 125.7, 125.0, 46.6, 33.9, 26.9, 9.3; FTIR (NaCl/thin film) 3055, 2969, 2934, 2887, 1599, 1489, 1092, 1012, 817, 746, 477 cm^{-1}; HRMS (EI+) [M]+ calculated for $C_{20}H_{19}Cl$ 294.1775, found: 294.1189.

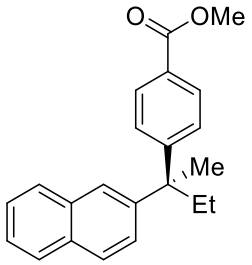

(*R*)-Methyl-4-(2-(naphthalen-2-yl)butan-2-yl)benzoate ((*R*)-2.28). Prepared via General Procedure A using **2.19** (prepared in 96% ee) except that 3.0 equiv of **2.21** were used and the reaction mixture was heated at 60 °C for 12 h. Compound **2.28** was obtained as a colorless oil (run 1: 114.5 mg, 90%; run 2: 105.6 mg, 83%). The enantiomeric excess was determined to be 96% (run 1: 96% ee, run 2: 96% ee) by chiral HPLC analysis (CHIRALPAK IC, 0.6 mL/min, 1% *i*-PrOH/hexane, λ=254 nm); t_R(major) = 30.604 min, t_R(minor) = 33.299 min. $[\alpha]_D^{24}$ = +8.1° (c 1.23, $CHCl_3$): ^{1}H NMR (600 MHz, $CDCl_3$) δ 7.98 – 7.90 (m, 2H), 7.85 – 7.81 (m, 1H), 7.81 – 7.76 (m, 2H), 7.69 (d, *J* = 8.7 Hz, 1H), 7.51 – 7.41 (m, 2H), 7.34 – 7.28 (m, 2H), 7.12 (dd, *J* = 8.6, 1.9 Hz, 1H), 3.90 (s, 3H), 2.34 – 2.22 (m, 2H), 1.72 (s, 3H), 0.77 (t, *J* = 7.4 Hz, 3H); ^{13}C NMR (151 MHz, $CDCl_3$) δ 167.2, 155.1, 146.2, 133.3, 131.9, 129.4, 128.1, 127.84, 127.75, 127.7, 127.6, 127.0, 126.1, 125.8, 125.0, 52.1, 47.2, 33.8, 26.8, 9.3; FTIR (NaCl/thin film) 3055, 2969, 2878, 1718, 1608, 1435, 1279, 1188, 1115, 1018, 854, 819, 747, 477 cm^{-1}; HRMS (CI+) $[M+H]^+$ calculated for $C_{22}H_{23}O_2$: 319.1698, found: 319.1708.

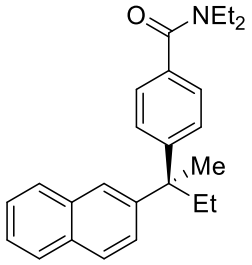

(*R*)-*N*,*N*-Diethyl-4-(2-(naphthalen-2-yl)butan-2-yl)benzamide ((*R*)-2.29). Prepared via General Procedure A using **2.21** (prepared in 96% ee) except that the reaction mixture was heated at 60 °C for 12 h. Compound **2.29** was obtained as white solid (mp 96−100 °C; run 1: 125 mg, 87%; run 2: 122 mg, 85%). The enantiomeric excess was determined to be 94% (run 1: 94% ee, run 2: 94% ee) by chiral HPLC analysis (CHIRALPAK IA, 0.8 mL/min, 8% *i*-PrOH/hexane, λ=254 nm); t_R(major) = 11.038 min, t_R(minor) = 10.179 min. $[\alpha]_D^{24}$ = +18.9° (c 1.16, $CHCl_3$): ^{1}H NMR (600 MHz, $CDCl_3$) δ 7.82 (d, *J* = 8.0 Hz, 1H), 7.80 – 7.76 (m, 2H), 7.69 (d, *J* = 8.7 Hz, 1H), 7.50 – 7.42 (m, 2H), 7.29 (d, *J* = 8.1 Hz, 2H), 7.24 (d, *J* = 8.4 Hz, 2H), 7.15 (dd, *J* = 8.7, 1.9 Hz, 1H), 3.54 (br s, 2H), 3.28 (br s, 2H), 2.33 – 2.18 (m, *J* = 7.1 Hz, 2H), 1.70 (s, 3H), 1.23 (br s, 3H), 1.12 (br s, 3H), 0.77 (t, *J* = 7.3 Hz, 3H); ^{13}C NMR (151 MHz, $CDCl_3$) δ 171.5, 150.9, 146.5, 134.6, 133.2, 131.9, 128.1, 127.7, 127.6, 127.5, 127.2, 126.3, 126.0, 125.7, 125.1, 46.9, 43.4, 39.3, 33.8, 26.9, 14.4, 13.0, 9.3; FTIR (NaCl/thin film) 3053, 2970, 2934, 2876, 1630, 1457, 1424, 1288, 1098, 1019, 819, 748, 478 cm^{-1}; HRMS (CI+) $[M+H]^+$ calculated for $C_{25}H_{30}NO$: 360.2327, found: 360.2347.

X-ray quality crystals were obtained from slow evaporation of **2.29** in EtOAc. The crystal structure demonstrates that the absolute configuration is *R* (Figure S1). The enantiomeric excess of the crystal was determined to be 96% ee by chiral HPLC analysis, with the major enantiomer matching that of the bulk material isolated as described above.

Figure 2.3. Molecular Diagram of (*R*)-**2.29** with Ellipsoids at 50% Probability. H-atoms Omitted for Clarity. (CCDC 1424635)

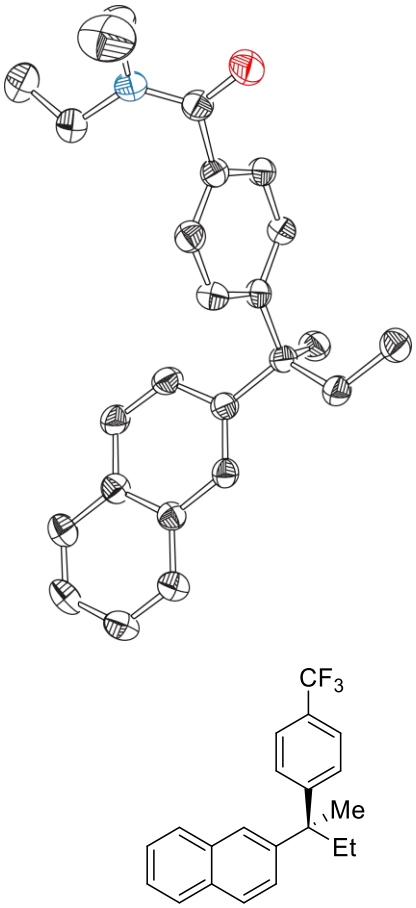

(*R*)-2-(2-(4-(Trifluoromethyl)phenyl)butan-2-yl)naphthalene ((*R*)-2.30). Prepared via General Procedure A using **2.19** (prepared in 96% ee) as a colorless oil (117 mg, 89%). The enantiomeric excess was determined to be 96% by chiral HPLC analysis (CHIRALPAK IB, 0.2 mL/min, 0% *i*-PrOH/hexane, λ=210 nm); t_R(major) = 39.173 min, t_R(minor) = 35.980 min. A second run using **2.19** (prepared in 95% ee) gave **2.30** (95 mg, 72%) in 95% ee. $[\alpha]_D^{24}$ = +9.9° (c 1.1, $CHCl_3$): ^{1}H NMR (400 MHz, $CDCl_3$) δ 7.91 – 7.84 (m, 1H), 7.84 – 7.79 (m, 2H), 7.73 (d, *J* = 8.6 Hz, 1H), 7.58 – 7.45 (m, 4H), 7.35 (d, *J* = 8.2 Hz, 2H), 7.13 (dd, *J* = 8.7, 1.9 Hz, 1H), 2.38 – 2.21 (m, 2H), 1.74 (s, 3H), 0.79 (t, *J* = 7.4 Hz, 3H); ^{13}C NMR (101 MHz, $CDCl_3$) δ 153.9, 145.9, 133.2, 131.9, 128.1, 128.02 (q, J_{C-F} = 32.9 Hz), 128.0, 127.9, 127.6, 126.9, 126.2, 125.8, 125.1,

125.0 (q, J_{C-F} = 3.8 Hz), 124.4 (q, J_{C-F} = 272.9 Hz), 47.0, 33.8, 26.8, 9.25; ^{19}F NMR (377 MHz, $CDCl_3$) δ –62.2; FTIR (NaCl/thin film) 3057, 2971, 2937, 2880, 1921, 1617, 1504, 1409, 1325, 1273, 1122, 1068, 1016, 948, 841, 748 cm^{-1}; HRMS (EI+) [M]+ calculated for $C_{21}H_{19}F_3$: 328.1439, found: 328.1447.

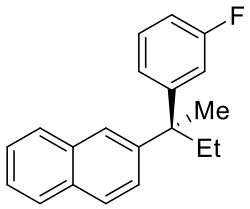

(*S*)-2-(2-(3-Fluorophenyl)butan-2-yl)naphthalene ((*S*)-2.31). Prepared via General Procedure A using **2.19** (prepared in 96% ee) as a colorless oil (run 1: 103.5 mg, 93%; run 2: 106.4 mg, 96%). The enantiomeric excess was determined to be 94% (run 1: 94% ee; run 2: 94% ee) by chiral SFC analysis (CHIRALCEL OJ-H (25 x 0.46 cm), 3.0 mL/min, 8% EtOH(0.1% diethylamine)/CO_2 (100 bar), λ=220 nm); t_R(major) = 5.22 min, t_R(minor) = 5.57 min. $[\alpha]_D^{24}$ = +7.5° (c 1.19, $CHCl_3$): ^{1}H NMR (600 MHz, $CDCl_3$) δ 7.83 (d, *J* = 7.9 Hz, 1H), 7.81 – 7.75 (m, 2H), 7.70 (d, *J* = 8.7 Hz, 1H), 7.52 – 7.41 (m, 2H), 7.21 (td, *J* = 8.0, 6.3 Hz, 1H), 7.15 (dd, *J* = 8.7, 1.9 Hz, 1H), 6.98 (dt, *J* = 8.0, 1.2 Hz, 1H), 6.95 (dt, *J* = 11.1, 2.2 Hz, 1H), 6.87 (td, *J* = 8.5, 2.7 Hz, 1H), 2.32 – 2.17 (m, 2H), 1.70 (s, 3H), 0.77 (t, *J* = 7.3 Hz, 3H); ^{13}C NMR (151 MHz, $CDCl_3$) δ 162.9 (d, J_{C-F} = 245 Hz), 152.6 (d, J_{C-F} = 6.4 Hz), 146.3, 133.3, 131.9, 129.4 (d, J_{C-F} = 8.2 Hz), 128.1, 127.8, 127.5, 127.0, 126.1, 125.7, 125.0, 123.4 (d, J_{C-F} = 2.7 Hz), 114.7 (d, J_{C-F} = 21.7 Hz), 112.7 (d, J_{C-F} = 21.2 Hz), 46.8 (d, J_{C-F} = 1.5 Hz), 33.8, 26.8, 9.3; ^{19}F NMR (565 MHz, $CDCl_3$) δ –113.6; FTIR (NaCl/thin film) 3056, 2970, 2878, 1612, 1585, 1485, 1433, 1243, 1163, 917, 818, 783, 477 cm^{-1}; HRMS (EI+) [M]+ calculated for $C_{20}H_{19}F$: 278.1471, found: 278.1479.

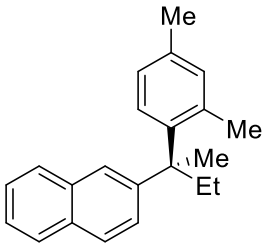

(*S*)-2-(2-(2,4-Dimethylphenyl)butan-2-yl)naphthalene ((*S*)-2.32). Prepared via General Procedure A using **2.19** (prepared in 96% ee) as a colorless oil (run 1: 103.8 mg, 90%; run 2: 100.4 mg, 87%). The enantiomeric excess was determined to be 95% (run 1: 95% ee; run 2: 95% ee) by chiral SFC analysis (CHIRALCEL OJ-H (25 x 0.46 cm), 3.0 mL/min, 8% EtOH(0.1% diethylamine)/CO_2 (100 bar), λ=220 nm); t_R(major) = 7.83 min, t_R(minor) = 8.59 min. $[\alpha]_D^{24} = -16.3°$ (c 1.02, $CHCl_3$): ^{1}H NMR (400 MHz, $CDCl_3$) δ 7.84 – 7.75 (m, 2H), 7.73 (d, *J* = 1.9 Hz, 1H), 7.67 (d, *J* = 8.6 Hz, 1H), 7.45 (dtd, *J* = 14.9, 7.5, 7.0, 5.4 Hz, 3H), 7.15 (dd, *J* = 8.6, 1.9 Hz, 1H), 7.11 – 7.06 (m, 1H), 6.91 – 6.85 (m, 1H), 2.46 – 2.30 (m, 4H), 2.27 – 2.14 (m, 1H), 1.71 (s, 3H), 1.68 (s, 3H), 0.71 (t, *J* = 7.3 Hz, 3H); ^{13}C NMR (101 MHz, $CDCl_3$) δ 148.2, 142.8, 137.2, 135.7, 133.5, 133.4, 131.7, 128.0, 127.7, 127.6, 127.5, 126.3, 126.1, 125.8, 125.3, 124.2, 46.9, 32.8, 28.0, 21.9, 20.9, 9.5; FTIR (NaCl/thin film) 3054, 2969, 2934, 2876 1630, 1598, 1502, 1455, 1376, 1265, 1130, 1040, 948, 894, 769, 476 cm^{-1}; HRMS (EI+) [M]+ calculated for $C_{22}H_{24}$: 288.1878, found: 288.1896.

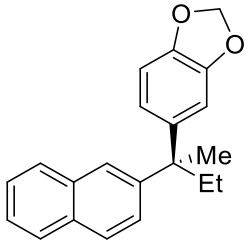

(*S*)-5-(2-(Naphthalen-2-yl)butan-2-yl)benzo-[1,3]-dioxole ((*S*)-2.33). Prepared via General Procedure A using **2.19** (prepared in 95% ee) as a colorless oil (run 1: 110 mg, 90%; run 2: 100 mg, 82%). The enantiomeric excess was determined to

be 92% (run 1: 92% ee; run 2: 92% ee) by chiral SFC analysis (CHIRALCEL OJ-H (25 x 0.46 cm), 3.0 mL/min, 30% EtOH(0.1% diethylamine)/CO_2 (100 bar), λ=220 nm); t_R(major) = 4.19 min, t_R(minor) = 4.93 min. $[\alpha]_D^{24}$ = +3.9° (c 4.57, $CHCl_3$): ^{1}H NMR (600 MHz, $CDCl_3$) δ 7.83 (dd, *J* = 8.0, 1.5 Hz, 1H), 7.81 – 7.77 (m, 2H), 7.70 (d, *J* = 8.7 Hz, 1H), 7.50 – 7.41 (m, 2H), 7.19 (dd, *J* = 8.7, 1.9 Hz, 1H), 6.74 (d, *J* = 1.3 Hz, 2H), 6.70 – 6.65 (m, 1H), 5.91 (s, 2H), 2.31 – 2.14 (m, 2H), 1.67 (s, 3H), 0.78 (t, *J* = 7.3 Hz, 3H); ^{13}C NMR (151 MHz, $CDCl_3$) δ 147.6, 147.1, 145.4, 143.8, 133.3, 131.9, 128.1, 127.7, 127.5, 127.1, 126.0, 125.6, 124.8, 120.4, 108.7, 107.6, 100.9, 46.6, 34.1, 27.1, 9.4; FTIR (NaCl/thin film) 3055, 2968, 2933, 2877, 1631, 1599, 1485, 1430, 1235, 1039, 938, 817, 746 cm^{-1}; HRMS (EI+) [M]+ calculated for $C_{21}H_{20}O$: 304.1463 found: 304.1482.

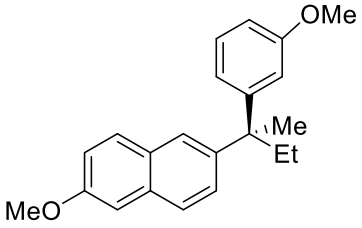

(*S*)-2-Methoxy-6-(2-(3-methoxyphenyl)butan-2-yl)naphthalene ((*S*)-2.34). Prepared via General Procedure A using **2.19a** (prepared in 92% ee) as a colorless sticky oil (run 1: 120 mg, 94%; run 2: 124.9 mg, 98%). The enantiomeric excess was determined to be 90% (run 1: 90% ee; run 2: 89% ee) by chiral HPLC analysis (CHIRALPAK IB, 0.6 mL/min, 0.1% *i*-PrOH/hexane, λ=254 nm); t_R(major) = 16.688 min, t_R(minor) = 18.948 min. $[\alpha]_D^{24}$ = +7.7° (c 4.28, $CHCl_3$): ^{1}H NMR (600 MHz, $CDCl_3$) δ 7.75 – 7.69 (m, 2H), 7.59 (d, *J* = 8.6 Hz, 1H), 7.21 – 7.12 (m, 3H), 7.10 (d, *J* = 2.5 Hz, 1H), 6.84 – 6.79 (m, 2H), 6.75 – 6.70 (m, 1H), 3.91 (s, 3H), 3.75 (s, 3H), 2.30 – 2.18 (m, 2H), 1.68 (s, 3H), 0.77 (t, *J* = 7.4 Hz, 3H); ^{13}C NMR (151 MHz, $CDCl_3$) δ 159.4, 157.6, 151.7, 144.6, 132.9, 129.6, 128.9, 128.7, 127.7, 126.6, 124.8, 120.4, 118.6,

114.3, 110.2, 105.7, 55.5, 55.2, 46.7, 33.9, 26.9, 9.4; FTIR (NaCl/thin film) 3057, 2967, 2936, 2834, 1609, 1488, 1456, 1388, 1264, 1198, 1032, 852, 779 cm^{-1}; HRMS (CI+) $[M+H]^+$ calculated for $C_{22}H_{25}O$: 321.1855, found: 321.1859.

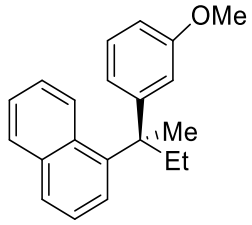

(*R*)-1-(2-(3-Methoxyphenyl)butan-2-yl)naphthalene ((*R*)-2.35). Prepared via General Procedure A using **2.19b** (prepared in 90% ee), except on a 0.30 mmol scale. Product **2.35** was isolated as a colorless sticky oil (58.6 mg, 67%). The enantiomeric excess was determined to be 88% by chiral HPLC analysis (CHIRALPAK IB, 0.6 mL/min, 0.1% *i*-PrOH/hexane, λ=254 nm); t_R(major) = 11.227 min, t_R(minor) = 14.389 min. A duplicate run was performed via General Procedure A using **2.19b** (prepared in 84% ee), except on a 0.3 mmol scale, to give **2.35** as a colorless oil (70.1 mg, 80%) in 83% ee. $[\alpha]_D^{24}$ = +17.1° (c 3.09, $CHCl_3$): ^{1}H NMR (600 MHz, $CDCl_3$) δ 7.81 – 7.77 (m, 1H), 7.75 (d, *J* = 8.1 Hz, 1H), 7.66 (dd, *J* = 7.3, 1.2 Hz, 1H), 7.56 (d, *J* = 8.8 Hz, 1H), 7.48 (t, *J* = 7.7 Hz, 1H), 7.30 (ddd, *J* = 8.0, 6.7, 1.1 Hz, 1H), 7.16 – 7.08 (m, 2H), 6.84 – 6.80 (m, 1H), 6.80 – 6.75 (m, 1H), 6.71 – 6.66 (m, 1H), 3.71 (s, 3H), 2.52 (dq, *J* = 14.6, 7.4 Hz, 1H), 2.25 (dq, *J* = 13.0, 7.3 Hz, 1H), 1.73 (s, 3H), 0.58 (t, *J* = 7.3 Hz, 3H); ^{13}C NMR (151 MHz, $CDCl_3$) δ 159.7, 153.1, 143.3, 135.0, 131.6, 129.3, 129.0, 127.9, 127.3, 125.3, 124.9, 124.8, 124.7, 119.4, 113.1, 110.0, 55.2, 47.5, 33.6, 29.4, 9.4; FTIR (NaCl/thin film) 3048, 2969, 2936, 2833, 1604, 1580, 1485, 1289, 1043, 877, 777, 705 cm^{-1}; HRMS (CI+) $[M+H]^+$ calculated for $C_{21}H_{23}O$: 291.1749, found: 291.1747.

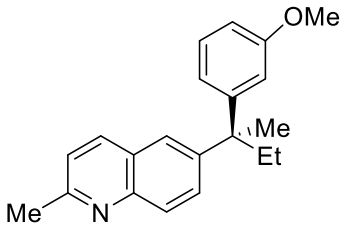

(*S*)-6-(2-(3-Methoxyphenyl)butan-2-yl)-2-methylquinoline ((*S*)-2.36). Prepared via General Procedure A using **2.19c** (prepared in 99% ee), except that **2.20** (133 mg, 0.332 mmol, 0.83 equiv.) was used in place of **2.21** and the reaction mixture was heated at 60 °C. Product **2.36** was isolated as a pale yellow oil (run 1: 91 mg, 74%; run 2: 102.9 mg, 84%). The enantiomeric excess was determined to be 97% (run 1: 97% ee; run 2: 97% ee) by chiral HPLC analysis (CHIRALPAK IA, 1.0 mL/min, 5% *i*-PrOH/hexane, λ=254 nm); t_R(major) = 8.758 min, t_R(minor) = 9.969 min. $[\alpha]_D^{24}$ = +5.7° (c 3.68, $CHCl_3$): ^{1}H NMR (600 MHz, $CDCl_3$) δ 8.01 (d, *J* = 8.4 Hz, 1H), 7.86 (d, *J* = 8.8 Hz, 1H), 7.68 (d, *J* = 2.1 Hz, 1H), 7.40 (dd, *J* = 8.8, 2.2 Hz, 1H), 7.29 – 7.24 (m, 1H), 7.19 (t, *J* = 7.9 Hz, 1H), 6.82 – 6.76 (m, 2H), 6.75 – 6.69 (m, 1H), 3.74 (s, 3H), 2.73 (s, 3H), 2.30 – 2.16 (m, 2H), 1.68 (s, 3H), 0.76 (t, *J* = 7.3 Hz, 3H); ^{13}C NMR (151 MHz, $CDCl_3$) δ 159.5, 158.6, 151.1, 146.9, 146.6, 136.4, 130.7, 129.0, 128.3, 126.1, 124.5, 122.0, 120.3, 114.3, 110.4, 55.2, 46.8, 33.9, 26.9, 25.4, 9.3; FTIR (NaCl/thin film) 3053, 2968, 2936, 2833, 1599, 1488, 1431, 1291, 1254, 1173, 1052, 837, 703 cm^{-1}; HRMS (LIFDI) [M]+ calculated for $C_{21}H_{23}NO$: 305.1780, found: 305.1759.

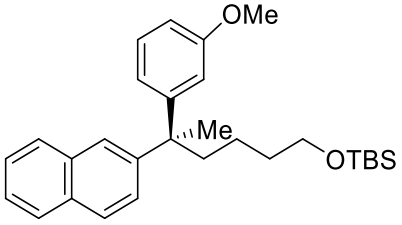

(*S*)-*tert*-Butyl((5-(3-methoxyphenyl)-5-(naphthalen-2-yl)hexyl)oxy)dimethylsilane ((*S*)-2.37). Prepared via General Procedure A using **2.19**d

(prepared in 99% ee) as a colorless sticky oil (159.8 mg, 89%). The enantiomeric excess was determined to be 99% by chiral HPLC analysis (CHIRALPAK IB, 0.4 mL/min, 100% hexane, λ=254 nm); t_R(major) = 33.672 min, t_R(minor) = 26.337 min. $[\alpha]_D^{24}$ = −11.0° (c 5.22, $CHCl_3$): ^{1}H NMR (600 MHz, $CDCl_3$) δ 7.82 (d, *J* = 8.0 Hz, 1H), 7.80 – 7.75 (m, 2H), 7.68 (d, *J* = 8.6 Hz, 1H), 7.45 (dddd, *J* = 19.3, 8.1, 6.8, 1.4 Hz, 2H), 7.21 – 7.15 (m, 2H), 6.83 – 6.78 (m, 2H), 6.75 – 6.70 (m, 1H), 3.75 (s, 3H), 3.55 (t, *J* = 6.6 Hz, 2H), 2.26 – 2.15 (m, 2H), 1.72 (s, 3H), 1.56 – 1.49 (m, 2H), 1.22 – 1.09 (m, 2H), 0.84 (s, 9H), –0.01 (s, 6H); ^{13}C NMR (151 MHz, $CDCl_3$) δ 159.4, 151.6, 147.0, 133.3, 131.9, 129.0, 128.1, 127.7, 127.5, 127.1, 125.9, 125.5, 124.7, 120.3, 114.2, 110.3, 63.2, 55.2, 46.6, 41.4, 33.7, 27.6, 26.1, 21.3, 18.4, –5.1; FTIR (NaCl/thin film) 3055, 2934, 2856, 1606, 1470, 1255, 1099, 1046, 836, 775, 705, 476 cm^{-1}; HRMS (LIFDI) [M]+ calculated for $C_{29}H_{40}O_2Si$: 448.2798, found: 448.2790.

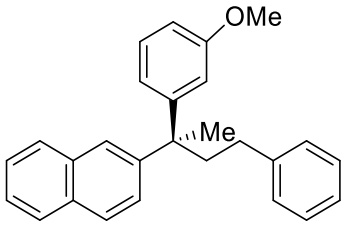

(*S*)-2-(2-(3-Methoxyphenyl)-4-phenylbutan-2-yl)naphthalene ((*S*)-2.38). Prepared via General Procedure A using **2.19e** (prepared in 94% ee), except that the reaction was run for 48 h. Product **2.38** was obtained as a colorless oil (run 1: 171.5 mg, 90%; run 2: 137.8 mg, 94%). The enantiomeric excess was determined to be 94% (run1: 94% ee; run 2: 94% ee) by chiral HPLC analysis (CHIRALPAK IB, 0.8 mL/min, 100% hexane, λ=210 nm); t_R(major) = 34.901 min, t_R(minor) = 31.785 min. [ ]$_D^{24}$ = −25.9° (c 4.54, $CHCl_3$): ^{1}H NMR (600 MHz, $CDCl_3$) δ 7.87 − 7.83 (m, 2H), 7.81 (dd, *J* = 7.8, 1.5 Hz, 1H), 7.73 (d, *J* = 8.7 Hz, 1H), 7.52 − 7.44 (m, 2H), 7.29 (t, *J* = 7.6 Hz, 2H), 7.25 – 7.17 (m, 3H), 7.17 – 7.13 (m, 2H), 6.88 – 6.85 (m, 2H), 6.76 (ddd, *J* = 8.3, 2.4, 1.0

Hz, 1H), 3.76 (s, 3H), 2.59 – 2.49 (m, 2H), 2.49 – 2.37 (m, 2H), 1.84 (s, 3H); ^{13}C NMR (151 MHz, $CDCl_3$) δ 159.6, 151.1, 146.6, 143.0, 133.3, 132.0, 129.1, 128.51, 128.50, 128.2, 127.9, 127.5, 127.0, 126.1, 125.9, 125.7, 124.8, 120.2, 114.2, 110.5, 55.3, 46.7, 43.9, 31.5, 27.5; FTIR (NaCl/thin film) 3056, 3024, 2946, 2867, 1600, 1283, 1494, 1291, 1047, 908, 818, 760 cm^{-1}; HRMS (EI+) [M]+ calculated for $C_{27}H_{26}O$: 366.1984, found: 366.1967.

Please note: The absolute configuration of **2.38** is tentatively assigned. The absolute configuration resulting from the method used in the preparation of its alcohol precursor **S-2.19e** has not been reported in the literature. Please see the experimental for **S-2.19e** below.

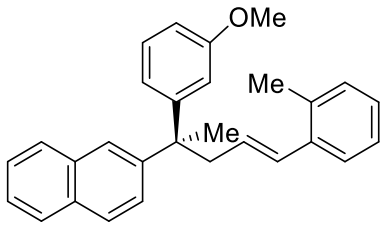

***(E)*-2-(2-(3-Methoxyphenyl)-5-(*o*-tolyl)pent-4-en-2-yl)naphthalene (2.39).** Prepared via General Procedure A using **2.19f** (prepared in 96% ee), except that **2.20** (133 mg, 0.332 mmol, 0.83 equiv.) was used in place of **2.21**. Product **2.39** was isolated as a colorless sticky oil (run 1: 125.6 mg, 80%; run 2: 119.7 mg, 76%). The enantiomeric excess was determined to be 95% (run 1: 95% ee; run 2: 94% ee) by chiral HPLC analysis (CHIRALPAK IC, 0.6 mL/min, 0.1% hexane, λ=210 nm); t_R(major) = 13.480 min, t_R(minor) = 15.096 min. $[\alpha]_D^{24}$ = +3.7° (c 4.84, $CHCl_3$): ^{1}H NMR (600 MHz, $CDCl_3$) δ 7.85 – 7.81 (m, 2H), 7.81 – 7.76 (m, 1H), 7.71 (d, *J* = 8.6 Hz, 1H), 7.50 – 7.42 (m, 2H), 7.24 (dd, *J* = 8.7, 2.0 Hz, 1H), 7.20 (t, *J* = 7.9 Hz, 1H), 7.17 (d, *J* = 7.3 Hz, 1H), 7.10 – 7.01 (m, 3H), 6.88 – 6.82 (m, 2H), 6.77 – 6.72 (m, 1H), 6.57 (d, *J* = 15.6 Hz, 1H), 5.76 (dt, *J* = 15.6, 7.2 Hz, 1H), 3.74 (s, 3H), 3.21 – 3.10 (m, 2H), 2.20 (s, 3H),

1.76 (s, 3H); ^{13}C NMR (151 MHz, $CDCl_3$) δ 159.5, 151.0, 146.5, 137.1, 135.1, 133.3, 132.0, 131.1, 130.1, 129.1, 128.5, 128.2, 127.8, 127.5, 127.1, 127.0, 126.04, 126.02, 125.9, 125.7, 124.8, 120.3, 114.2, 110.6, 55.3, 46.8, 45.6, 27.7, 19.8; FTIR (NaCl/thin film) 3054, 2965, 2933, 1599, 1485, 1431, 1258, 1047, 967, 818, 754 cm^{-1}; HRMS (LIFDI) [M]+ calculated for $C_{29}H_{28}O$: 392.2140, found: 392.2137.

Please note: The absolute configuration of **2.39** is tentatively assigned. The absolute configuration resulting from the method used in the preparation of its acetate precursor **2.19f** has not been reported in the literature. Please see the experimental for **2.19f** below.

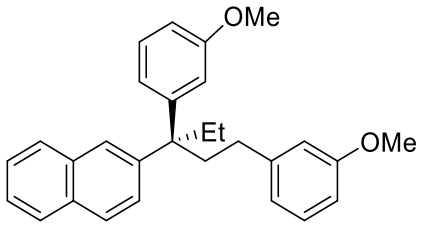

(*S*)-2-(1,3-Bis(3-methoxyphenyl)pentan-3-yl)naphthalene ((*S*)-2.40). Prepared via General Procedure A using **2.19g** (prepared in 89% ee), except that **2.20** (133 mg, 0.332 mmol, 0.83 equiv.) was used in place of **2.21**. Product **2.40** was isolated as a colorless sticky oil (127 mg, 77%). The enantiomeric excess was determined to be 87% by chiral SFC analysis (CHIRALCEL OJ-H(25 x 0.46 cm), 3.0 mL/min, 20% MeOH (0.1% diethylamine)/CO_2 (100 bar), λ=220 nm); t_R(major) = 9.10 min, t_R(minor) = 7.81 min. A duplicate experiment was conducted with **2.19g** (prepared in 87% ee) to give **22** (103 mg, 63%) in 86% ee. $[\alpha]_D^{24} = -30.5°$ (c 3.04, $CHCl_3$): ^{1}H NMR (600 MHz, $CDCl_3$) δ 7.87 – 7.81 (m, 2H), 7.78 (d, *J* = 7.8 Hz, 1H), 7.68 (d, *J* = 8.7 Hz, 1H), 7.51 – 7.41 (m, 2H), 7.19 (td, *J* = 7.9, 4.1 Hz, 2H), 7.14 (dd, *J* = 8.7, 1.9 Hz, 1H), 6.86 – 6.81 (m, 2H), 6.77 – 6.67 (m, 3H), 6.65 – 6.61 (m, 1H), 3.78 (s, 3H), 3.75 (s, 3H), 2.50 – 2.44 (m, 2H), 2.36 – 2.22 (m, 4H), 0.75 (t, *J* = 7.3 Hz, 3H); ^{13}C NMR (151 MHz, $CDCl_3$)

δ 159.8, 159.4, 150.1, 145.7, 144.8, 133.2, 131.9, 129.5, 128.9, 128.2, 127.7, 127.51, 127.48, 126.0, 125.6, 125.5, 120.93, 120.92, 114.9, 114.4, 111.0, 110.4, 55.29, 55.28, 50.0, 38.9, 30.9, 29.5, 8.6; FTIR (NaCl/thin film) 3054, 2955, 2833, 1600, 1487, 1257, 1153, 1050, 908, 813, 782 cm^{-1}; HRMS (LIFDI) [M]+ calculated for $C_{29}H_{30}O_2$: 410.2246, found: 410.2238.

Please note: The absolute configuration of **2.40** is tentatively assigned. The absolute configuration resulting from the method used in the preparation of its alcohol precursor **S-2.19g** has not been reported in the literature. Please see the experimental for **S-2.19g** below.

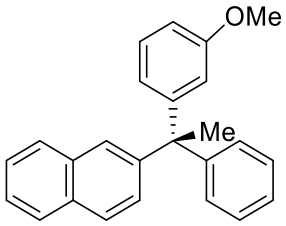

(*R*)-2-(1-(3-Methoxyphenyl)-1-phenylethyl)naphthalene ((*R*)-2.41). Prepared via General Procedure A using **2.19h** (prepared in 96% ee) as a colorless oil (run 1: 95 mg, 70%; run 2: 101 mg, 75%). The enantiomeric excess was determined to be 94% (run 1: 94%; run 2: 94%) by chiral HPLC analysis (CHIRALPAK IB, 0.2 mL/min, 0.1% hexane, λ=210 nm); t_R(major) = 49.084 min, t_R(minor) = 52.102 min. $[\alpha]_D^{24}$ = +15.0° (c 0.86, $CHCl_3$): ^{1}H NMR (600 MHz, $CDCl_3$) δ 7.82 – 7.79 (m, 1H), 7.74 (d, *J* = 8.7 Hz, 1H), 7.72 – 7.67 (m, 1H), 7.49 – 7.41 (m, 3H), 7.32 (dd, *J* = 8.6, 2.0 Hz, 1H), 7.28 (t, *J* = 7.4 Hz, 2H), 7.25 – 7.19 (m, 2H), 7.19 – 7.14 (m, 2H), 6.81 – 6.74 (m, 2H), 6.72 (t, *J* = 2.1 Hz, 1H), 3.72 (s, 3H), 2.27 (s, 3H); ^{13}C NMR (151 MHz, $CDCl_3$) δ 159.4, 150.6, 148.8, 146.5, 133.2, 132.0, 130.6, 128.94, 128.91, 128.3, 128.1, 127.8, 127.5, 127.0, 126.2, 126.0, 125.9, 121.7, 115.6, 110.9, 55.3, 52.9, 30.6; FTIR (NaCl/thin

film) 3055, 2978, 2934, 2833, 1597, 1487, 1256, 1044, 820, 745, 701 cm^{-1}; HRMS (CI+) $[M+H]^+$ calculated for $C_{25}H_{23}O$: 339.1749, found: 339.1742.

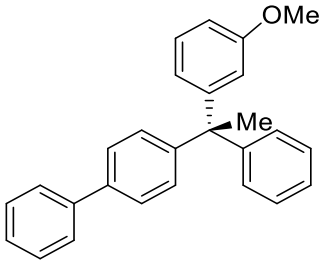

(*R*)-4-(1-(3-Methoxyphenyl)-1-phenylethyl)-1,1'-biphenyl ((*R*)-2.42). Prepared via General Procedure A using **2.19i** (prepared as 91% ee), except with 10 mol % $NiCl_2$·DME, 10 mol % CyJohnPhos, 60 °C, 48 h. Product **2.42** was isolated as a colorless oil (run 1: 84.4 mg, 58%; run 2: 96.2 mg, 66%). The enantiomeric excess was determined to be 91% (run 1: 91% ee; run 2: 91% ee) by chiral HPLC analysis (CHIRALPAK IB, 0.6 mL/min, 0.1% hexane, λ=254 nm); t_R(major) = 18.913 min, t_R(minor) = 18.288 min. $[\alpha]_D^{24}$ = +31.5° (c 1.68, $CHCl_3$): ^{1}H NMR (600 MHz, $CDCl_3$) δ 7.60 (dd, *J* = 8.1, 1.4 Hz, 2H), 7.54 – 7.48 (m, 2H), 7.43 (t, *J* = 7.7 Hz, 2H), 7.35 – 7.31 (m, 1H), 7.29 (dd, *J* = 8.4, 6.9 Hz, 2H), 7.22 (td, *J* = 7.6, 4.0 Hz, 2H), 7.20 – 7.14 (m, 4H), 6.80 – 6.73 (m, 2H), 6.71 (t, *J* = 2.1 Hz, 1H), 3.74 (s, 3H), 2.22 (s, 3H); ^{13}C NMR (151 MHz, $CDCl_3$) δ 159.4, 150.8, 149.0, 148.2, 140.9, 138.8, 129.3, 128.90, 128.86, 128.85, 128.0, 127.3, 127.1, 126.6, 126.2, 121.6, 115.6, 110.8, 55.3, 52.5, 30.6; FTIR (NaCl/thin film) 3055, 3028, 2979, 2833, 1598, 1486, 1290, 1254, 1040, 845, 735, 699 cm^{-1}; HRMS (CI+) $[M+H]^+$ calculated for $C_{27}H_{25}O$: 365.1905, found: 365.1907.

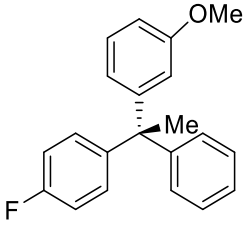

(*R*)-1-(1-(4-Fluorophenyl)-1-phenylethyl)-3-methoxybenzene ((*R*)-2.46). Prepared via General Procedure A using **2.19j** (prepared as 90% ee), except with 10 mol % $NiCl_2$·DME, 25 mol % $PCy_2(o\text{-}MeC_6H_4)$, 60 °C, 48 h. Product **2.46** was isolated as a colorless oil (run 1: 89.4 mg, 73%; run 2: 84.6 mg, 69%). The enantiomeric excess was determined to be 76% (run 1: 77% ee; run 2: 74% ee) by chiral HPLC analysis (CHIRALPAK IB, 0.6 mL/min, 0.1% hexane, λ=254 nm); t_R(major) = 13.431 min, t_R(minor) = 14.101 min. $[\alpha]_D^{24}$ = +2.61° (c 0.88, $CHCl_3$): ^{1}H NMR (400 MHz, $CDCl_3$) δ 7.32 – 7.17 (m, 1H), 7.12 – 7.03 (m, 1H), 6.95 (t, *J* = 8.7 Hz, 1H), 6.77 (ddd, *J* = 8.2, 2.6, 0.8 Hz, 1H), 6.69 (ddd, *J* = 7.8, 1.7, 0.4 Hz, 1H), 6.63 (t, J = 2.2 Hz, 1H), 3.73 (s, 3H), 2.17 (s, 3H); ^{13}C NMR (101 MHz, $CDCl_3$) δ 161.67, 159.23, 158.56, 149.94, 148.06, 144.06 (d, $J_{C\text{-}F}$ = 3.3 Hz), 144.01 (d, $J_{C\text{-}F}$ = 3.3 Hz), 129.67(d, $J_{C\text{-}F}$ = 7.9 Hz), 129.55 (d, $J_{C\text{-}F}$ = 7.9 Hz), 128.19, 127.94, 127.30, 125.49 120.65, 114.71 (d, $J_{C\text{-}F}$ = 21.0 Hz), 114.0 (d, $J_{C\text{-}F}$ = 21.0 Hz), 113.79, 109.99, 54.47, 51.42, 29.96; ^{19}F NMR (377 MHz, $CDCl_3$) δ –117.44; FTIR (NaCl/thin film) 3057, 3029, 2980, 2937, 2834, 1895, 1598, 1507, 1315, 1291, 1164, 1047, 917, 838, 806, 701, 674, 575 cm^{-1}; HRMS (CI+) $[M+H]^+$ calculated for $C_{21}H_{20}OF$: 307.1420, found: 307.1493.

2.4.2.2 General Procedure B: Preparation of (S)-2-(Naphthalen-2-yl)butan-2-yl Acetate (2.19)

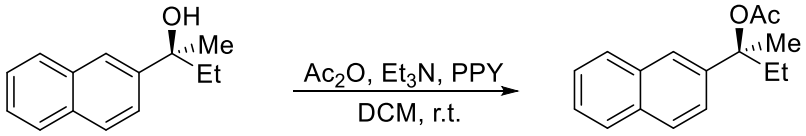

2.18 **2.19**

In an oven-dried 100-mL round-bottomed flask, was placed 2-(naphthalen-2-yl)butan-2-ol (**2.18**, prepared in 96% ee, 1.5 g, 7.5 mmol, 1.0 equiv.), 4-pyrrolidinopyridine (PPY, 168 mg, 1.13 mmol, 0.150 equiv.), and CH_2Cl_2 (25 mL, 0.3

M). Then flask was placed in an ice/water bath. Et_3N (3.1 mL, 23 mmol, 3.0 equiv.) was added, followed by acetic anhydride (1.4 mL, 15 mmol, 2.0 equiv.). The solution was then stirred at room temperature for 14 h. Sat. $NaHCO_3$ (100 mL) was added, and the product was extracted with CH_2Cl_2 (3 x 25 mL). The combined organic layers were washed with sat. NaCl, dried (Na_2SO_4), filtered and concentrated. The crude mixture was purified by silica gel chromatography (0−20% EtOAc/hexanes) to give **2.19** as a viscous oil (1.45 g, 80%). The enantiomeric excess was determined to be 96% by chiral HPLC analysis (CHIRALPAK IB, 1 mL/min, 1% *i*-PrOH/hexane, λ=254 nm); t_R(major) = 8.234 min, t_R(minor) = 6.313 min. $[\alpha]_D^{24}$ = +5.0° (c 3.59, $CHCl_3$): ^{1}H NMR (600 MHz, $CDCl_3$) δ 7.86 – 7.78 (m, 3H), 7.77 – 7.74 (m, 1H), 7.51 – 7.39 (m, 3H), 2.18 – 2.08 (m, 5H), 1.92 (s, 3H), 0.81 (t, *J* = 7.4 Hz, 3H); ^{13}C NMR (151 MHz, $CDCl_3$) δ 169.8, 142.4, 133.2, 132.5, 128.3, 128.1, 127.6, 126.2, 125.9, 123.6, 123.2, 84.6, 35.1, 24.5, 22.4, 8.3; FTIR (NaCl/thin film) 3057, 2977, 2938, 2880, 1734, 1458, 1366, 1246, 1128, 1017, 817, 747, 477 cm^{-1}; HRMS (EI+) [M]+ calculated for $C_{16}H_{18}O_2$: 242.1307, found: 242.1309.

This type of compound decomposed to olefins quickly in pure form at room temperature, but is relatively stable in cold solution. Our suggestion is to immediately dissolve in anhydrous 2-Me-THF and store in fridge under N_2.

A crystal suitable for X-ray diffraction analysis was obtained upon cooling the viscous oil isolated above neat at -35 ^{o} C. The crystal structure demonstrates that the absolute configuration is *S*. (Figure 2.4)

Figure 2.4. Molecular Diagram of (*S*)-**2.19** with Ellipsoids at 50% Probability, H-atoms Omitted for Clarity. (CCDC 1502353)

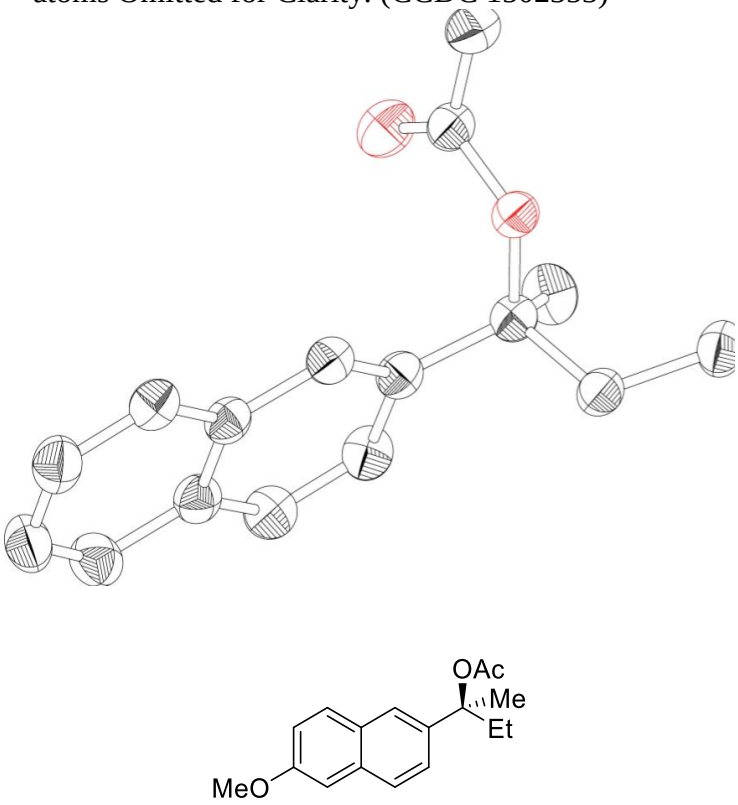

(*S*)-2-(6-Methoxynaphthalen-2-yl)butan-2-yl acetate ((*S*)-2.19a). Prepared via General Procedure B using **2.18a** (prepared as 92% ee) as a colorless oil (75%). The enantiomeric excess was assumed to be 92% based on the starting material (**2.18a**). $[\alpha]_D^{24}$ = +42° (c 1.5, $CHCl_3$): ^{1}H NMR (600 MHz, $CDCl_3$) δ 7.74 – 7.66 (m, 3H), 7.40 (dd, *J* = 8.6, 1.9 Hz, 1H), 7.14 (dd, *J* = 8.8, 2.5 Hz, 1H), 7.11 (d, *J* = 2.5 Hz, 1H), 3.91 (s, 3H), 2.16 – 2.06 (m, 5H), 1.90 (s, 3H), 0.80 (t, *J* = 7.4 Hz, 3H); ^{13}C NMR (151 MHz, $CDCl_3$) δ 169.9, 157.8, 140.1, 133.6, 129.8, 128.7, 126.9, 123.8, 123.5, 119.0, 105.7, 84.7, 55.5, 35.1, 24.5, 22.4, 8.3; FTIR (NaCl/thin film) 2975, 2937, 1734, 1608, 1367, 1247, 1204, 1164, 1031, 850 cm^{-1}; HRMS (CI+) [M]+H calculated for $C_{17}H_{21}O_3$: 273.1491, found: 273.1501.

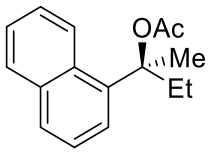

(*S*)-2-(Naphthalen-1-yl)butan-2-yl acetate ((*S*)-2.19b). Prepared via General Procedure B using **2.18b** (90% ee) as a colorless oil (58%). The enantiomeric excess was determined to be 90% by chiral HPLC analysis (CHIRALPAK IB, 0.7 mL/min, 2.0% *i*-PrOH/hexanes, λ=254 nm); t_R(major) = 9.214 min, t_R(minor) = 8.322 min. $[\alpha]_D^{24}$ = +10.2° (c 0.88, $CHCl_3$): ^{1}H NMR (600 MHz, $CDCl_3$) δ 8.55 (dd, *J* = 8.5, 1.5 Hz, 1H), 7.87 (dd, *J* = 7.7, 1.9 Hz, 1H), 7.78 (d, *J* = 8.1 Hz, 1H), 7.52 (dd, *J* = 7.3, 1.3 Hz, 1H), 7.50 – 7.41 (m, 3H), 2.48 (dq, *J* = 14.7, 7.5 Hz, 1H), 2.25 (dq, *J* = 14.6, 7.5 Hz, 1H), 2.04 (s, 3H), 2.02 (s, 3H), 0.87 (t, *J* = 7.5 Hz, 3H); ^{13}C NMR (151 MHz, $CDCl_3$) δ 169.5, 139.9, 134.9, 130.4, 129.7, 128.7, 125.6, 125.5, 125.1, 125.0, 124.3, 85.6, 34.0, 24.6, 21.8, 8.7; FTIR (NaCl/thin film) 2979, 2940, 1734, 1653, 1558, 1507, 1364, 1242, 1107, 1015, 804, 776 cm^{-1}; HRMS (EI+) [M]+ calculated for $C_{16}H_{18}O_2$: 242.1307, found: 242.1316.

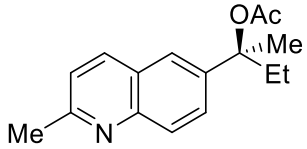

(*S*)-2-(2-Methylquinolin-6-yl)butan-2-yl acetate ((*S*)-2.19c). Prepared via General Procedure B using **2.18c** (99% ee) as a yellow oil (87%). The enantiomeric excess was determined to be 99% by chiral HPLC analysis (CHIRLPAK IB, 1.0 mL/min, 6.0% *i*-PrOH/hexanes, λ=254 nm); t_R(major) = 13.331 min, t_R(minor) = 9.787 min. $[\alpha]_D^{24}$ = +7.8° (c 1.51, $CHCl_3$): ^{1}H NMR (600 MHz, $CDCl_3$) δ 8.01 (d, *J* = 8.4 Hz, 1H), 7.97 (d, *J* = 8.8 Hz, 1H), 7.67 (d, *J* = 2.1 Hz, 1H), 7.63 (dd, *J* = 8.8, 2.2 Hz, 1H), 7.27 (s, 1H), 2.72 (s, 3H), 2.10 (s, 5H), 1.90 (s, 3H), 0.79 (t, *J* = 7.4 Hz, 3H); ^{13}C NMR (151 MHz, $CDCl_3$) δ 169.8, 159.0, 147.1, 142.2, 136.5, 128.7, 126.7, 126.1, 123.2, 122.3,

84.3, 35.1, 25.4, 24.4, 22.3, 8.3; FTIR (NaCl/thin film) 2977, 2938, 1739, 1601, 1368, 1247, 1136, 1078, 834 cm^{-1}; HRMS (CI+) [M]+H calculated for $C_{16}H_{20}NO_2$: 258.1494, found: 258.1488.

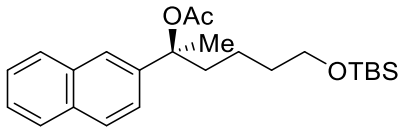

(*S*)-6-((tert-Butyldimethylsilyl)oxy)-2-(naphthalen-2-yl)hexan-2-yl acetate ((*S*)-2.19d). Prepared via General Procedure B using **2.18d** (99% ee) as a colorless oil (75%). The enantiomeric excess was determined to be 99% by chiral HPLC analysis (CHIRLCEL OD-H, 1.0 mL/min, 0.5% *i*-PrOH/hexanes, λ=254 nm); t_R(major) = 21.535 min, t_R(minor) = 14.469 min. $[\alpha]_D^{24}$ = +15.4° (c 4.73, $CHCl_3$): ^{1}H NMR (600 MHz, $CDCl_3$) δ 7.81 (dd, *J* = 11.1, 8.5 Hz, 3H), 7.76 – 7.71 (m, 1H), 7.48 – 7.41 (m, 3H), 3.53 (t, *J* = 6.4 Hz, 2H), 2.14 – 2.03 (m, 5H), 1.93 (s, 3H), 1.46 (p, *J* = 7.0 Hz, 2H), 1.31 – 1.22 (m, 2H), 0.83 (s, 9H), –0.01 (s, 6H); ^{13}C NMR (101 MHz, $CDCl_3$) δ 169.9, 142.5, 133.2, 132.5, 128.3, 128.1, 127.6, 126.1, 125.9, 123.5, 123.1, 84.2, 63.0, 42.4, 33.0, 26.0, 24.8, 22.4, 20.3, 18.4, –5.2; FTIR (NaCl/thin film) 3058, 2952, 2929, 2857, 1739, 1366, 1248, 1101, 836, 775 cm^{-1}; HRMS (LIFDI) [M]+ calculated for $C_{24}H_{36}O_3Si$: 400.2434, found: 400.2435.

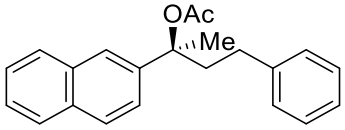

(*S*)-2-(Naphthalen-2-yl)-4-phenylbutan-2-yl acetate ((*S*)-2.19e). Prepared via General Procedure B as a colorless oil (96%). The enantiomeric excess was determined to be 94% by chiral HPLC analysis (CHIRALPAK IA, 1.0 mL/min, 0.5% *i*-PrOH/hexanes, λ=254 nm); t_R(major) = 11.227 min, t_R(minor) = 12.577 min. $[\alpha]_D^{24}$ = −74.8° (c 1.1, $CHCl_3$): ^{1}H NMR (400 MHz, $CDCl_3$) δ 7.89 – 7.77 (m, 4H), 7.52 – 7.43

(m, 3H), 7.26 – 7.21 (m, 2H), 7.16 (d, *J* = 7.3 Hz, 1H), 7.13 – 7.07 (m, 2H), 2.58 – 2.34 (m, 4H), 2.12 (s, 3H), 2.01 (s, 3H); ^{13}C NMR (101 MHz, $CDCl_3$) δ 169.9, 142.2, 141.8, 133.2, 132.5, 128.49, 128.46, 128.4, 128.3, 127.6, 126.3, 126.01, 126.00, 123.6, 123.0, 84.0, 44.1, 30.4, 25.3, 22.4; FTIR (NaCl/thin film) 3059,3 025, 2937, 1734, 1717, 1652, 1558, 1506, 1244, 747 cm^{-1}; HRMS (LIFDI) [M]+ calculated for $C_{22}H_{22}O_2$: 318.1620, found: 318.1648.

Please note: The absolute configuration of **2.19e** is tentatively assigned. The absolute configuration resulting from the method used in the preparation of its alcohol precursor **2.18e** has not been reported in the literature. Please see the experimental for **2.18e** below.

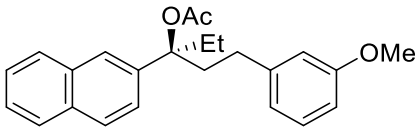

(*S*)-1-(3-Methoxyphenyl)-3-(naphthalen-2-yl)pentan-3-yl acetate ((*S*)-2.19g). Prepared via General Procedure B using **2.18g** (89% ee) as a colorless oil (80%). The enantiomeric excess was assumed to be 89% based on the starting material. $[\alpha]_D^{24}$ = +30.5° (c 1.50, $CHCl_3$): ^{1}H NMR (600 MHz, $CDCl_3$) δ 7.91 – 7.84 (m, 4H), 7.55 – 7.46 (m, 3H), 7.16 (t, *J* = 7.9 Hz, 1H), 6.70 (ddd, *J* = 13.7, 7.8, 2.0 Hz, 2H), 6.65 – 6.61 (m, 1H), 3.76 (s, 3H), 2.97 – 2.85 (m, 1H), 2.62 (dq, *J* = 14.6, 7.3 Hz, 1H), 2.51 – 2.41 (m, 2H), 2.39 – 2.29 (m, 1H), 2.27 – 2.16 (m, 4H), 0.74 (t, *J* = 7.4 Hz, 3H); ^{13}C NMR (151 MHz, $CDCl_3$) δ 169.7, 159.7, 143.6, 140.6, 133.2, 132.5, 129.4, 128.4, 128.2, 127.6, 126.3, 126.0, 124.5, 123.2, 120.9, 114.2, 111.3, 87.8, 55.2, 39.4, 30.9, 30.1, 22.2, 7.8; FTIR (NaCl/thin film) 3056, 2970, 2937, 1733, 1600, 1489, 1455, 1366, 1242, 1046, 1021, 819, 748 cm^{-1}; HRMS (LIFDI) [M]+ calculated for $C_{24}H_{26}O_3$: 362.1882, found: 362.1906.

Please note: The absolute configuration of **2.19g** is tentatively assigned. The absolute configuration resulting from the method used in the preparation of its alcohol precursor **2.18g** has not been reported in the literature. Please see the experimental for **2.18g** below.

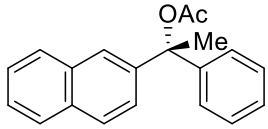

(*R*)-1-(Naphthalen-2-yl)-1-phenylethyl acetate ((*R*)-2.19h). Prepared via General Procedure B using **2.18h** (96% ee) as a colorless sticky oil (54%). The enantiomeric excess was determined to be 96% by chiral HPLC analysis (CHIRLPAK IB, 1.0 mL/min, 1.0% *i*-PrOH/hexanes, λ=254 nm); t_R(major) = 8.923 min, t_R(minor) = 7.511 min. $[\alpha]_D^{24}$ = +15.3° (c 4.1, $CHCl_3$): ^{1}H NMR (600 MHz, $CDCl_3$) δ 7.89 – 7.87 (m, 1H), 7.84 (dd, *J* = 7.4, 1.8 Hz, 1H), 7.79 (dd, *J* = 7.4, 1.7 Hz, 1H), 7.75 (d, *J* = 8.7 Hz, 1H), 7.50 – 7.44 (m, 2H), 7.38 – 7.29 (m, 5H), 7.26 – 7.23 (m, 1H), 2.30 (s, 3H), 2.16 (s, 3H); ^{13}C NMR (151 MHz, $CDCl_3$) δ 169.4, 145.6, 142.9, 133.0, 132.6, 128.5, 128.3, 128.1, 127.7, 127.3, 126.3, 126.2, 126.1, 124.6, 124.5, 84.8, 27.0, 22.6; FTIR (NaCl/thin film) 3056, 3024, 2981, 1739, 1368, 1241, 1188, 749, 699 cm^{-1}; HRMS (LIFDI) [M]+ calculated for $C_{20}H_{18}O_2$: 290.1307, found: 290.1328.

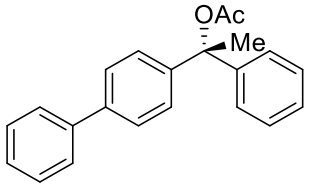

(*R*)-1-([1,1'-Biphenyl]-4-yl)-1-phenylethyl acetate ((*R*)-2.19i). Prepared via General Procedure B using **2.18i** (91% ee) as a colorless oil (61%). The enantiomeric excess was assumed to be 91% based on the starting material. $[\alpha]_D^{24}$ = −17.8° (c 0.84, $CHCl_3$): ^{1}H NMR (600 MHz, $CDCl_3$) δ 7.61 – 7.57 (m, 2H), 7.57 – 7.53 (m, 2H), 7.44

(t, J = 7.7 Hz, 2H), 7.42 – 7.32 (m, 7H), 7.29 – 7.26 (m, 1H), 2.25 (s, 3H), 2.16 (s, 3H); ^{13}C NMR (151 MHz, $CDCl_3$) δ 169.4, 145.7, 144.8, 140.8, 140.1, 128.9, 128.3, 127.4, 127.3, 127.2, 127.0, 126.5, 126.0, 84.6, 27.0, 22.6; FTIR (NaCl/thin film) 3057, 3029, 2939, 1739, 1600, 1582, 1487, 1446, 1368, 1238, 1057, 875, 761 cm^{-1}; HRMS (LIFDI) [M]+ calculated for $C_{22}H_{20}O_2$: 316.1463, found: 316.1485.

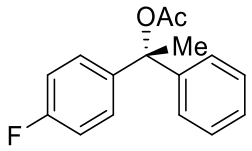

(*R*)-1-(4-Fluorophenyl)-1-phenylethyl acetate ((*R*)-2.19j). Prepared via General Procedure B using **2.18j** (90% ee) as a colorless oil (95%). The enantiomeric excess was assumed to be 93% based on the starting material. $[\alpha]_D^{24}$ = −12.4° (c 0.84, $CHCl_3$): ^{1}H NMR (400 MHz, $CDCl_3$) δ 7.34 – 7.27 (m, 7H), 7.01 – 6.97 (m, 2H), 2.18 (s, 3H), 2.12 (s, 3H); ^{13}C NMR (101 MHz, $CDCl_3$) δ 169.37, 163.08, 160.64, 145.61, 141.54 (d, $J_{C\text{-}F}$ = 3.3 Hz), 141.51 (d, $J_{C\text{-}F}$ = 3.3 Hz), 128.31, 127.95 (d, $J_{C\text{-}F}$ = 8.1 Hz), 127.87 (d, $J_{C\text{-}F}$ = 8.1 Hz), 127.37, 125.89, 115.16 (d, $J_{C\text{-}F}$ = 21.4 Hz), 114.95 (d, $J_{C\text{-}F}$ = 21.4 Hz), 84.25, 27.15, 22.54; ^{19}F NMR (377 MHz, $CDCl_3$) δ –115.58; FTIR (NaCl/thin film) 3463, 3061, 2983, 2939, 1740, 1602, 1509, 1447, 1370, 1237, 1115, 947, 699, 560 cm^{-1}; HRMS (LIFDI) [M]+ calculated for $C_{16}H_{15}FO_2$: 258.1132, found: 258.1358.

Please note: The absolute configuration of **2.19j** is tentatively assigned. The absolute configuration resulting from the method used in the preparation of its alcohol precursor **2.18j** has not been reported in the literature. Please see the experimental for **2.18j** below.

2.4.2.3 Preparation of (*S*,*E*)-2-(Naphthalen-2-yl)-5-(*o*-tolyl)pent-4-en-2-yl acetate ((*S*)-2.19f)

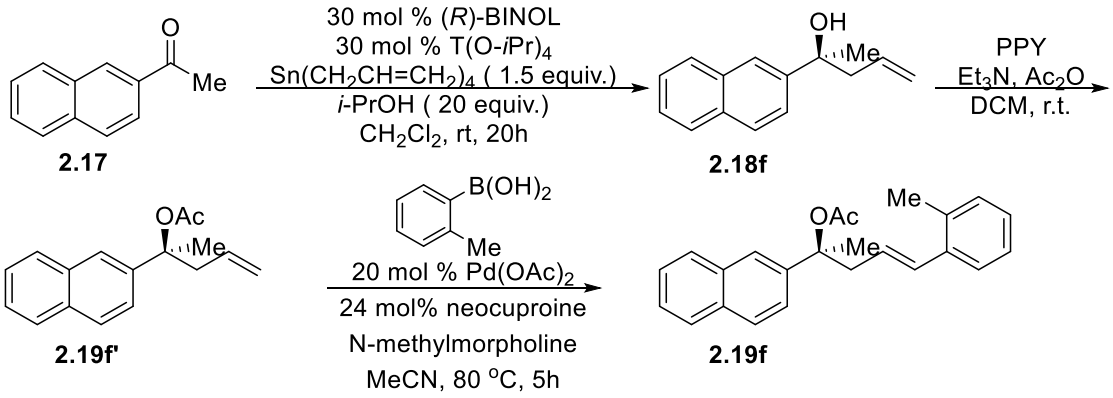

2-(Naphthalen-2-yl)pent-4-en-2-ol (2.18f). This procedure was adapted from that reported in the literature.[12] In an oven-dried, 50-mL, round-bottomed flask was placed (*R*)-BINOL (312 mg, 1.09 mmol, 0.300 equiv.) in CH_2Cl_2 (9.0 mL). Ti(O-*i*Pr)$_4$ (0.33 mL, 1.1 mmol, 0.30 equiv.) was added at room temperature. The mixture was stirred for 10 min. Then *i*PrOH (5.6 mL, 73 mmol, 20 equiv.) was added, followed by a solution of 2-acetonaphthone (618 mg, 3.63 mmol, 1.00 equiv.) and CH_2Cl_2 (3.0 mL), and then tetraallyltin (0.96 mL, 4.0 mmol, 1.1 equiv.). The orange solution was stirred at room temperature for 22 h and quenched with sat. $NaHCO_3$ (40 mL). To remove solids, the mixture was filtered through Celite®, which was then washed with CH_2Cl_2. The layers were separated, and the organic layer was washed with sat. NaCl, dried (Na_2SO_4), filtered, and concentrated. The crude mixture was purified on silica gel chromatography (0−20% EtOAc/hexanes) to give a 2-(naphthalen-2-yl)pent-4-en-2-ol as a clear oil (634.2 mg, 82%). The enantiomeric excess was determined to be 96% by chiral HPLC analysis (CHIRALPAK IC, 1 mL/min, 3% i-PrOH/hexane, λ=254 nm); t_R(major) = 12.164 min, t_R(minor) = 10.175 min. The spectral data of this compound matches of that reported in the literature.[13]

Please note: The absolute configuration of 2-(naphthalene-2-yl)pent-4-en-2-ol is tentatively assigned. The absolute configuration resulting from this allylation procedure has not been reported in the literature. [REF: Walsh ACIE 2002]

2-(Naphthalen-2-yl)pent-4-en-2-yl acetate (2.19f'). Using General Procedure B, 2-(naphthalen-2-yl)pent-4-en-2-yl acetate was obtained as a colorless oil (632.5 mg, 86%) from 2-(naphthalen-2-yl)pent-4-en-2-ol (611 mg, 2.88 mmol, 96% ee): ^{1}H NMR (600 MHz, $CDCl_3$) δ 7.90 – 7.80 (m, 3H), 7.79 – 7.72 (m, 1H), 7.46 (dtd, *J* = 9.2, 6.9, 5.4 Hz, 3H), 5.63 (ddt, *J* = 17.3, 10.2, 7.2 Hz, 1H), 5.11 – 4.95 (m, 2H), 2.94 (dd, *J* = 14.0, 7.1 Hz, 1H), 2.85 (dd, *J* = 14.0, 7.3 Hz, 1H), 2.09 (s, 3H), 1.91 (s, 3H); ^{13}C NMR (151 MHz, $CDCl_3$) δ 169.8, 142.2, 133.2, 133.0, 132.6, 128.4, 128.2, 127.6, 126.2, 126.0, 123.6, 123.1, 118.8, 83.4, 46.4, 25.1, 22.4.

(*S*,*E*)-2-(Naphthalen-2-yl)-5-(*o*-tolyl)pent-4-en-2-yl acetate ((*S*)-2.19f). The procedure was adapted from reported literature.[14] In 25-mL, round-bottomed flask was placed 2-(naphthalen-2-yl)pent-4-en-2-yl acetate (632 mg, 2.49 mmol, 1.00 equiv.), 2-methylphenyl boronic acid (677 mg, 5.00 mmol, 2.00 equiv.), *N*-methylmorpholine (0.55 mL, 5.0 mmol, 2.0 equiv.), and MeCN (10 mL). The flask was exposed to open air. $Pd(OAc)_2$ (335 mg, 0.498 mmol, 20 mol %) and neocuproine (125 mg, 0.598 mmol, 24 mol %) were added. The mixture was heated at 80 °C for 22 h. The mixture was cooled to room temperature and diluted with CH_2Cl_2 (30 mL). The solid was removed by filtration through a pad of Celite®, and the organic layer was concentrated. The crude mixture was purified via silica gel chromatography (0−15% EtOAc/hexanes) to give **2.19f** as a colorless oil (351 mg, 41%). The enantiomeric excess was determined to be 96% by chiral HPLC analysis (CHIRALPAK IA, 0.8 mL/min, 1% *i*-PrOH/hexane, λ=254 nm); t_R(major) = 15.924 min, t_R(minor) = 21.866 min. $[\alpha]_D^{24}$ = +10.7° (c 1.12,

$CHCl_3$): ^{1}H NMR (600 MHz, $CDCl_3$) δ 7.85 – 7.78 (m, 4H), 7.52 – 7.44 (m, 3H), 7.28 (dd, *J* = 7.4, 2.2 Hz, 1H), 7.14 – 7.07 (m, 3H), 6.62 – 6.56 (m, 1H), 5.87 (dt, *J* = 15.3, 7.4 Hz, 1H), 3.12 – 2.99 (m, 2H), 2.22 (s, 3H), 2.10 (s, 3H), 1.97 (s, 3H); ^{13}C NMR (151 MHz, $CDCl_3$) δ 169.8, 142.2, 136.8, 135.3, 133.2, 132.6, 132.1, 130.2, 128.4, 128.2, 127.6, 127.3, 126.3, 126.1, 126.05, 126.03, 125.9, 123.6, 123.2, 83.8, 45.9, 25.3, 22.4, 19.8; FTIR (NaCl/thin film) 2955, 2921, 2850, 1713, 1464, 1364, 1232, 1076, 748 cm^{-1}; HRMS (LIFDI) [M]+ calculated for $C_{24}H_{24}O_2$: 344.1776, found: 344.1769.

Please note: The absolute configuration of **2.19f** is tentatively assigned. The absolute configuration resulting from the method used in the preparation of its alcohol precursor has not been reported in the literature, as discussed above.

2.4.2.4 Preparation of Tertiary Benzyl Alcohols

2.4.2.4.1 Preparation of 2.18, 2.18a – 2.18c.

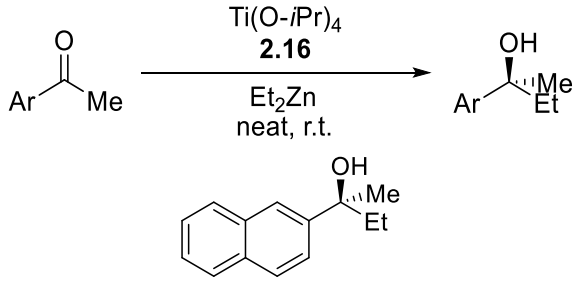

(*S*)-2-(Naphthalen-2-yl)butan-2-ol ((*S*)-2.18). This procedure was adapted from that reported in the literature.[15] In an oven-dried, 100-mL, round-bottomed flask was placed **2.16** (33 mg, 0.060 mmol, 0.010 equiv.) and Et_2Zn (0.73 mL, 7.2 mmol, 1.2 equiv.). Ti(O-*i*Pr)$_4$ (2.1 mL, 7.2 mmol, 1.2 equiv.) was added. The resulting greenish solution was stirred at room temperature for 5 min. 2-Acetonaphthalone (1.02 g, 6.00 mmol, 1.00 equiv.) was added into the flask in one portion. The mixture was stirred at room temperature for 17 h. The resulting brown sticky oil was diluted with EtOAc (50

mL) and quenched with HCl (1 N). The product was extracted from the aqueous layer with EtOAc (25 mL x 2). The combined organic layers were washed with sat. NaCl, dried ($MgSO_4$), filtered, and concentrated. The residue was purified via silica gel chromatography (5−10% Et_2O/hexanes) to give **(*S*)-2.18** (470 mg, 39%) as a colorless oil. The enantiomeric excess was determined to be 97% by chiral HPLC analysis (CHIRLPAK IB, 1.0 mL/min, 3.0% *i*-PrOH/hexanes, λ=254 nm); t_R(major) = 10.269 min, t_R(minor) = 11.370 min. Based on the optical rotation, $[\alpha]_D^{24} = -9.5°$ (c 1.0, MeOH) (Literature data: $[\alpha]_D^{24} = +16.3°$ (c 1.0, MeOH) for *R* configuration),[14b] the absolute configuration of **2.18** was assigned as *S*. The spectral data of this compound matched that reported in the literature. [15]

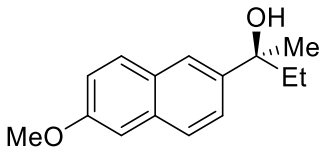

(*S*)-2-(6-Methoxynaphthalen-2-yl)butan-2-ol ((*S*)-2.18a). Prepared via the procedure described above for preparation of **(*S*)-2.18** as a colorless oil (32%). The enantiomeric excess was determined to be 92% by chiral HPLC analysis (CHIRLPAK IC, 1.0 mL/min, 3.0% *i*-PrOH/hexanes, λ=254 nm); t_R(major) = 21.219 min, t_R(minor) = 16.516 min. $[\alpha]_D^{24} = +5.1°$ (c 3.02, $CHCl_3$): ^{1}H NMR (600 MHz, $CDCl_3$) δ 7.83 (d, *J* = 1.9 Hz, 1H), 7.73 (dd, *J* = 12.2, 8.7 Hz, 2H), 7.50 (dd, *J* = 8.6, 1.9 Hz, 1H), 7.16 – 7.11 (m, 2H), 3.92 (s, 3H), 1.99 – 1.85 (m, 2H), 1.79 (d, *J* = 3.6 Hz, 1H), 1.63 (s, 3H), 0.82 (td, *J* = 7.4, 1.0 Hz, 3H); ^{13}C NMR (151 MHz, $CDCl_3$) δ 157.7, 143.0, 133.4, 129.7, 128.8, 126.8, 124.4, 123.3, 118.9, 105.7, 75.2, 55.5, 36.7, 29.9, 8.5; FTIR (NaCl/thin film) 3447 (br s), 3059, 2969, 2935, 1634, 4606, 1504, 1485, 1462, 1388, 1265, 1199, 1033, 852, 810 cm^{-1}; HRMS (CI+) [M]+H calculated for $C_{15}H_{19}O_2$: 231.1385, found: 231.1400.

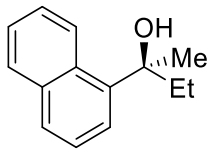

(*S*)-2-(Naphthalen-1-yl)butan-2-ol ((*S*)-2.18b). Prepared via the procedure described above for preparation of **(*S*)-2.18** as a colorless oil (9%). The enantiomeric excess was determined as 90% by chiral HPLC analysis (CHIRLPAK IB, 0.7 mL/min, 2.0% *i*-PrOH/hexanes, λ=254 nm); t_R(major) = 15.085 min, t_R(minor) = 17.287 min. $[\alpha]_D^{24}$ = +33.7° (c 1.91, $CHCl_3$): ^{1}H NMR (600 MHz, $CDCl_3$) δ 8.79 – 8.75 (m, 1H), 7.87 (dd, *J* = 7.8, 1.9 Hz, 1H), 7.77 (d, *J* = 8.2 Hz, 1H), 7.58 (dd, *J* = 7.3, 1.3 Hz, 1H), 7.48 (pd, *J* = 6.8, 1.6 Hz, 2H), 7.42 (t, *J* = 7.7 Hz, 1H), 2.30 – 2.17 (m, 2H), 2.02 (s, 1H), 1.82 (s, 3H), 0.83 (t, *J* = 7.5 Hz, 3H); ^{13}C NMR (151 MHz, $CDCl_3$) δ 142.4, 135.0, 131.1, 129.3, 128.6, 127.1, 125.3, 125.2, 124.9, 124.0, 76.9, 35.4, 29.5, 9.0; FTIR (NaCl/thin film) 3420 (brs), 3048, 2971, 2936, 2877, 1653, 1508, 1456, 1374, 1117, 804, 777 cm^{-1}; HRMS (EI+) [M]+H calculated for $C_{14}H_{16}O$: 200.1201, found: 200.1205.

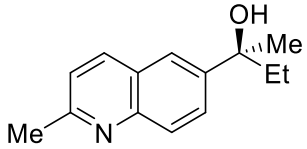

(*S*)-2-(2-Methylquinolin-6-yl)butan-2-ol ((*S*)-2.18c). Prepared via the procedure described above for preparation of **(*S*)-2.18** as a pale yellow solid (mp 86–89°, 41%). The enantiomeric excess was determined as 99% by chiral HPLC analysis (CHIRLPAK IC, 1 mL/min, 8.0% *i*-PrOH/hexanes, λ=230 nm); t_R(major) = 23.228 min, t_R(minor) = 19.313 min. $[\alpha]_D^{24}$ = +33° (c 1.03, $CHCl_3$): ^{1}H NMR (600 MHz, $CDCl_3$) δ 8.04 (d, *J* = 8.4 Hz, 1H), 7.98 (d, *J* = 8.8 Hz, 1H), 7.85 (d, *J* = 2.1 Hz, 1H), 7.71 (dd, *J* = 8.9, 2.1 Hz, 1H), 7.28 (d, *J* = 8.4 Hz, 1H), 2.74 (s, 3H), 1.93 (ddt, *J* = 27.2, 14.1, 7.1 Hz, 2H), 1.64 (s, 3H), 0.81 (t, *J* = 7.5 Hz, 3H); ^{13}C NMR (151 MHz, $CDCl_3$) δ 158.9, 147.0, 145.1, 136.5, 128.6, 127.4, 126.2, 123.1, 122.3, 75.1, 36.7, 30.0, 25.5, 8.4; FTIR

(NaCl/thin film) 3355 (brs), 2969, 2933, 2878, 1601, 1497, 1457, 1374, 1165, 1126, 837, 755 cm^{-1}; HRMS (CI+) [M]+H calculated for $C_{14}H_{18}NO$: 216.1388, found: 216.1398.

A crystal suitable for X-ray diffraction analysis was obtained via diffusion of hexanes into a solution of **2.18c** in EtOAc at –18 °C. The crystal structure demonstrates that the absolute configuration is *S* (Figure 2.5).

Figure 2.5. Molecular Diagram of (*S*)-**2.18c** with Ellipsoids at 50% Probability, All Non-Oxygen Bound H-atoms Omitted for Clarity. (CCDC 1424634)

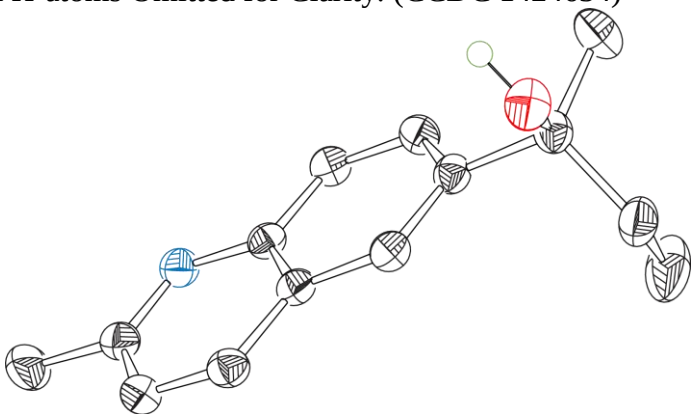

2.4.2.4.2 Preparation of 2.18d

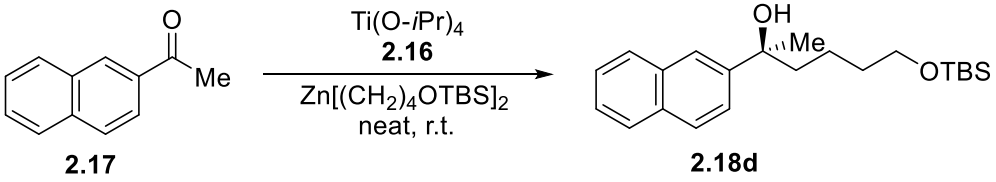

2.17 **2.18d**

(*S*)-6-((*tert*-Butyldimethylsilyl)oxy)-2-(4-nitrophenyl)hexan-2-ol ((*S*)-2.18d). Prepared via the procedure described above for preparation of **(*S*)-2.18d**, except that bis(4-((*tert*-butyldimethylsilyl)oxy)butyl)zinc was used instead of Et_2Zn, as a colorless oil (30%). The enantiomeric excess was determined to be 99% by chiral HPLC analysis (CHIRLPAK IA, 0.6 mL/min, 3.0% *i*-PrOH/hexanes, λ=254 nm); t_R(major) = 14.468

min, t_R(minor) = 13.695 min. $[\alpha]_D^{24}$ = +10.2° (c 2.63, $CHCl_3$): ^{1}H NMR (600 MHz, $CDCl_3$) δ 7.93 – 7.89 (m, 1H), 7.86 – 7.79 (m, 3H), 7.52 (dd, *J* = 8.6, 1.9 Hz, 1H), 7.50 – 7.42 (m, 2H), 3.54 (t, *J* = 6.5 Hz, 2H), 2.01 – 1.84 (m, 3H), 1.65 (s, 3H), 1.53 – 1.45 (m, 2H), 1.40 – 1.28 (m, 1H), 1.27 – 1.17 (m, 1H), 0.83 (s, 9H), –0.01 (d, *J* = 2.3 Hz, 6H); ^{13}C NMR (151 MHz, $CDCl_3$) δ 145.5, 133.3, 132.4, 128.3, 128.0, 127.6, 126.1, 125.8, 123.8, 123.3, 75.1, 63.1, 43.8, 33.1, 30.4, 26.1, 20.6, 18.4, –5.16, –5.17; FTIR (NaCl/thin film) 3432 (brs), 3056, 2952, 2929, 2857, 1471, 1254, 1101, 836, 775, 476 cm^{-1}; HRMS (LIFDI) [M]+ calculated for $C_{24}H_{26}O_3$: 358.2328, found: 358.2343.

2.4.2.4.3 Preparation of 2.18e and 2.18g

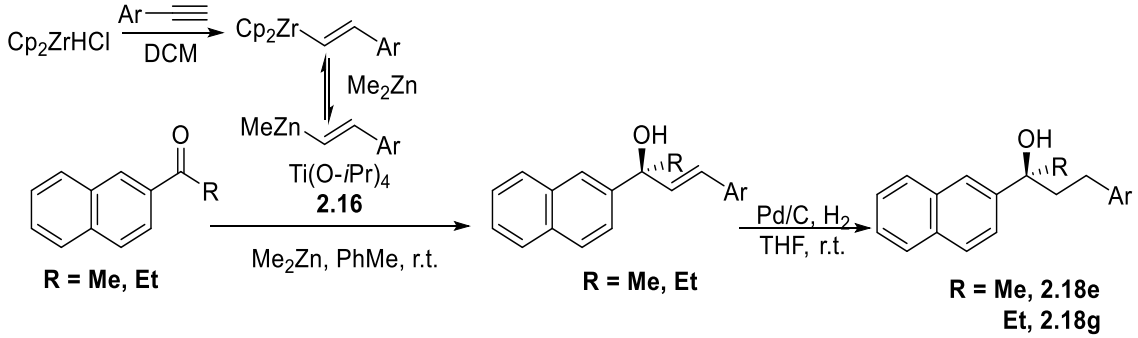

(*S*)-2-(naphthalen-2-yl)-4-phenylbutan-2-ol (*S*)-2.18e. The procedure for formation of the allylic alcohol was adapted from a reported procedure.[16] For preparation the vinylzinc reagent, in an oven-dried, round-bottomed flask was placed Cp_2ZrHCl (346 mg, 1.20 mmol, 1.20 equiv.) and CH_2Cl_2 (4.0 mL). At room temperature, phenylacetylene (0.13 mL, 1.2 mmol, 1.2 equiv.) was added into the flask and stirred for 10 min. The solvent was removed, and the orange solid was dissolved in PhMe (4.0 mL). The solution was cooled to –78 °C, before Me_2Zn (1.0 mL, 1.2 mmol, 1.2 equiv., 1.2 M in PhMe) was added. The mixture was stirred at –78 °C for 10 min. The resulting solution was assumed to be the vinylzinc in PhMe solution. In a separate flask was

placed **2.16** (54.5 mg, 0.10 mmol, 0.10 equiv.), Me_2Zn (0.33 mL, 0.40 mmol, 0.40 equiv., 1.2 M in PhMe), and PhMe (2.0 mL). To this mixture was added Ti(O-*i*Pr)$_4$ (0.36 mL, 1.2 mmol, 1.2 equiv.) at room temperature. The mixture was stirred at room temperature for 15 min, then the solution was added into the pre-formed vinylzinc solution at –78 °C via cannula. The combined solution was warmed to 0 °C, and treated with a solution of 2-acetylnaphthalone (170 mg, 1.0 mmol, 1.0 equiv.) and PhMe (1.0 mL). The resulting reddish solution was stirred at room temperature for 16 h and then quenched with sat. $NaHCO_3$ aq. (20 mL). The solid was removed via filtration through a pad of Celite®. The product was extracted with EtOAc. The combined organic layers were washed with sat. NaCl, dried (Na_2SO_4), filtered, and concentrated. The residue was purified via silica gel chromatography (0–10% EtOAc/hexanes) to give (*E*)-2-(naphthalen-2-yl)-4-phenylbut-3-en-2-ol as a colorless oil (202 mg, 77%), which was used directly in next step.

Please note: We assume the same absolute configuration using these homemade vinylzinc reagents as when Et_2Zn is used. However, the absolute configuration obtained for this procedure has not been reported in the literature.[16]

(*E*)-2-(Naphthalen-2-yl)-4-phenylbut-3-en-2-ol (202 mg, 0.736 mmol) was dissolved in THF (7 mL) at room temperature. Pd/C (39 mg, 0.037 mmol, 10% w) was added. The headspace of the flask was evacuated and refilled with H_2 three times. The mixture was then stirred at room temperature for 12 h under H_2 (1 atm). The solid was removed via filtration through a tight-packed pad of Celite®. The filtrate was concentrated and purified via silica gel chromatography (0–10% EtOAc/hexanes) to give **(*S*)-2.18e** (189 mg, 93%) as a white solid (mp 76–79°). $[\alpha]_D^{24}$ = +43.6° (c 2.2, $CHCl_3$): ^{1}H NMR (600 MHz, $CDCl_3$) δ 8.02 – 7.98 (m, 1H), 7.92 – 7.86 (m, 3H), 7.60

(dd, *J* = 8.6, 1.9 Hz, 1H), 7.52 (pd, *J* = 6.8, 1.5 Hz, 2H), 7.29 – 7.21 (m, 2H), 7.21 – 7.16 (m, 1H), 7.16 – 7.13 (m, 2H), 2.69 (ddd, *J* = 13.7, 11.8, 5.6 Hz, 1H), 2.48 (ddd, *J* = 13.6, 11.8, 4.9 Hz, 1H), 2.33 – 2.20 (m, 2H), 1.93 (s, 1H), 1.73 (s, 3H); ^{13}C NMR (151 MHz, $CDCl_3$) δ 145.0, 142.3, 133.4, 132.4, 128.51, 128.46, 128.3, 128.2, 127.6, 126.3, 125.90, 125.89, 123.7, 123.4, 75.1, 45.9, 30.8, 30.7; FTIR (NaCl/thin film) 3446 (brs), 3057, 3024, 2972, 2932, 1601, 1496, 1455, 819, 747, 700, 487 cm^{-1}; HRMS (EI+) [M]+ calculated for $C_{20}H_{20}O$: 276.1514, found: 276.1514.

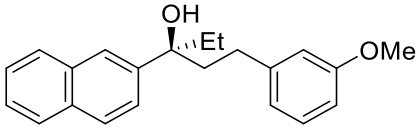

(*S*)-1-(3-methoxyphenyl)-3-(naphthalen-2-yl)pentan-3-ol ((*S*)-2.18g). Following a similar procedure as for the preparation of **(*S*)-2.18e** above, **(*S*)-2.18g** was prepared as a colorless oil (40% overall yield from 1-(naphthalene-2-yl)propan-1-one). The enantiomeric excess was determined to be 89% ee by chiral HPLC analysis (CHIRLPAK IC, 1.0 mL/min, 5.0% *i*-PrOH/hexanes, λ=254 nm); t_R(major) = 9.989 min, t_R(minor) = 10.700 min. $[\alpha]_D^{24}$ = +41.3° (c 0.92, $CHCl_3$): ^{1}H NMR (600 MHz, $CDCl_3$) δ 7.98 – 7.93 (m, 1H), 7.90 – 7.84 (m, 3H), 7.50 (dtd, *J* = 9.4, 7.0, 5.3 Hz, 3H), 7.17 (t, *J* = 7.9 Hz, 1H), 6.71 (dd, *J* = 8.0, 2.1 Hz, 2H), 6.66 (t, *J* = 2.0 Hz, 1H), 3.76 (s, 3H), 2.66 (ddd, *J* = 13.6, 11.7, 5.5 Hz, 1H), 2.35 (ddd, *J* = 13.6, 11.8, 4.7 Hz, 1H), 2.32 – 2.17 (m, 2H), 2.03 (dq, *J* = 14.9, 7.4 Hz, 1H), 1.95 (dq, *J* = 14.5, 7.4 Hz, 1H), 1.88 (s, 1H), 0.81 (t, *J* = 7.4 Hz, 3H); ^{13}C NMR (151 MHz, $CDCl_3$) δ 159.8, 144.2, 143.0, 133.3, 132.3, 129.5, 128.3, 128.1, 127.6, 126.2, 125.8, 124.4, 123.9, 120.8, 114.2, 111.2, 77.6, 55.2, 44.5, 35.9, 30.3, 7.9; FTIR (NaCl/thin film) 3486 (brs), 3054, 2964, 2936, 1680, 1489, 1455, 1258, 1152, 1048, 819, 748, 698, 477 cm^{-1}; HRMS (EI+) [M]+ calculated for $C_{22}H_{24}O_2$: 320.1776, found: 320.1753.

Please note: We assume the same absolute configuration using these homemade vinylzinc reagents as when Et_2Zn is used. However, the absolute configuration obtained for this procedure has not been reported in the literature.[16]

2.4.2.4.4 Preparation of 2.18h – 2.18j

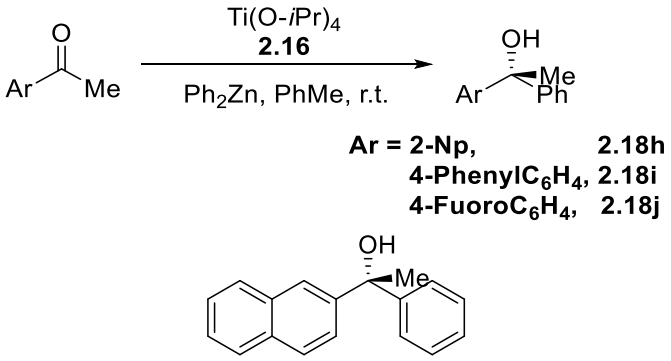

(*R*)-1-(naphthalen-2-yl)-1-phenylethan-1-ol ((*R*)-2.18h). The procedure was adapted from that reported in the literature.[17] In an oven-dried, 50-mL, round-bottomed flask was placed **2.16** (54.5 mg, 0.100 mmol, 0.100 equiv.), Ph_2Zn (351 mL, 1.60 mmol, 1.60 equiv.), and PhMe (10 mL) at room temperature. Ti(O-*i*Pr)$_4$ (0.1 mL, 0.60 mmol, 0.60 equiv.) was added. The mixture was stirred at room temperature for 15 min. A solution of 2-acetonaphthalone (170 mg, 1.0 mmol, 1.0 equiv) and PhMe (5 mL) was added into the flask. The mixture was stirred at room temperature for 17 h. The reaction was then quenched with sat. NH_4Cl aq. (20 mL). The solids were removed via filtration through a pad of Celite®. The mixture was extracted with EtOAc (25 mL x 2). The combined organic layers were washed with sat. NaCl, dried ($NaSO_4$), filtered, and concentrated. The residue was purified via silica gel chromatography (5−15% Et_2O/hexanes) to give **(*R*)-2. 18h** (203.7 mg, 82%) as a colorless oil. The enantiomeric excess was determined to be 95% by chiral HPLC analysis (CHIRLPAK IB, 1.0 mL/min, 4.0% *i*-PrOH/hexanes, λ=254 nm); t_R(major) = 13.183 min, t_R(minor) = 14.119 min.

$[\alpha]_D^{24}$ = +10.7° (c 0.82, $CHCl_3$): ^{1}H NMR (600 MHz, $CDCl_3$) δ 8.00 – 7.95 (m, 1H), 7.87 – 7.83 (m, 1H), 7.81 (dd, *J* = 7.5, 1.8 Hz, 1H), 7.77 (d, *J* = 8.6 Hz, 1H), 7.52 – 7.44 (m, 4H), 7.42 (dd, *J* = 8.6, 1.9 Hz, 1H), 7.33 (dd, *J* = 8.5, 7.0 Hz, 2H), 7.27 (d, *J* = 6.6 Hz, 1H), 2.29 (s, 1H), 2.06 (s, 3H); ^{13}C NMR (151 MHz, $CDCl_3$) δ 147.9, 145.4, 133.1, 132.5, 128.40, 128.38, 128.1, 127.6, 127.2, 126.3, 126.10, 126.09, 125.1, 123.9, 76.5, 30.9; FTIR (NaCl/thin film) 3560 (brs), 3056, 2978, 2931, 1599, 1505, 1493, 14461, 1372, 1126, 1065, 909, 858 cm^{-1}; HRMS (EI+) [M]+ calculated for $C_{18}H_{16}BO$: 248.1201, found: 248.1193.

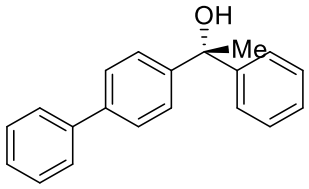

(*R*)-1-([1,1'-biphenyl]-4-yl)-1-phenylethan-1-ol ((*R*)-2.18i). Following a similar procedure as described for **(*R*)-2.18h** above, compound **(*R*)-2.18i** was prepared as a white solid (mp 108–111 °C, 72%). The enantiomeric excess was determined to be 91% by chiral HPLC analysis (CHIRLPAK IB, 1.0 mL/min, 2.0% *i*-PrOH/hexanes, λ=254 nm); t_R(major) = 34.792 min, t_R(minor) = 18.929 min. $[\alpha]_D^{24}$ = +9.0° (c 1.0, $CHCl_3$): ^{1}H NMR (600 MHz, $CDCl_3$) δ 7.61 – 7.57 (m, 2H), 7.57 – 7.54 (m, 2H), 7.51 – 7.46 (m, 4H), 7.43 (dd, *J* = 8.4, 7.0 Hz, 2H), 7.38 – 7.32 (m, 3H), 7.29 – 7.26 (m, 1H), 2.22 (s, 1H), 2.00 (s, 3H); ^{13}C NMR (151 MHz, $CDCl_3$) δ 148.0, 147.2, 140.9, 140.0, 128.9, 128.4, 127.4, 127.21, 127.17, 127.1, 126.4, 126.0, 76.3, 31.0; FTIR (NaCl/thin film) 3458 (brs), 3056, 3028, 2978, 1599, 1486, 1449, 1401, 1266, 1171, 1068, 907, 845 cm^{-1}; HRMS (CI+) [M]+H calculated for $C_{20}H_{19}O$: 275.1436, found: 275.1444.

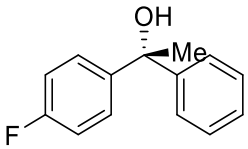

(*R*)-1-(4-fluorophenyl)-1-phenylethan-1-ol ((*R*)-2.18i). Following a similar procedure as described for **(*R*)-2.18h** above, compound **(*R*)-2.18i** was prepared as a colorless oil (95% overall yield from 4-fluoroacetophenone). The enantiomeric excess was determined to be 90% by chiral HPLC analysis (CHIRLPAK IB, 0.4 mL/min, 1.0% *i*-PrOH/hexanes, λ=254 nm); t_R(major) = 52.679 min, t_R(minor) = 49.042 min. $[\alpha]_D^{24}$ = +8.5° (c 1.2, $CHCl_3$): ^{1}H NMR (600 MHz, $CDCl_3$) δ 7.44 – 7.37 (m, 4H), 7.34 (dd, *J* = 8.5, 6.9 Hz, 2H), 7.29 – 7.27 (m, 1H), 7.02 – 6.99 (m, *J* = 8.4, 7.0 Hz, 2H), 2.19 (s, 1H), 1.96 (s, 3H); ^{13}C NMR (151 MHz, $CDCl_3$) δ 162.71, 161.08, 147.92, 144.01 (d, J_{C-F} = 3.2 Hz), 144.00 (d, J_{C-F} = 3.2 Hz), 128.40, 127.75 (d, J_{C-F} = 8.0 Hz), 127.73 (d, J_{C-F} = 8.0 Hz), 127.26, 125.90, 115.07 (d, J_{C-F} = 21.2 Hz), 114.99 (d, J_{C-F} = 21.2 Hz), 76.03, 31.18; ^{19}F NMR (377 MHz, $CDCl_3$) δ –116.17; FTIR (NaCl/thin film) 3410 (brs), 2977, 1652, 1601, 1507, 1384, 1226, 1159, 1070, 835, 701, 567 cm^{-1}; EI-MS (m/z) $[M]^+$ calculated for $C_{14}H_{13}OF$: 216.26, found: 216.13.

2.4.3 Evidence for Stereoretention

As discussed above, the absolute configurations of **2.18c**, **(*S*)-2.19**, and **(*R*)-2.29** were determined by X-ray crystallography. The arylation of **(*S*)-2.19** produced **(*R*)- 2.29**, demonstrating that this arylation proceeds with overall retention of absolute

stereochemistry.

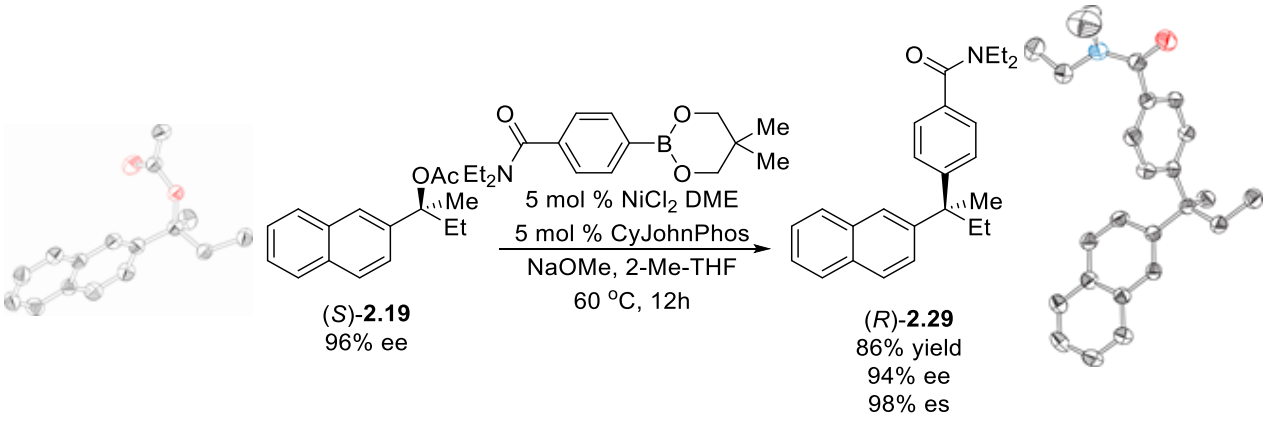

2.4.3.1 Crystal Structure Data for (*R*)-2.29

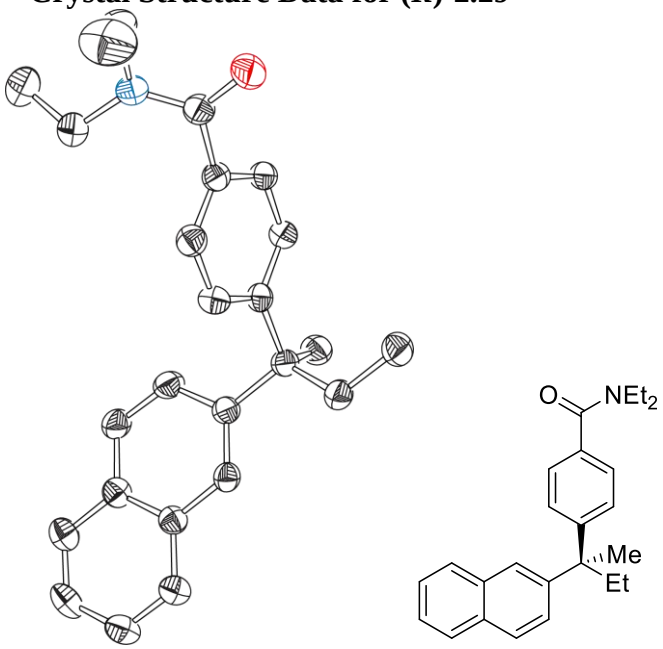

Table 2.4. Sample and crystal data for **(*R*)-2.29**.

Identification code	mary029
Chemical formula	$C_{25}H_{29}NO$
Formula weight	359.49
Temperature	200(2) K
Wavelength	1.54178 Å
Crystal size	0.248 x 0.378 x 0.487 mm
Crystal system	orthorhombic
Space group	P 21 21 21

Unit cell dimensions	a = 8.1727(3) Å	α = 90°
	b = 12.9877(5) Å	β = 90°
	c = 19.1341(7) Å	γ = 90°
Volume	2030.98(13) $Å^3$	
Z	4	
Density (calculated)	1.176 g/cm^3	
Absorption coefficient	0.540 mm^{-1}	
F(000)	776	

Table 2.5. Data collection and structure refinement for **(*R*)-2.29**.

Theta range for data collection	4.11 to 59.90°	
Index ranges	-8<=h<=9, -14<=k<=13, -21<=l<=19	
Reflections collected	6276	
Independent reflections	2630 [R(int) = 0.0365]	
Coverage of independent reflections	95.1%	
Absorption correction	multi-scan	
Max. and min. transmission	0.8780 and 0.7080	
Refinement method	Full-matrix least-squares on F^2	
Refinement program	SHELXL-2014/7 (Sheldrick, 2014)	
Function minimized	$\Sigma\, w(F_o^2 - F_c^2)^2$	
Data / restraints / parameters	2630 / 0 / 249	
Goodness-of-fit on F^2	0.860	
Final R indices	2423 data; I>2σ(I)	R1 = 0.0373, wR2 = 0.1046
	all data	R1 = 0.0407, wR2 = 0.1084
Weighting scheme	$w=1/[\sigma^2(F_o^2)+(0.1000P)^2]$ where $P=(F_o^2+2F_c^2)/3$	
Absolute structure parameter	0.0(3)	
Extinction coefficient	0.0058(9)	
Largest diff. peak and hole	0.135 and -0.151 $eÅ^{-3}$	
R.M.S. deviation from mean	0.037 $eÅ^{-3}$	

Table 2.6. Atomic coordinates and equivalent isotropic atomic displacement parameters ($Å^2$) for **(*R*)-2.29**.

U(eq) is defined as one third of the trace of the orthogonalized U_{ij} tensor.

x/a	**y/b**	**z/c**	**U(eq)**

O1	0.4981(3)	0.50887(17)	0.01225(10)	0.0528(6)
N1	0.5202(3)	0.39117(18)	0.09868(13)	0.0412(6)
C1	0.6431(3)	0.61242(19)	0.24991(13)	0.0288(6)
C2	0.5755(3)	0.5641(2)	0.30982(14)	0.0311(7)
C3	0.4047(4)	0.5453(2)	0.31633(15)	0.0364(7)
C4	0.3434(4)	0.4997(2)	0.37492(16)	0.0445(8)
C5	0.4486(4)	0.4689(2)	0.42913(16)	0.0455(8)
C6	0.6129(4)	0.4850(2)	0.42429(15)	0.0403(7)
C7	0.6800(3)	0.5343(2)	0.36502(14)	0.0334(7)
C8	0.8496(3)	0.5562(2)	0.35893(14)	0.0377(7)
C9	0.9094(3)	0.6044(2)	0.30127(14)	0.0376(8)
C10	0.8070(3)	0.6340(2)	0.24435(13)	0.0305(6)
C11	0.8828(3)	0.6918(2)	0.18274(13)	0.0298(6)
C12	0.9236(4)	0.8013(2)	0.20884(16)	0.0396(7)
C13	0.7628(3)	0.6988(2)	0.12036(13)	0.0354(7)
C14	0.8307(4)	0.7444(2)	0.05339(14)	0.0435(8)
C15	0.0316(3)	0.5282(2)	0.14805(14)	0.0342(7)
C16	0.1636(3)	0.4742(2)	0.12206(14)	0.0355(7)
C17	0.3068(3)	0.5257(2)	0.10319(12)	0.0295(6)
C18	0.3106(3)	0.6315(2)	0.11035(13)	0.0305(6)
C19	0.1794(3)	0.6850(2)	0.13789(13)	0.0303(6)
C20	0.0364(3)	0.6345(2)	0.15721(13)	0.0290(6)
C21	0.4492(4)	0.4735(2)	0.06862(14)	0.0354(7)
C22	0.6428(4)	0.3346(3)	0.05765(18)	0.0536(9)
C23	0.5677(6)	0.2525(3)	0.0140(3)	0.0894(15)
C24	0.4761(4)	0.3501(2)	0.16769(16)	0.0459(8)
C25	0.6199(4)	0.3331(3)	0.21548(18)	0.0530(9)

Table 2.7. Bond lengths (Å) for **(*R*)-2.29**.

O1-C21	1.239(3)	N1-C21	1.345(4)
N1-C24	1.469(4)	N1-C22	1.470(4)
C1-C10	1.373(4)	C1-C2	1.419(4)
C1-H1	0.95	C2-C7	1.413(4)
C2-C3	1.422(4)	C3-C4	1.363(4)
C3-H3	0.95	C4-C5	1.406(4)
C4-H4	0.95	C5-C6	1.361(5)
C5-H5	0.95	C6-C7	1.414(4)
C6-H6	0.95	C7-C8	1.419(4)
C8-C9	1.359(4)	C8-H8	0.95
C9-C10	1.426(4)	C9-H9	0.95
C10-C11	1.529(4)	C11-C20	1.539(4)

C11-C12	1.543(4)	C11-C13	1.548(4)
C12-H12A	0.98	C12-H12B	0.98
C12-H12C	0.98	C13-C14	1.517(4)
C13-H13A	0.99	C13-H13B	0.99
C14-H14A	0.98	C14-H14B	0.98
C14-H14C	0.98	C15-C16	1.379(4)
C15-C20	1.393(4)	C15-H15	0.95
C16-C17	1.396(4)	C16-H16	0.95
C17-C18	1.381(4)	C17-C21	1.501(4)
C18-C19	1.382(4)	C18-H18	0.95
C19-C20	1.390(4)	C19-H19	0.95
C22-C23	1.487(5)	C22-H22A	0.99
C22-H22B	0.99	C23-H23A	0.98
C23-H23B	0.98	C23-H23C	0.98
C24-C25	1.506(5)	C24-H24A	0.99
C24-H24B	0.99	C25-H25A	0.98
C25-H25B	0.98	C25-H25C	0.98

Table 2.8. Bond angles (°) for **(*R*)-2.29**.

C21-N1-C24	124.5(2)	C21-N1-C22	117.6(2)
C24-N1-C22	117.8(2)	C10-C1-C2	122.2(2)
C10-C1-H1	118.9	C2-C1-H1	118.9
C7-C2-C1	119.3(2)	C7-C2-C3	118.8(3)
C1-C2-C3	121.9(3)	C4-C3-C2	120.5(3)
C4-C3-H3	119.8	C2-C3-H3	119.8
C3-C4-C5	120.4(3)	C3-C4-H4	119.8
C5-C4-H4	119.8	C6-C5-C4	120.6(3)
C6-C5-H5	119.7	C4-C5-H5	119.7
C5-C6-C7	120.5(3)	C5-C6-H6	119.8
C7-C6-H6	119.8	C2-C7-C6	119.3(3)
C2-C7-C8	118.3(2)	C6-C7-C8	122.4(3)
C9-C8-C7	120.7(3)	C9-C8-H8	119.7
C7-C8-H8	119.7	C8-C9-C10	122.2(3)
C8-C9-H9	118.9	C10-C9-H9	118.9
C1-C10-C9	117.3(2)	C1-C10-C11	123.7(2)
C9-C10-C11	118.9(2)	C10-C11-C20	109.7(2)
C10-C11-C12	106.9(2)	C20-C11-C12	111.8(2)
C10-C11-C13	111.5(2)	C20-C11-C13	107.5(2)
C12-C11-C13	109.4(2)	C11-C12-H12A	109.5
C11-C12-H12B	109.5	H12A-C12-H12B	109.5
C11-C12-H12C	109.5	H12A-C12-H12C	109.5

H12B-C12-H12C	109.5	C14-C13-C11	116.3(2)
C14-C13-H13A	108.2	C11-C13-H13A	108.2
C14-C13-H13B	108.2	C11-C13-H13B	108.2
H13A-C13-H13B	107.4	C13-C14-H14A	109.5
C13-C14-H14B	109.5	H14A-C14-H14B	109.5
C13-C14-H14C	109.5	H14A-C14-H14C	109.5
H14B-C14-H14C	109.5	C16-C15-C20	121.8(3)
C16-C15-H15	119.1	C20-C15-H15	119.1
C15-C16-C17	120.4(3)	C15-C16-H16	119.8
C17-C16-H16	119.8	C18-C17-C16	118.1(2)
C18-C17-C21	118.4(2)	C16-C17-C21	123.2(2)
C17-C18-C19	121.4(3)	C17-C18-H18	119.3
C19-C18-H18	119.3	C18-C19-C20	121.1(2)
C18-C19-H19	119.5	C20-C19-H19	119.5
C19-C20-C15	117.3(2)	C19-C20-C11	122.8(2)
C15-C20-C11	119.8(2)	O1-C21-N1	121.9(3)
O1-C21-C17	117.8(3)	N1-C21-C17	120.4(2)
N1-C22-C23	112.1(3)	N1-C22-H22A	109.2
C23-C22-H22A	109.2	N1-C22-H22B	109.2
C23-C22-H22B	109.2	H22A-C22-H22B	107.9
C22-C23-H23A	109.5	C22-C23-H23B	109.5
H23A-C23-H23B	109.5	C22-C23-H23C	109.5
H23A-C23-H23C	109.5	H23B-C23-H23C	109.5
N1-C24-C25	114.1(3)	N1-C24-H24A	108.7
C25-C24-H24A	108.7	N1-C24-H24B	108.7
C25-C24-H24B	108.7	H24A-C24-H24B	107.6
C24-C25-H25A	109.5	C24-C25-H25B	109.5
H25A-C25-H25B	109.5	C24-C25-H25C	109.5
H25A-C25-H25C	109.5	H25B-C25-H25C	109.5

Table 2.9. Torsion angles (°) for **(*R*)-2.29**.

C10-C1-C2-C7	-1.8(4)	C10-C1-C2-C3	177.7(3)
C7-C2-C3-C4	0.3(4)	C1-C2-C3-C4	-179.2(3)
C2-C3-C4-C5	-1.3(4)	C3-C4-C5-C6	0.7(5)
C4-C5-C6-C7	0.9(5)	C1-C2-C7-C6	-179.2(2)
C3-C2-C7-C6	1.3(4)	C1-C2-C7-C8	1.4(4)
C3-C2-C7-C8	-178.2(3)	C5-C6-C7-C2	-1.9(4)
C5-C6-C7-C8	177.5(3)	C2-C7-C8-C9	-0.2(4)
C6-C7-C8-C9	-179.6(3)	C7-C8-C9-C10	-0.7(5)
C2-C1-C10-C9	1.0(4)	C2-C1-C10-C11	-176.1(2)

C8-C9-C10-C1	0.3(4)	C8-C9-C10-C11	177.5(3)
C1-C10-C11-C20	-133.0(3)	C9-C10-C11-C20	50.0(3)
C1-C10-C11-C12	105.5(3)	C9-C10-C11-C12	-71.5(3)
C1-C10-C11-C13	-14.1(4)	C9-C10-C11-C13	168.9(2)
C10-C11-C13-C14	-173.7(2)	C20-C11-C13-C14	-53.4(3)
C12-C11-C13-C14	68.3(3)	C20-C15-C16-C17	-0.8(4)
C15-C16-C17-C18	-1.0(4)	C15-C16-C17-C21	-174.3(2)
C16-C17-C18-C19	2.5(4)	C21-C17-C18-C19	176.1(2)
C17-C18-C19-C20	-2.2(4)	C18-C19-C20-C15	0.4(4)
C18-C19-C20-C11	-175.2(2)	C16-C15-C20-C19	1.1(4)
C16-C15-C20-C11	176.8(2)	C10-C11-C20-C19	-138.7(3)
C12-C11-C20-C19	-20.3(4)	C13-C11-C20-C19	99.9(3)
C10-C11-C20-C15	45.9(3)	C12-C11-C20-C15	164.3(2)
C13-C11-C20-C15	-75.6(3)	C24-N1-C21-O1	175.3(3)
C22-N1-C21-O1	-8.8(4)	C24-N1-C21-C17	-4.5(4)
C22-N1-C21-C17	171.3(3)	C18-C17-C21-O1	-48.9(4)
C16-C17-C21-O1	124.4(3)	C18-C17-C21-N1	131.0(3)
C16-C17-C21-N1	-55.7(4)	C21-N1-C22-C23	-88.4(4)
C24-N1-C22-C23	87.7(4)	C21-N1-C24-C25	-129.8(3)
C22-N1-C24-C25	54.3(4)		

Table 2.10. Anisotropic atomic displacement parameters (Å^2) for **(*R*)-2.29**.
The anisotropic atomic displacement factor exponent takes the form: $-2\pi^2[h^2 a^{*2} U_{11} + ... + 2 h k a^* b^* U_{12}]$

	U_{11}	**U_{22}**	**U_{33}**	**U_{23}**	**U_{13}**	**U_{12}**
O1	0.0573(14)	0.0621(14)	0.0391(12)	0.0079(11)	0.0201(12)	0.0140(12)
N1	0.0358(14)	0.0424(14)	0.0453(14)	0.0030(12)	0.0100(12)	0.0097(12)
C1	0.0289(14)	0.0312(14)	0.0262(14)	0.0003(12)	-0.0029(12)	0.0033(11)
C2	0.0331(15)	0.0278(15)	0.0323(16)	-0.0029(12)	0.0014(13)	-0.0010(12)
C3	0.0313(15)	0.0395(17)	0.0384(17)	0.0019(14)	0.0009(14)	-0.0025(13)
C4	0.0386(17)	0.0449(18)	0.0499(19)	0.0010(16)	0.0045(15)	-0.0121(14)
C5	0.0537(19)	0.0443(18)	0.0385(18)	0.0054(14)	0.0095(15)	-0.0116(15)
C6	0.0464(18)	0.0413(17)	0.0332(16)	0.0040(13)	0.0004(15)	-0.0025(14)
C7	0.0356(15)	0.0325(15)	0.0319(15)	-0.0034(13)	-0.0005(13)	0.0001(12)
C8	0.0315(15)	0.0515(18)	0.0301(15)	0.0065(14)	-0.0023(14)	0.0056(13)
C9	0.0252(15)	0.0516(19)	0.0360(17)	0.0004(14)	-0.0015(13)	0.0014(13)
C10	0.0276(13)	0.0337(15)	0.0302(14)	0.0024(12)	0.0000(13)	0.0047(12)
C11	0.0230(13)	0.0367(15)	0.0295(14)	0.0017(12)	0.0004(12)	0.0030(11)
C12	0.0370(16)	0.0366(16)	0.0453(17)	-0.0011(14)	0.0076(14)	0.0029(13)
C13	0.0297(15)	0.0412(16)	0.0353(16)	0.0038(13)	0.0005(12)	0.0052(13)

C14	0.0436(19)	0.0510(17)	0.0359(15)	0.0077(15)	0.0006(15)	0.0077(15)
C15	0.0274(14)	0.0372(17)	0.0379(15)	0.0044(13)	0.0035(13)	-0.0020(12)
C16	0.0367(16)	0.0305(15)	0.0392(16)	-0.0013(13)	0.0041(13)	0.0014(13)
C17	0.0300(14)	0.0378(16)	0.0207(13)	0.0026(12)	0.0005(12)	0.0046(13)
C18	0.0255(13)	0.0392(16)	0.0269(13)	0.0054(12)	-0.0017(12)	-0.0016(12)
C19	0.0290(15)	0.0312(14)	0.0309(14)	0.0011(12)	0.0013(13)	0.0009(12)
C20	0.0278(14)	0.0329(16)	0.0262(14)	0.0039(12)	-0.0015(12)	0.0009(11)
C21	0.0330(15)	0.0413(17)	0.0319(16)	-0.0020(13)	0.0045(13)	0.0039(13)
C22	0.0482(19)	0.0486(19)	0.064(2)	-0.0055(18)	0.0122(18)	0.0142(16)
C23	0.092(3)	0.063(2)	0.113(4)	-0.035(3)	0.027(3)	-0.003(2)
C24	0.0411(17)	0.0452(18)	0.0513(18)	0.0145(15)	0.0062(16)	0.0087(14)
C25	0.051(2)	0.0470(19)	0.061(2)	0.0045(16)	-0.0059(18)	0.0073(16)

Table 2.11. Hydrogen atomic coordinates and isotropic atomic displacement parameters ($Å^2$) for **(*R*)-2.29**.

	x/a	**y/b**	**z/c**	**U(eq)**
H1	-0.4274	0.6304	0.2124	0.035
H3	-0.6672	0.5646	0.2796	0.044
H4	-0.7711	0.4887	0.3792	0.053
H5	-0.5952	0.4366	0.4695	0.055
H6	-0.3172	0.4629	0.4610	0.048
H8	-0.0780	0.5370	0.3955	0.045
H9	0.0232	0.6188	0.2988	0.045
H12A	-0.1767	0.8350	0.2251	0.059
H12B	-0.0286	0.8413	0.1705	0.059
H12C	0.0021	0.7970	0.2475	0.059
H13A	-0.2777	0.6285	0.1100	0.042
H13B	-0.3326	0.7405	0.1350	0.042
H14A	-0.1280	0.8139	0.0626	0.065
H14B	-0.2562	0.7477	0.0182	0.065
H14C	-0.0799	0.7010	0.0361	0.065
H15	-0.0653	0.4918	0.1600	0.041
H16	0.1570	0.4016	0.1170	0.043
H18	0.4054	0.6682	0.0960	0.037
H19	0.1871	0.7575	0.1437	0.036
H22A	0.7236	0.3032	0.0898	0.064
H22B	0.7019	0.3834	0.0270	0.064
H23A	0.5062	0.2051	0.0440	0.134
H23B	0.6538	0.2145	-0.0105	0.134
H23C	0.4934	0.2837	-0.0201	0.134
H24A	0.4182	0.2838	0.1613	0.055

H24B	0.3992	0.3985	0.1905	0.055
H25A	0.6849	0.2750	0.1984	0.079
H25B	0.5805	0.3181	0.2628	0.079
H25C	0.6879	0.3953	0.2164	0.079

2.4.3.2 Crystal Structure Data for (*S*)-2.19

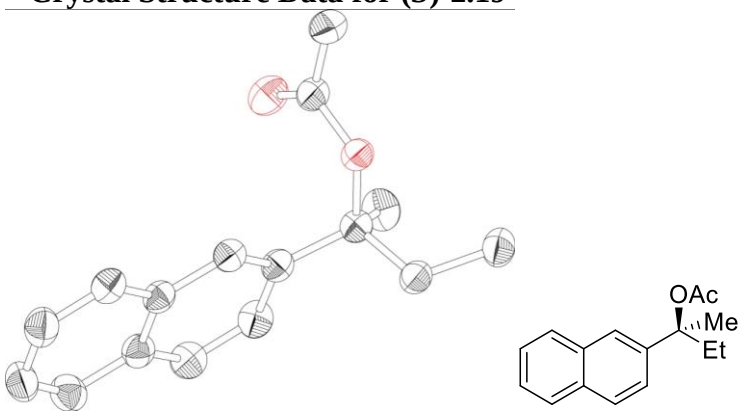

Table 2.12. Sample and crystal data for **(*S*)-2.19.**

Identification code	mary035	
Chemical formula	$C_{16}H_{18}O_2$	
Formula weight	242.30 g/mol	
Temperature	200(2) K	
Wavelength	1.54178 Å	
Crystal size	0.144 x 0.196 x 0.269 mm	
Crystal system	monoclinic	
Space group	C 1 2 1	
Unit cell dimensions	a = 21.7695(7) Å	α = 90°
	b = 5.8807(2) Å	β = 97.282(2)°
	c = 10.4637(3) Å	γ = 90°
Volume	1328.76(7) $Å^3$	
Z	4	
Density (calculated)	1.211 g/cm^3	
Absorption coefficient	0.620 mm^{-1}	

F(000)	520

Table 2.13. Data collection and structure refinement for **(*S*)-2.19.**

Theta range for data collection	4.09 to 75.07°	
Index ranges	-27<=h<=26, -7<=k<=7, -13<=l<=12	
Reflections collected	13728	
Independent reflections	2708 [R(int) = 0.0319]	
Coverage of independent reflections	99.4%	
Absorption correction	multi-scan	
Max. and min. transmission	0.7539 and 0.6441	
Structure solution technique	direct methods	
Structure solution program	SHELXS-97 (Sheldrick 2008)	
Refinement method	Full-matrix least-squares on F^2	
Refinement program	SHELXL-2014/7 (Sheldrick, 2014)	
Function minimized	$\Sigma\ w(F_o^2 - F_c^2)^2$	
Data / restraints / parameters	2708 / 1 / 166	
Goodness-of-fit on F^2	1.035	
Final R indices	2626 data; I>2σ(I)	R1 = 0.0349, wR2 = 0.0937
	all data	R1 = 0.0359, wR2 = 0.0948
Weighting scheme	$w=1/[\sigma^2(F_o^2)+(0.0638P)^2+0.1971P]$ where $P=(F_o^2+2F_c^2)/3$	
Absolute structure parameter	-0.1(1)	
Largest diff. peak and hole	0.193 and -0.164 eÅ^{-3}	
R.M.S. deviation from mean	0.034 eÅ^{-3}	

Table 2.14. Atomic coordinates and equivalent isotropic atomic displacement parameters (Å^2) for **(*S*)-2.19.**

U(eq) is defined as one third of the trace of the orthogonalized U_{ij} tensor.

	x/a	**y/b**	**z/c**	**U(eq)**
O1	0.40605(5)	0.6779(2)	0.16441(11)	0.0352(3)
O2	0.32500(7)	0.4448(3)	0.10507(15)	0.0560(4)
C1	0.44069(7)	0.5057(3)	0.24545(16)	0.0324(4)
C2	0.45441(10)	0.3005(3)	0.1639(2)	0.0452(4)
C3	0.50055(7)	0.6315(3)	0.29722(16)	0.0353(4)
C4	0.54151(8)	0.6990(4)	0.19539(19)	0.0444(4)
C5	0.35048(8)	0.6252(4)	0.09814(17)	0.0407(4)
C6	0.32655(9)	0.8226(5)	0.0164(2)	0.0528(5)
C7	0.40667(7)	0.4437(3)	0.35920(16)	0.0324(4)
C8	0.42021(8)	0.2325(3)	0.42318(19)	0.0378(4)
C9	0.39467(8)	0.1768(3)	0.53140(18)	0.0398(4)
C10	0.35368(8)	0.3262(3)	0.58396(18)	0.0358(4)

C11	0.32657(9)	0.2747(4)	0.69691(19)	0.0445(4)
C12	0.28692(9)	0.4252(4)	0.74387(19)	0.0481(5)
C13	0.27174(9)	0.6322(4)	0.67982(19)	0.0453(5)
C14	0.29716(8)	0.6866(3)	0.57105(18)	0.0381(4)
C15	0.33914(7)	0.5370(3)	0.52055(17)	0.0325(4)
C16	0.36692(7)	0.5906(3)	0.40857(16)	0.0327(3)

Table 2.15. Bond lengths (Å) for **(*S*)-2.19.**

O1-C5	1.352(2)	O1-C1	1.466(2)
O2-C5	1.204(3)	C1-C7	1.524(2)
C1-C2	1.529(2)	C1-C3	1.536(2)
C2-H2A	0.98	C2-H2B	0.98
C2-H2C	0.98	C3-C4	1.526(2)
C3-H3A	0.99	C3-H3B	0.99
C4-H4A	0.98	C4-H4B	0.98
C4-H4C	0.98	C5-C6	1.496(3)
C6-H6A	0.98	C6-H6B	0.98
C6-H6C	0.98	C7-C16	1.369(2)
C7-C8	1.424(2)	C8-C9	1.363(3)
C8-H8	0.95	C9-C10	1.413(3)
C9-H9	0.95	C10-C11	1.419(3)
C10-C15	1.423(2)	C11-C12	1.370(3)
C11-H11	0.95	C12-C13	1.409(3)
C12-H12	0.95	C13-C14	1.365(3)
C13-H13	0.95	C14-C15	1.418(2)
C14-H14	0.95	C15-C16	1.420(2)
C16-H16	0.95		

Table 2.16. Bond angles (°) for **(*S*)-2.19.**

C5-O1-C1	119.98(14)	O1-C1-C7	110.59(12)
O1-C1-C2	110.15(14)	C7-C1-C2	113.31(15)
O1-C1-C3	102.86(13)	C7-C1-C3	108.33(13)
C2-C1-C3	111.09(14)	C1-C2-H2A	109.5
C1-C2-H2B	109.5	H2A-C2-H2B	109.5
C1-C2-H2C	109.5	H2A-C2-H2C	109.5
H2B-C2-H2C	109.5	C4-C3-C1	115.06(14)
C4-C3-H3A	108.5	C1-C3-H3A	108.5
C4-C3-H3B	108.5	C1-C3-H3B	108.5
H3A-C3-H3B	107.5	C3-C4-H4A	109.5
C3-C4-H4B	109.5	H4A-C4-H4B	109.5
C3-C4-H4C	109.5	H4A-C4-H4C	109.5

H4B-C4-H4C	109.5	O2-C5-O1	124.07(19)
O2-C5-C6	126.06(18)	O1-C5-C6	109.87(17)
C5-C6-H6A	109.5	C5-C6-H6B	109.5
H6A-C6-H6B	109.5	C5-C6-H6C	109.5
H6A-C6-H6C	109.5	H6B-C6-H6C	109.5
C16-C7-C8	118.41(16)	C16-C7-C1	122.46(15)
C8-C7-C1	118.95(15)	C9-C8-C7	121.23(17)
C9-C8-H8	119.4	C7-C8-H8	119.4
C8-C9-C10	121.20(17)	C8-C9-H9	119.4
C10-C9-H9	119.4	C9-C10-C11	122.78(17)
C9-C10-C15	118.34(16)	C11-C10-C15	118.88(16)
C12-C11-C10	120.54(19)	C12-C11-H11	119.7
C10-C11-H11	119.7	C11-C12-C13	120.54(18)
C11-C12-H12	119.7	C13-C12-H12	119.7
C14-C13-C12	120.26(19)	C14-C13-H13	119.9
C12-C13-H13	119.9	C13-C14-C15	120.91(18)
C13-C14-H14	119.5	C15-C14-H14	119.5
C14-C15-C16	122.12(16)	C14-C15-C10	118.86(16)
C16-C15-C10	119.02(15)	C7-C16-C15	121.79(16)
C7-C16-H16	119.1	C15-C16-H16	119.1

Table 2.17. Torsion angles (°) for **(*S*)-2.19.**

C5-O1-C1-C7	-66.62(18)	C5-O1-C1-C2	59.41(19)
C5-O1-C1-C3	177.89(14)	O1-C1-C3-C4	-64.92(17)
C7-C1-C3-C4	177.97(16)	C2-C1-C3-C4	52.9(2)
C1-O1-C5-O2	3.6(3)	C1-O1-C5-C6	-176.21(14)
O1-C1-C7-C16	-26.1(2)	C2-C1-C7-C16	-150.35(16)
C3-C1-C7-C16	85.91(18)	O1-C1-C7-C8	158.93(14)
C2-C1-C7-C8	34.7(2)	C3-C1-C7-C8	-89.05(18)
C16-C7-C8-C9	-0.3(3)	C1-C7-C8-C9	174.88(16)
C7-C8-C9-C10	0.2(3)	C8-C9-C10-C11	-179.53(18)
C8-C9-C10-C15	0.5(3)	C9-C10-C11-C12	-179.82(18)
C15-C10-C11-C12	0.2(3)	C10-C11-C12-C13	0.9(3)
C11-C12-C13-C14	-1.0(3)	C12-C13-C14-C15	0.0(3)
C13-C14-C15-C16	-179.14(16)	C13-C14-C15-C10	1.1(3)
C9-C10-C15-C14	178.85(16)	C11-C10-C15-C14	-1.2(2)
C9-C10-C15-C16	-0.9(2)	C11-C10-C15-C16	179.06(16)
C8-C7-C16-C15	-0.2(2)	C1-C7-C16-C15	-175.20(14)
C14-C15-C16-C7	-178.95(15)	C10-C15-C16-C7	0.8(2)

Table 2.18. Anisotropic atomic displacement parameters ($Å^2$) for **(*S*)-2.19.**

The anisotropic atomic displacement factor exponent takes the form: $-2\pi^2[h^2 a^{*2} U_{11} + ... + 2 h k a^* b^* U_{12}]$

	U_{11}	U_{22}	U_{33}	U_{23}	U_{13}	U_{12}
O1	0.0306(6)	0.0377(6)	0.0366(6)	0.0034(5)	0.0016(4)	-0.0007(5)
O2	0.0427(7)	0.0672(10)	0.0555(8)	-0.0023(8)	-0.0033(6)	-0.0155(8)
C1	0.0318(7)	0.0301(8)	0.0353(8)	-0.0008(7)	0.0035(6)	0.0007(6)
C2	0.0510(11)	0.0386(10)	0.0478(10)	-0.0099(8)	0.0134(8)	-0.0023(8)
C3	0.0299(8)	0.0387(9)	0.0368(8)	-0.0010(7)	0.0029(6)	-0.0005(7)
C4	0.0357(9)	0.0512(11)	0.0472(10)	-0.0004(9)	0.0085(7)	-0.0061(8)
C5	0.0320(8)	0.0560(12)	0.0341(8)	-0.0024(8)	0.0037(6)	-0.0019(8)
C6	0.0387(9)	0.0745(15)	0.0443(10)	0.0088(10)	0.0016(8)	0.0103(10)
C7	0.0308(7)	0.0296(8)	0.0363(8)	-0.0022(7)	0.0025(6)	-0.0018(6)
C8	0.0376(8)	0.0283(8)	0.0479(10)	-0.0003(7)	0.0071(7)	0.0030(7)
C9	0.0420(9)	0.0291(8)	0.0478(10)	0.0037(8)	0.0036(7)	0.0002(7)
C10	0.0334(8)	0.0342(8)	0.0391(8)	0.0004(7)	0.0025(6)	-0.0048(7)
C11	0.0469(10)	0.0434(10)	0.0432(10)	0.0055(8)	0.0059(8)	-0.0062(8)
C12	0.0482(10)	0.0577(12)	0.0407(9)	-0.0002(9)	0.0146(8)	-0.0094(9)
C13	0.0395(9)	0.0528(12)	0.0448(10)	-0.0086(8)	0.0100(7)	-0.0004(8)
C14	0.0337(8)	0.0379(9)	0.0425(9)	-0.0033(8)	0.0036(6)	0.0010(7)
C15	0.0287(7)	0.0307(8)	0.0374(8)	-0.0006(6)	0.0013(6)	-0.0029(6)
C16	0.0320(7)	0.0282(8)	0.0374(8)	0.0006(6)	0.0024(6)	-0.0005(6)

Table 2.19. Hydrogen atomic coordinates and isotropic atomic displacement parameters ($Å^2$) for **(*S*)-2.19.**

	x/a	**y/b**	**z/c**	**U(eq)**
H2A	0.4184	0.1992	0.1532	0.068
H2B	0.4904	0.2184	0.2070	0.068
H2C	0.4633	0.3526	0.0791	0.068
H3A	0.4894	0.7708	0.3422	0.042
H3B	0.5249	0.5333	0.3617	0.042
H4A	0.5574	0.5617	0.1577	0.067
H4B	0.5763	0.7908	0.2354	0.067
H4C	0.5172	0.7877	0.1276	0.067
H6A	0.3521	0.8435	-0.0533	0.079
H6B	0.3282	0.9605	0.0693	0.079
H6C	0.2836	0.7932	-0.0204	0.079
H8	0.4476	0.1286	0.3898	0.045
H9	0.4046	0.0348	0.5722	0.048
H11	0.3360	0.1347	0.7403	0.053
H12	0.2695	0.3896	0.8202	0.058
H13	0.2437	0.7343	0.7124	0.054
H14	0.2866	0.8267	0.5286	0.046

H16	0.3577	0.7322	0.3668	0.039

2.4.3.3 Crystal Structure Data for (*S*)-2.18c

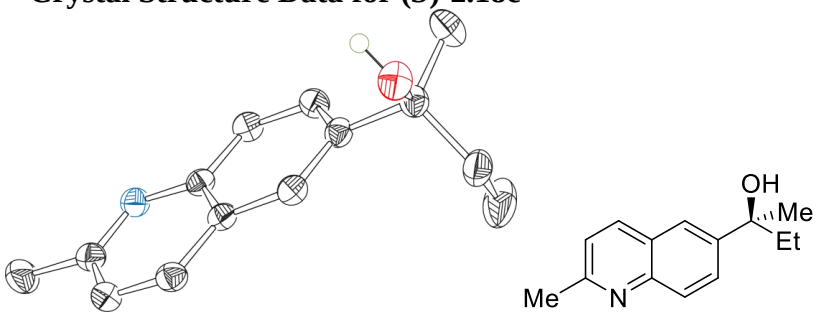

Table 2.20. Sample and crystal data for **(*S*)-2.18c**.

Identification code	mary026	
Chemical formula	$C_{14}H_{17}NO$	
Formula weight	215.28	
Temperature	200(2) K	
Wavelength	1.54178 Å	
Crystal size	0.216 x 0.425 x 0.545 mm	
Crystal system	orthorhombic	
Space group	P 21 21 21	
Unit cell dimensions	a = 5.9000(2) Å	α = 90°
	b = 8.4404(3) Å	β = 90°
	c = 23.7442(10) Å	γ = 90°
Volume	1182.42(8) $Å^3$	
Z	4	
Density (calculated)	1.209 g/cm^3	
Absorption coefficient	0.591 mm^{-1}	
F(000)	464	

Table 2.21. Data collection and structure refinement for **(*S*)-2.18c**.

Theta range for data collection	3.72 to 74.70°
Index ranges	-7<=h<=7, -10<=k<=10, -29<=l<=29
Reflections collected	19673
Independent reflections	2415 [R(int) = 0.0388]
Max. and min. transmission	0.8830 and 0.7390
Refinement method	Full-matrix least-squares on F^2
Refinement program	SHELXL-2014/7 (Sheldrick, 2014)

Function minimized	$\Sigma w(F_o^2 - F_c^2)^2$	
Data / restraints / parameters	2415 / 0 / 150	
Goodness-of-fit on F^2	1.020	
Δ/σ_{max}	0.001	
Final R indices	2389 data; I>2σ(I)	R1 = 0.0333, wR2 = 0.0953
	all data	R1 = 0.0337, wR2 = 0.0976
Weighting scheme	$w=1/[\sigma^2(F_o^2)+(0.0716P)^2+0.1296P]$ where $P=(F_o^2+2F_c^2)/3$	
Absolute structure parameter	-0.1(1)	
Extinction coefficient	0.0143(18)	
Largest diff. peak and hole	0.213 and -0.198 eÅ^{-3}	
R.M.S. deviation from mean	0.044 eÅ^{-3}	

Table 2.22. Atomic coordinates and equivalent isotropic atomic displacement parameters (Å^2) for **(*S*)-2.18c**.
U(eq) is defined as one third of the trace of the orthogonalized U_{ij} tensor.

	x/a	**y/b**	**z/c**	**U(eq)**
N1	0.7994(2)	0.02782(15)	0.06577(6)	0.0283(3)
O1	0.37311(19)	0.72139(14)	0.84869(5)	0.0341(3)
C1	0.7123(4)	0.1740(2)	0.15036(7)	0.0426(4)
C2	0.6518(3)	0.12030(18)	0.09177(6)	0.0297(3)
C3	0.4435(3)	0.16671(18)	0.06700(7)	0.0309(4)
C4	0.3886(3)	0.11487(18)	0.01428(6)	0.0275(3)
C5	0.5437(3)	0.01707(16)	0.98464(6)	0.0244(3)
C6	0.5001(2)	0.95546(17)	0.93022(6)	0.0256(3)
C7	0.6555(3)	0.86111(17)	0.90266(6)	0.0254(3)
C8	0.8641(3)	0.82844(17)	0.92987(6)	0.0275(3)
C9	0.9091(2)	0.88311(18)	0.98318(6)	0.0275(3)
C10	0.7501(3)	0.97764(16)	0.01203(6)	0.0243(3)
C11	0.5951(3)	0.79050(17)	0.84508(6)	0.0273(3)
C12	0.7606(3)	0.6636(2)	0.82559(7)	0.0408(4)
C13	0.5692(3)	0.9218(2)	0.80068(7)	0.0376(4)
C14	0.7760(5)	0.0252(3)	0.79252(8)	0.0610(7)

Table 2.23. Bond lengths (Å) for **(*S*)-2.18c**.

N1-C2	1.322(2)	N1-C10	1.376(2)
O1-C11	1.4365(19)	O1-H1	0.84

C1-C2	1.506(2)	C1-H1A	0.98
C1-H1B	0.98	C1-H1C	0.98
C2-C3	1.418(2)	C3-C4	1.365(2)
C3-H3	0.95	C4-C5	1.419(2)
C4-H4	0.95	C5-C6	1.416(2)
C5-C10	1.420(2)	C6-C7	1.379(2)
C6-H6	0.95	C7-C8	1.417(2)
C7-C11	1.5335(19)	C8-C9	1.373(2)
C8-H8	0.95	C9-C10	1.409(2)
C9-H9	0.95	C11-C12	1.522(2)
C11-C13	1.537(2)	C12-H12A	0.98
C12-H12B	0.98	C12-H12C	0.98
C13-C14	1.512(3)	C13-H13A	0.99
C13-H13B	0.99	C14-H14A	0.98
C14-H14B	0.98	C14-H14C	0.98

Table 2.24. Bond angles (°) for **(*S*)-2.18c**.

C2-N1-C10	118.39(14)	C11-O1-H1	109.5
C2-C1-H1A	109.5	C2-C1-H1B	109.5
H1A-C1-H1B	109.5	C2-C1-H1C	109.5
H1A-C1-H1C	109.5	H1B-C1-H1C	109.5
N1-C2-C3	122.71(14)	N1-C2-C1	116.91(15)
C3-C2-C1	120.37(15)	C4-C3-C2	119.84(14)
C4-C3-H3	120.1	C2-C3-H3	120.1
C3-C4-C5	119.22(14)	C3-C4-H4	120.4
C5-C4-H4	120.4	C6-C5-C4	123.29(14)
C6-C5-C10	119.17(13)	C4-C5-C10	117.53(13)
C7-C6-C5	121.61(13)	C7-C6-H6	119.2
C5-C6-H6	119.2	C6-C7-C8	118.24(13)
C6-C7-C11	119.53(13)	C8-C7-C11	122.19(13)
C9-C8-C7	121.53(14)	C9-C8-H8	119.2
C7-C8-H8	119.2	C8-C9-C10	120.62(14)
C8-C9-H9	119.7	C10-C9-H9	119.7
N1-C10-C9	118.97(14)	N1-C10-C5	122.28(14)
C9-C10-C5	118.75(13)	O1-C11-C12	108.50(13)
O1-C11-C7	108.45(11)	C12-C11-C7	113.30(13)
O1-C11-C13	104.08(12)	C12-C11-C13	111.28(14)
C7-C11-C13	110.75(12)	C11-C12-H12A	109.5
C11-C12-H12B	109.5	H12A-C12-H12B	109.5
C11-C12-H12C	109.5	H12A-C12-H12C	109.5

H12B-C12-H12C	109.5	C14-C13-C11	115.07(16)
C14-C13-H13A	108.5	C11-C13-H13A	108.5
C14-C13-H13B	108.5	C11-C13-H13B	108.5
H13A-C13-H13B	107.5	C13-C14-H14A	109.5
C13-C14-H14B	109.5	H14A-C14-H14B	109.5
C13-C14-H14C	109.5	H14A-C14-H14C	109.5
H14B-C14-H14C	109.5		

Table 2.25. Torsion angles (°) for **(*S*)-2.18c**.

C10-N1-C2-C3	1.4(2)	C10-N1-C2-C1	-179.53(14)
N1-C2-C3-C4	0.3(2)	C1-C2-C3-C4	-178.76(15)
C2-C3-C4-C5	-1.1(2)	C3-C4-C5-C6	178.91(13)
C3-C4-C5-C10	0.2(2)	C4-C5-C6-C7	179.80(14)
C10-C5-C6-C7	-1.5(2)	C5-C6-C7-C8	-0.9(2)
C5-C6-C7-C11	176.90(12)	C6-C7-C8-C9	2.6(2)
C11-C7-C8-C9	-175.20(13)	C7-C8-C9-C10	-1.7(2)
C2-N1-C10-C9	178.04(13)	C2-N1-C10-C5	-2.3(2)
C8-C9-C10-N1	178.83(13)	C8-C9-C10-C5	-0.8(2)
C6-C5-C10-N1	-177.24(13)	C4-C5-C10-N1	1.5(2)
C6-C5-C10-C9	2.4(2)	C4-C5-C10-C9	-178.84(13)
C6-C7-C11-O1	-47.66(18)	C8-C7-C11-O1	130.09(14)
C6-C7-C11-C12	-168.19(14)	C8-C7-C11-C12	9.6(2)
C6-C7-C11-C13	65.96(18)	C8-C7-C11-C13	-116.29(16)
O1-C11-C13-C14	174.47(15)	C12-C11-C13-C14	-68.9(2)
C7-C11-C13-C14	58.1(2)		

Table 2.26. Anisotropic atomic displacement parameters (Å^2) for **(*S*)-2.18c**.
The anisotropic atomic displacement factor exponent takes the form: $-2\pi^2[h^2 a^{*2} U_{11} + ... + 2 h k a^* b^* U_{12}]$

	U_{11}	**U_{22}**	**U_{33}**	**U_{23}**	**U_{13}**	**U_{12}**
N1	0.0306(7)	0.0276(6)	0.0268(6)	-0.0002(5)	-0.0030(5)	0.0005(5)
O1	0.0311(6)	0.0391(6)	0.0321(6)	-0.0004(4)	-0.0023(4)	-0.0084(5)
C1	0.0553(11)	0.0413(9)	0.0311(8)	-0.0072(7)	-0.0055(8)	0.0079(8)
C2	0.0365(8)	0.0247(6)	0.0279(7)	0.0000(6)	-0.0006(6)	-0.0004(6)
C3	0.0348(8)	0.0276(7)	0.0301(7)	-0.0007(6)	0.0041(6)	0.0036(6)
C4	0.0253(7)	0.0265(6)	0.0308(7)	0.0018(6)	-0.0003(6)	0.0023(6)
C5	0.0242(7)	0.0225(6)	0.0264(7)	0.0033(5)	0.0005(5)	-0.0006(6)
C6	0.0230(7)	0.0270(7)	0.0268(7)	0.0021(5)	-0.0021(6)	-0.0004(6)

C7	0.0262(7)	0.0257(6)	0.0242(6)	0.0019(5)	0.0011(5)	-0.0031(6)
C8	0.0235(7)	0.0290(7)	0.0301(7)	-0.0010(6)	0.0016(6)	0.0023(6)
C9	0.0226(7)	0.0293(7)	0.0305(7)	0.0011(6)	-0.0028(5)	0.0006(6)
C10	0.0245(7)	0.0222(6)	0.0260(7)	0.0021(5)	-0.0016(5)	-0.0022(6)
C11	0.0278(7)	0.0293(7)	0.0249(7)	-0.0013(5)	-0.0009(5)	-0.0025(6)
C12	0.0406(9)	0.0441(9)	0.0377(8)	-0.0141(7)	-0.0021(7)	0.0055(8)
C13	0.0509(10)	0.0376(8)	0.0242(7)	0.0019(6)	-0.0016(7)	-0.0046(8)
C14	0.0884(17)	0.0595(12)	0.0351(9)	0.0044(8)	0.0028(11)	-0.0373(13)

Table 2.27. Hydrogen atomic coordinates and isotropic atomic displacement parameters ($Å^2$) for **(*S*)-2.18c**.

	x/a	**y/b**	**z/c**	**U(eq)**
H1	0.3743	0.6477	0.8725	0.051
H1A	0.6046	1.1287	1.1773	0.064
H1B	0.7057	1.2898	1.1523	0.064
H1C	0.8659	1.1382	1.1596	0.064
H3	0.3423	1.2337	1.0870	0.037
H4	0.2483	1.1439	0.9976	0.033
H6	0.3605	0.9797	0.9123	0.031
H8	0.9754	0.7673	0.9108	0.033
H9	1.0488	0.8570	1.0008	0.033
H12A	0.7689	0.5794	0.8539	0.061
H12B	0.9111	0.7106	0.8205	0.061
H12C	0.7085	0.6189	0.7898	0.061
H13A	0.5308	0.8720	0.7642	0.045
H13B	0.4402	0.9903	0.8116	0.045
H14A	0.8085	1.0824	0.8275	0.091
H14B	0.7473	1.1013	0.7622	0.091
H14C	0.9062	0.9587	0.7825	0.091

REFERENCES

(1) (a) Feng, C.; Kaneko, Y.; Kobayashi, Y. *Tetrahedron Lett.* **2013**, *54*, 4629. (b) Feng, C.; Kobayashi, Y. *J. Org. Chem.* **2013**, *78*, 3755. (c) Potter, B.; Edelstein, E. K.; Morken, J. P. *Organic Letters.* **2016**, *18*, 3286.

(2) (a) Joshi-Pangu, A.; Wang, C.-Y.; Biscoe, M. R. *J. Am. Chem. Soc.* **2011**, *133*, 8478. (b) Zultanski, S. L.; Fu, G. C. *J. Am. Chem. Soc.* **2013**, *135*, 624. (c). Huang, C.-Y.; Doyle, A. G. *J. Am. Chem. Soc.* **2015**, *137*, 5638.

(3) (a) Zhou, Q.; Srinivas, H. D.; Dasgupta, S.; Watson, M. P. *J. Am. Chem. Soc.* **2013,** *135*, 3307. (b) Maity, P.; Shacklady-McAtee, D. M.; Yap, G. P. A.; Sirianni, E. R.; Watson, M. P. *J. Am. Chem. Soc.* **2013,** *135*, 280.

(4) Jeon, S.-J.; Li, H.; Walsh, P. J. *J. Am. Chem. Soc.* **2005**, *127*, 16416.

(5) Balsells, J.; Walsh, P. J. *J. Am. Chem. Soc.* **2000**, *122*, 3250

(6) (a) Yagupsky, G.; Mowat, W.; Shortland, A.; Wilkinson, G. *Journal of the Chemical Society D: Chemical Communications* **1970**, 1369. (b) Martin, R.; Buchwald, S. L. *Acc. Chem. Res.* **2008**, *41*, 1461. (c) Surry, D. S.; Buchwald, S. L. *Angew. Chem. Int. Ed*. **2008**, *47*, 6338.

(7) Parsons, S.; Flack, H. D.; Wagner, T. *Acta Cryst. B* **2013**, *69*, 249.

(8) Zhou, Q.; Cobb, K. M.; Tan, T.; Watson, M. P. *J. Am. Chem. Soc.* **2016**, *138*, 12057.

(9) Pangborn, A. B.; Giardello, M. A.; Grubbs, R. H.; Rosen, R. K.; Timmers, F. J. *Organometallics* **1996**, *15*, 1518.

(10) Walsh, P.J. U.S. Patent 0191345 A1, October 9, 2003.

(11) Langer, F.; Schwink, L.; Devasagayaraj, A.; Chavant, P.-Y.; Knochel P. *J. Org. Chem.*, **1996**, *61*, 8229.

(12) Waltz, K.M.; Gavenonis, J.; Walsh, P.J.; *Angew. Chem. Int. Ed.* **2002**, *41*, 3697.

(13) Williams, F.J.; Crote, R.E.; Jarvo, E.R.; *Chem. Commun.* **2012**, *48*, 1496.

(14) Enquist, P.-A.; Lindh, J.; Nilsson, P.; Larhed, M. *Green Chem.* **2006**, *8*, 338.

(15) (a) Jeon, S.-J.; Li, H.M.; Walsh, P.J. *J. Am. Chem. Soc.* **2005**, *127*, 16416. (b) Derwing, C.; Hoppe, D. *Synthesis* 1996, 149.

(16) Li. H.; Walsh, P. J. *J. Am. Chem. Soc.* **2004**, *126*, 6538.

(17) García, C.; Walsh, P.J. *Org. Lett.* **2003**, *5*, 3641.

Appendix A

NMR AND HPLC SPECTRA

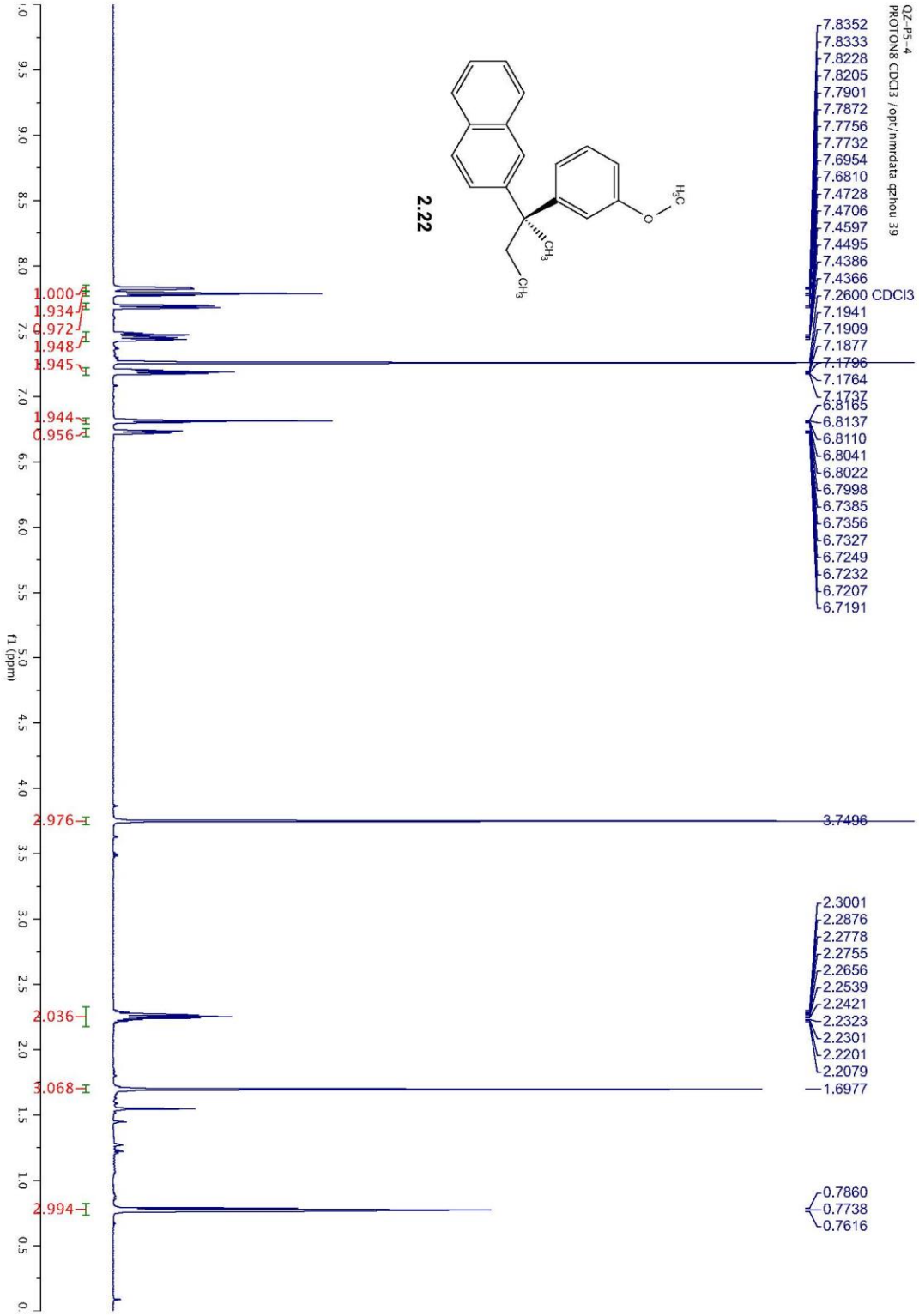
2.22
QZ-P5-4
PROTON8 CDCl3 /opt/nmrdata qzhou 39
7.8352
7.8333
7.8228
7.8205
7.7901
7.7872
7.7756
7.7732
7.6954
7.6810
7.4728
7.4706
7.4597
7.4495
7.4386
7.4366
7.2600 CDCl3
7.1941
7.1909
7.1877
7.1796
7.1764
7.1737
6.8165
6.8137
6.8110
6.8041
6.8022
6.7998
6.7385
6.7356
6.7327
6.7249
6.7232
6.7207
6.7191
3.7496
2.3001
2.2876
2.2778
2.2755
2.2656
2.2539
2.2421
2.2323
2.2301
2.2201
2.2079
1.6977
0.7860
0.7738
0.7616
1.000
1.934
0.972
1.948
1.945
1.944
0.956
2.976
2.036
3.068
2.994
f1 (ppm)

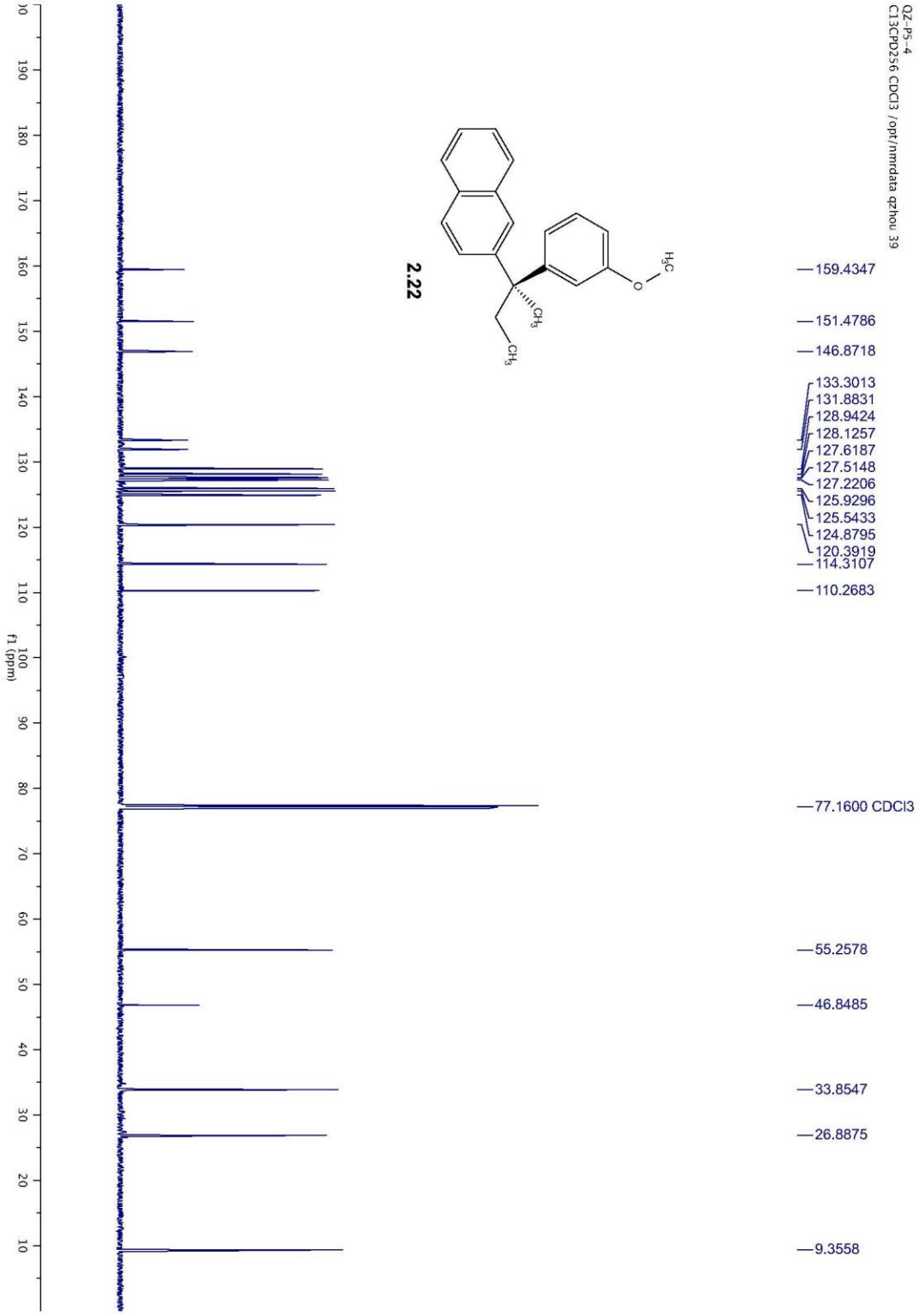
QZ-P5-4
C13CPD256 CDCl3 /opt/nmrdata qzhou 39
2.22
H3C
O
CH3
CH3
159.4347
151.4786
146.8718
133.3013
131.8831
128.9424
128.1257
127.6187
127.5148
127.2206
125.9296
125.5433
124.8795
120.3919
114.3107
110.2683
77.1600 CDCl3
55.2578
46.8485
33.8547
26.8875
9.3558
f1 (ppm)

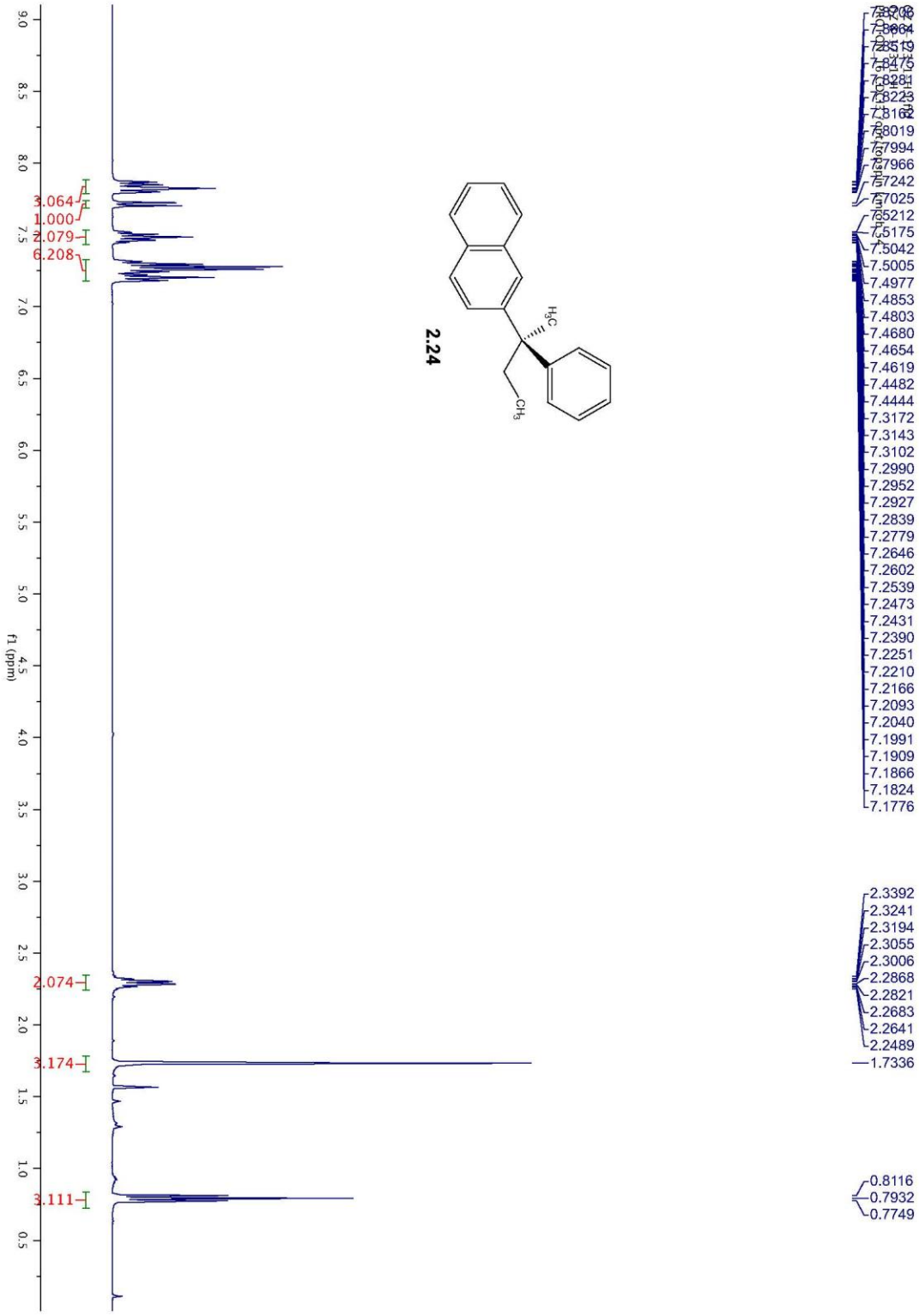
3.064
1.000
2.079
6.208
2.074
3.174
3.111
f1 (ppm)
2.24
H3C
CH3
7.5212
7.5175
7.5042
7.5005
7.4977
7.4853
7.4803
7.4680
7.4654
7.4619
7.4482
7.4444
7.3172
7.3143
7.3102
7.2990
7.2952
7.2927
7.2839
7.2779
7.2646
7.2602
7.2539
7.2473
7.2431
7.2390
7.2251
7.2210
7.2166
7.2093
7.2040
7.1991
7.1909
7.1866
7.1824
7.1776
2.3392
2.3241
2.3194
2.3055
2.3006
2.2868
2.2821
2.2683
2.2641
2.2489
1.7336
0.8116
0.7932
0.7749

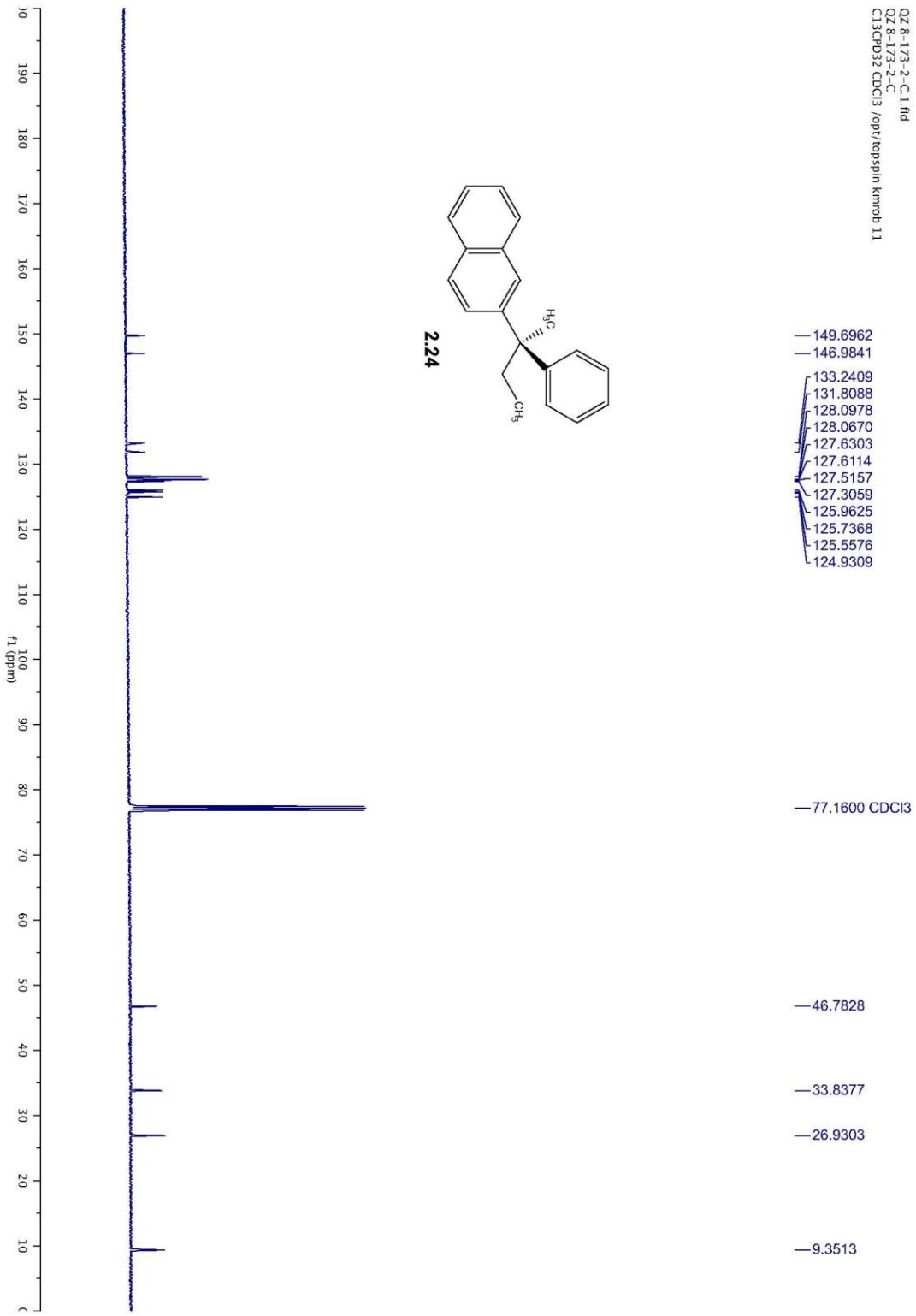
QZ 8-173-2-C.1.fid
QZ 8-173-2-C
C13CPD32 CDCl3 /opt/topspin kmrob 11
2.24
149.6962
146.9841
133.2409
131.8088
128.0978
128.0670
127.6303
127.6114
127.5157
127.3059
125.9625
125.7368
125.5576
124.9309
77.1600 CDCl3
46.7828
33.8377
26.9303
9.3513
f1 (ppm)

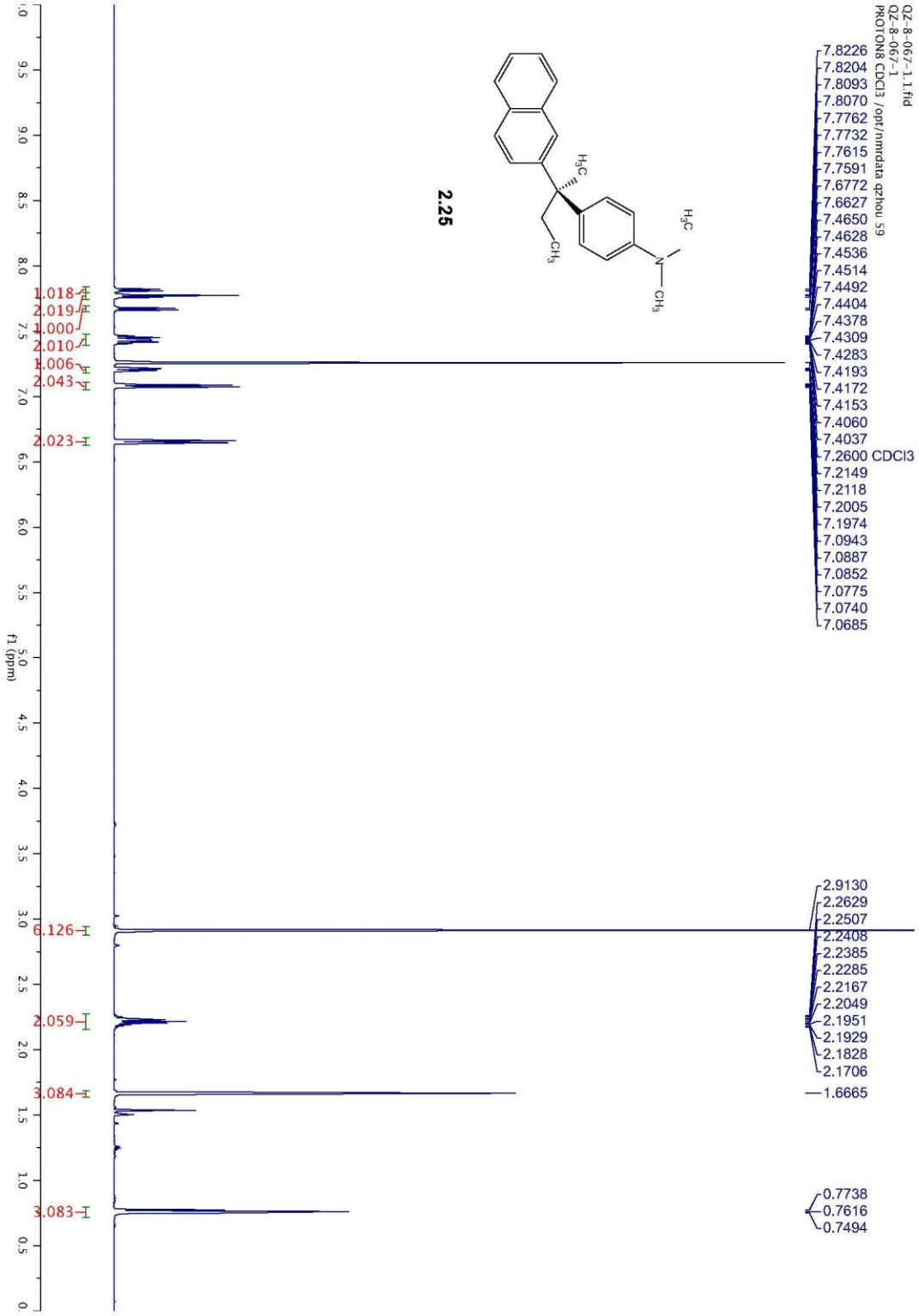
QZ-8-067-1.1.fid
QZ-8-067-1
PROTON8 CDCl3 /opt/nmrdata qzhou 59
2.25
7.8226
7.8204
7.8093
7.8070
7.7762
7.7732
7.7615
7.7591
7.6772
7.6627
7.4650
7.4628
7.4536
7.4514
7.4492
7.4404
7.4378
7.4309
7.4283
7.4193
7.4172
7.4153
7.4060
7.4037
7.2600 CDCl3
7.2149
7.2118
7.2005
7.1974
7.0943
7.0887
7.0852
7.0775
7.0740
7.0685
2.9130
2.2629
2.2507
2.2408
2.2385
2.2285
2.2167
2.2049
2.1951
2.1929
2.1828
2.1706
1.6665
0.7738
0.7616
0.7494
1.018
2.019
1.000
2.010
1.006
2.043
2.023
6.126
2.059
3.084
3.083
f1 (ppm)

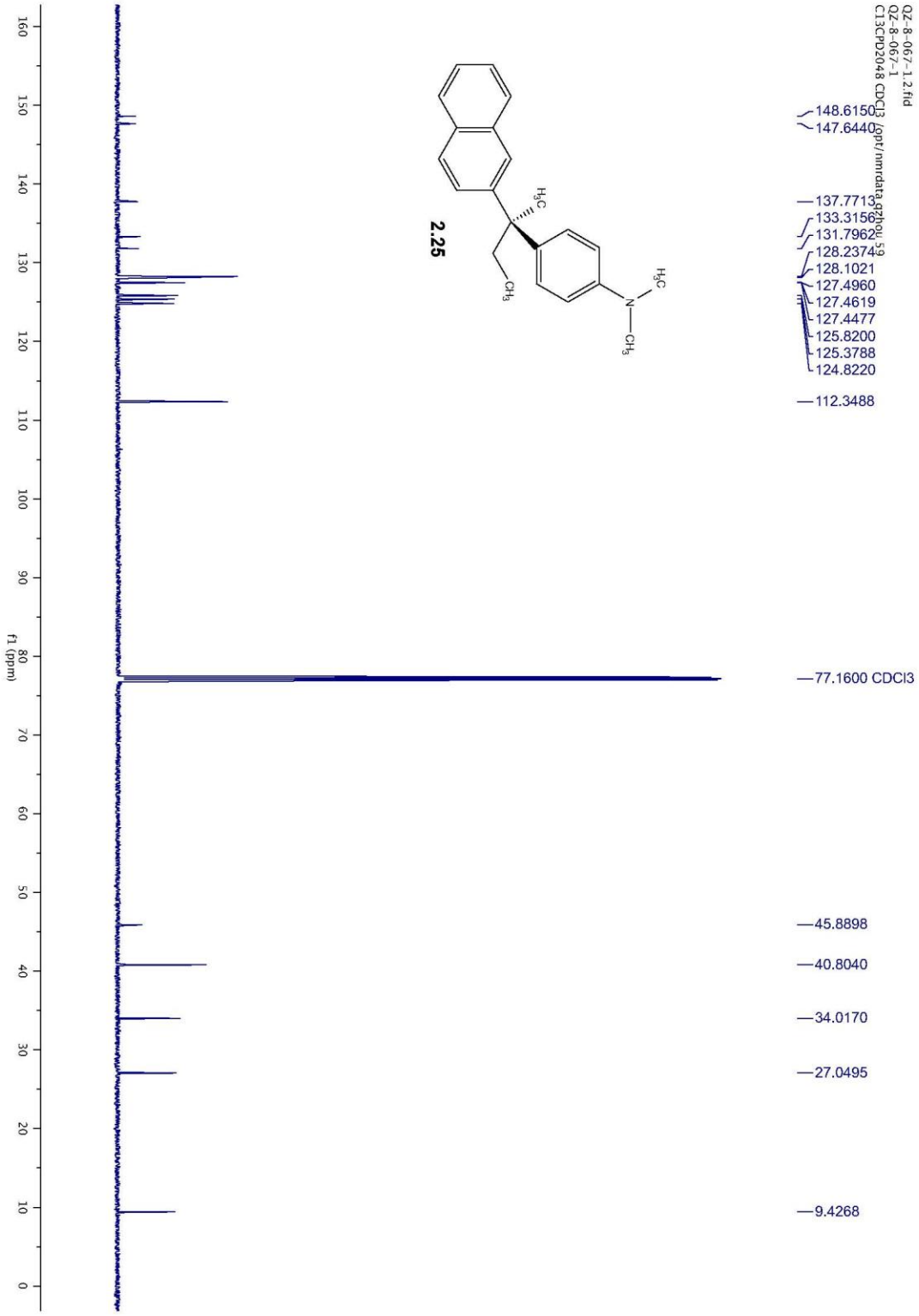
QZ-8-067-1.2.fid
QZ-8-067-1
C13CPD2048 CDCl3 /opt/nmrdata azhou 58
148.6150
147.6440
137.7713
133.3156
131.7962
128.2374
128.1021
127.4960
127.4619
127.4477
125.8200
125.3788
124.8220
112.3488
77.1600 CDCl3
45.8898
40.8040
34.0170
27.0495
9.4268
2.25
f1 (ppm)

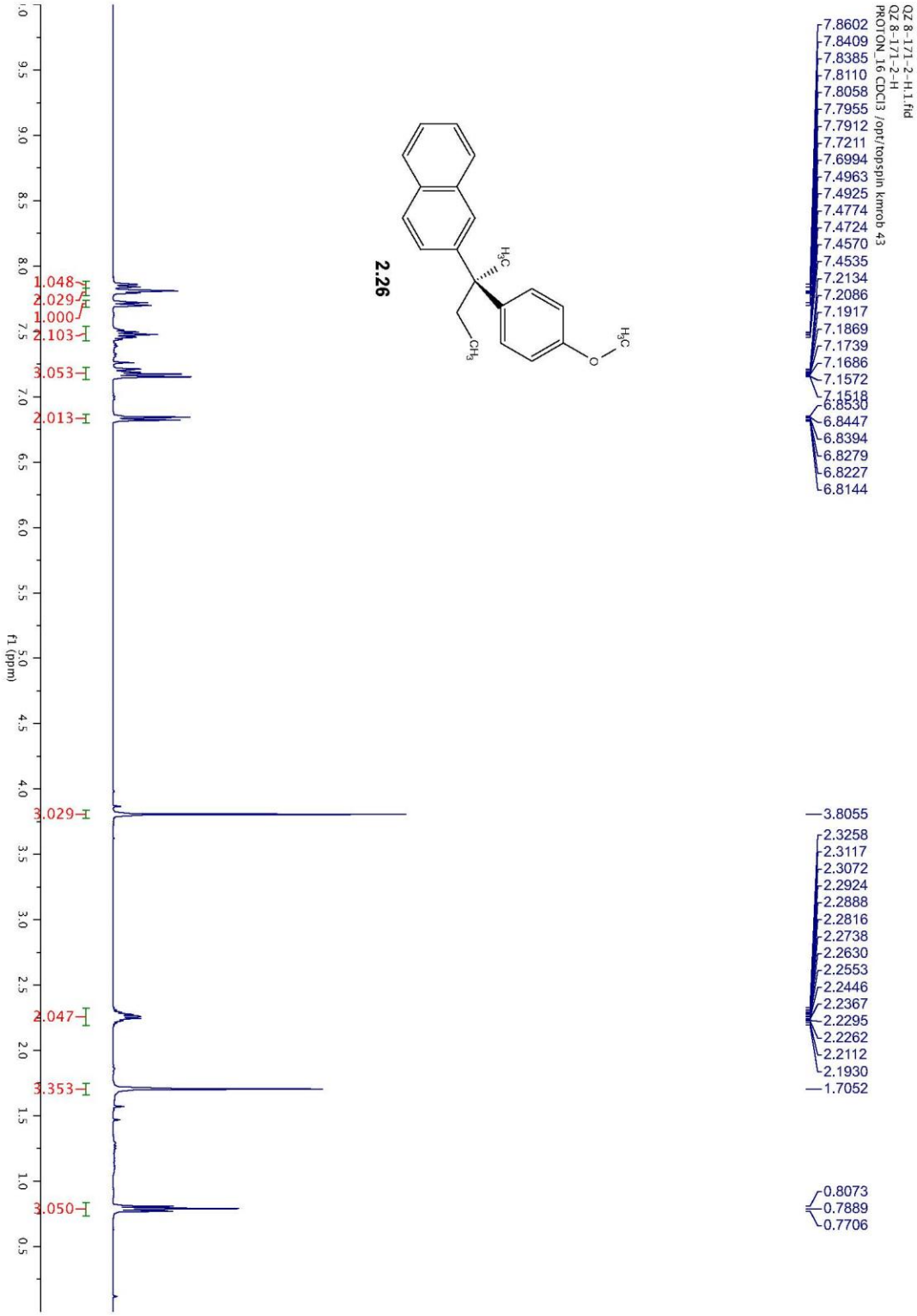
QZ 8-171-2-H.1.fid
QZ 8-171-2-H
PROTON_16 CDCl3 /opt/topspin kmrob 43
2.26
f1 (ppm)
1.048
2.029
1.000
2.103
3.053
2.013
3.029
2.047
3.353
3.050
7.8602
7.8409
7.8385
7.8110
7.8058
7.7955
7.7912
7.7211
7.6994
7.4963
7.4925
7.4774
7.4724
7.4570
7.4535
7.2134
7.2086
7.1917
7.1869
7.1739
7.1686
7.1572
7.1518
6.8530
6.8447
6.8394
6.8279
6.8227
6.8144
3.8055
2.3258
2.3117
2.3072
2.2924
2.2888
2.2816
2.2738
2.2630
2.2553
2.2446
2.2367
2.2295
2.2262
2.2112
2.1930
1.7052
0.8073
0.7889
0.7706

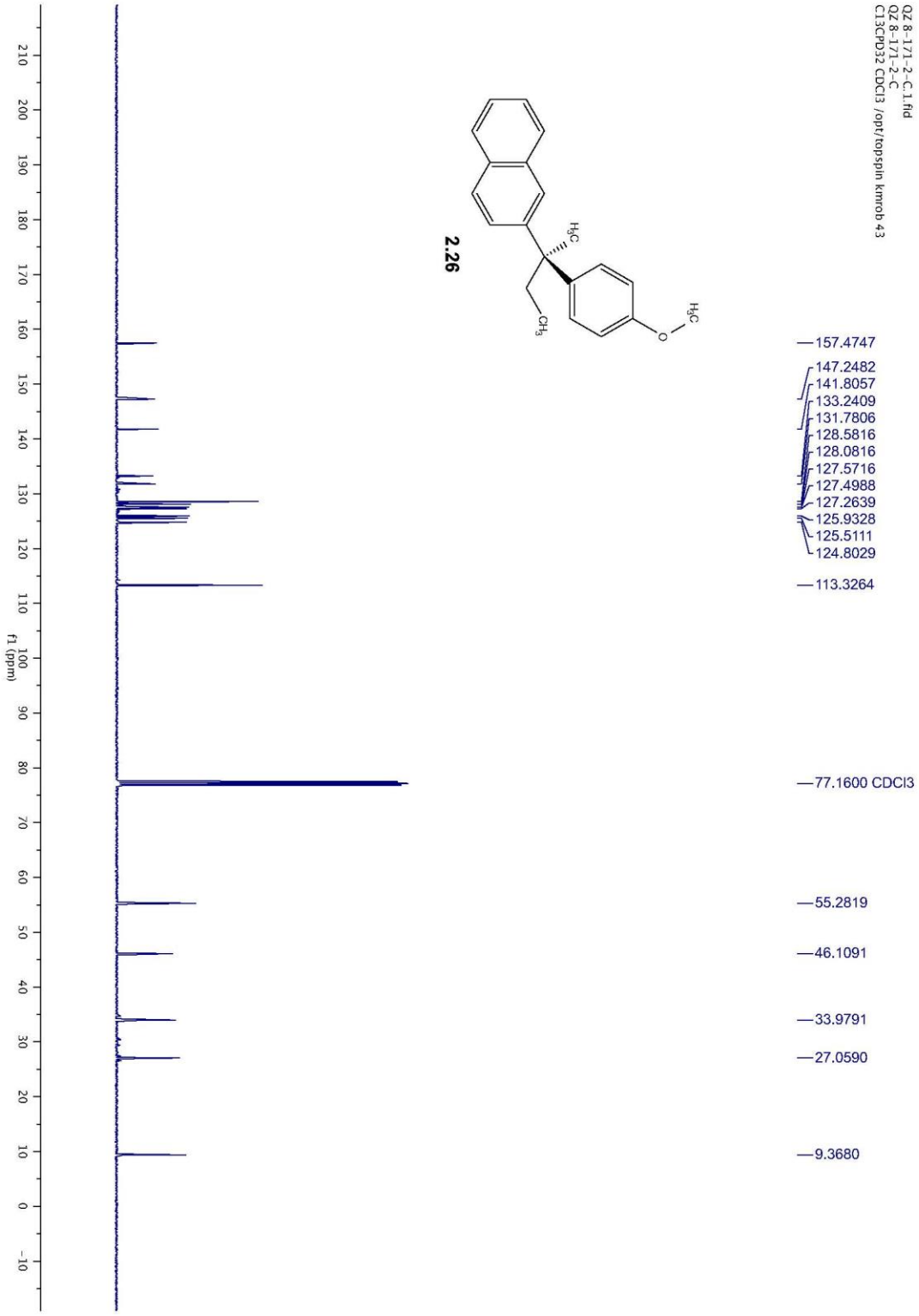
QZ 8-171-2-C.1.fid
QZ 8-171-2-C
C13CPD32 CDCl3 /opt/topspin kmrob 43
2.26
H3C
CH3
O
H3C
157.4747
147.2482
141.8057
133.2409
131.7806
128.5816
128.0816
127.5716
127.4988
127.2639
125.9328
125.5111
124.8029
113.3264
77.1600 CDCl3
55.2819
46.1091
33.9791
27.0590
9.3680
f1 (ppm)

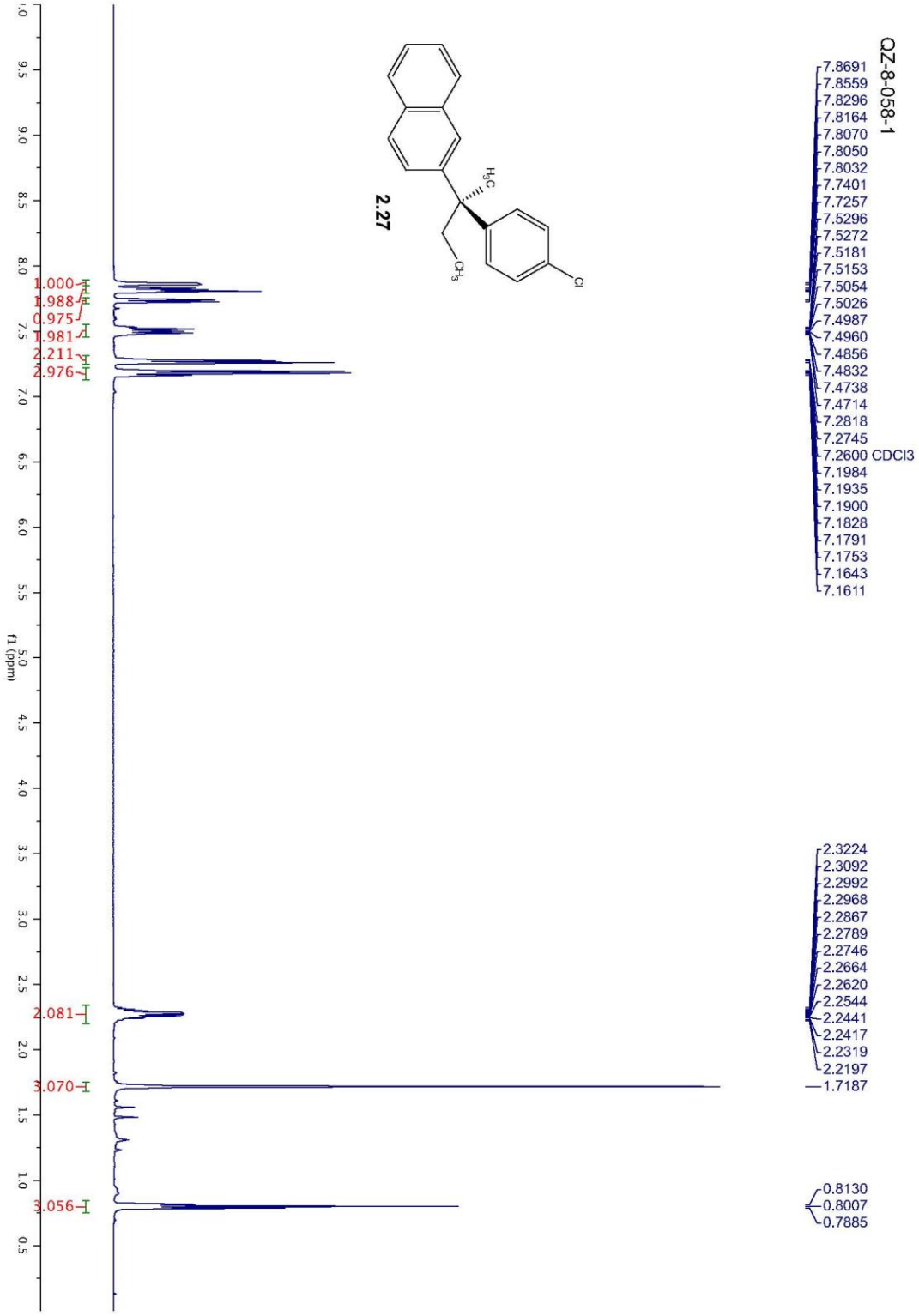
QZ-8-058-1
2.27
H3C
CH3
Cl
7.8691
7.8559
7.8296
7.8164
7.8070
7.8050
7.8032
7.7401
7.7257
7.5296
7.5272
7.5181
7.5153
7.5054
7.5026
7.4987
7.4960
7.4856
7.4832
7.4738
7.4714
7.2818
7.2745
7.2600 CDCl3
7.1984
7.1935
7.1900
7.1828
7.1791
7.1753
7.1643
7.1611
2.3224
2.3092
2.2992
2.2968
2.2867
2.2789
2.2746
2.2664
2.2620
2.2544
2.2441
2.2417
2.2319
2.2197
1.7187
0.8130
0.8007
0.7885
1.000
1.988
0.975
1.981
2.211
2.976
2.081
3.070
3.056
f1 (ppm)

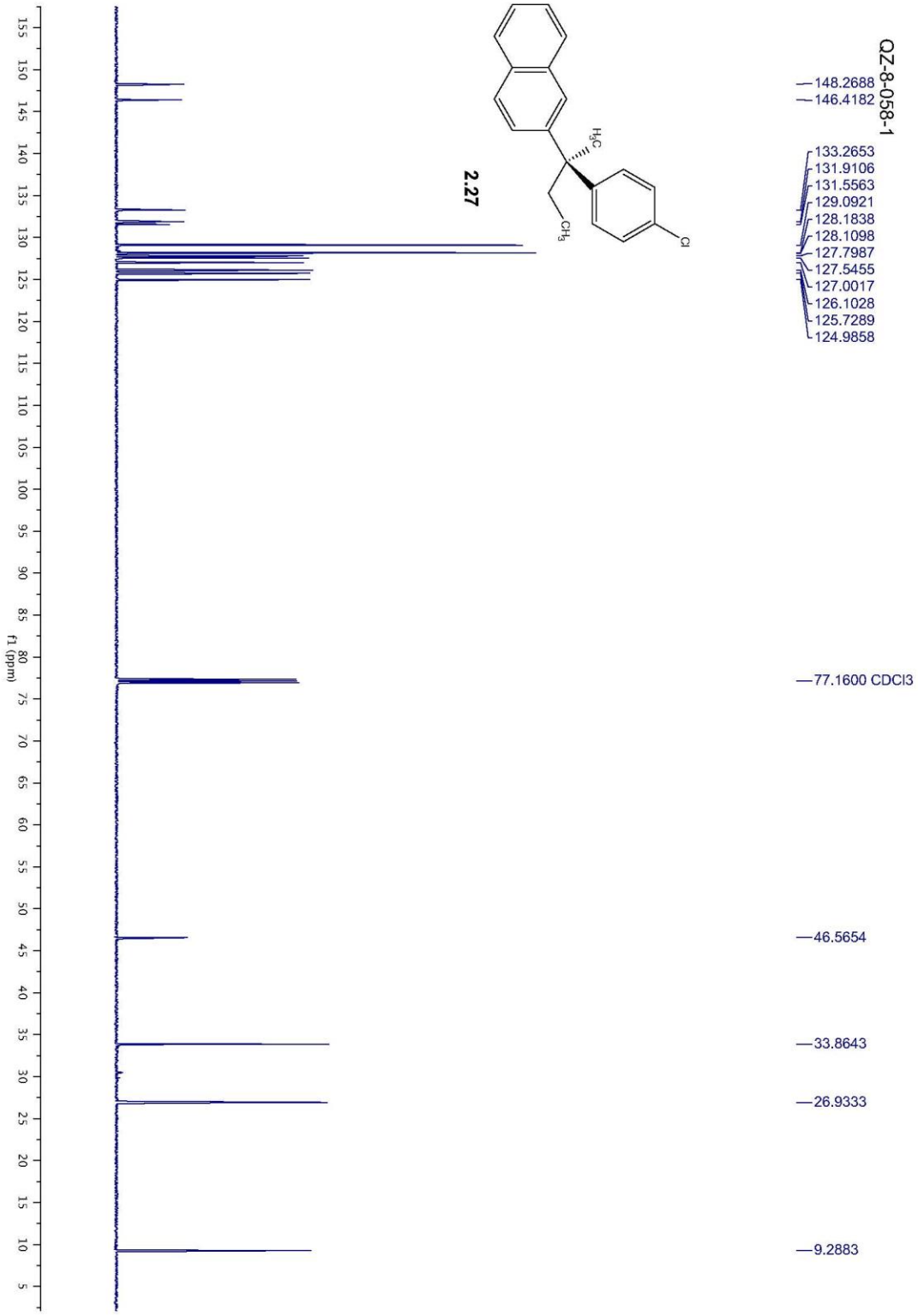
QZ-8-058-1
148.2688
146.4182
133.2653
131.9106
131.5563
129.0921
128.1838
128.1098
127.7987
127.5455
127.0017
126.1028
125.7289
124.9858
77.1600 CDCl3
46.5654
33.8643
26.9333
9.2883
f1 (ppm)
2.27
H3C
CH3
Cl

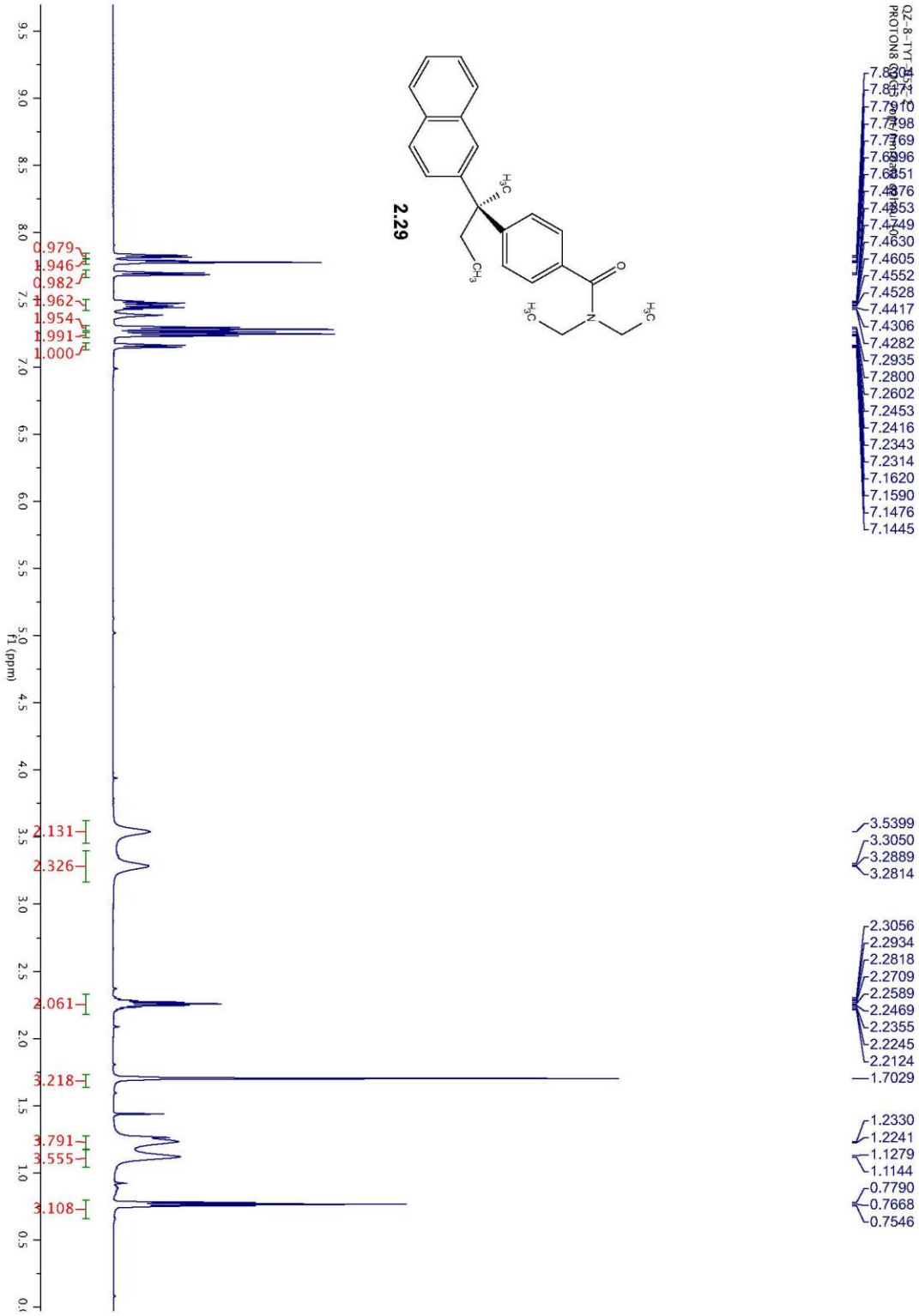
2.29
f1 (ppm)
0.979
1.946
0.982
1.962
1.954
1.991
1.000
2.131
2.326
2.061
3.218
3.791
3.555
3.108
7.8304
7.8171
7.7910
7.7798
7.7369
7.6396
7.6351
7.4876
7.4753
7.4749
7.4630
7.4605
7.4552
7.4528
7.4417
7.4306
7.4282
7.2935
7.2800
7.2602
7.2453
7.2416
7.2343
7.2314
7.1620
7.1590
7.1476
7.1445
3.5399
3.3050
3.2889
3.2814
2.3056
2.2934
2.2818
2.2709
2.2589
2.2469
2.2355
2.2245
2.2124
1.7029
1.2330
1.2241
1.1279
1.1144
0.7790
0.7668
0.7546

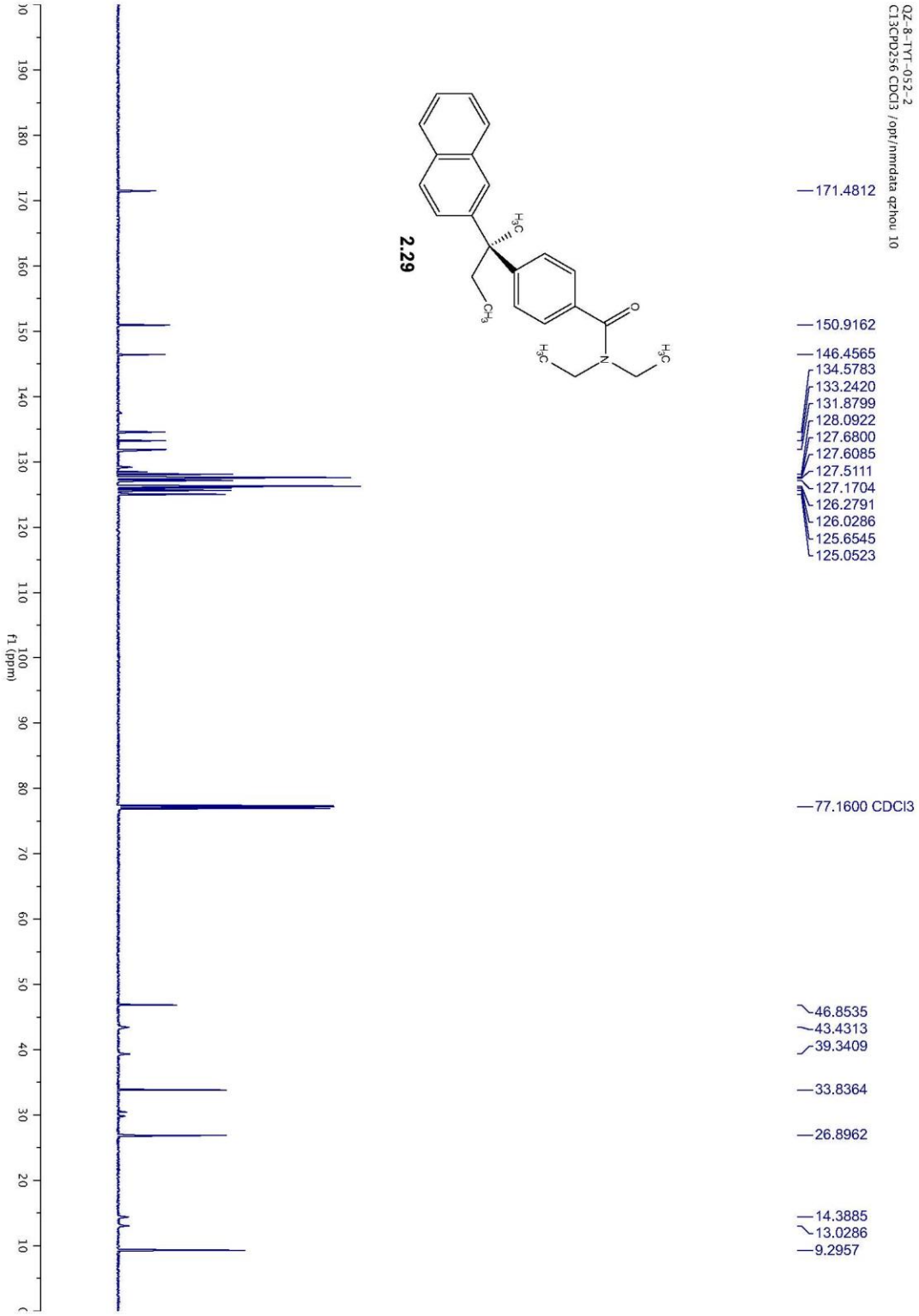
QZ-8-TYT-052-2
C13CPD256 CDCl3 /opt/nmrdata qzhou 10
171.4812
150.9162
146.4565
134.5783
133.2420
131.8799
128.0922
127.6800
127.6085
127.5111
127.1704
126.2791
126.0286
125.6545
125.0523
77.1600 CDCl3
46.8535
43.4313
39.3409
33.8364
26.8962
14.3885
13.0286
9.2957
2.29
f1 (ppm)

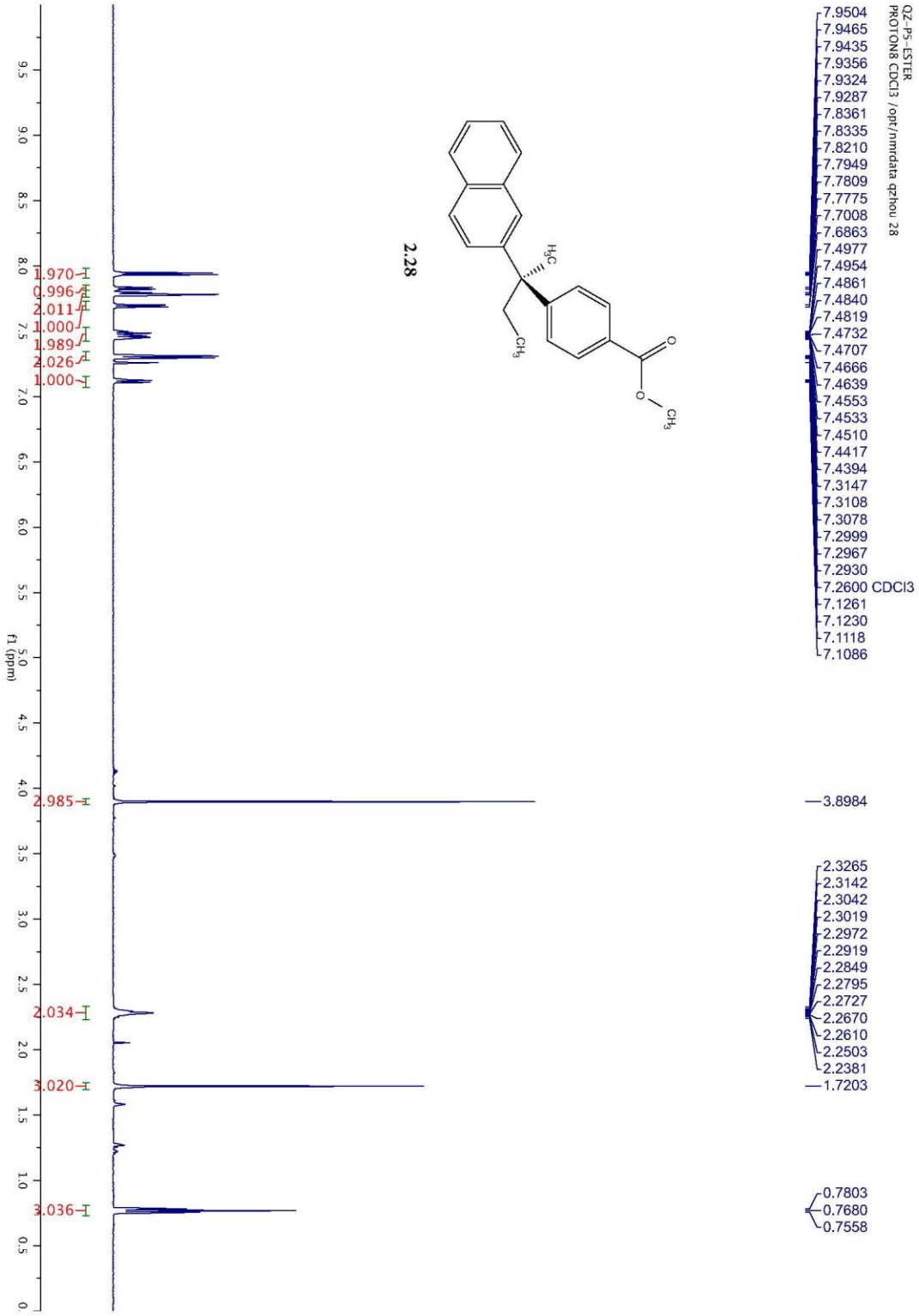
QZ-P5--ESTER
PROTON8 CDCl3 /opt/nmrdata qzhou 28
7.9504
7.9465
7.9435
7.9356
7.9324
7.9287
7.8361
7.8335
7.8210
7.7949
7.7809
7.7775
7.7008
7.6863
7.4977
7.4954
7.4861
7.4840
7.4819
7.4732
7.4707
7.4666
7.4639
7.4553
7.4533
7.4510
7.4417
7.4394
7.3147
7.3108
7.3078
7.2999
7.2967
7.2930
7.2600 CDCl3
7.1261
7.1230
7.1118
7.1086
2.28
H3C
CH3
O
O
CH3
1.970
0.996
2.011
1.000
1.989
2.026
1.000
2.985
3.8984
2.034
3.020
1.7203
3.036
2.3265
2.3142
2.3042
2.3019
2.2972
2.2919
2.2849
2.2795
2.2727
2.2670
2.2610
2.2503
2.2381
0.7803
0.7680
0.7558
f1 (ppm)

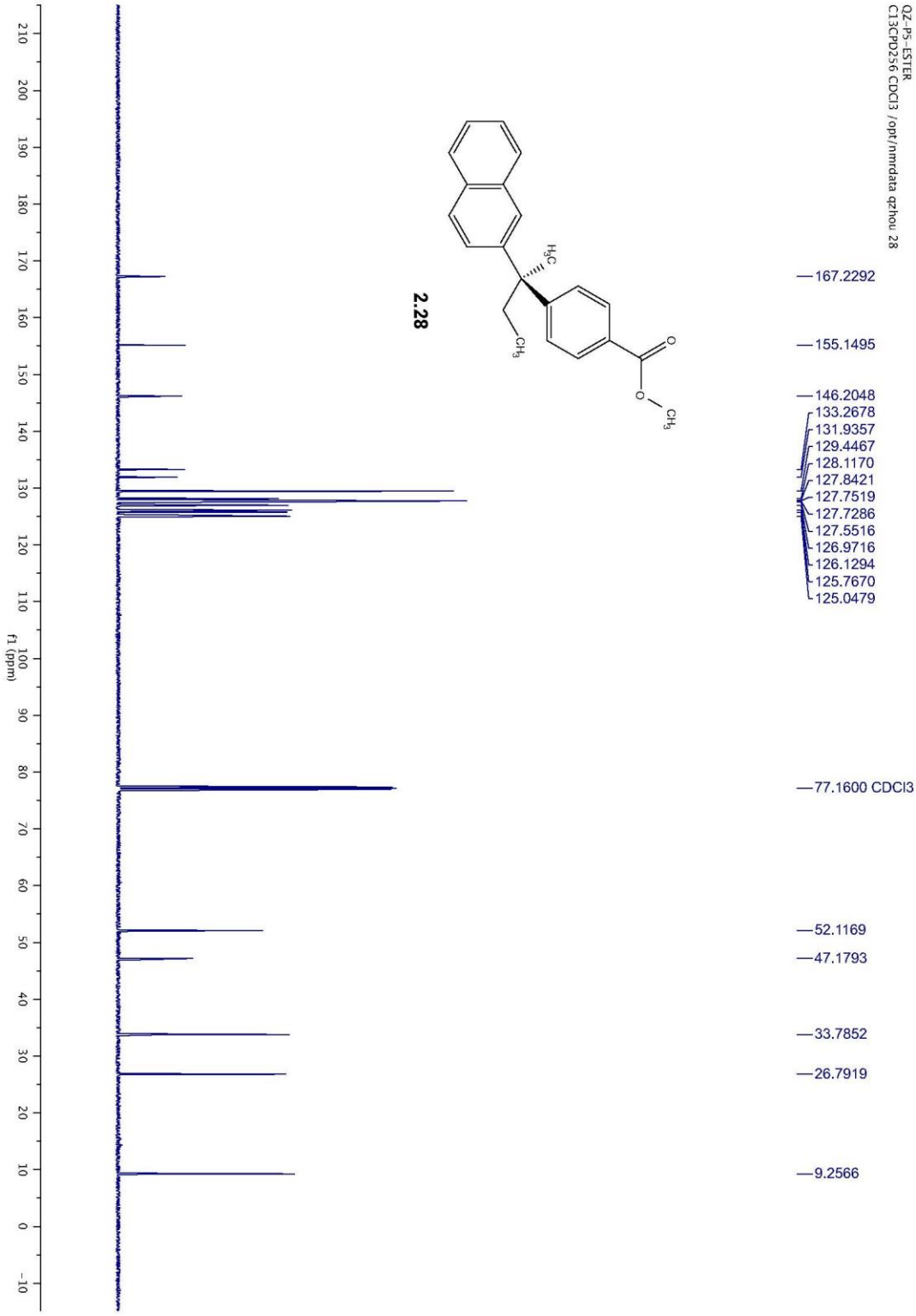
QZ-P5--ESTER
C13CPD256 CDCl3 /opt/nmrdata qzhou 28
2.28
H3C
CH3
O
O
CH3
f1 (ppm)
210
200
190
180
170
160
150
140
130
120
110
100
90
80
70
60
50
40
30
20
10
0
-10
167.2292
155.1495
146.2048
133.2678
131.9357
129.4467
128.1170
127.8421
127.7519
127.7286
127.5516
126.9716
126.1294
125.7670
125.0479
77.1600 CDCl3
52.1169
47.1793
33.7852
26.7919
9.2566

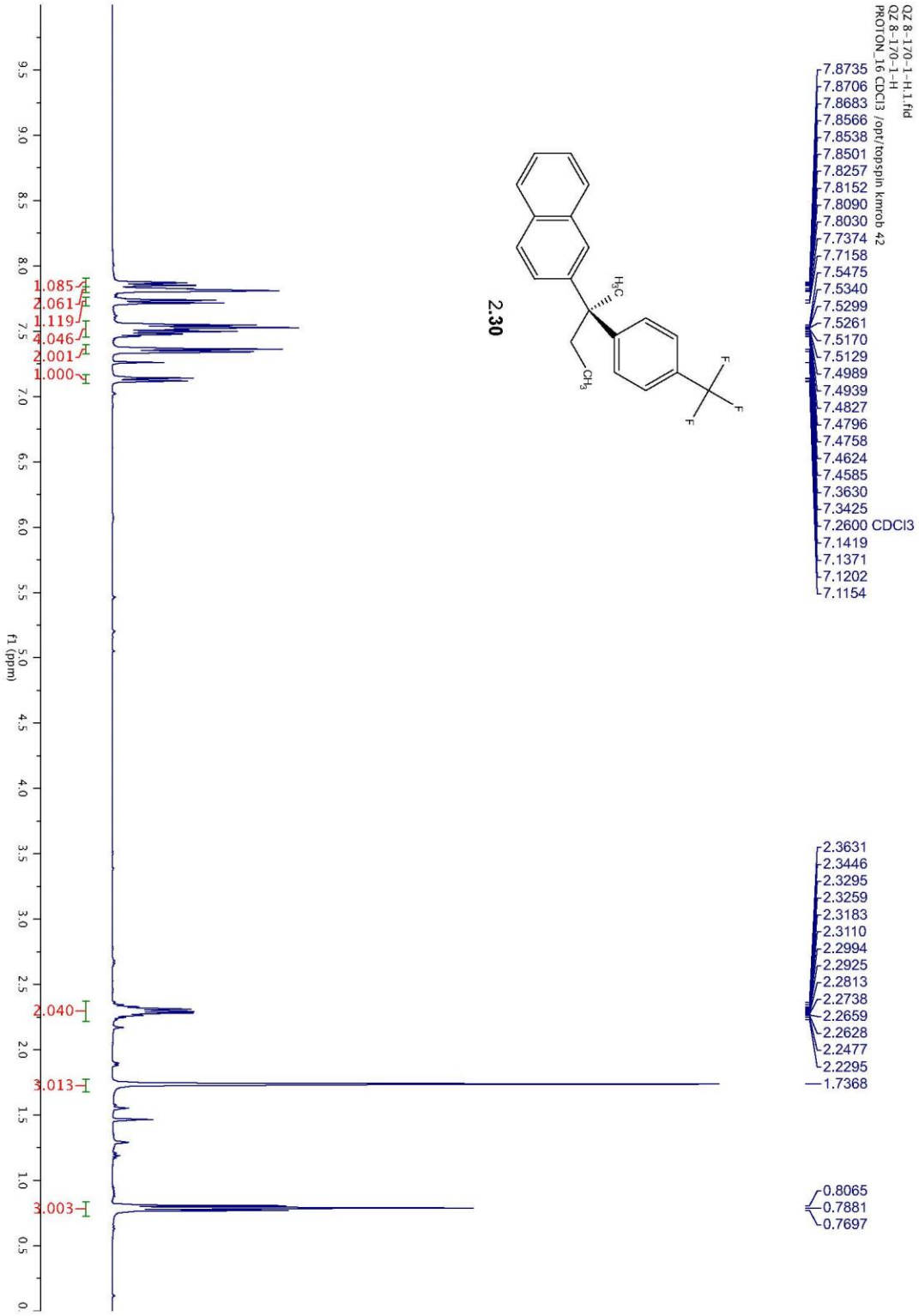
QZ 8-170-1-H.1.fid
QZ 8-170-1-H
PROTON_16 CDCl3 /opt/topspin kmrob 42
7.8735
7.8706
7.8683
7.8566
7.8538
7.8501
7.8257
7.8152
7.8090
7.8030
7.7374
7.7158
7.5475
7.5340
7.5299
7.5261
7.5170
7.5129
7.4989
7.4939
7.4827
7.4796
7.4758
7.4624
7.4585
7.3630
7.3425
7.2600 CDCl3
7.1419
7.1371
7.1202
7.1154
2.3631
2.3446
2.3295
2.3259
2.3183
2.3110
2.2994
2.2925
2.2813
2.2738
2.2659
2.2628
2.2477
2.2295
1.7368
0.8065
0.7881
0.7697
1.085
2.061
1.119
4.046
2.001
1.000
2.040
3.013
3.003
f1 (ppm)
2.30
H3C
CH3
F
F
F

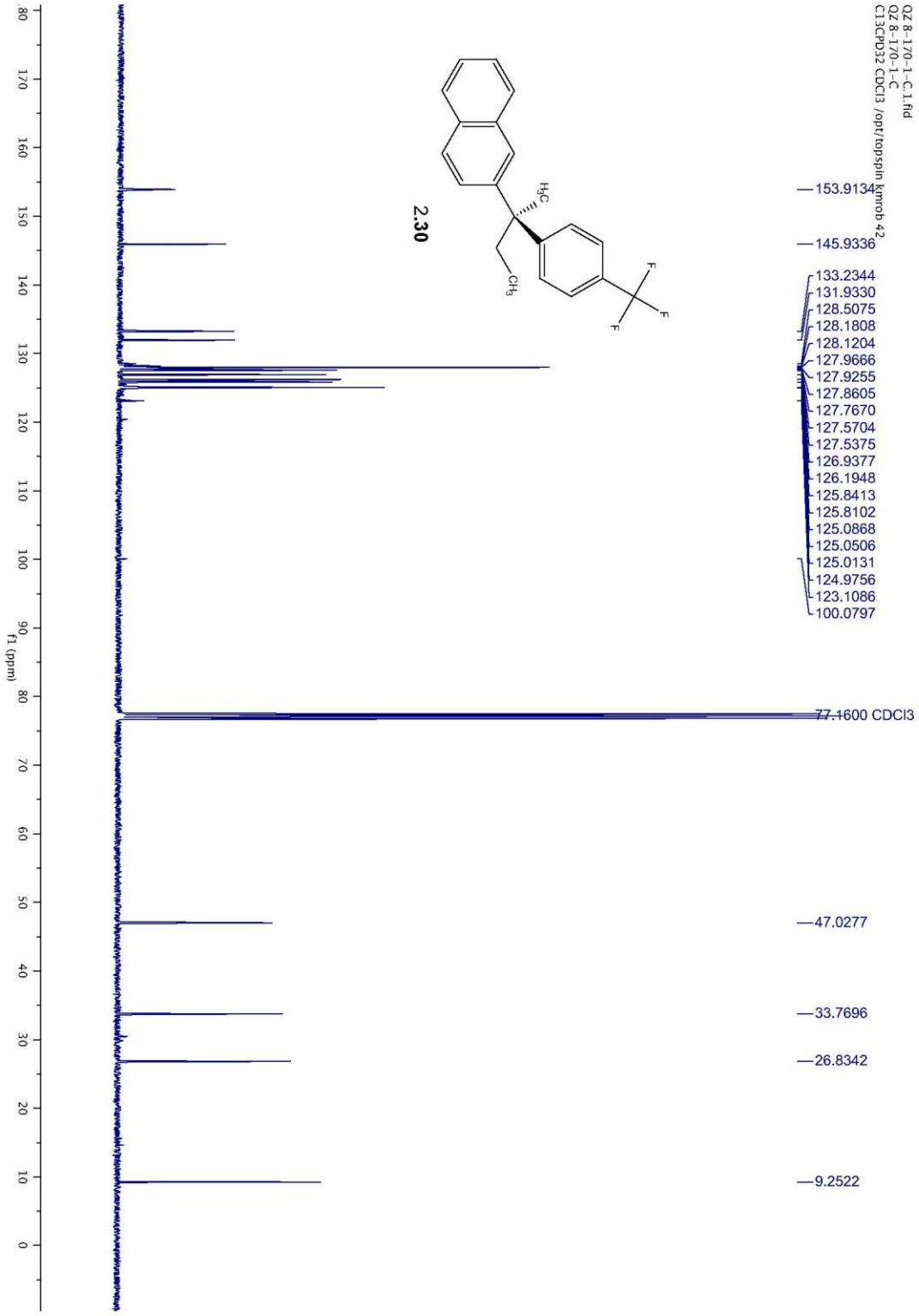
QZ 8-170-1-C.1.fid
QZ 8-170-1-C
C13CPD32 CDCl3 /opt/topspin kmrob 42
153.9134
145.9336
133.2344
131.9330
128.5075
128.1808
128.1204
127.9666
127.9255
127.8605
127.7670
127.5704
127.5375
126.9377
126.1948
125.8413
125.8102
125.0868
125.0506
125.0131
124.9756
123.1086
100.0797
77.1600 CDCl3
47.0277
33.7696
26.8342
9.2522
f1 (ppm)
2.30

QZ 8-170-1-F.1.fid
QZ 8-170-1-F
F19CPD CDCl3 /opt/topspin kmrob 42

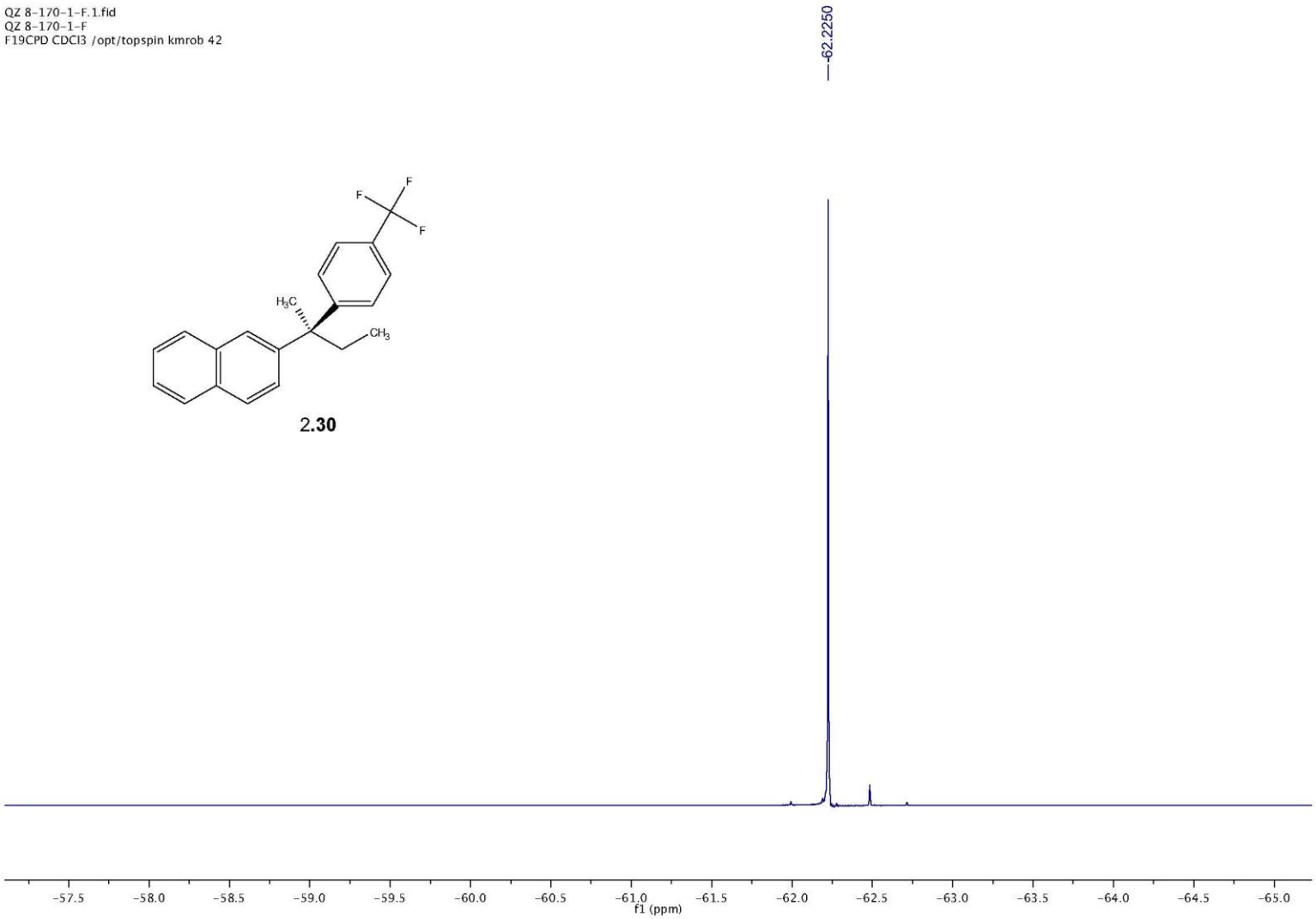

2.30

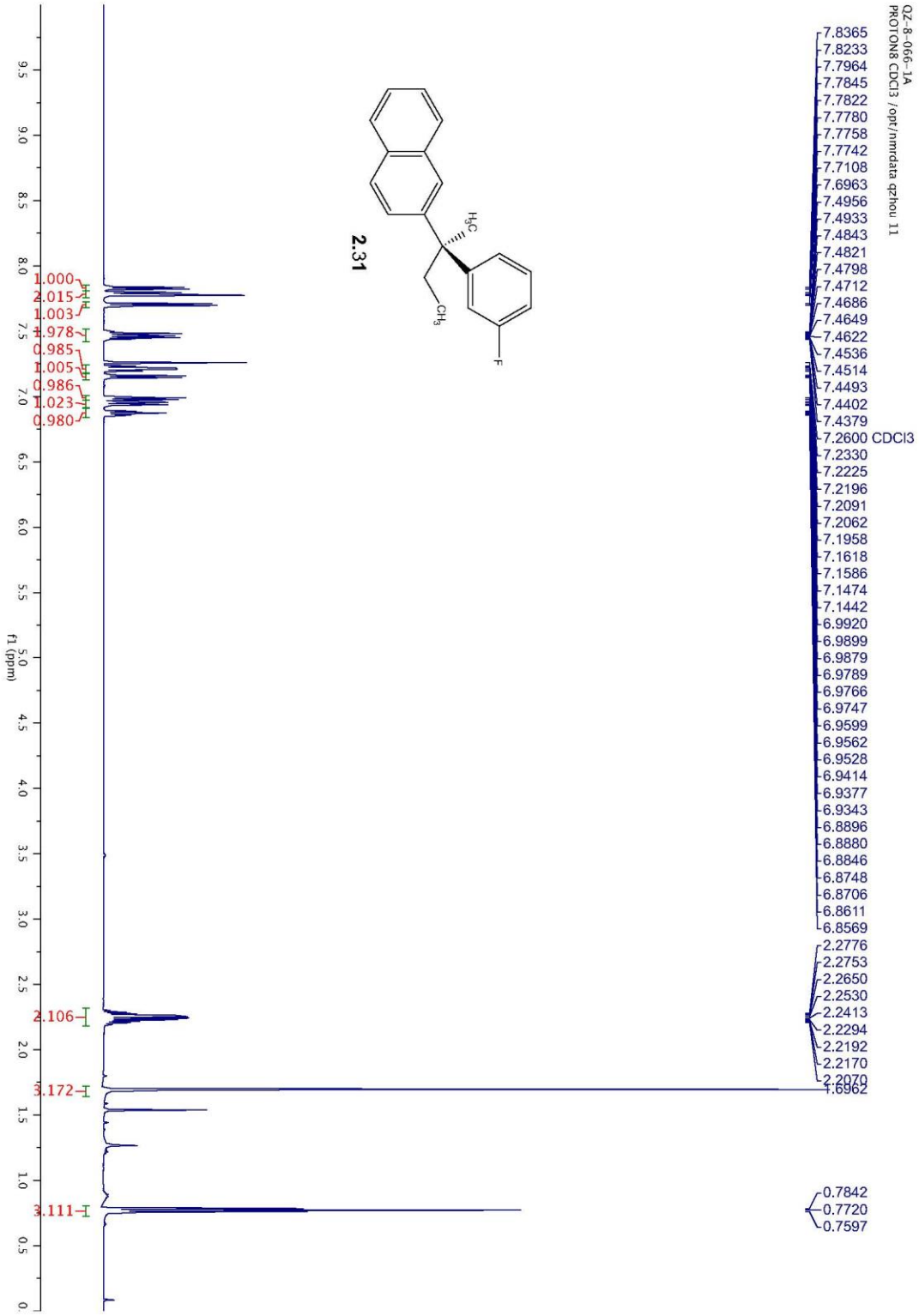
QZ-8-066-1A
PROTON8 CDCl3 /opt/nmrdata qzhou 11
2.31
CDCl3
f1 (ppm)

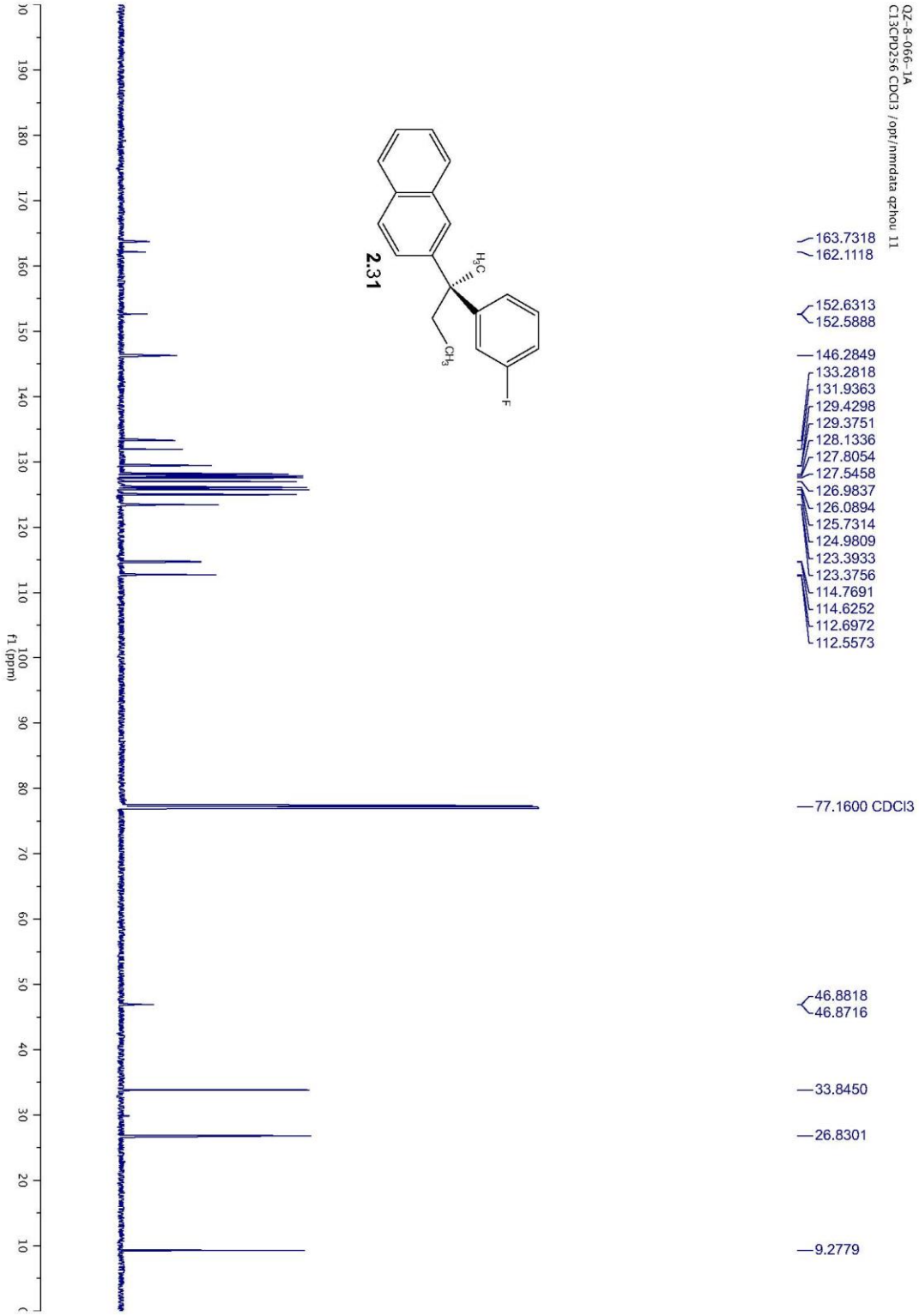
QZ-8-066-1A
C13CPD256 CDCl3 /opt/nmrdata qzhou 11
2.31
H3C
CH3
F
163.7318
162.1118
152.6313
152.5888
146.2849
133.2818
131.9363
129.4298
129.3751
128.1336
127.8054
127.5458
126.9837
126.0894
125.7314
124.9809
123.3933
123.3756
114.7691
114.6252
112.6972
112.5573
77.1600 CDCl3
46.8818
46.8716
33.8450
26.8301
9.2779
f1 (ppm)

QZ-8-066-1A
F19CPD16 CDCl3 /opt/nmrdata qzhou 11

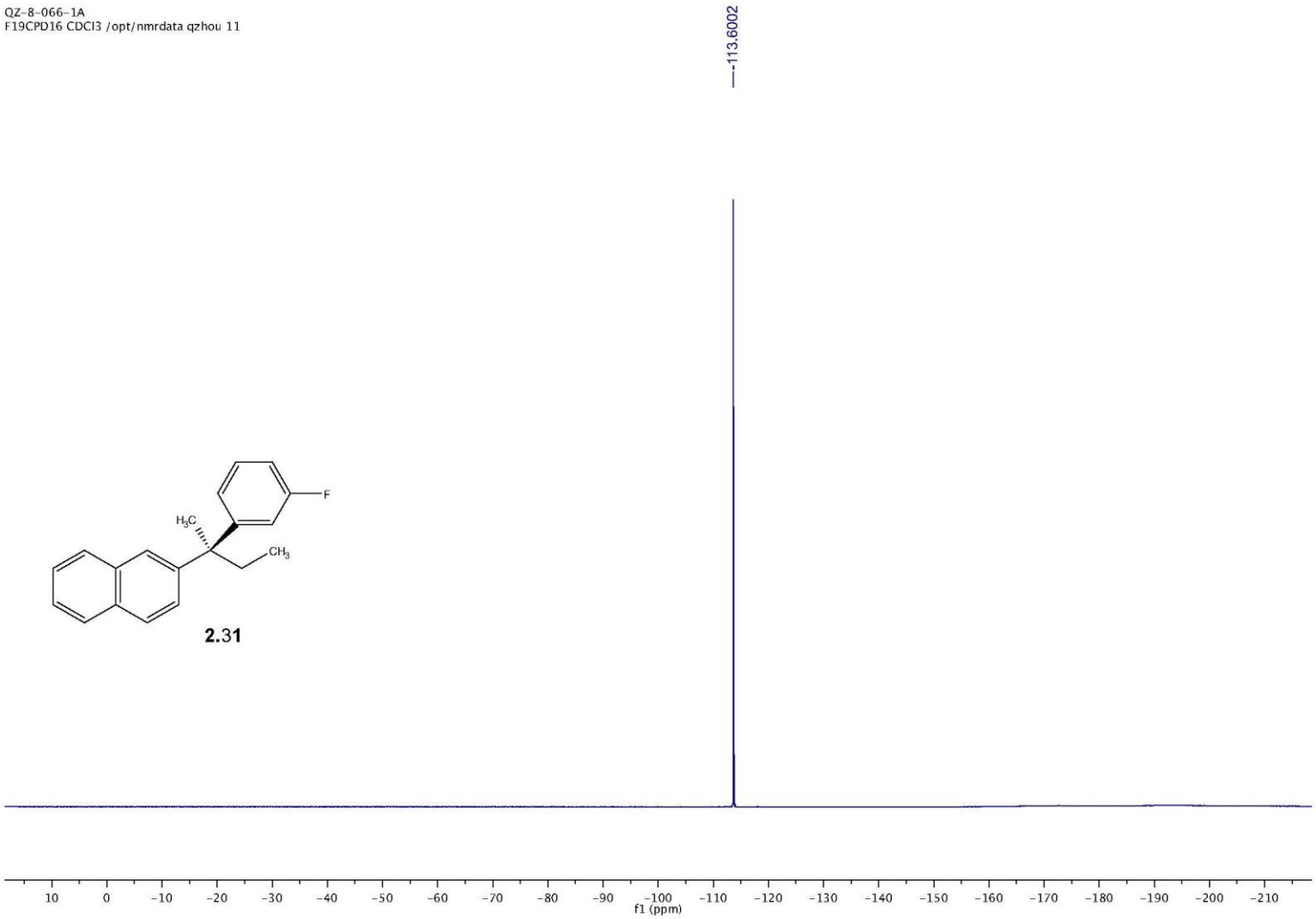

2.31

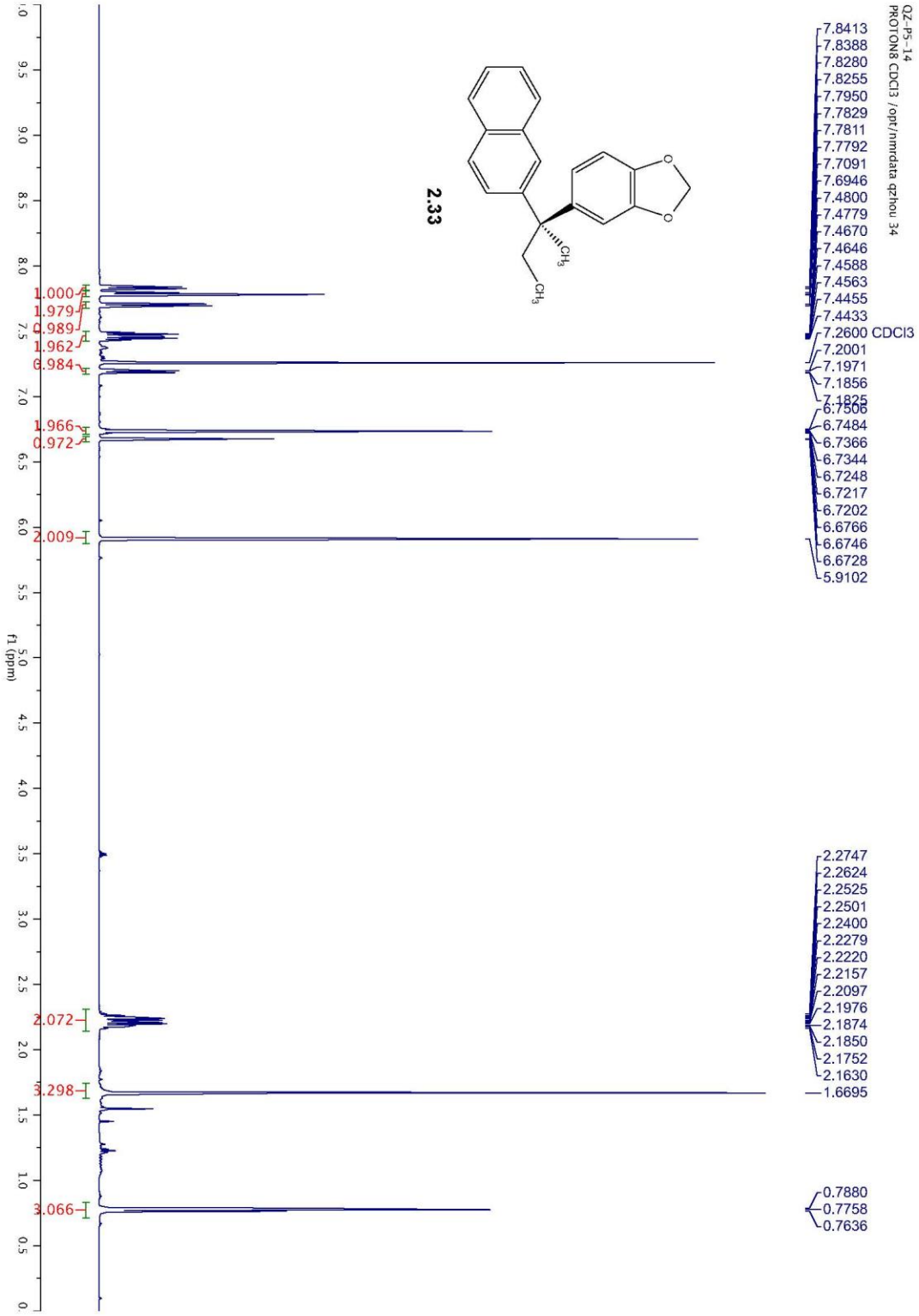
2.33
QZ-P5-14
PROTON6 CDCl3 /opt/nmrdata qzhou 34
7.8413
7.8388
7.8280
7.8255
7.7950
7.7829
7.7811
7.7792
7.7091
7.6946
7.4800
7.4779
7.4670
7.4646
7.4588
7.4563
7.4455
7.4433
7.2600 CDCl3
7.2001
7.1971
7.1856
7.1825
6.7506
6.7484
6.7366
6.7344
6.7248
6.7217
6.7202
6.6766
6.6746
6.6728
5.9102
2.2747
2.2624
2.2525
2.2501
2.2400
2.2279
2.2220
2.2157
2.2097
2.1976
2.1874
2.1850
2.1752
2.1630
1.6695
0.7880
0.7758
0.7636
1.000
1.979
0.989
1.962
0.984
1.966
0.972
2.009
2.072
3.298
3.066
f1 (ppm)

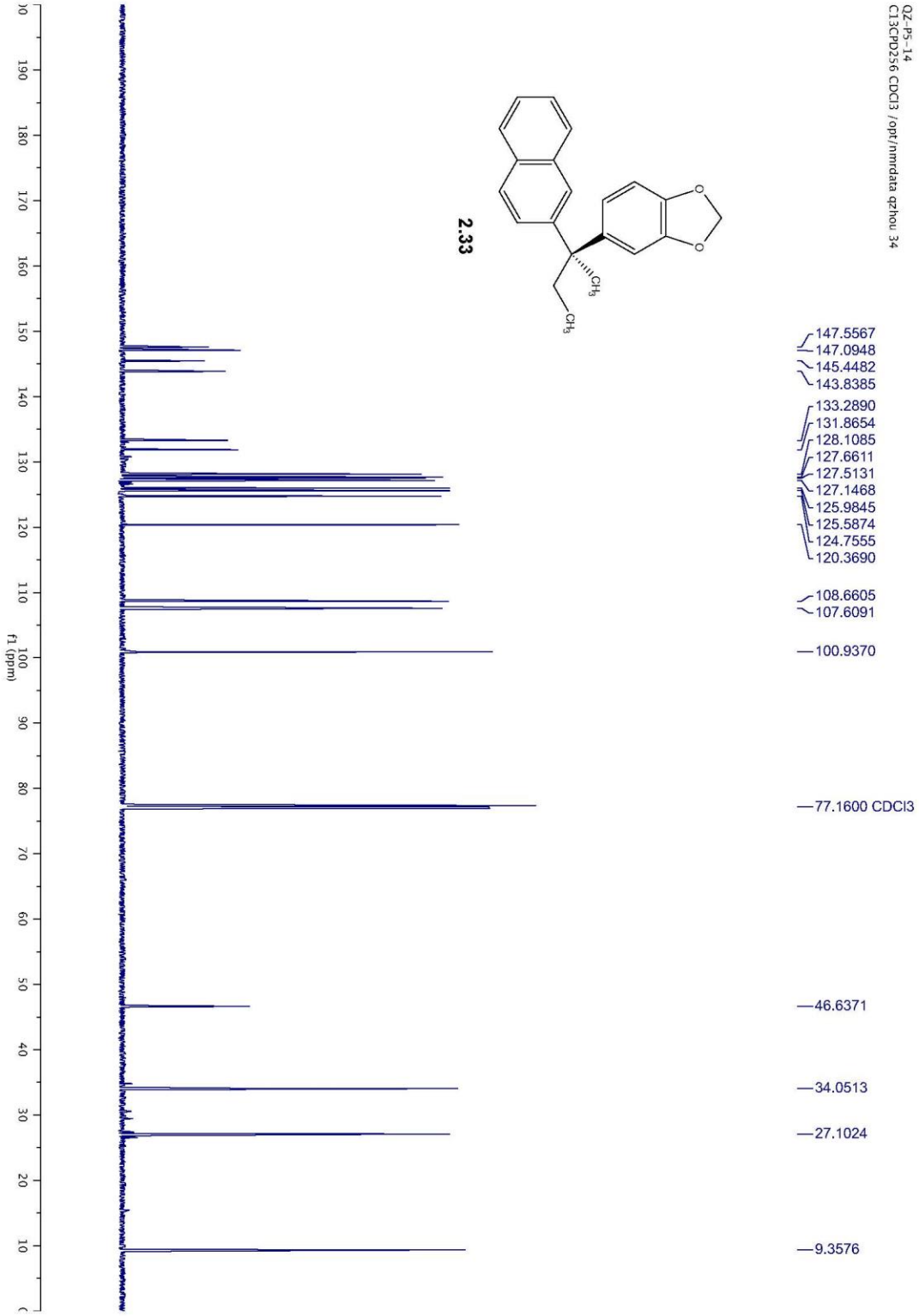
QZ-P5-14
C13CPD256 CDCl3 /opt/nmrdata qzhou 34
2.33
147.5567
147.0948
145.4482
143.8385
133.2890
131.8654
128.1085
127.6611
127.5131
127.1468
125.9845
125.5874
124.7555
120.3690
108.6605
107.6091
100.9370
77.1600 CDCl3
46.6371
34.0513
27.1024
9.3576
f1 (ppm)

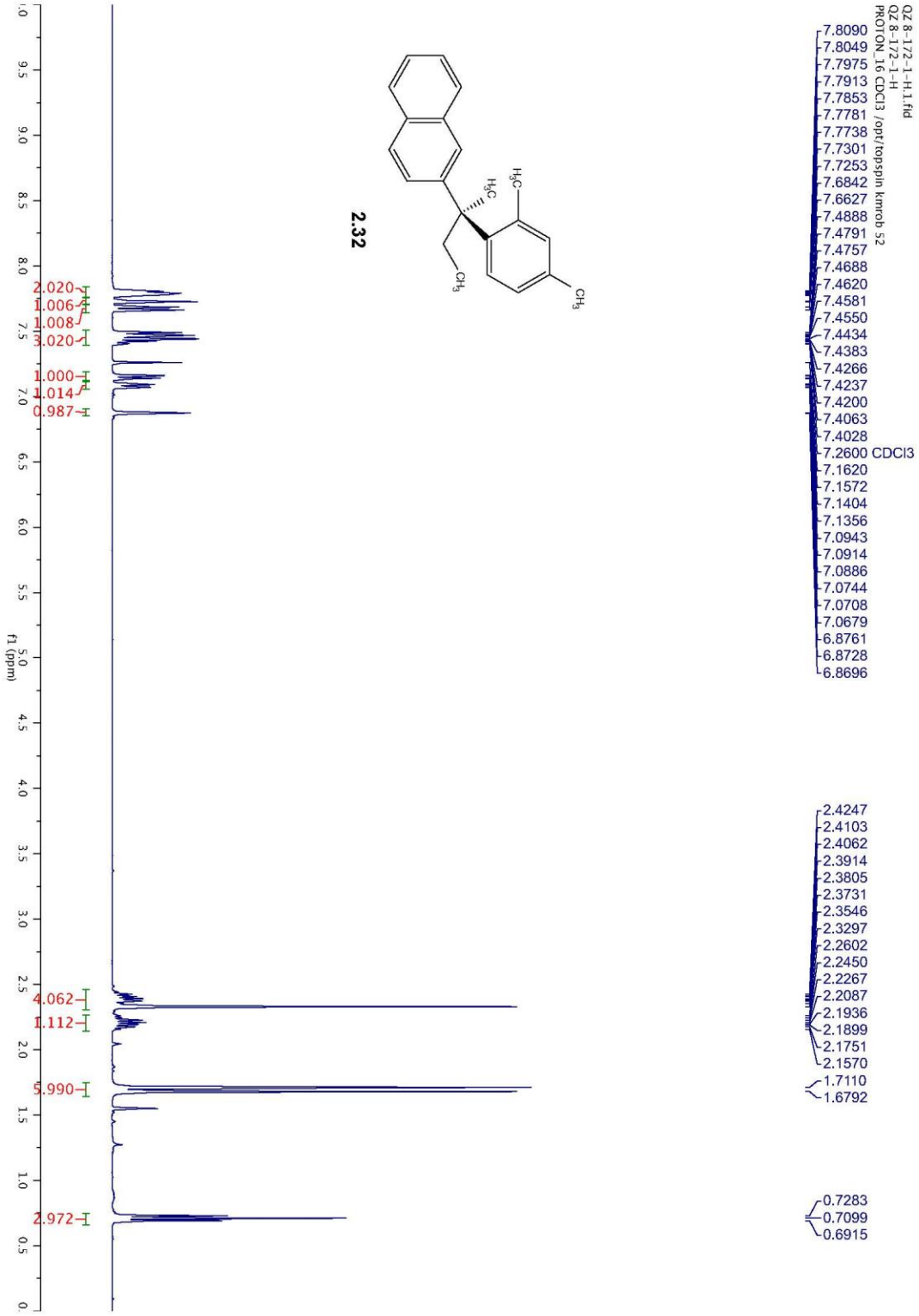
2.32
QZ 8-172-1-H.1.fid
QZ 8-172-1-H
PROTON_16 CDCl3 /opt/topspin kmrob 52
7.8090
7.8049
7.7975
7.7913
7.7853
7.7781
7.7738
7.7301
7.7253
7.6842
7.6627
7.4888
7.4791
7.4757
7.4688
7.4620
7.4581
7.4550
7.4434
7.4383
7.4266
7.4237
7.4200
7.4063
7.4028
7.2600 CDCl3
7.1620
7.1572
7.1404
7.1356
7.0943
7.0914
7.0886
7.0744
7.0708
7.0679
6.8761
6.8728
6.8696
2.4247
2.4103
2.4062
2.3914
2.3805
2.3731
2.3546
2.3297
2.2602
2.2450
2.2267
2.2087
2.1936
2.1899
2.1751
2.1570
1.7110
1.6792
0.7283
0.7099
0.6915
2.020
1.006
1.008
3.020
1.000
1.014
0.987
4.062
1.112
5.990
2.972
f1 (ppm)

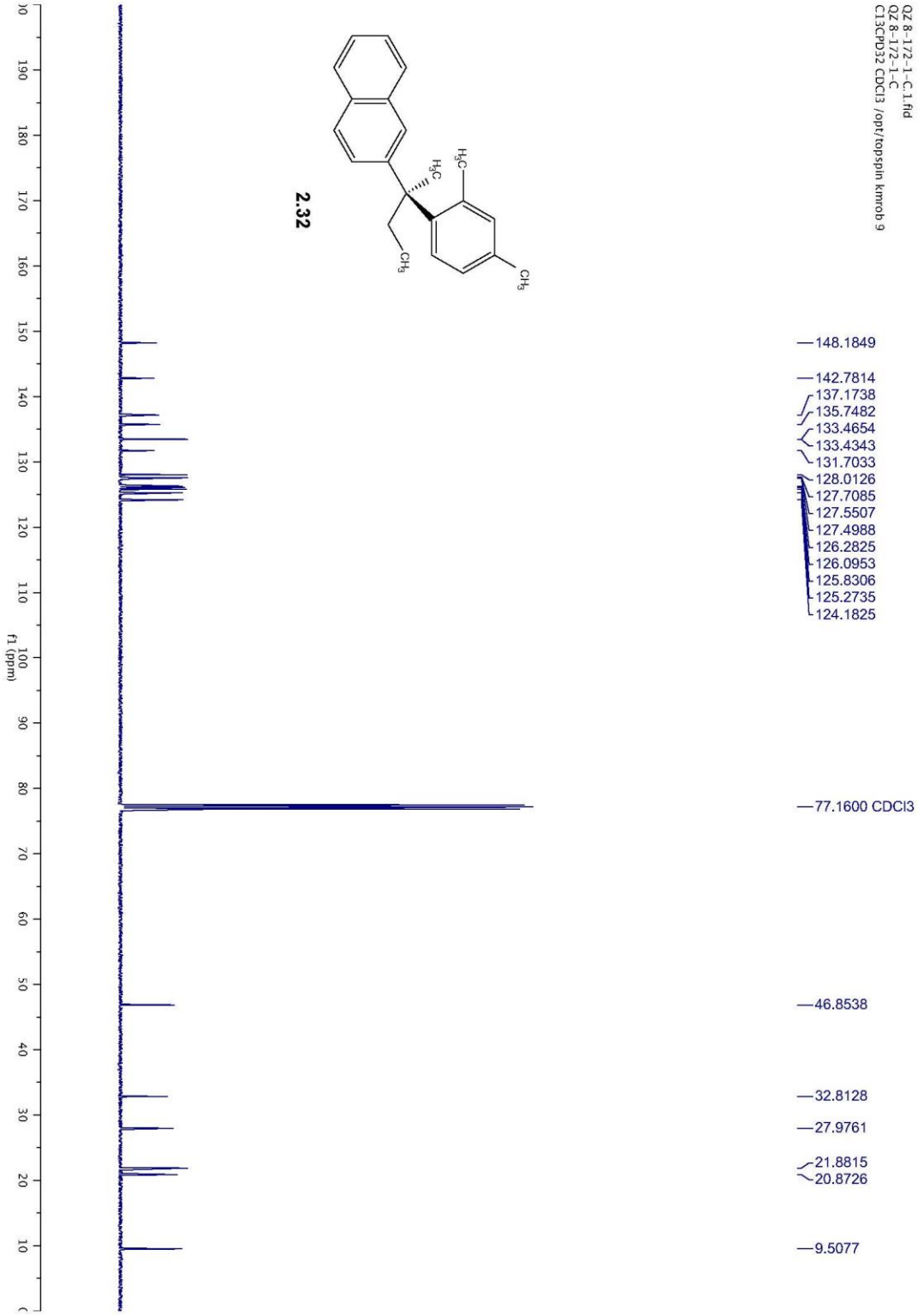
QZ 8-172-1-C.1.fid
QZ 8-172-1-C
C13CPD32 CDCl3 /opt/topspin kmrob 9
2.32
148.1849
142.7814
137.1738
135.7482
133.4654
133.4343
131.7033
128.0126
127.7085
127.5507
127.4988
126.2825
126.0953
125.8306
125.2735
124.1825
77.1600 CDCl3
46.8538
32.8128
27.9761
21.8815
20.8726
9.5077
f1 (ppm)

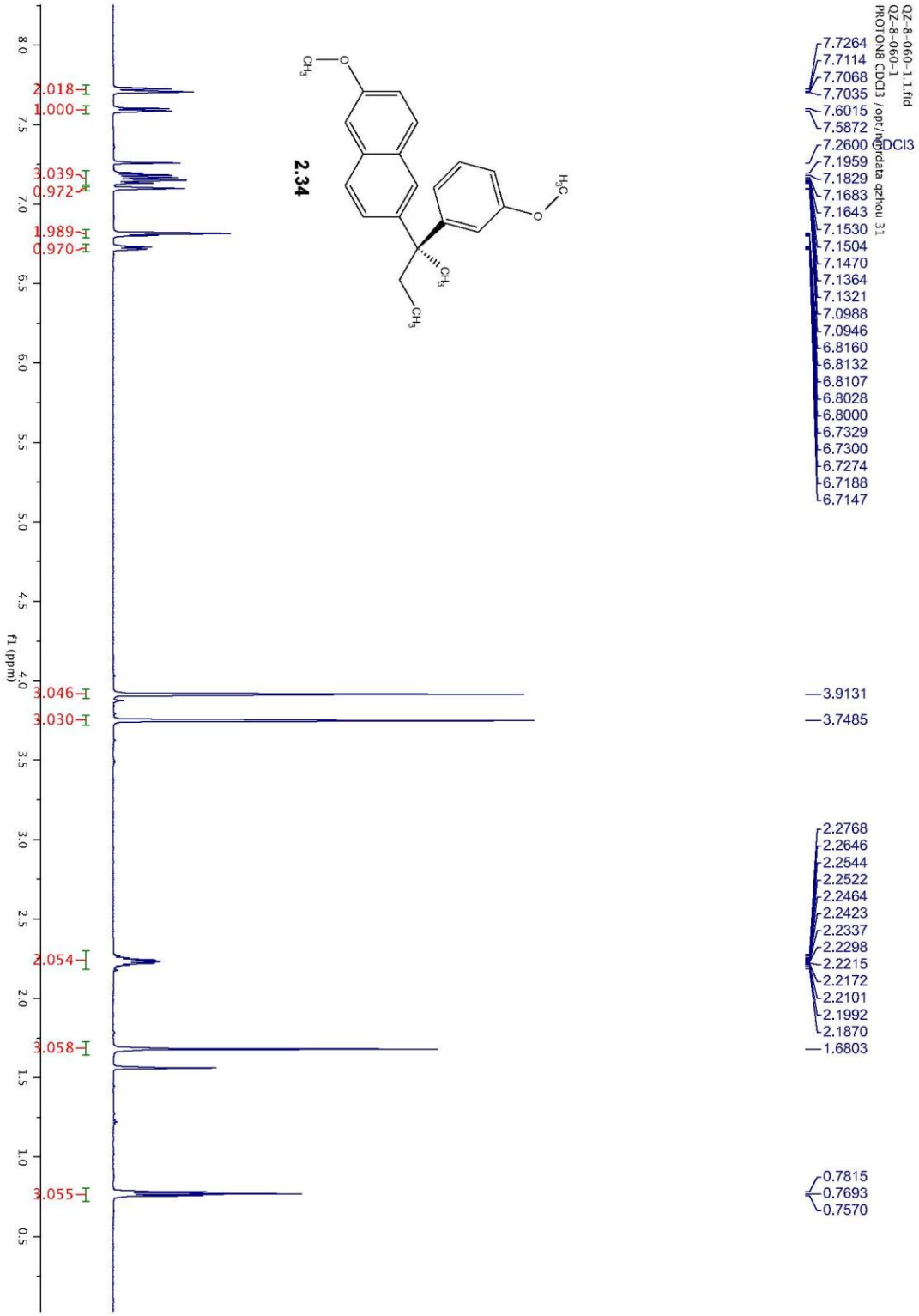
2.34
QZ-8-060-1.1.fid
QZ-8-060-1
PROTON8 CDCl3 /opt/nmrdata qzhou 31
CDCl3
7.7264
7.7114
7.7068
7.7035
7.6015
7.5872
7.2600
7.1959
7.1829
7.1683
7.1643
7.1530
7.1504
7.1470
7.1364
7.1321
7.0988
7.0946
6.8160
6.8132
6.8107
6.8028
6.8000
6.7329
6.7300
6.7274
6.7188
6.7147
3.9131
3.7485
2.2768
2.2646
2.2544
2.2522
2.2464
2.2423
2.2337
2.2298
2.2215
2.2172
2.2101
2.1992
2.1870
1.6803
0.7815
0.7693
0.7570
2.018
1.000
3.039
0.972
1.989
0.970
3.046
3.030
2.054
3.058
3.055
f1 (ppm)

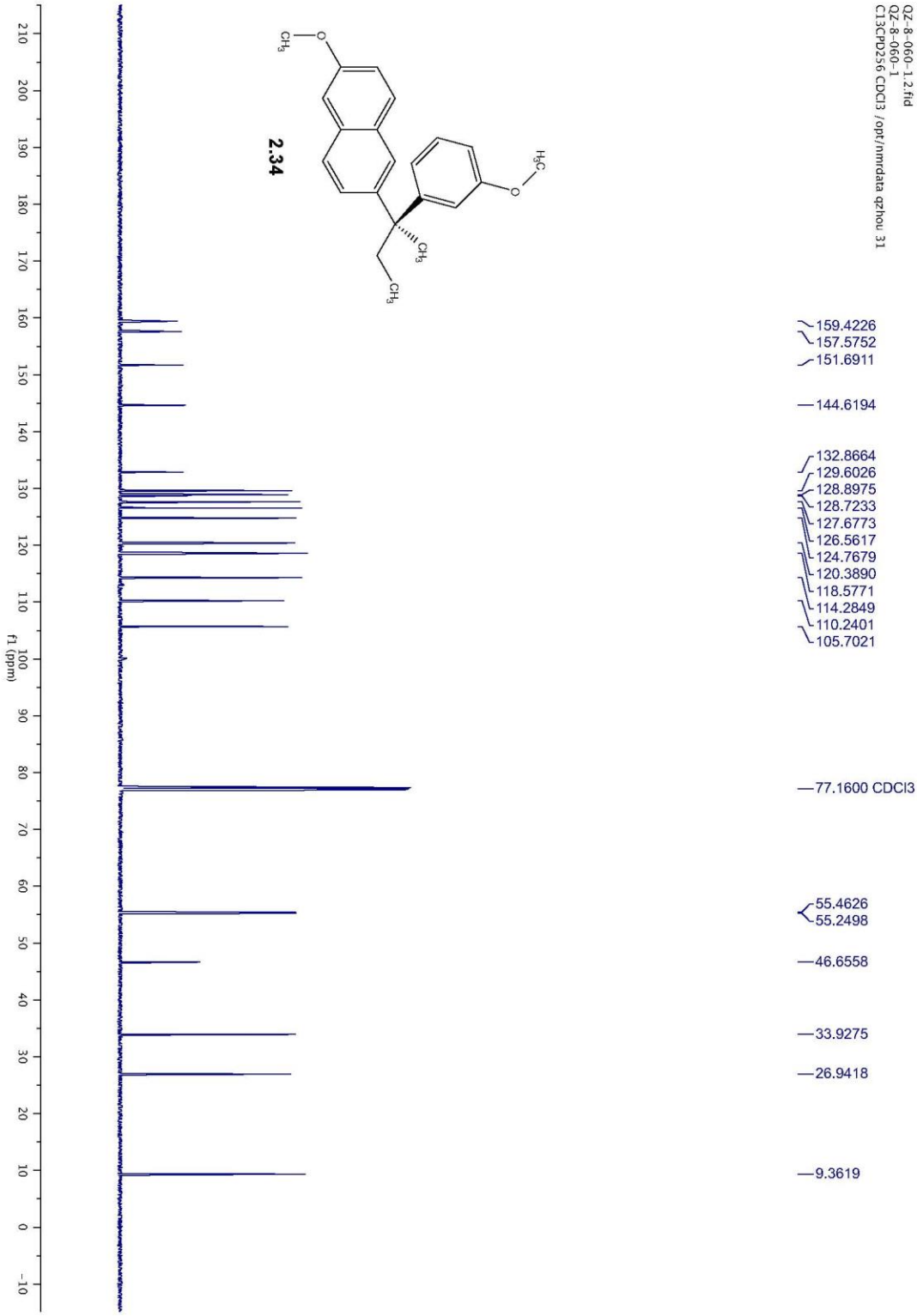
QZ-8-060-1.2.fid
QZ-8-060-1
C13CPD256 CDCl3 /opt/nmrdata qzhou 31
2.34
159.4226
157.5752
151.6911
144.6194
132.8664
129.6026
128.8975
128.7233
127.6773
126.5617
124.7679
120.3890
118.5771
114.2849
110.2401
105.7021
77.1600 CDCl3
55.4626
55.2498
46.6558
33.9275
26.9418
9.3619
f1 (ppm)

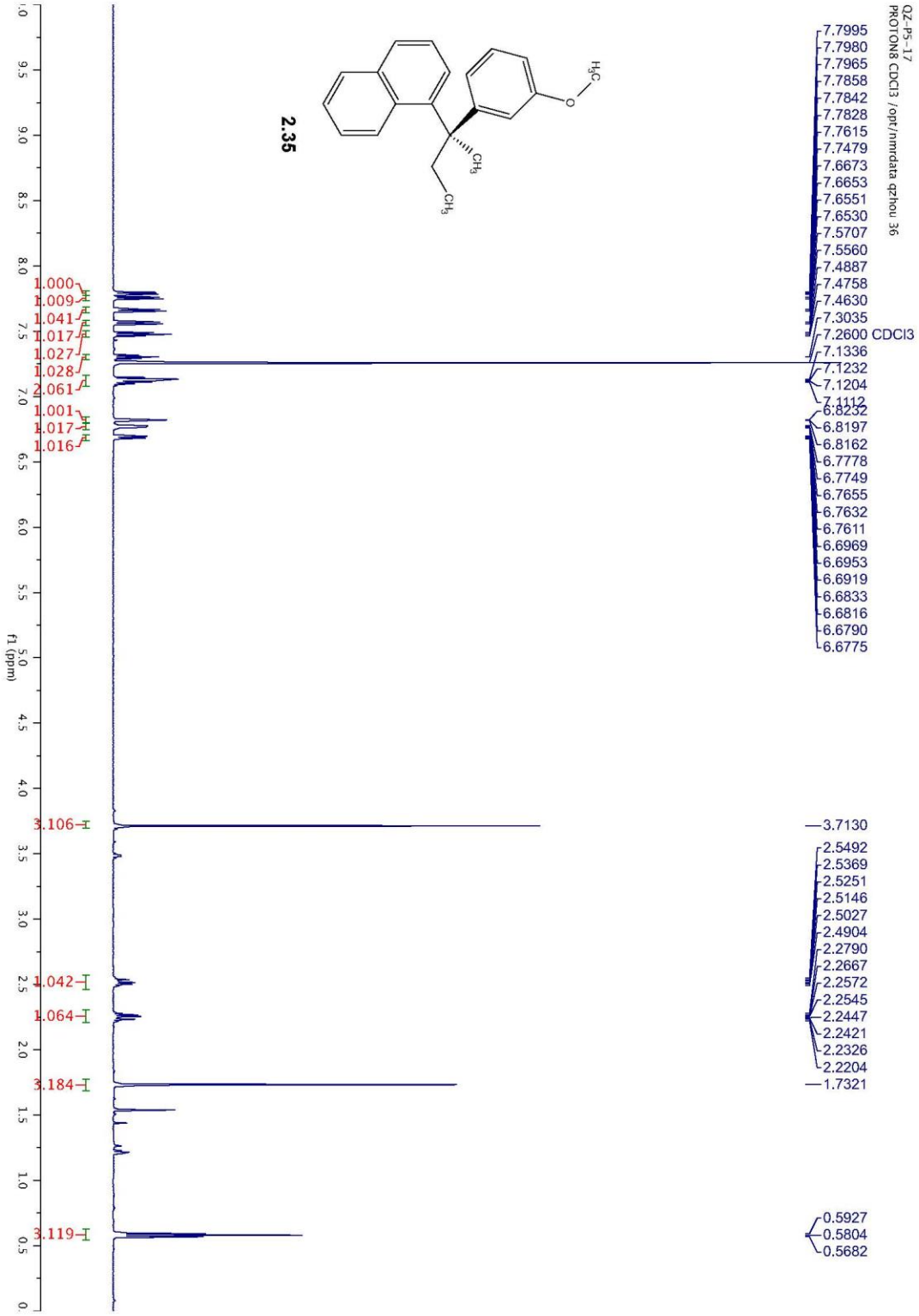
2.35
QZ-P5-17
PROTON8 CDCl3 /opt/nmrdata qzhou 36
7.7995
7.7980
7.7965
7.7858
7.7842
7.7828
7.7615
7.7479
7.6673
7.6653
7.6551
7.6530
7.5707
7.5560
7.4887
7.4758
7.4630
7.3035
7.2600 CDCl3
7.1336
7.1232
7.1204
7.1112
6.8232
6.8197
6.8162
6.7778
6.7749
6.7655
6.7632
6.7611
6.6969
6.6953
6.6919
6.6833
6.6816
6.6790
6.6775
3.7130
2.5492
2.5369
2.5251
2.5146
2.5027
2.4904
2.2790
2.2667
2.2572
2.2545
2.2447
2.2421
2.2326
2.2204
1.7321
0.5927
0.5804
0.5682
1.000
1.009
1.041
1.017
1.027
1.028
2.061
1.001
1.017
1.016
3.106
1.042
1.064
3.184
3.119
f1 (ppm)

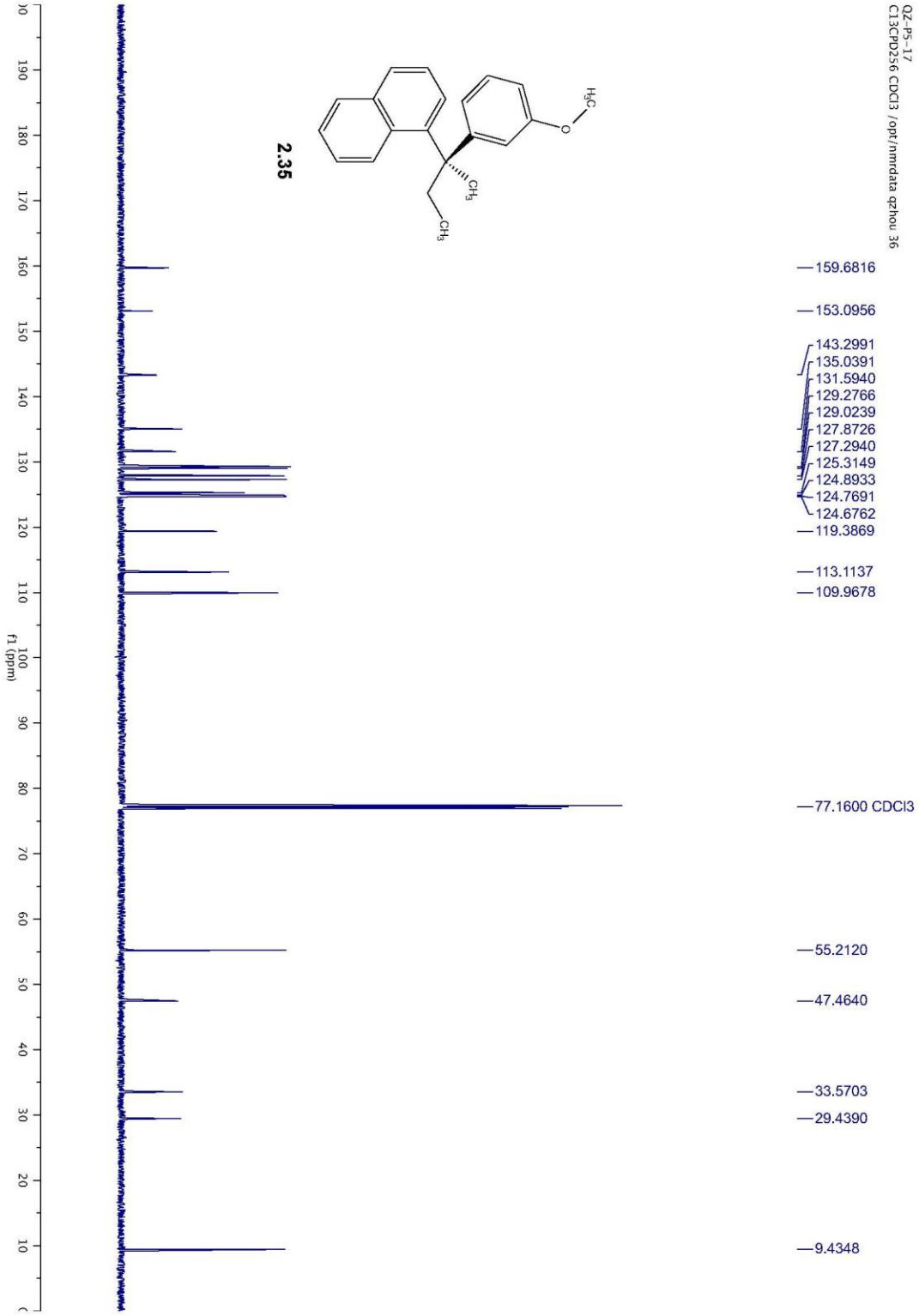
QZ-P5-17
C13CPD256 CDCl3 /opt/nmrdata qzhou 36
2.35
H3C
O
CH3
CH3
159.6816
153.0956
143.2991
135.0391
131.5940
129.2766
129.0239
127.8726
127.2940
125.3149
124.8933
124.7691
124.6762
119.3869
113.1137
109.9678
77.1600 CDCl3
55.2120
47.4640
33.5703
29.4390
9.4348
f1 (ppm)

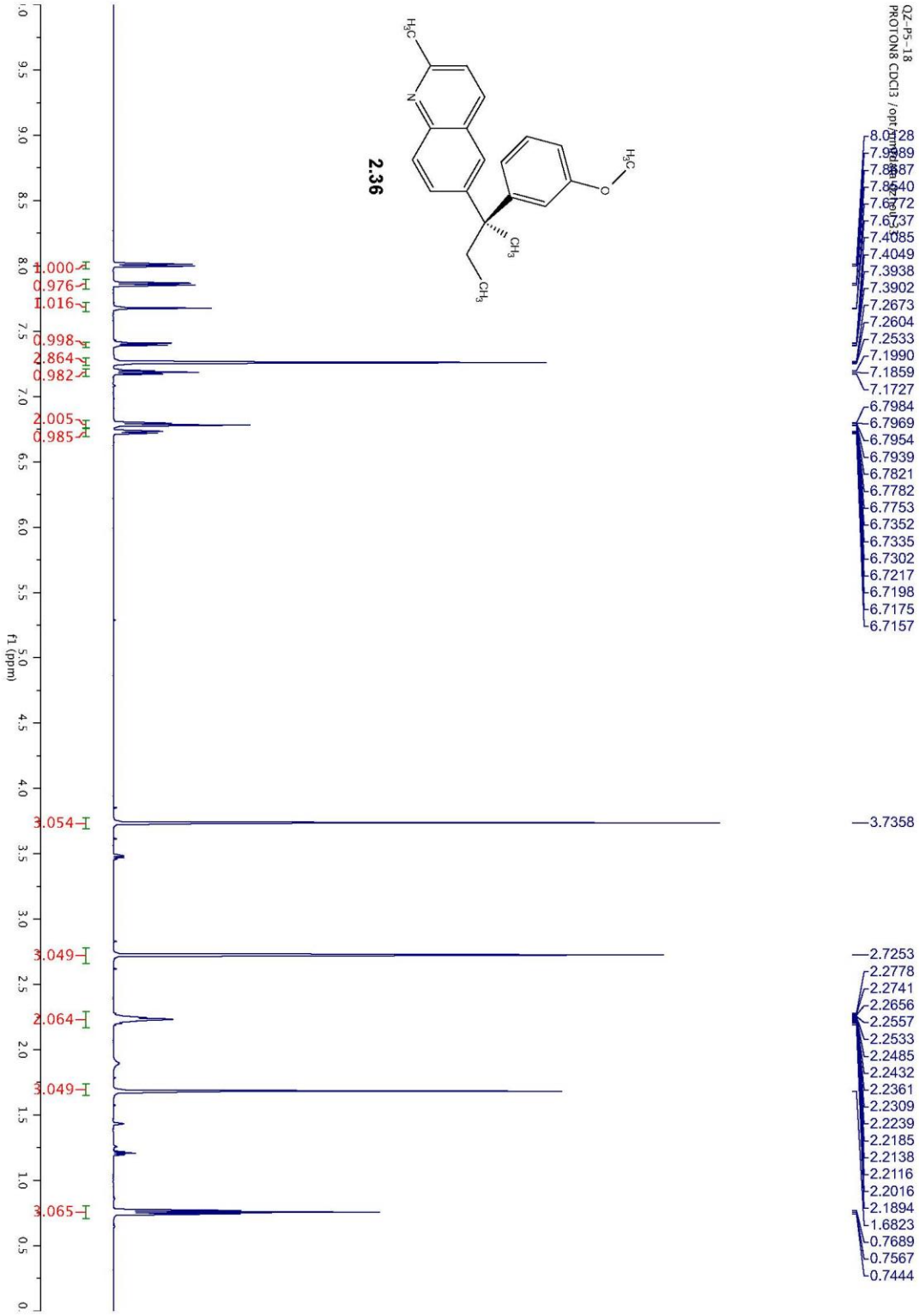
2.36
QZ-P5-18
PROTON8 CDCl3 /opt/data
1.000
0.976
1.016
0.998
2.864
0.982
2.005
0.985
3.054
3.049
2.064
3.049
3.065
f1 (ppm)
8.0128
7.9389
7.8587
7.8540
7.6772
7.6737
7.4085
7.4049
7.3938
7.3902
7.2673
7.2604
7.2533
7.1990
7.1859
7.1727
6.7984
6.7969
6.7954
6.7939
6.7821
6.7782
6.7753
6.7352
6.7335
6.7302
6.7217
6.7198
6.7175
6.7157
3.7358
2.7253
2.2778
2.2741
2.2656
2.2557
2.2533
2.2485
2.2432
2.2361
2.2309
2.2239
2.2185
2.2138
2.2116
2.2016
2.1894
1.6823
0.7689
0.7567
0.7444

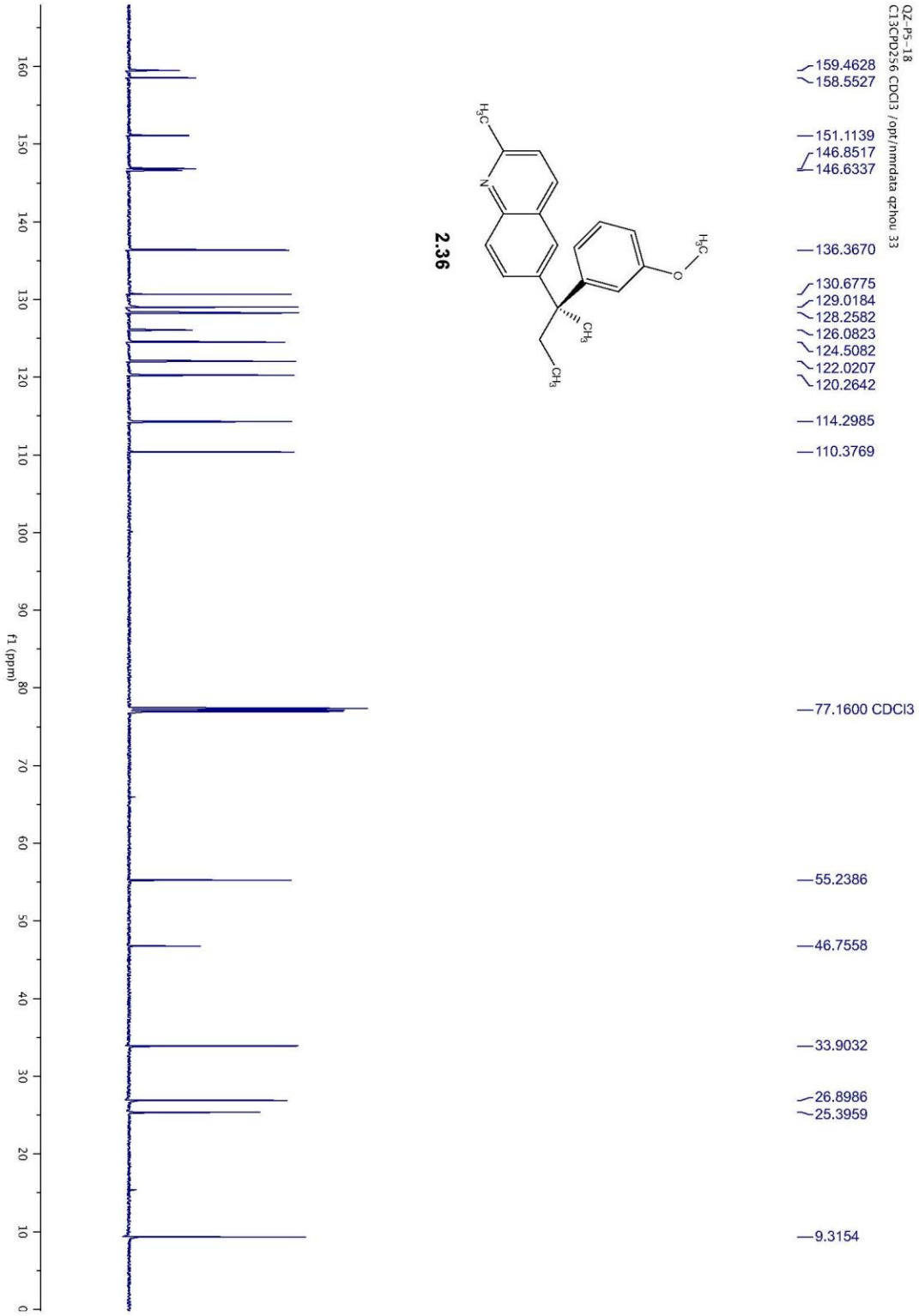
QZ-P5-18
C13CPD256 CDCl3 /opt/nmrdata qzhou 33
159.4628
158.5527
151.1139
146.8517
146.6337
136.3670
130.6775
129.0184
128.2582
126.0823
124.5082
122.0207
120.2642
114.2985
110.3769
77.1600 CDCl3
55.2386
46.7558
33.9032
26.8986
25.3959
9.3154
2.36
f1 (ppm)

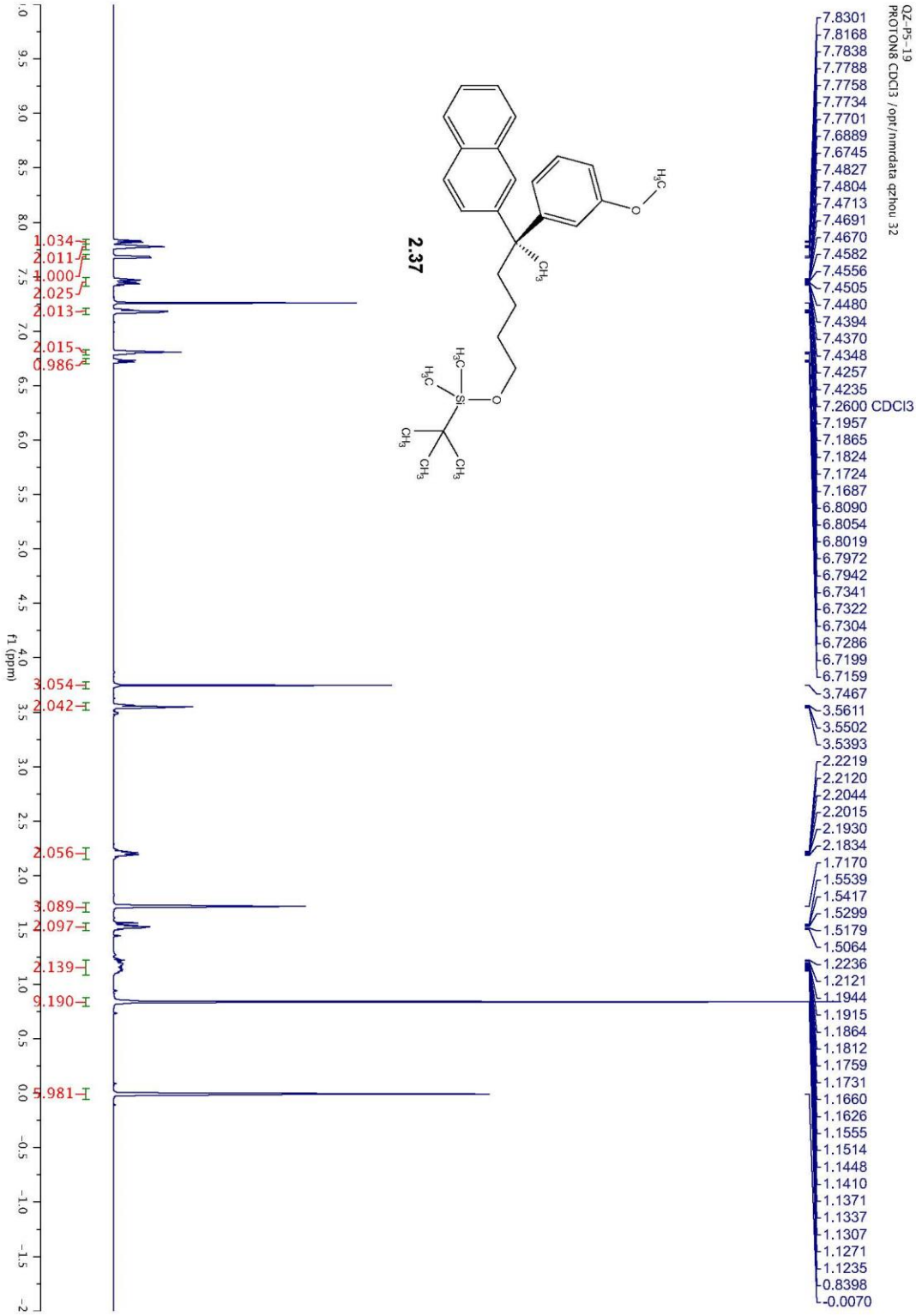
QZ-P5-19
PROTON6 CDCl3 /opt/nmrdata qzhou 32
2.37
f1 (ppm)
1.034
2.011
1.000
2.025
2.013
2.015
0.986
3.054
2.042
2.056
3.089
2.097
2.139
9.190
5.981
7.8301
7.8168
7.7838
7.7788
7.7758
7.7734
7.7701
7.6889
7.6745
7.4827
7.4804
7.4713
7.4691
7.4670
7.4582
7.4556
7.4505
7.4480
7.4394
7.4370
7.4348
7.4257
7.4235
7.2600 CDCl3
7.1957
7.1865
7.1824
7.1724
7.1687
6.8090
6.8054
6.8019
6.7972
6.7942
6.7341
6.7322
6.7304
6.7286
6.7199
6.7159
3.7467
3.5611
3.5502
3.5393
2.2219
2.2120
2.2044
2.2015
2.1930
2.1834
1.7170
1.5539
1.5417
1.5299
1.5179
1.5064
1.2236
1.2121
1.1944
1.1915
1.1864
1.1812
1.1759
1.1731
1.1660
1.1626
1.1555
1.1514
1.1448
1.1410
1.1371
1.1337
1.1307
1.1271
1.1235
0.8398
-0.0070

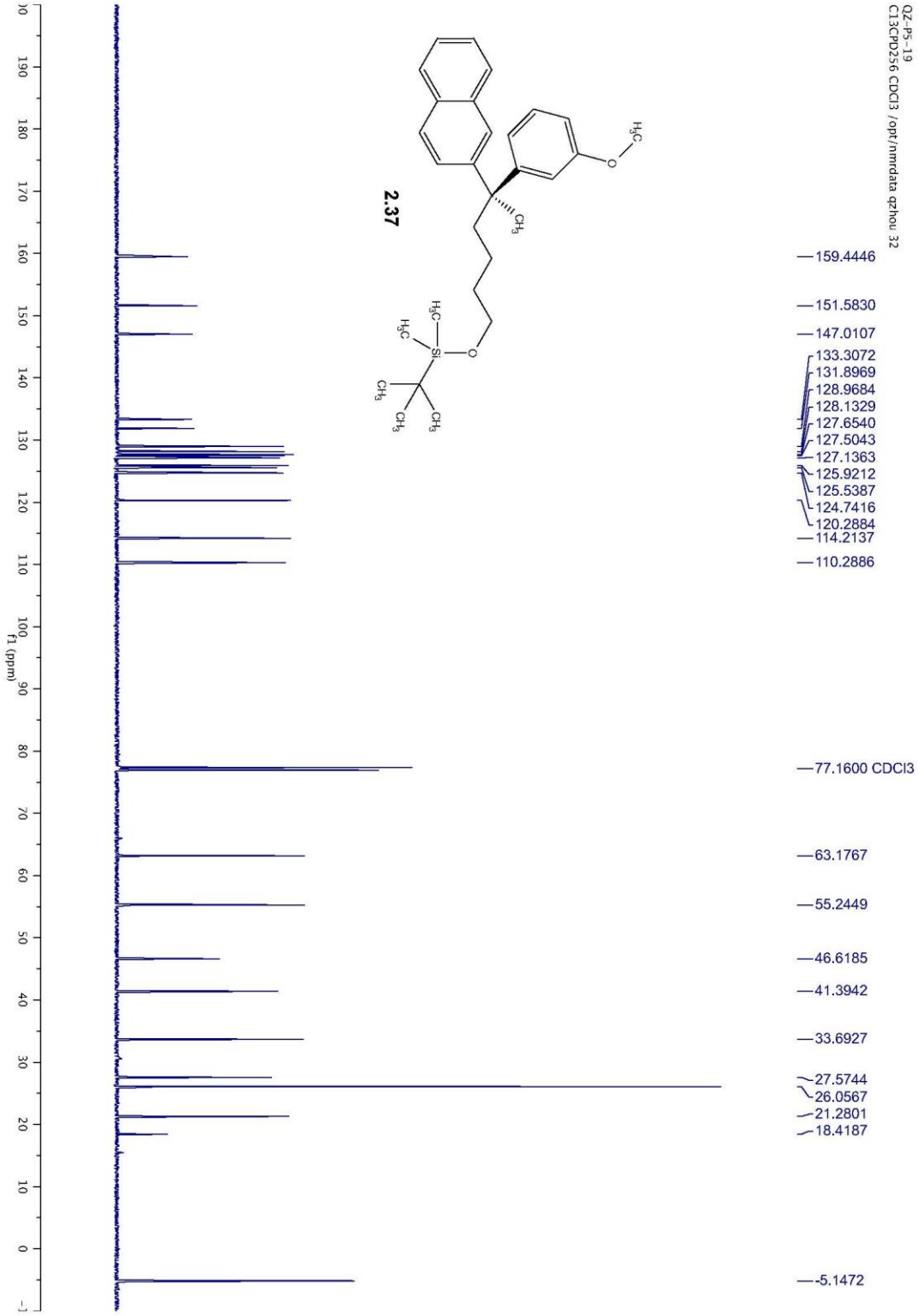
QZ-P5-19
C13CPD256 CDCl3 /opt/nmrdata qzhou 32
2.37
159.4446
151.5830
147.0107
133.3072
131.8969
128.9684
128.1329
127.6540
127.5043
127.1363
125.9212
125.5387
124.7416
120.2884
114.2137
110.2886
77.1600 CDCl3
63.1767
55.2449
46.6185
41.3942
33.6927
27.5744
26.0567
21.2801
18.4187
-5.1472
f1 (ppm)

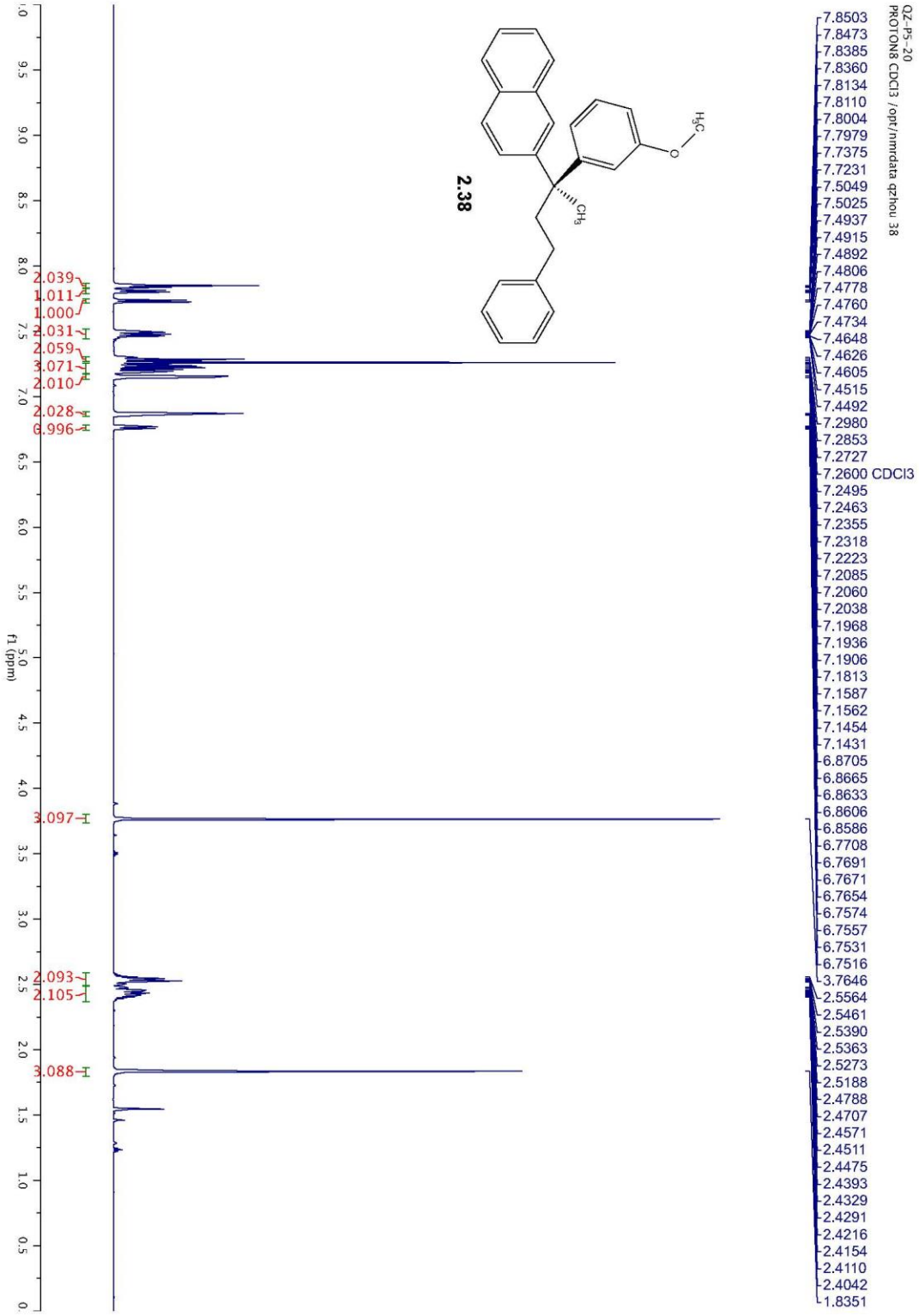
2.38
H3C
CH3
O
f1 (ppm)
2.039
1.011
1.000
2.031
2.059
3.071
2.010
2.028
0.996
3.097
2.093
2.105
3.088
QZ-P5-20
PROTON8 CDCl3 /opt/nmrdata qzhou 38
7.8503
7.8473
7.8385
7.8360
7.8134
7.8110
7.8004
7.7979
7.7375
7.7231
7.5049
7.5025
7.4937
7.4915
7.4892
7.4806
7.4778
7.4760
7.4734
7.4648
7.4626
7.4605
7.4515
7.4492
7.2980
7.2853
7.2727
7.2600 CDCl3
7.2495
7.2463
7.2355
7.2318
7.2223
7.2085
7.2060
7.2038
7.1968
7.1936
7.1906
7.1813
7.1587
7.1562
7.1454
7.1431
6.8705
6.8665
6.8633
6.8606
6.8586
6.7708
6.7691
6.7671
6.7654
6.7574
6.7557
6.7531
6.7516
3.7646
2.5564
2.5461
2.5390
2.5363
2.5273
2.5188
2.4788
2.4707
2.4571
2.4511
2.4475
2.4393
2.4329
2.4291
2.4216
2.4154
2.4110
2.4042
1.8351

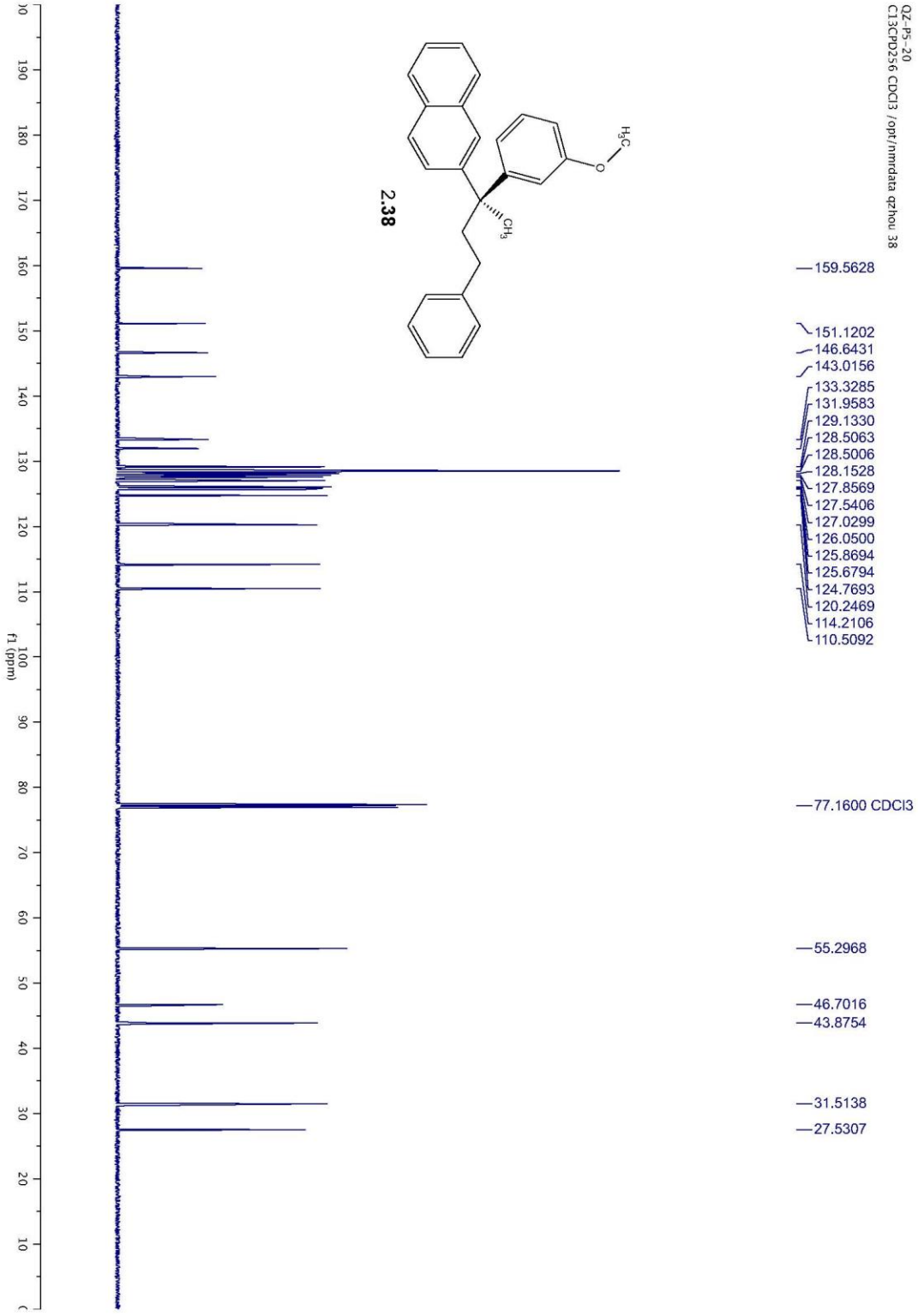
QZ-P5-20
C13CPD256 CDCl3 /opt/nmrdata qzhou 38
2.38
159.5628
151.1202
146.6431
143.0156
133.3285
131.9583
129.1330
128.5063
128.5006
128.1528
127.8569
127.5406
127.0299
126.0500
125.8694
125.6794
124.7693
120.2469
114.2106
110.5092
77.1600 CDCl3
55.2968
46.7016
43.8754
31.5138
27.5307
f1 (ppm)

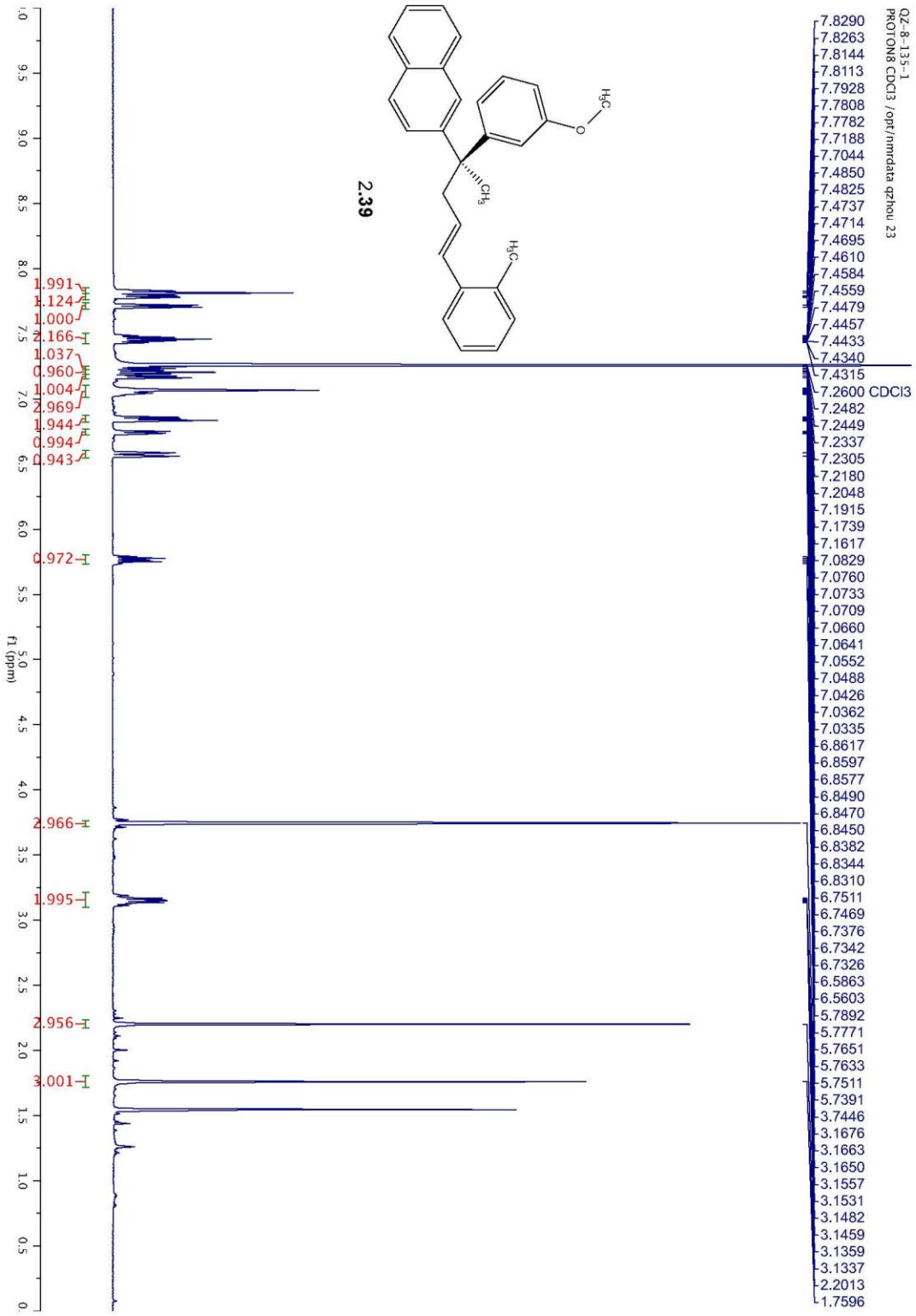
2.39
QZ-8-135-1
PROTON8 CDCl3 /opt/nmrdata qzhou 23
f1 (ppm)
1.991
1.124
1.000
2.166
1.037
0.960
1.004
2.969
1.944
0.994
0.943
0.972
2.966
1.995
2.956
3.001
7.8290
7.8263
7.8144
7.8113
7.7928
7.7808
7.7782
7.7188
7.7044
7.4850
7.4825
7.4737
7.4714
7.4695
7.4610
7.4584
7.4559
7.4479
7.4457
7.4433
7.4340
7.4315
7.2600 CDCl3
7.2482
7.2449
7.2337
7.2305
7.2180
7.2048
7.1915
7.1739
7.1617
7.0829
7.0760
7.0733
7.0709
7.0660
7.0641
7.0552
7.0488
7.0426
7.0362
7.0335
6.8617
6.8597
6.8577
6.8490
6.8470
6.8450
6.8382
6.8344
6.8310
6.7511
6.7469
6.7376
6.7342
6.7326
6.5863
6.5603
5.7892
5.7771
5.7651
5.7633
5.7511
5.7391
3.7446
3.1676
3.1663
3.1650
3.1557
3.1531
3.1482
3.1459
3.1359
3.1337
2.2013
1.7596

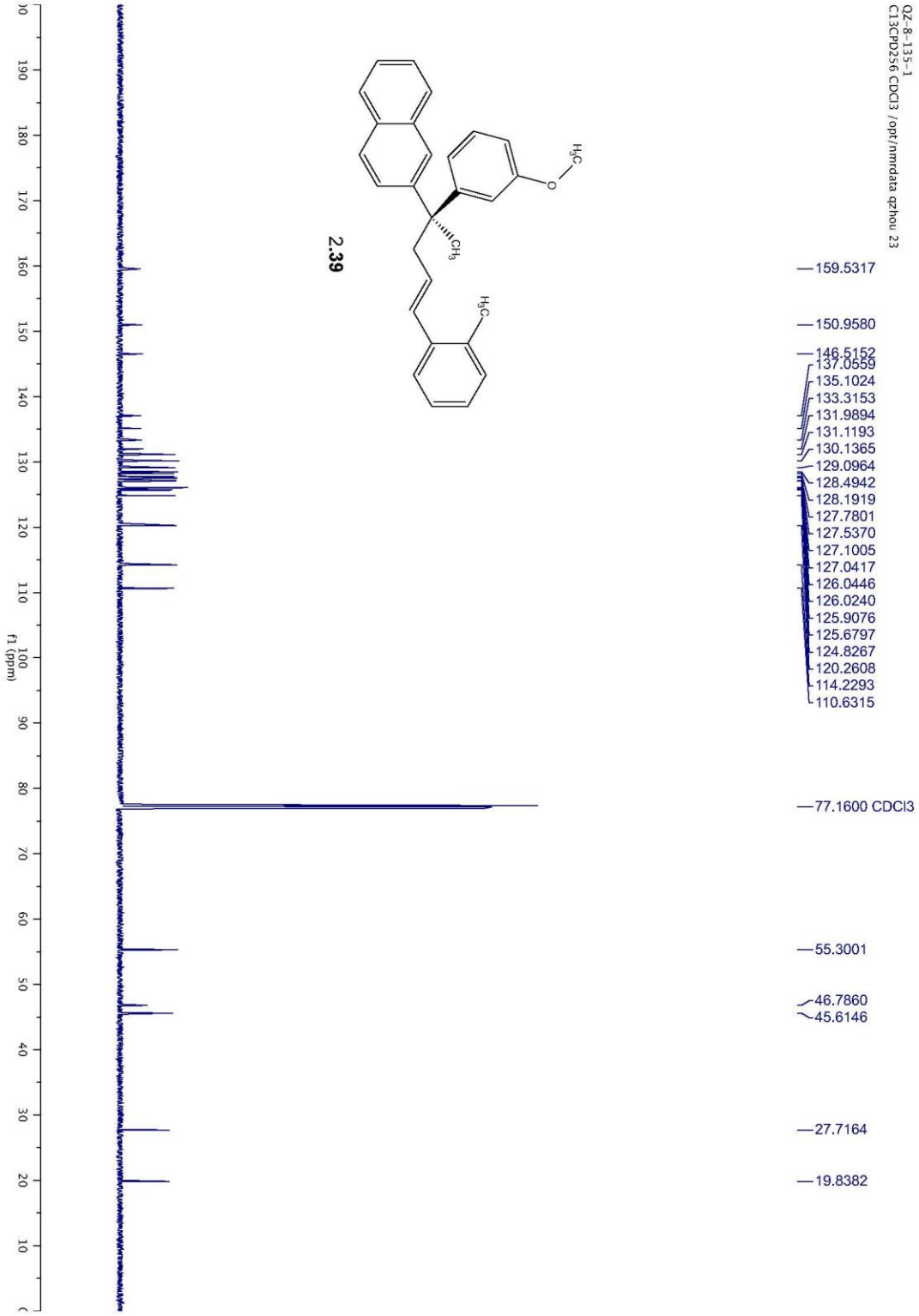
QZ-8-135-1
C13CPD256 CDCl3 /opt/nmrdata qzhou 23
2.39
159.5317
150.9580
146.5152
137.0559
135.1024
133.3153
131.9894
131.1193
130.1365
129.0964
128.4942
128.1919
127.7801
127.5370
127.1005
127.0417
126.0446
126.0240
125.9076
125.6797
124.8267
120.2608
114.2293
110.6315
77.1600 CDCl3
55.3001
46.7860
45.6146
27.7164
19.8382
f1 (ppm)

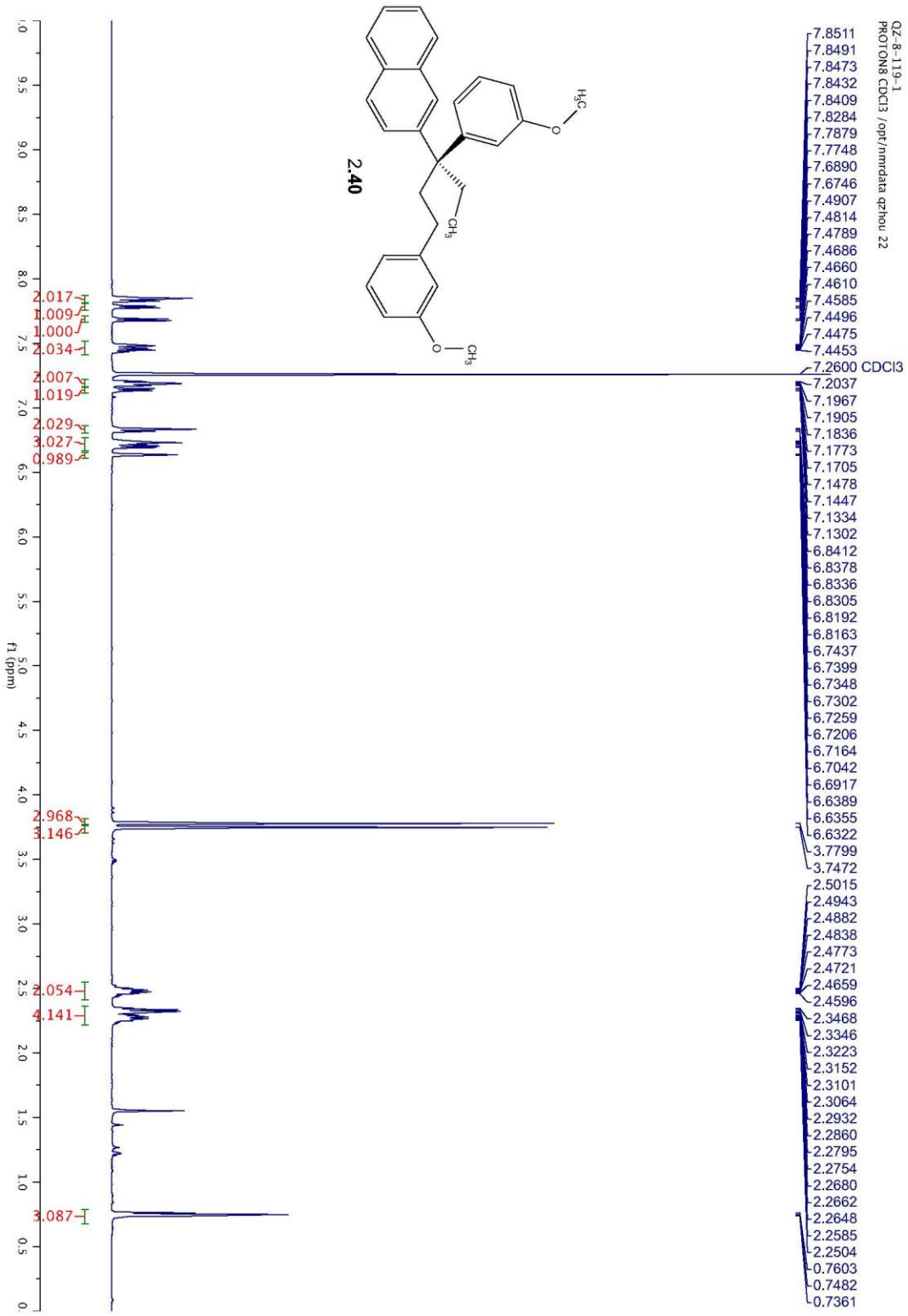
2.40
QZ-8-119-1
PROTON8 CDCl3 /opt/nmrdata qzhou 22
7.8511
7.8491
7.8473
7.8432
7.8409
7.8284
7.7879
7.7748
7.6890
7.6746
7.4907
7.4814
7.4789
7.4686
7.4660
7.4610
7.4585
7.4496
7.4475
7.4453
7.2600 CDCl3
7.2037
7.1967
7.1905
7.1836
7.1773
7.1705
7.1478
7.1447
7.1334
7.1302
6.8412
6.8378
6.8336
6.8305
6.8192
6.8163
6.7437
6.7399
6.7348
6.7302
6.7259
6.7206
6.7164
6.7042
6.6917
6.6389
6.6355
6.6322
3.7799
3.7472
2.5015
2.4943
2.4882
2.4838
2.4773
2.4721
2.4659
2.4596
2.3468
2.3346
2.3223
2.3152
2.3101
2.3064
2.2932
2.2860
2.2795
2.2754
2.2680
2.2662
2.2648
2.2585
2.2504
0.7603
0.7482
0.7361
2.017
1.009
1.000
2.034
2.007
1.019
2.029
3.027
0.989
2.968
3.146
2.054
4.141
3.087
f1 (ppm)

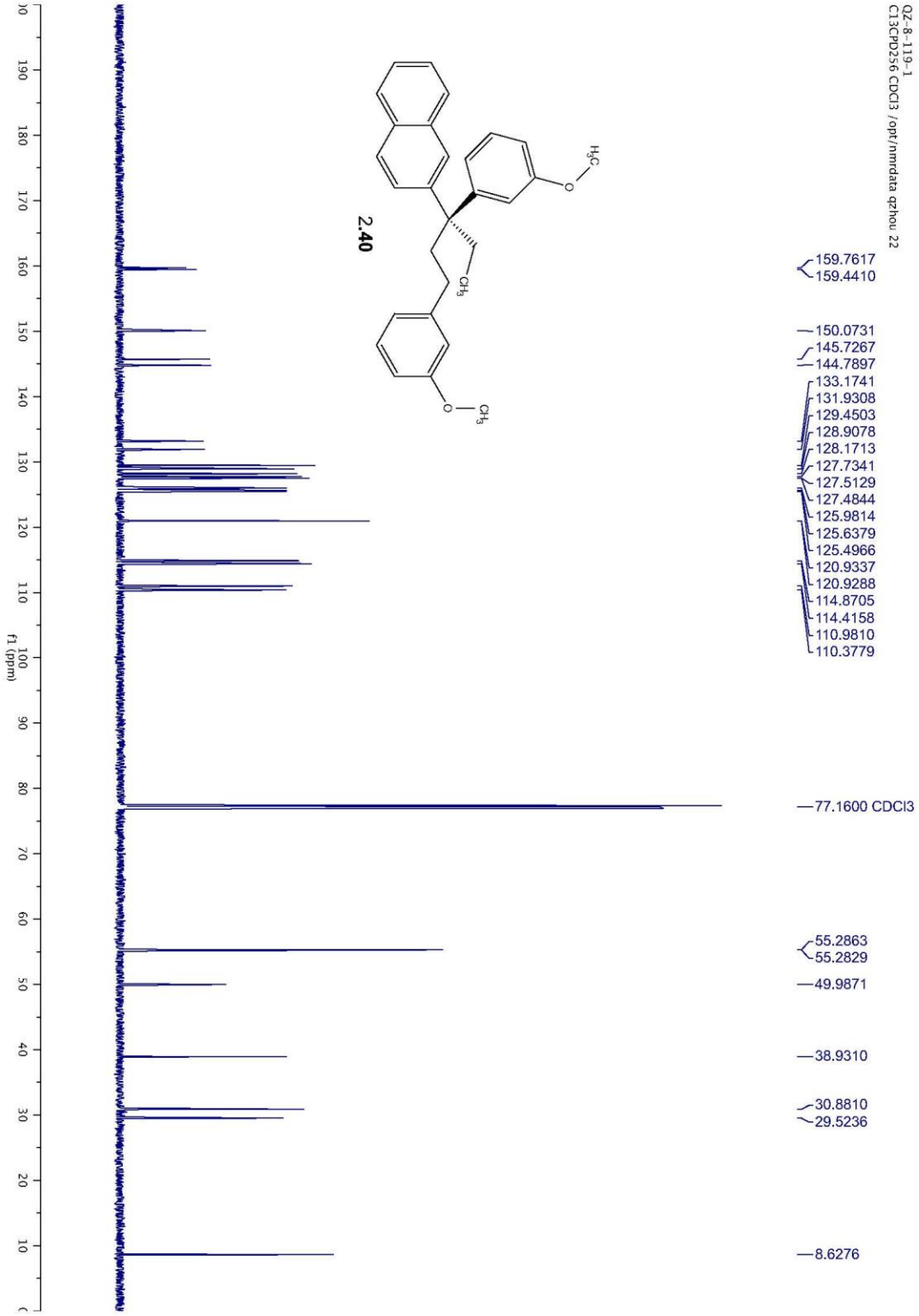
QZ-8-119-1
C13CPD256 CDCl3 /opt/nmrdata qzhou 22
2.40
159.7617
159.4410
150.0731
145.7267
144.7897
133.1741
131.9308
129.4503
128.9078
128.1713
127.7341
127.5129
127.4844
125.9814
125.6379
125.4966
120.9337
120.9288
114.8705
114.4158
110.9810
110.3779
77.1600 CDCl3
55.2863
55.2829
49.9871
38.9310
30.8810
29.5236
8.6276
f1 (ppm)

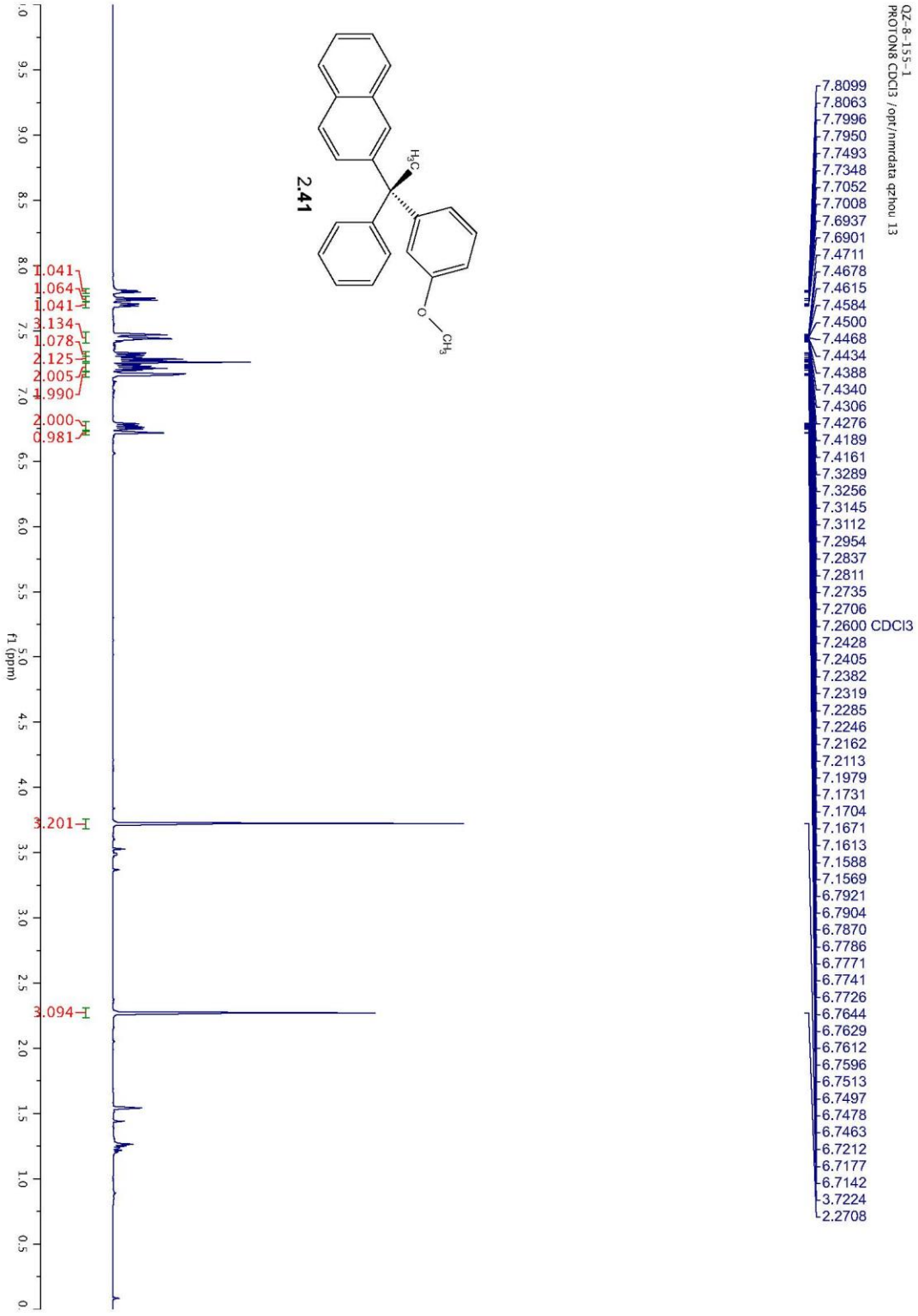
2.41
H3C
O
CH3
1.041
1.064
1.041
3.134
1.078
2.125
2.005
1.990
2.000
0.981
3.201
3.094
f1 (ppm)
QZ-8-155-1
PROTON8 CDCl3 /opt/nmrdata qzhou 13
7.8099
7.8063
7.7996
7.7950
7.7493
7.7348
7.7052
7.7008
7.6937
7.6901
7.4711
7.4678
7.4615
7.4584
7.4500
7.4468
7.4434
7.4388
7.4340
7.4306
7.4276
7.4189
7.4161
7.3289
7.3256
7.3145
7.3112
7.2954
7.2837
7.2811
7.2735
7.2706
7.2600 CDCl3
7.2428
7.2405
7.2382
7.2319
7.2285
7.2246
7.2162
7.2113
7.1979
7.1731
7.1704
7.1671
7.1613
7.1588
7.1569
6.7921
6.7904
6.7870
6.7786
6.7771
6.7741
6.7726
6.7644
6.7629
6.7612
6.7596
6.7513
6.7497
6.7478
6.7463
6.7212
6.7177
6.7142
3.7224
2.2708

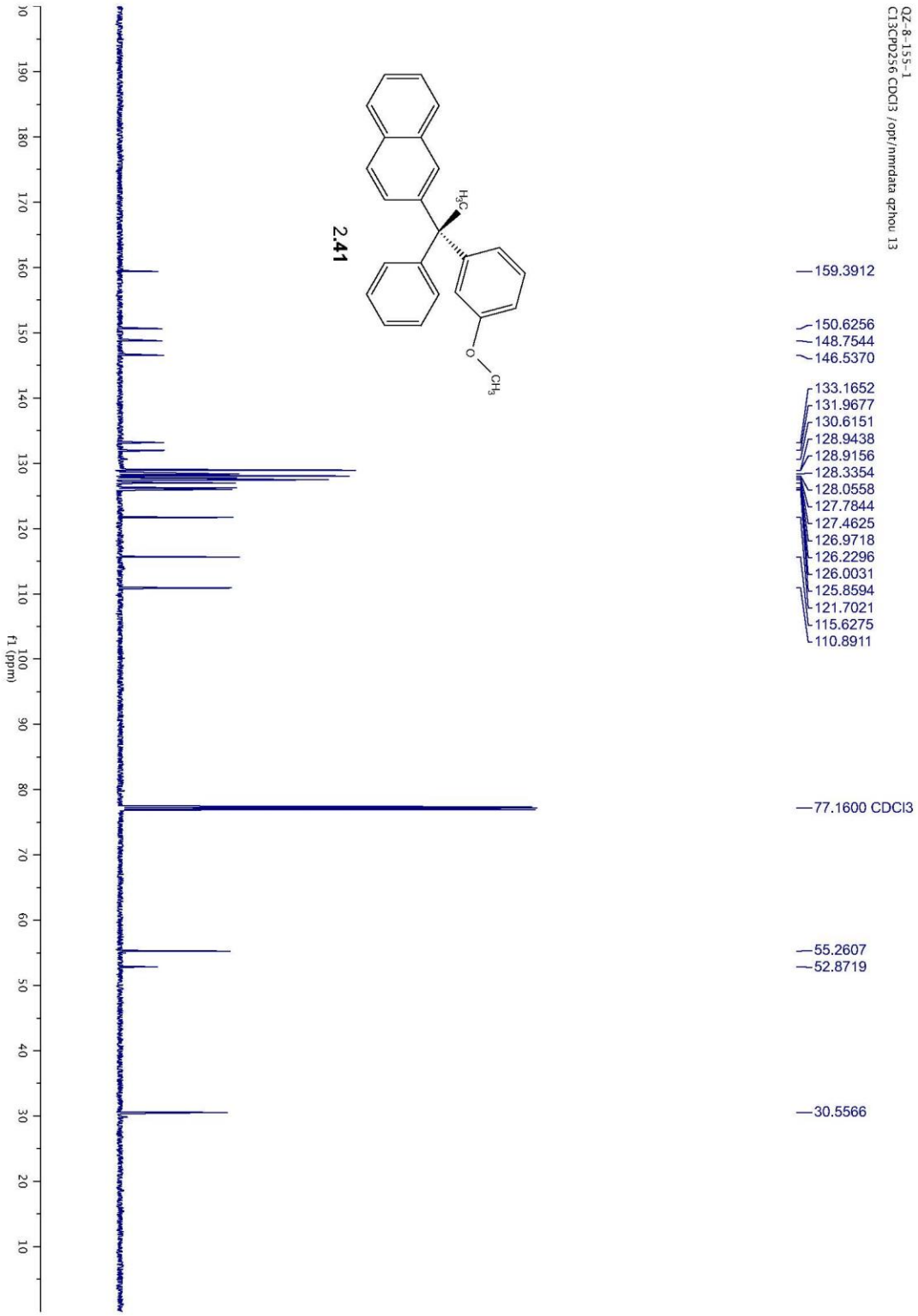
QZ-8-155-1
C13CPD256 CDCl3 /opt/nmrdata qzhou 13
2.41
159.3912
150.6256
148.7544
146.5370
133.1652
131.9677
130.6151
128.9438
128.9156
128.3354
128.0558
127.7844
127.4625
126.9718
126.2296
126.0031
125.8594
121.7021
115.6275
110.8911
77.1600 CDCl3
55.2607
52.8719
30.5566
f1 (ppm)

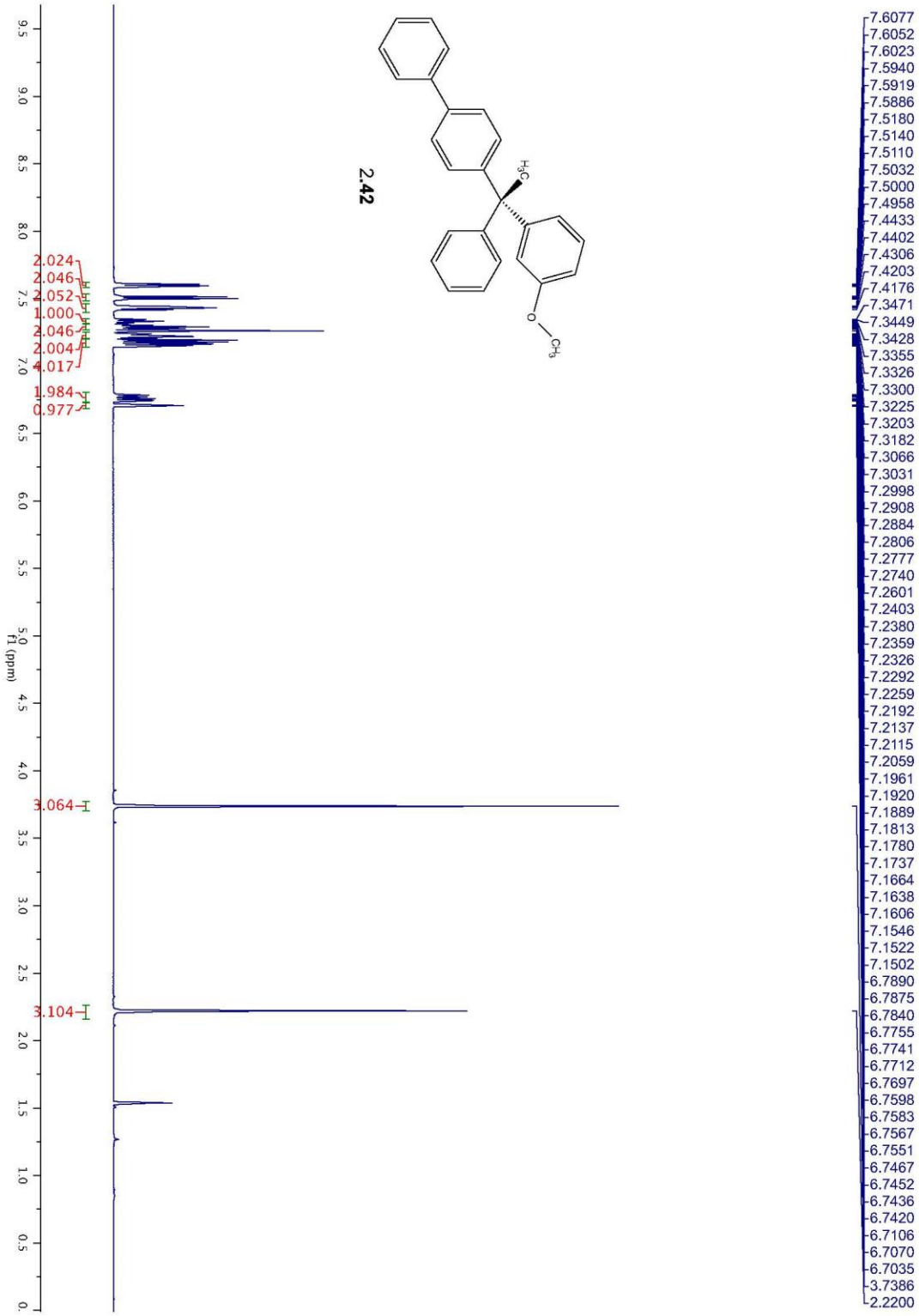
2.42
2.024
2.046
2.052
1.000
2.046
2.004
4.017
1.984
0.977
3.064
3.104
f1 (ppm)
7.6077
7.6052
7.6023
7.5940
7.5919
7.5886
7.5180
7.5140
7.5110
7.5032
7.5000
7.4958
7.4433
7.4402
7.4306
7.4203
7.4176
7.3471
7.3449
7.3428
7.3355
7.3326
7.3300
7.3225
7.3203
7.3182
7.3066
7.3031
7.2998
7.2908
7.2884
7.2806
7.2777
7.2740
7.2601
7.2403
7.2380
7.2359
7.2326
7.2292
7.2259
7.2192
7.2137
7.2115
7.2059
7.1961
7.1920
7.1889
7.1813
7.1780
7.1737
7.1664
7.1638
7.1606
7.1546
7.1522
7.1502
6.7890
6.7875
6.7840
6.7755
6.7741
6.7712
6.7697
6.7598
6.7583
6.7567
6.7551
6.7467
6.7452
6.7436
6.7420
6.7106
6.7070
6.7035
3.7386
2.2200

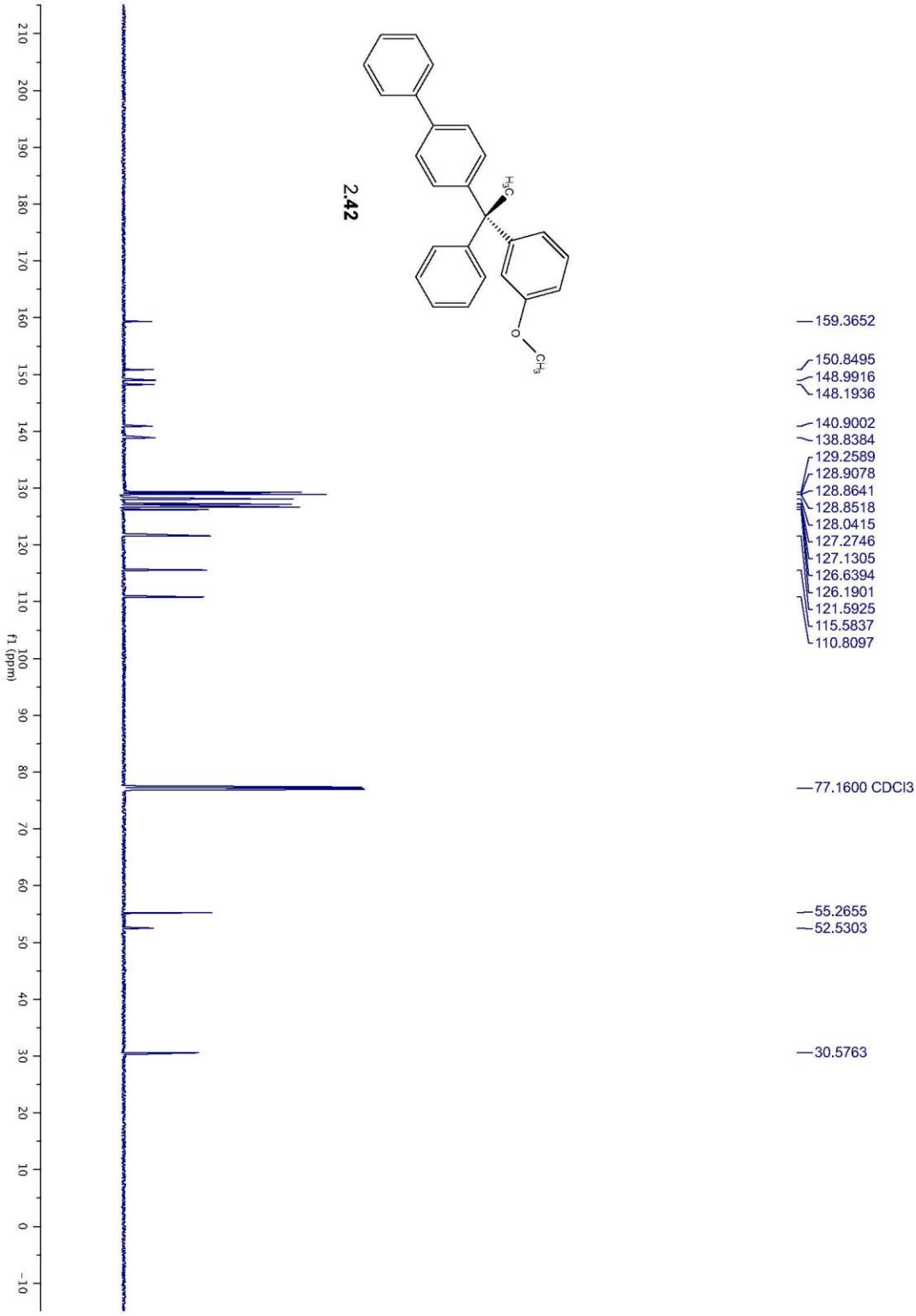
2.42
159.3652
150.8495
148.9916
148.1936
140.9002
138.8384
129.2589
128.9078
128.8641
128.8518
128.0415
127.2746
127.1305
126.6394
126.1901
121.5925
115.5837
110.8097
77.1600 CDCl3
55.2655
52.5303
30.5763
f1 (ppm)

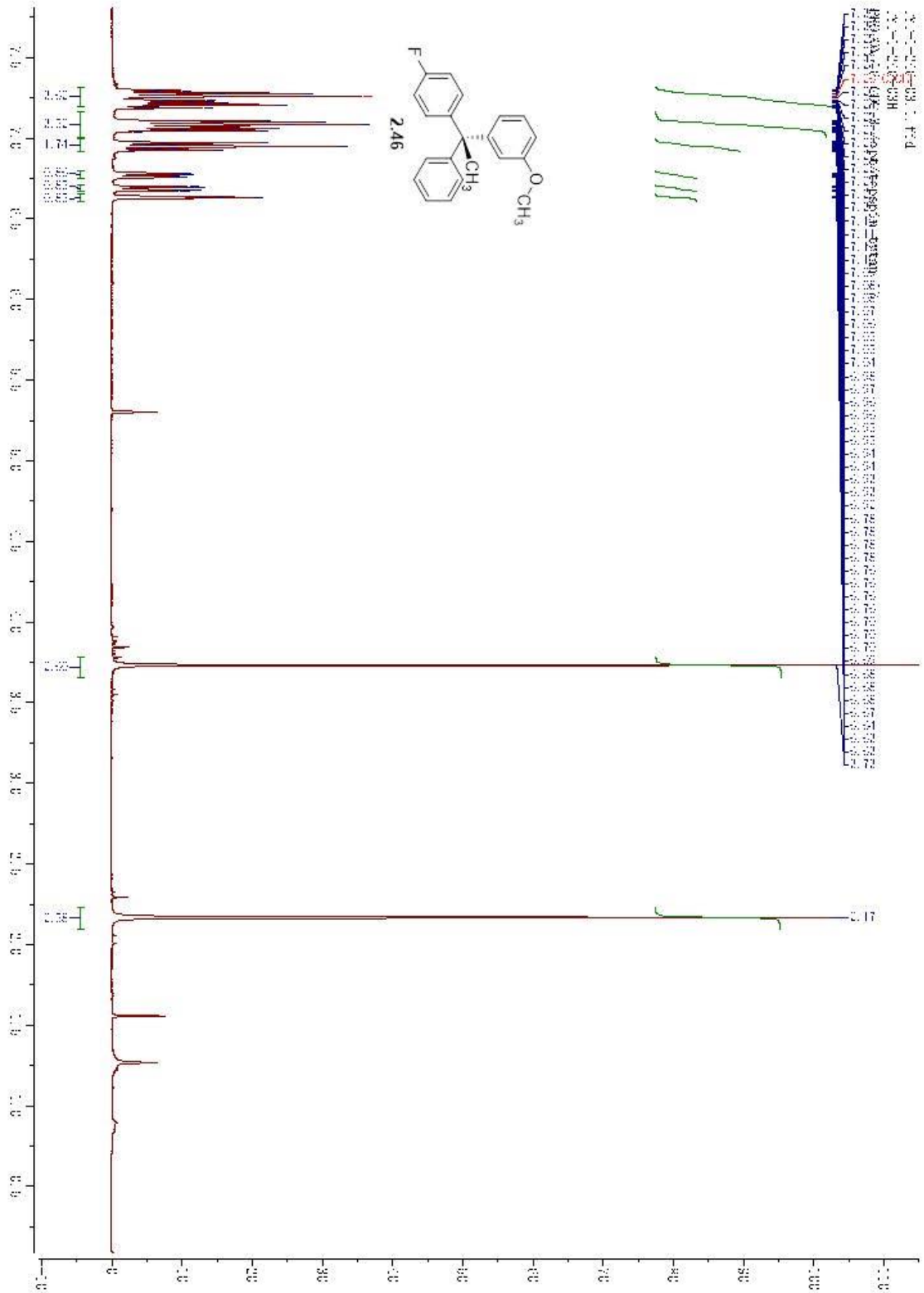
F
CH3
O
CH3
2.46

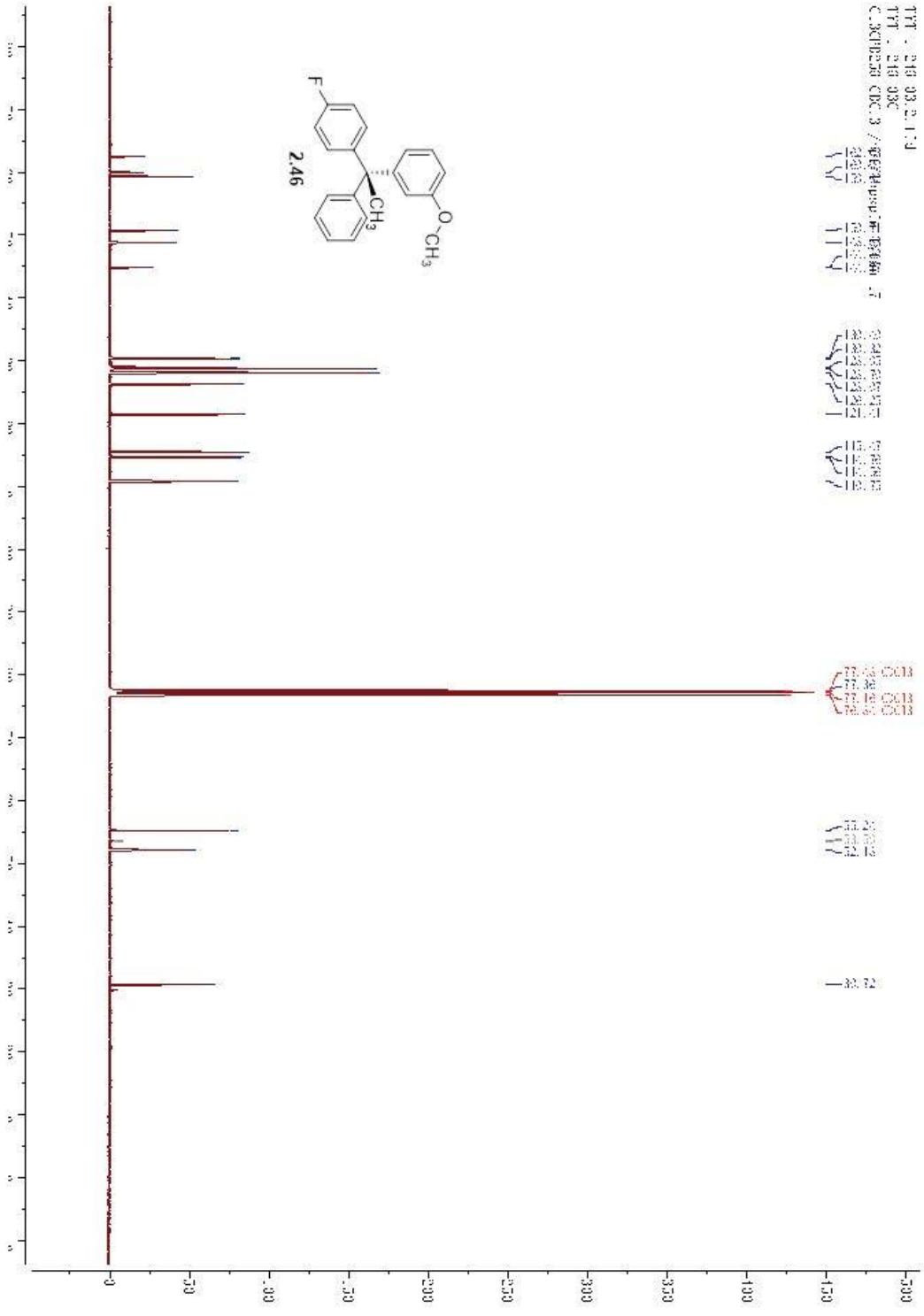
F
CH3
O
CH3
2.46

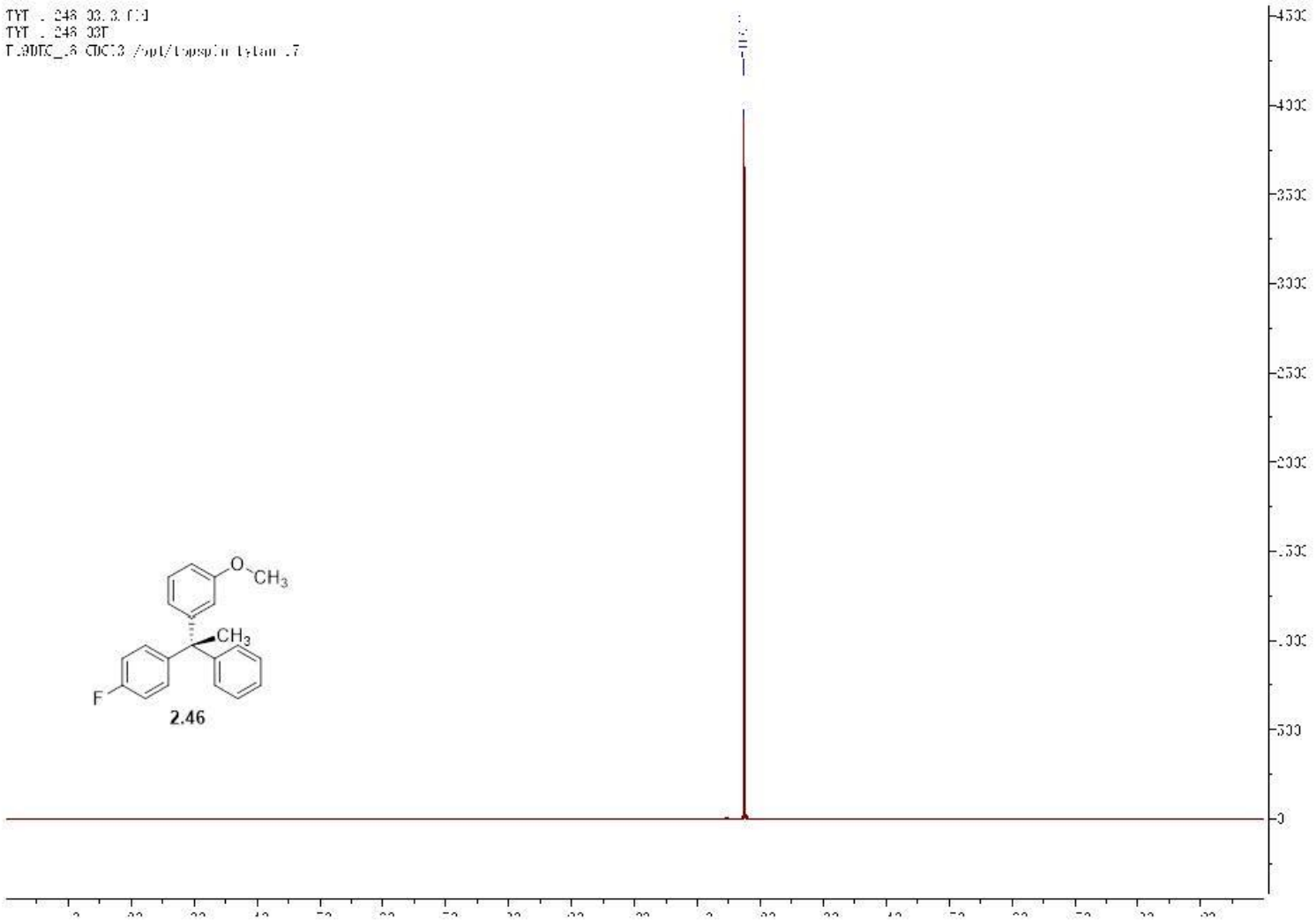

2.46

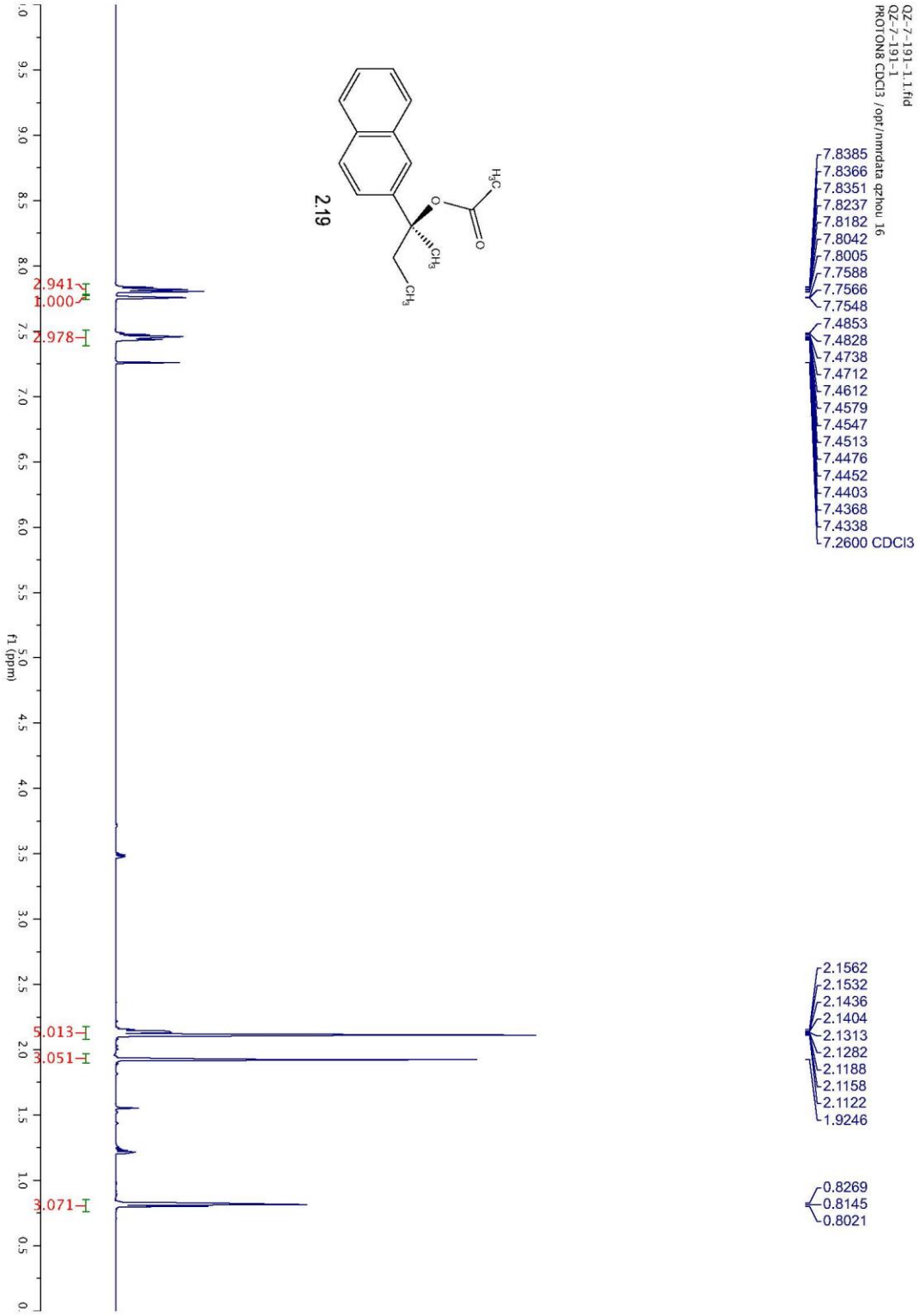
QZ-7-191-1.1.fid
QZ-7-191-1
PROTON8 CDCl3 /opt/nmrdata qzhou 16
2.19
f1 (ppm)
2.941
1.000
2.978
5.013
3.051
3.071
7.8385
7.8366
7.8351
7.8237
7.8182
7.8042
7.8005
7.7588
7.7566
7.7548
7.4853
7.4828
7.4738
7.4712
7.4612
7.4579
7.4547
7.4513
7.4476
7.4452
7.4403
7.4368
7.4338
7.2600 CDCl3
2.1562
2.1532
2.1436
2.1404
2.1313
2.1282
2.1188
2.1158
2.1122
1.9246
0.8269
0.8145
0.8021

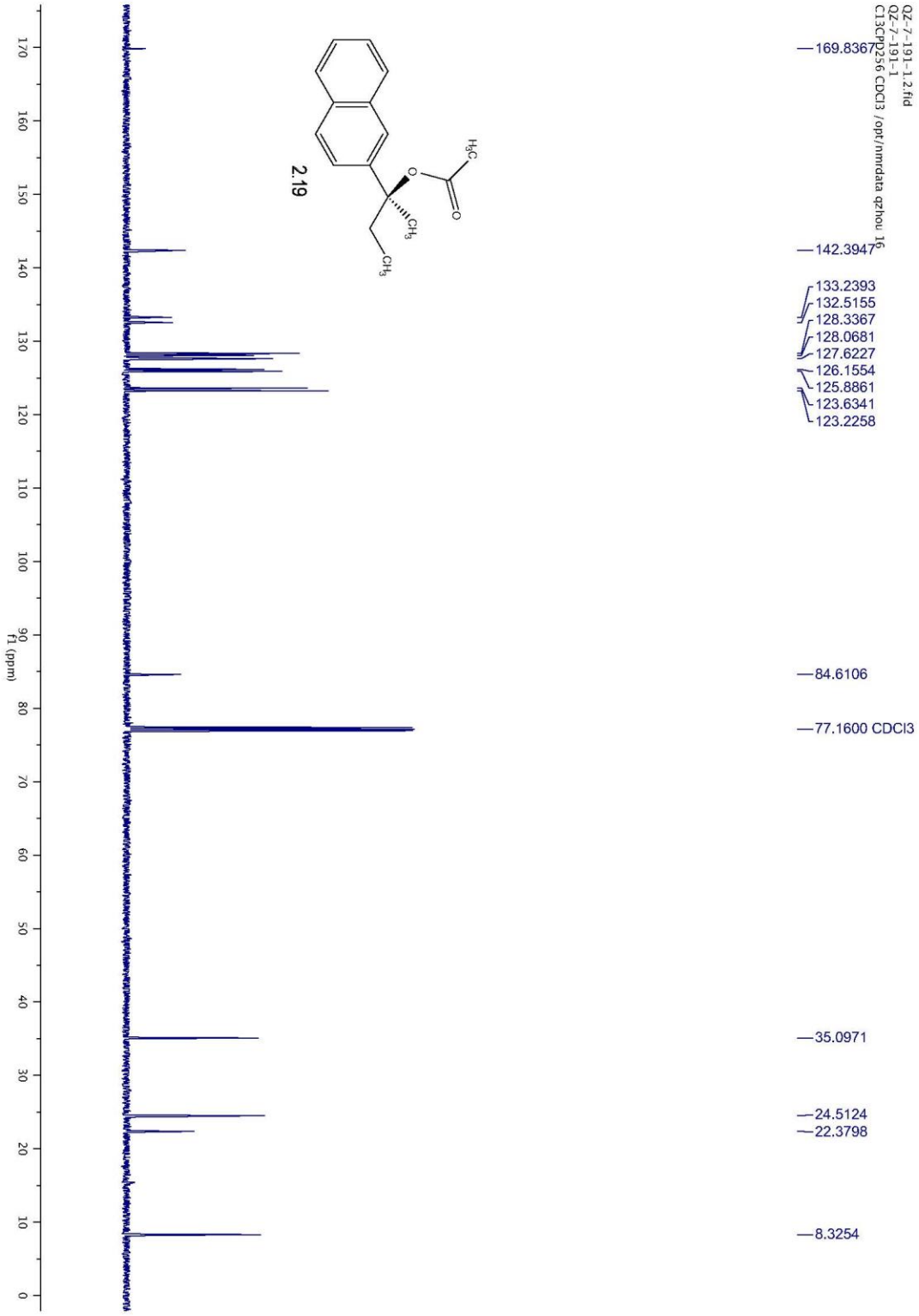
QZ-7-191-1.2.fid
QZ-7-191-1
C13CPD256 CDCl3 /opt/nmrdata qzhou 16
169.8367
142.3947
133.2393
132.5155
128.3367
128.0681
127.6227
126.1554
125.8861
123.6341
123.2258
84.6106
77.1600 CDCl3
35.0971
24.5124
22.3798
8.3254
2.19
f1 (ppm)

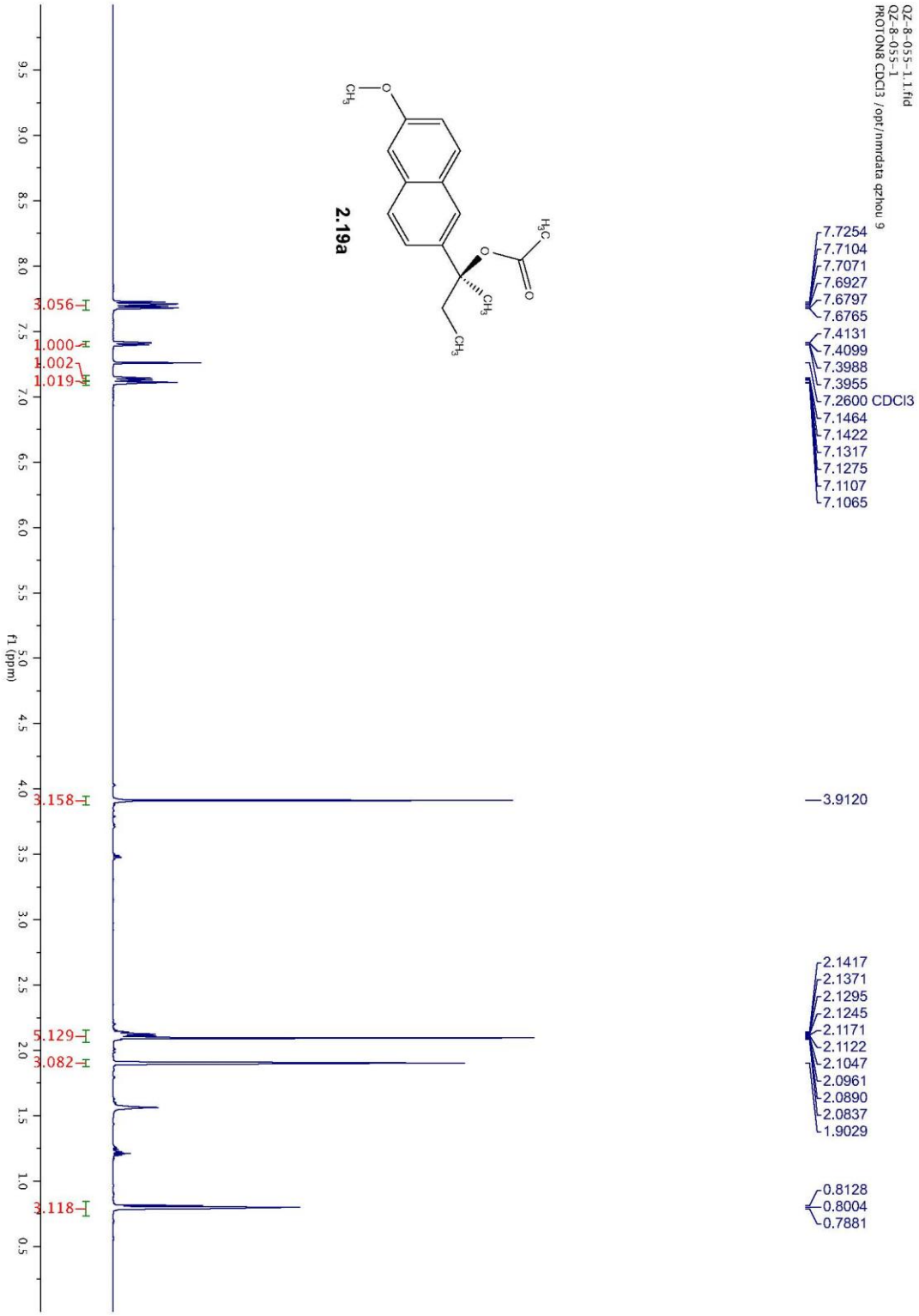
QZ-8-055-1.1.fid
QZ-8-055-1
PROTON8 CDCl3 /opt/nmrdata qzhou 9
2.19a
7.7254
7.7104
7.7071
7.6927
7.6797
7.6765
7.4131
7.4099
7.3988
7.3955
7.2600 CDCl3
7.1464
7.1422
7.1317
7.1275
7.1107
7.1065
3.9120
2.1417
2.1371
2.1295
2.1245
2.1171
2.1122
2.1047
2.0961
2.0890
2.0837
1.9029
0.8128
0.8004
0.7881
3.056
1.000
1.002
1.019
3.158
5.129
3.082
3.118
f1 (ppm)

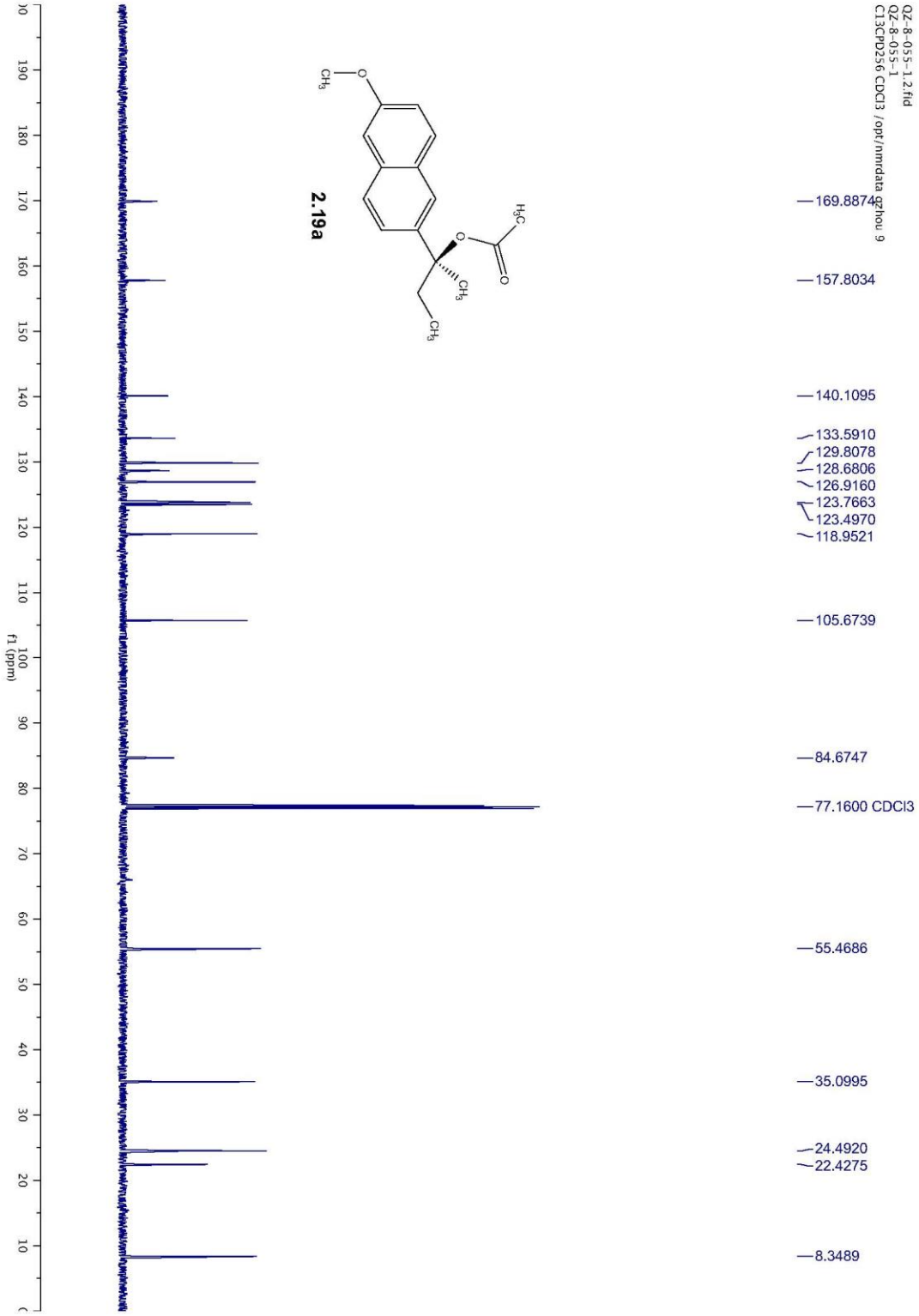
QZ-8-055-1.2.fid
QZ-8-055-1
C13CPD256 CDCl3 /opt/nmrdata qzhou 9
2.19a
169.8874
157.8034
140.1095
133.5910
129.8078
128.6806
126.9160
123.7663
123.4970
118.9521
105.6739
84.6747
77.1600 CDCl3
55.4686
35.0995
24.4920
22.4275
8.3489
f1 (ppm)

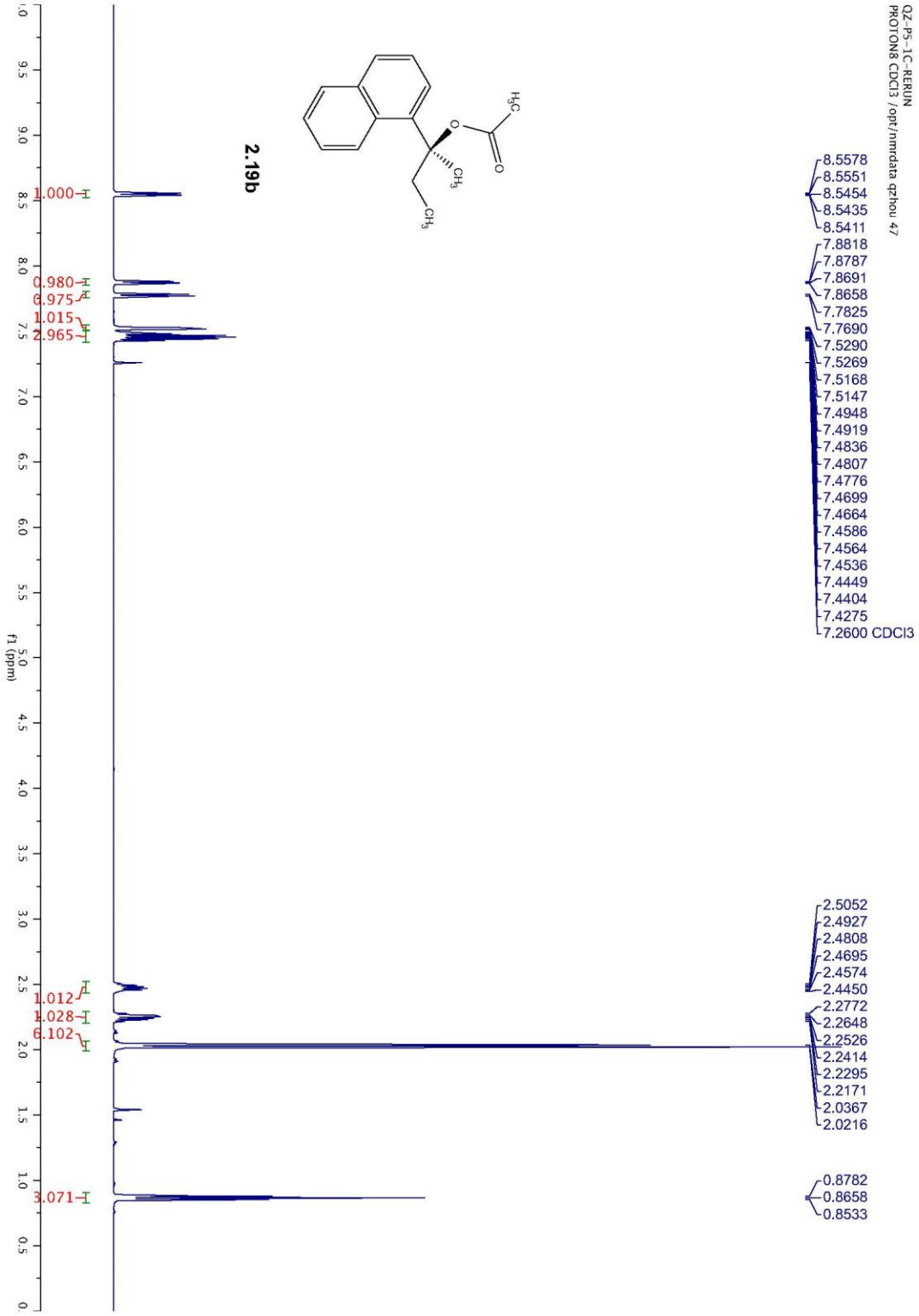
QZ-P5-1C-RERUN
PROTON8 CDCl3 /opt/nmrdata qzhou 47
2.19b
f1 (ppm)
1.000
0.980
0.975
1.015
2.965
1.012
1.028
6.102
3.071
8.5578
8.5551
8.5454
8.5435
8.5411
7.8818
7.8787
7.8691
7.8658
7.7825
7.7690
7.5290
7.5269
7.5168
7.5147
7.4948
7.4919
7.4836
7.4807
7.4776
7.4699
7.4664
7.4586
7.4564
7.4536
7.4449
7.4404
7.4275
7.2600 CDCl3
2.5052
2.4927
2.4808
2.4695
2.4574
2.4450
2.2772
2.2648
2.2526
2.2414
2.2295
2.2171
2.0367
2.0216
0.8782
0.8658
0.8533

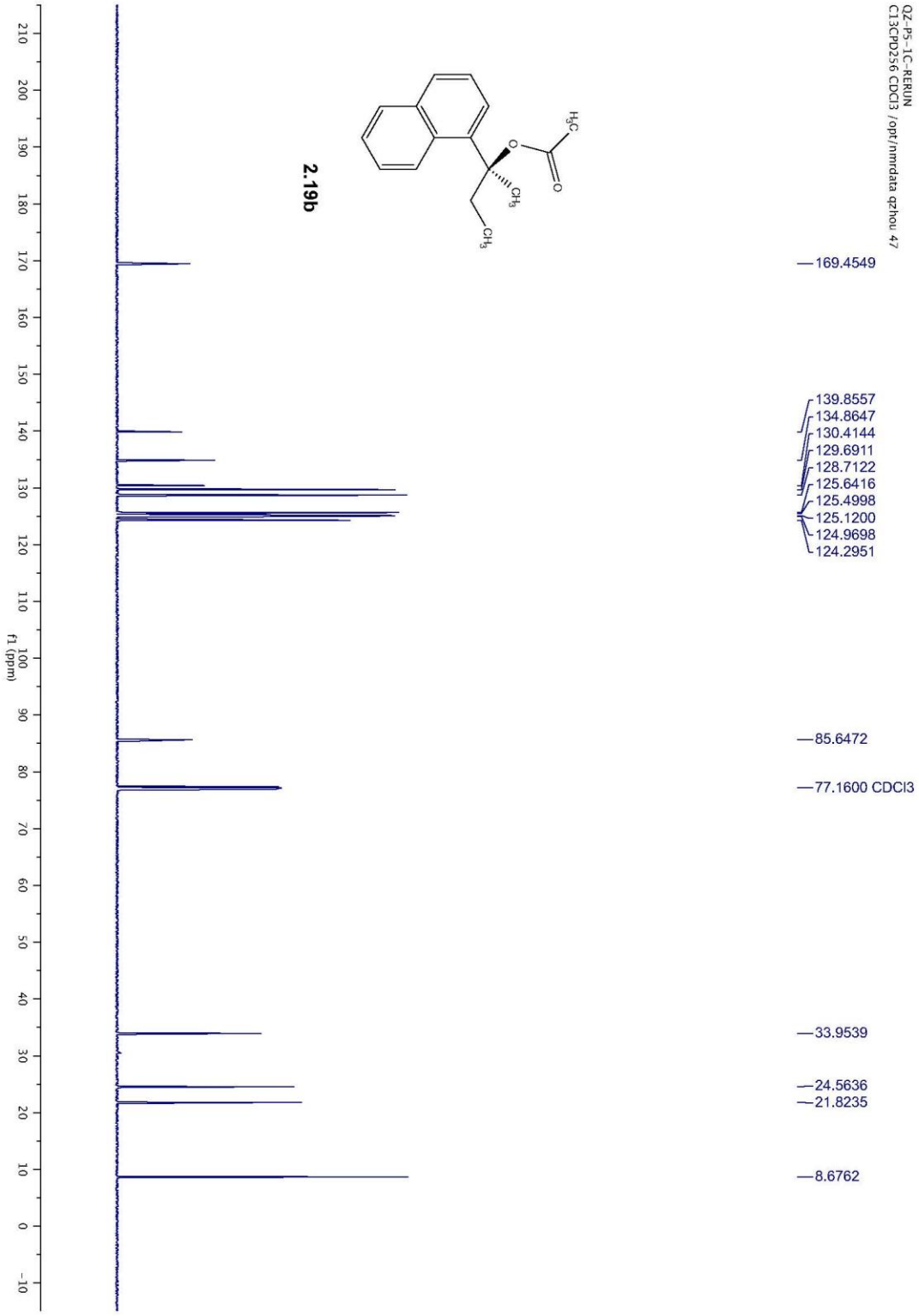
QZ-P5-1C-RERUN
C13CPD256 CDCl3 /opt/nmrdata qzhou 47
2.19b
f1 (ppm)
169.4549
139.8557
134.8647
130.4144
129.6911
128.7122
125.6416
125.4998
125.1200
124.9698
124.2951
85.6472
77.1600 CDCl3
33.9539
24.5636
21.8235
8.6762

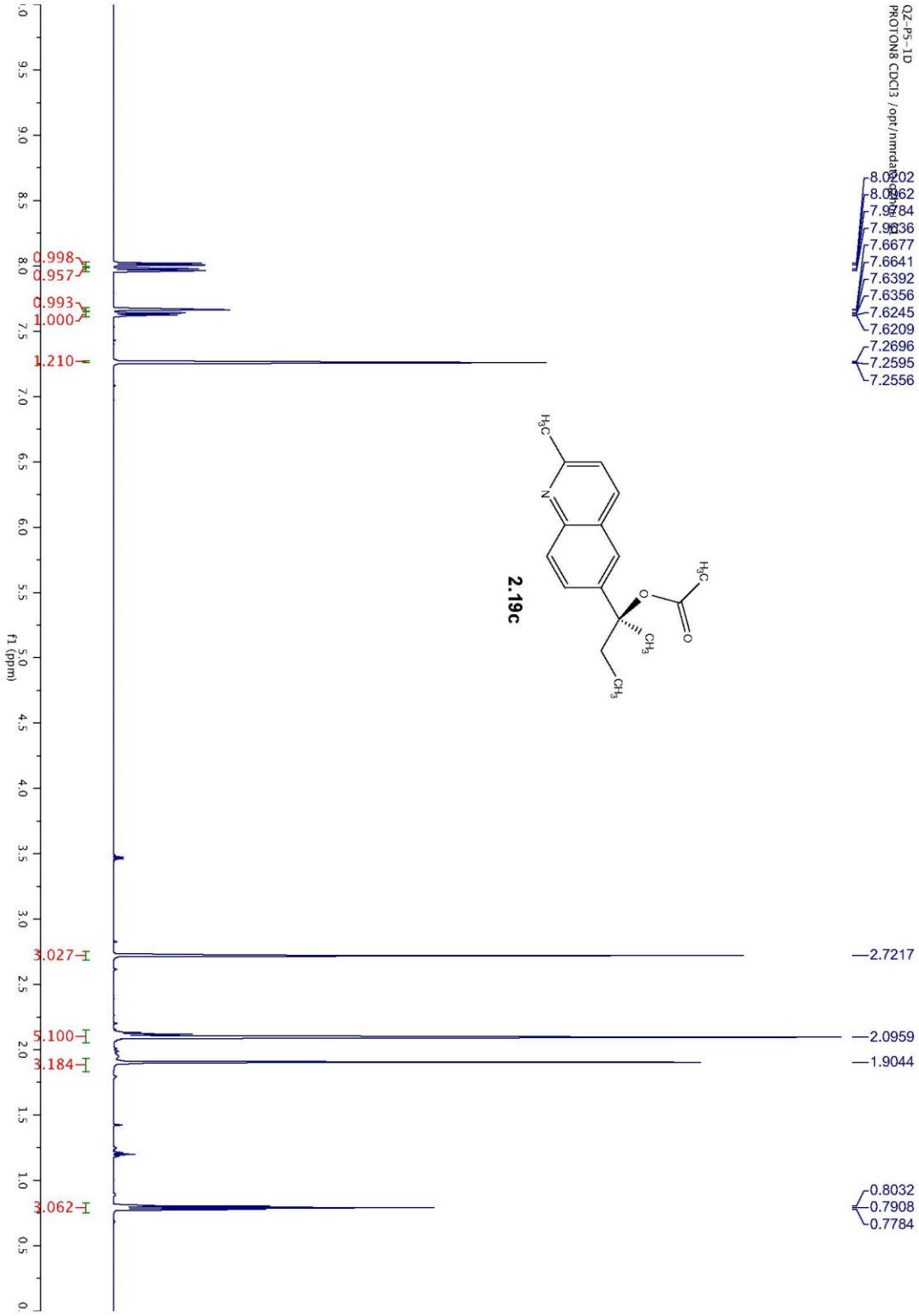
QZ-P5-1D
PROTON8 CDCl3 /opt/nmrdata/data
8.0202
8.0062
7.9784
7.9636
7.6677
7.6641
7.6392
7.6356
7.6245
7.6209
7.2696
7.2595
7.2556
0.998
0.957
0.993
1.000
1.210
3.027
5.100
3.184
3.062
2.7217
2.0959
1.9044
0.8032
0.7908
0.7784
f1 (ppm)
2.19c

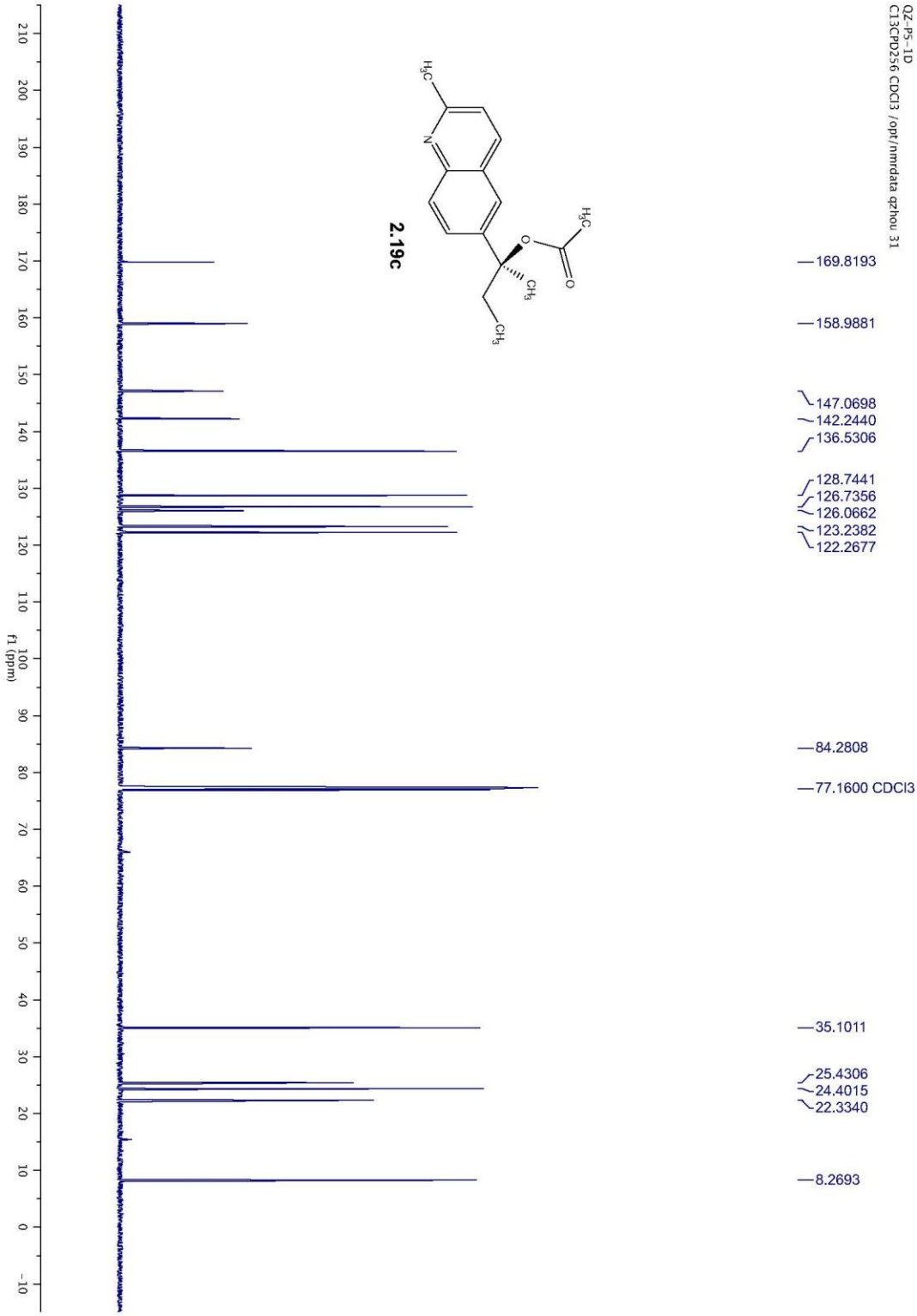
QZ-P5-1D
C13CPD256 CDCl3 /opt/nmrdata qzhou 31
2.19c
169.8193
158.9881
147.0698
142.2440
136.5306
128.7441
126.7356
126.0662
123.2382
122.2677
84.2808
77.1600 CDCl3
35.1011
25.4306
24.4015
22.3340
8.2693
f1 (ppm)

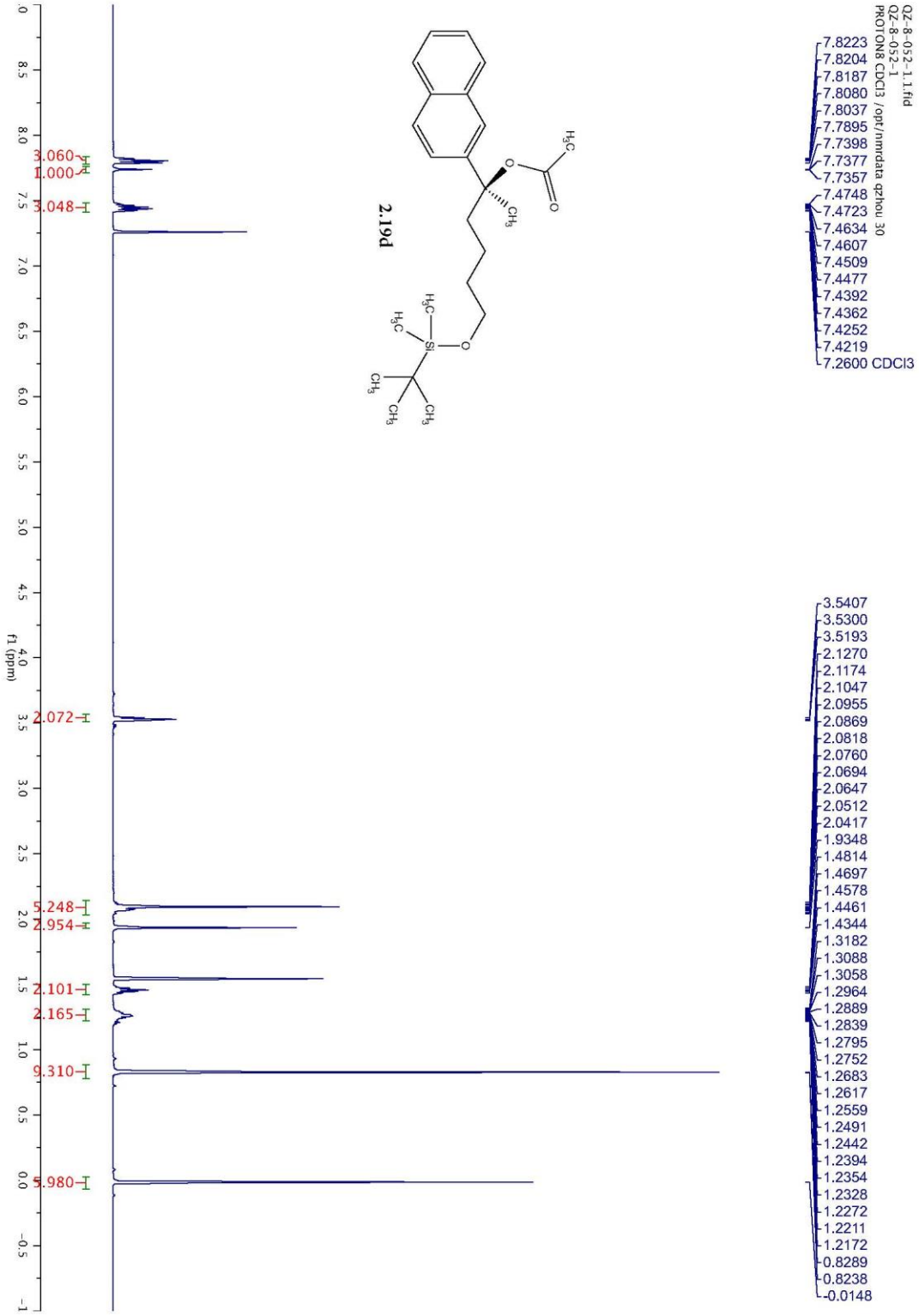
2.19d
QZ-8-052-1.1.fid
QZ-8-052-1
PROTON8 CDCl3 /opt/nmrdata qzhou 30
7.8223
7.8204
7.8187
7.8080
7.8037
7.7895
7.7398
7.7377
7.7357
7.4748
7.4723
7.4634
7.4607
7.4509
7.4477
7.4392
7.4362
7.4252
7.4219
7.2600 CDCl3
3.5407
3.5300
3.5193
2.1270
2.1174
2.1047
2.0955
2.0869
2.0818
2.0760
2.0694
2.0647
2.0512
2.0417
1.9348
1.4814
1.4697
1.4578
1.4461
1.4344
1.3182
1.3088
1.3058
1.2964
1.2889
1.2839
1.2795
1.2752
1.2683
1.2617
1.2559
1.2491
1.2442
1.2394
1.2354
1.2328
1.2272
1.2211
1.2172
0.8289
0.8238
-0.0148
3.060
1.000
3.048
2.072
5.248
2.954
2.101
2.165
9.310
5.980
f1 (ppm)

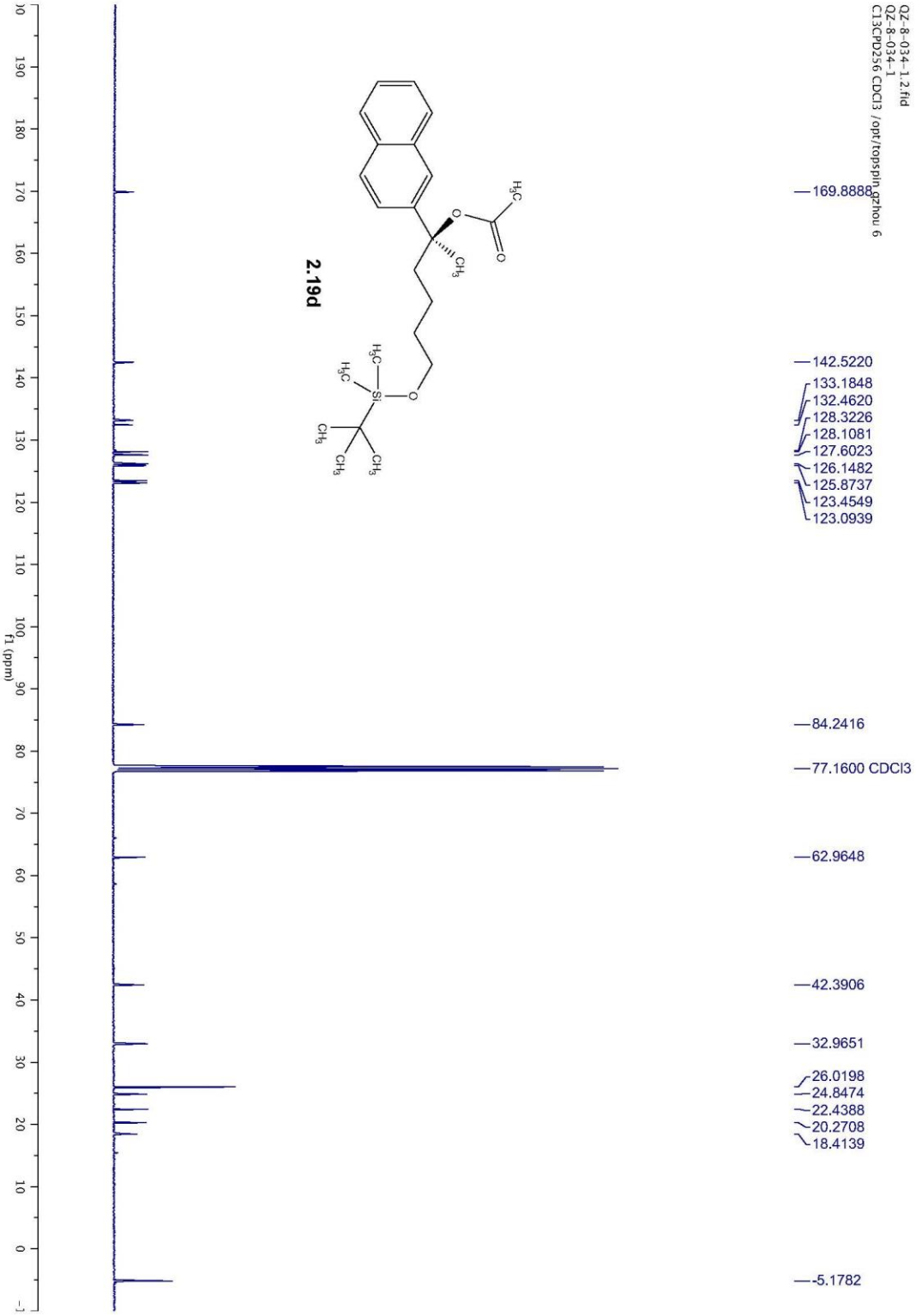
QZ-8-034-1.2.fid
QZ-8-034-1
C13CPD256 CDCl3 /opt/topspin_gzhou 6
2.19d
f1 (ppm)
169.8888
142.5220
133.1848
132.4620
128.3226
128.1081
127.6023
126.1482
125.8737
123.4549
123.0939
84.2416
77.1600 CDCl3
62.9648
42.3906
32.9651
26.0198
24.8474
22.4388
20.2708
18.4139
-5.1782

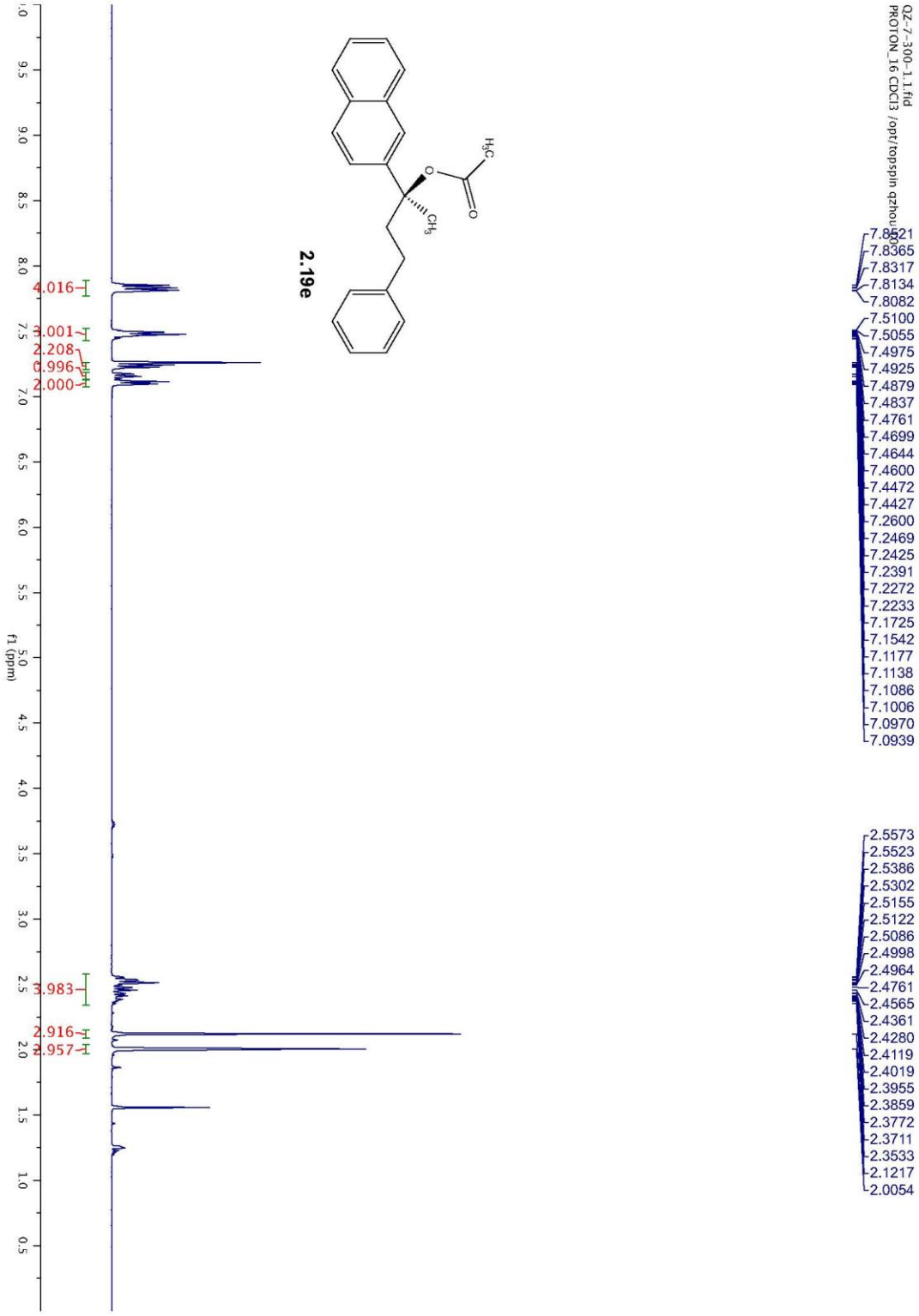
QZ-7-300-1.1.fid
PROTON_16 CDCl3 /opt/topspin qzhou
2.19e
4.016
3.001
2.208
0.996
2.000
3.983
2.916
2.957
f1 (ppm)
7.8521
7.8365
7.8317
7.8134
7.8082
7.5100
7.5055
7.4975
7.4925
7.4879
7.4837
7.4761
7.4699
7.4644
7.4600
7.4472
7.4427
7.2600
7.2469
7.2425
7.2391
7.2272
7.2233
7.1725
7.1542
7.1177
7.1138
7.1086
7.1006
7.0970
7.0939
2.5573
2.5523
2.5386
2.5302
2.5155
2.5122
2.5086
2.4998
2.4964
2.4761
2.4565
2.4361
2.4280
2.4119
2.4019
2.3955
2.3859
2.3772
2.3711
2.3533
2.1217
2.0054

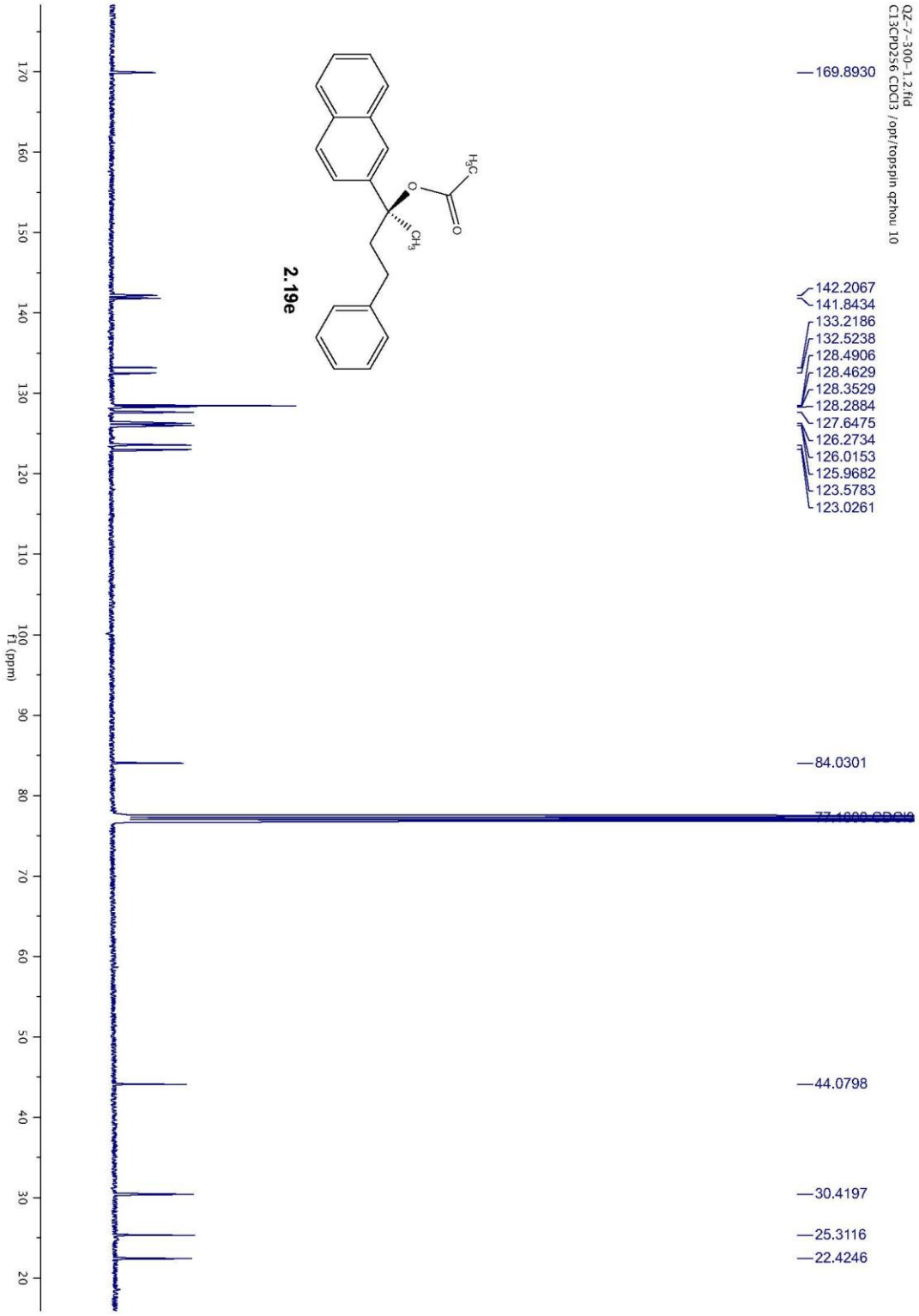
QZ-7-300-1.2.fid
C13CPD256 CDCl3 /opt/topspin qzhou 10
169.8930
142.2067
141.8434
133.2186
132.5238
128.4906
128.4629
128.3529
128.2884
127.6475
126.2734
126.0153
125.9682
123.5783
123.0261
84.0301
77.1999 CDCl3
44.0798
30.4197
25.3116
22.4246
2.19e
f1 (ppm)

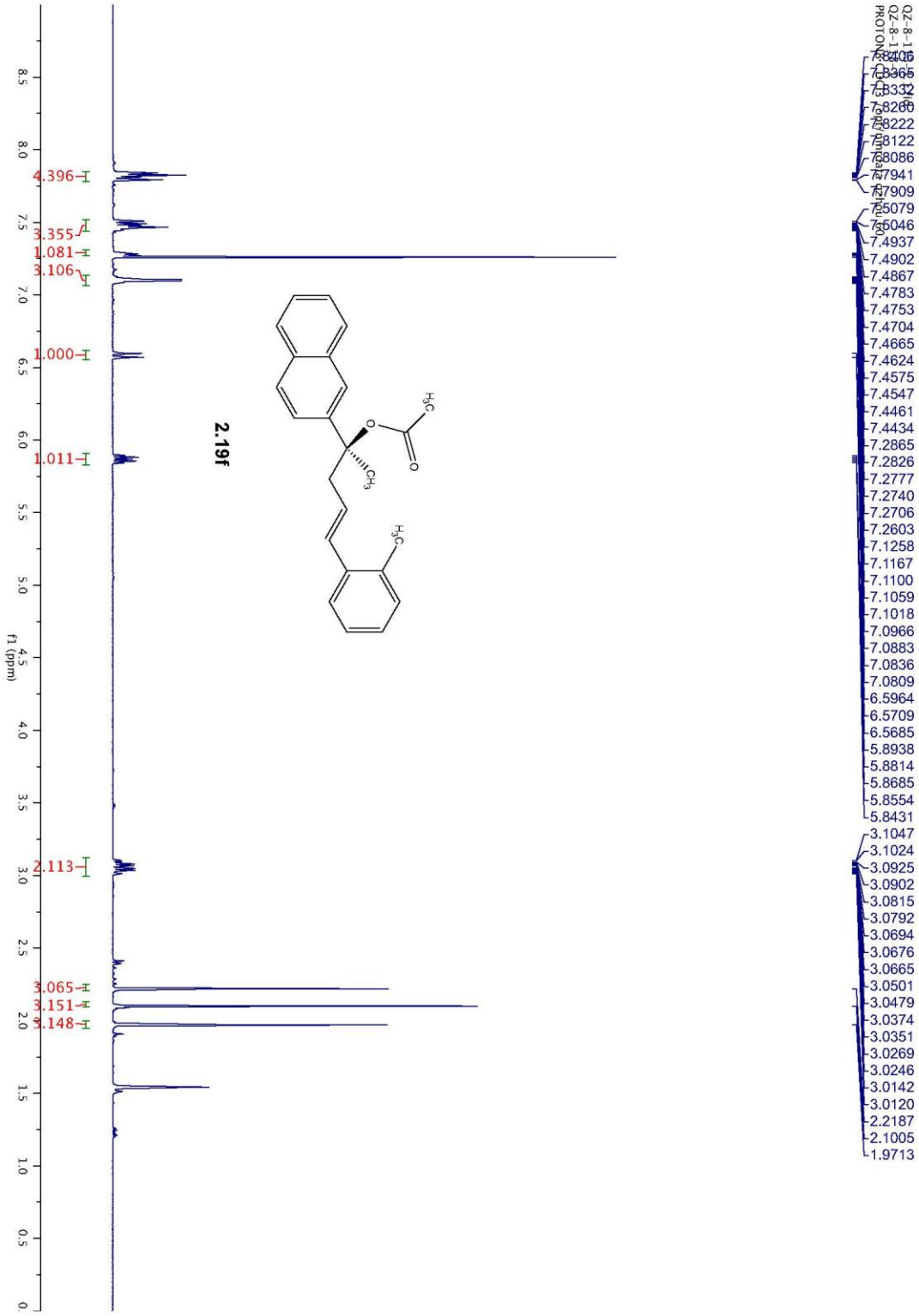
4.396
3.355
1.081
3.106
1.000
1.011
2.113
3.065
3.151
3.148
f1 (ppm)
2.19f
H3C
O
O
CH3
H3C
QZ-8-1
PROTON
7.8406
7.8365
7.8332
7.8260
7.8222
7.8122
7.8086
7.7941
7.7909
7.5079
7.5046
7.4937
7.4902
7.4867
7.4783
7.4753
7.4704
7.4665
7.4624
7.4575
7.4547
7.4461
7.4434
7.2865
7.2826
7.2777
7.2740
7.2706
7.2603
7.1258
7.1167
7.1100
7.1059
7.1018
7.0966
7.0883
7.0836
7.0809
6.5964
6.5709
6.5685
5.8938
5.8814
5.8685
5.8554
5.8431
3.1047
3.1024
3.0925
3.0902
3.0815
3.0792
3.0694
3.0676
3.0665
3.0501
3.0479
3.0374
3.0351
3.0269
3.0246
3.0142
3.0120
2.2187
2.1005
1.9713

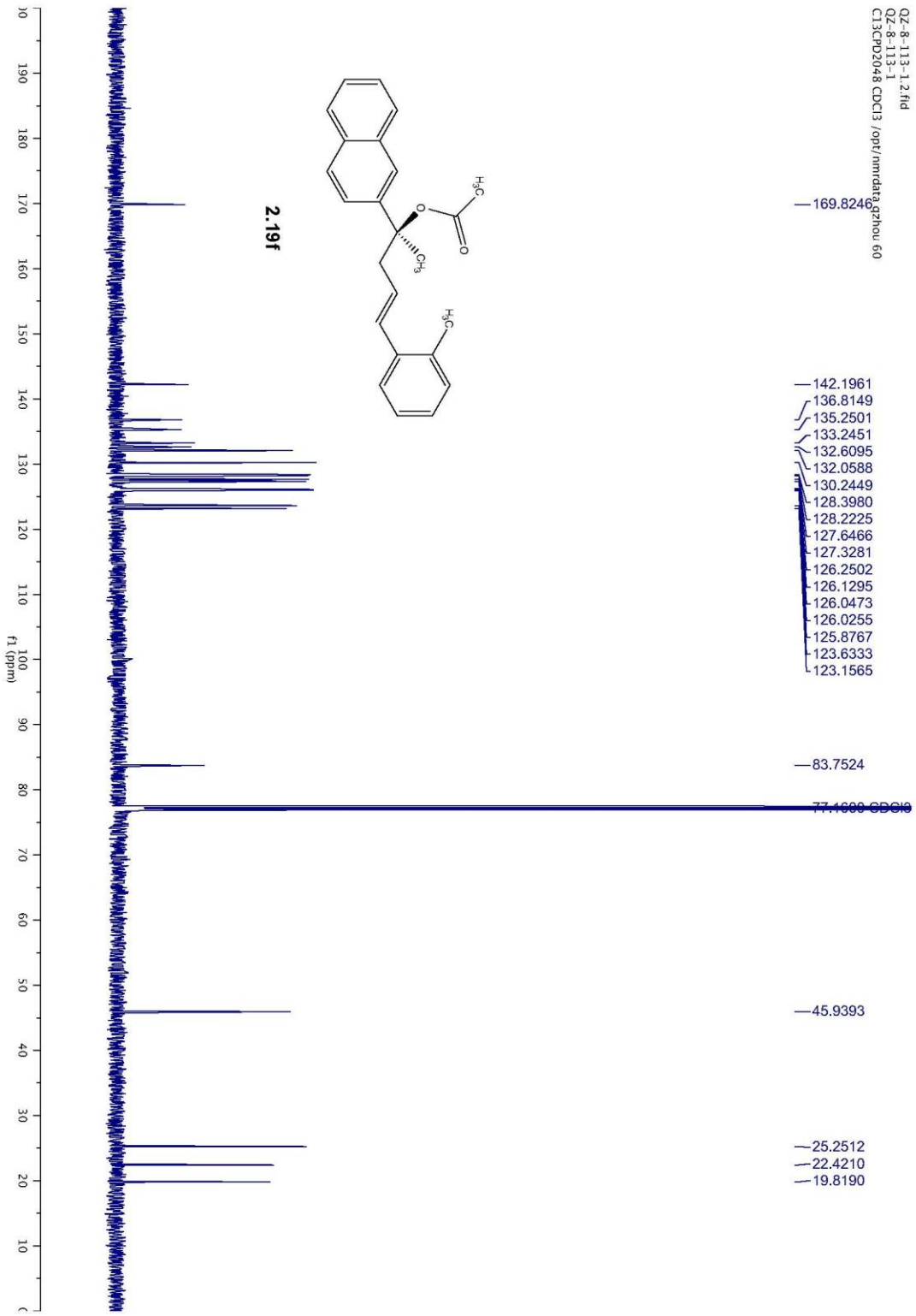
QZ-8-113-1.2.fid
QZ-8-113-1
C13CPD2048 CDCl3 /opt/nmrdata/qzhou 60
2.19f
169.8246
142.1961
136.8149
135.2501
133.2451
132.6095
132.0588
130.2449
128.3980
128.2225
127.6466
127.3281
126.2502
126.1295
126.0473
126.0255
125.8767
123.6333
123.1565
83.7524
77.1600 CDCl3
45.9393
25.2512
22.4210
19.8190
f1 (ppm)

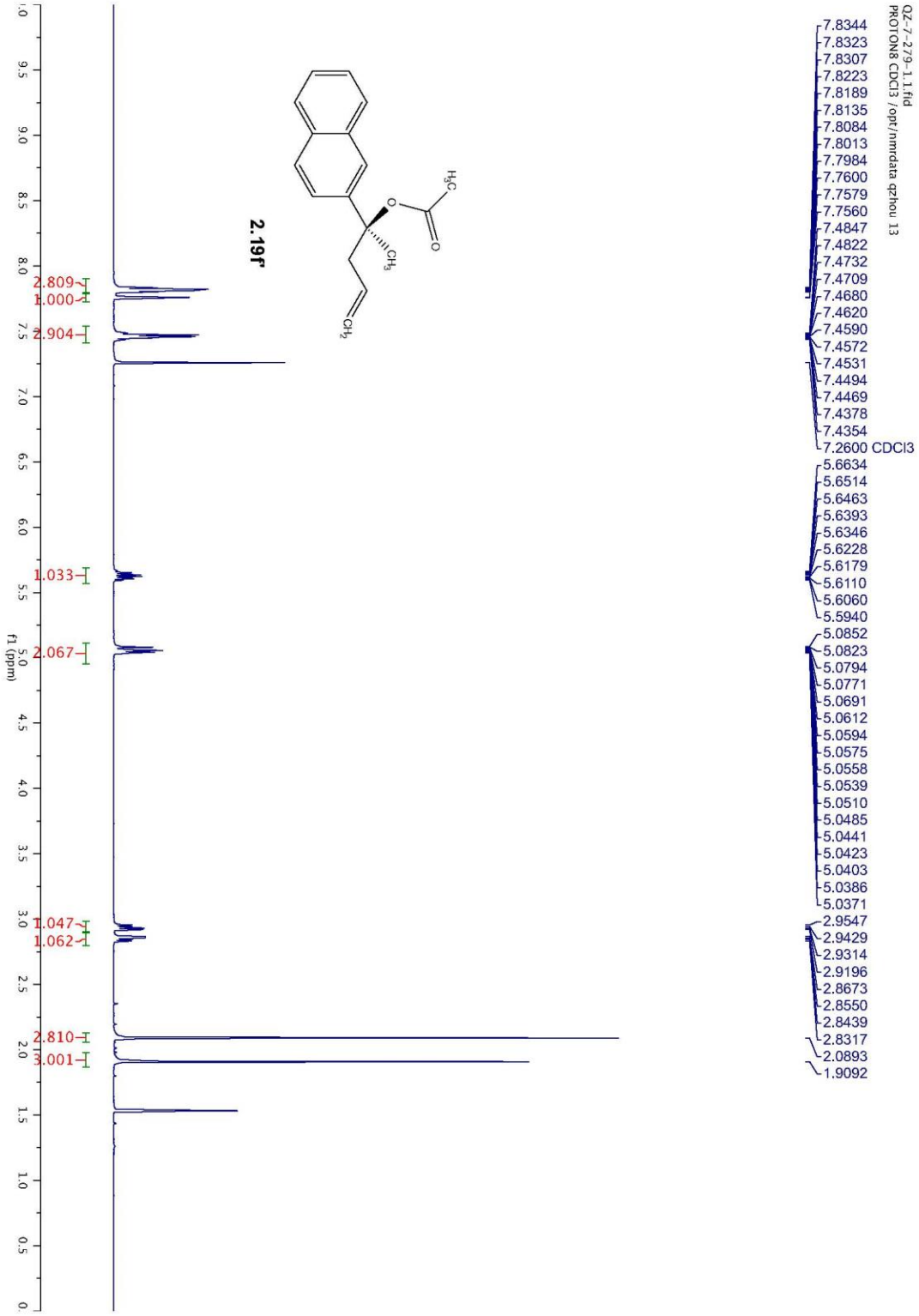
2.19f
2.809
1.000
2.904
1.033
2.067
1.047
1.062
2.810
3.001
f1 (ppm)
QZ-7-279-1.1.fid
PROTON8 CDCl3 /opt/nmrdata qzhou 13
7.8344
7.8323
7.8307
7.8223
7.8189
7.8135
7.8084
7.8013
7.7984
7.7600
7.7579
7.7560
7.4847
7.4822
7.4732
7.4709
7.4680
7.4620
7.4590
7.4572
7.4531
7.4494
7.4469
7.4378
7.4354
7.2600 CDCl3
5.6634
5.6514
5.6463
5.6393
5.6346
5.6228
5.6179
5.6110
5.6060
5.5940
5.0852
5.0823
5.0794
5.0771
5.0691
5.0612
5.0594
5.0575
5.0558
5.0539
5.0510
5.0485
5.0441
5.0423
5.0403
5.0386
5.0371
2.9547
2.9429
2.9314
2.9196
2.8673
2.8550
2.8439
2.8317
2.0893
1.9092

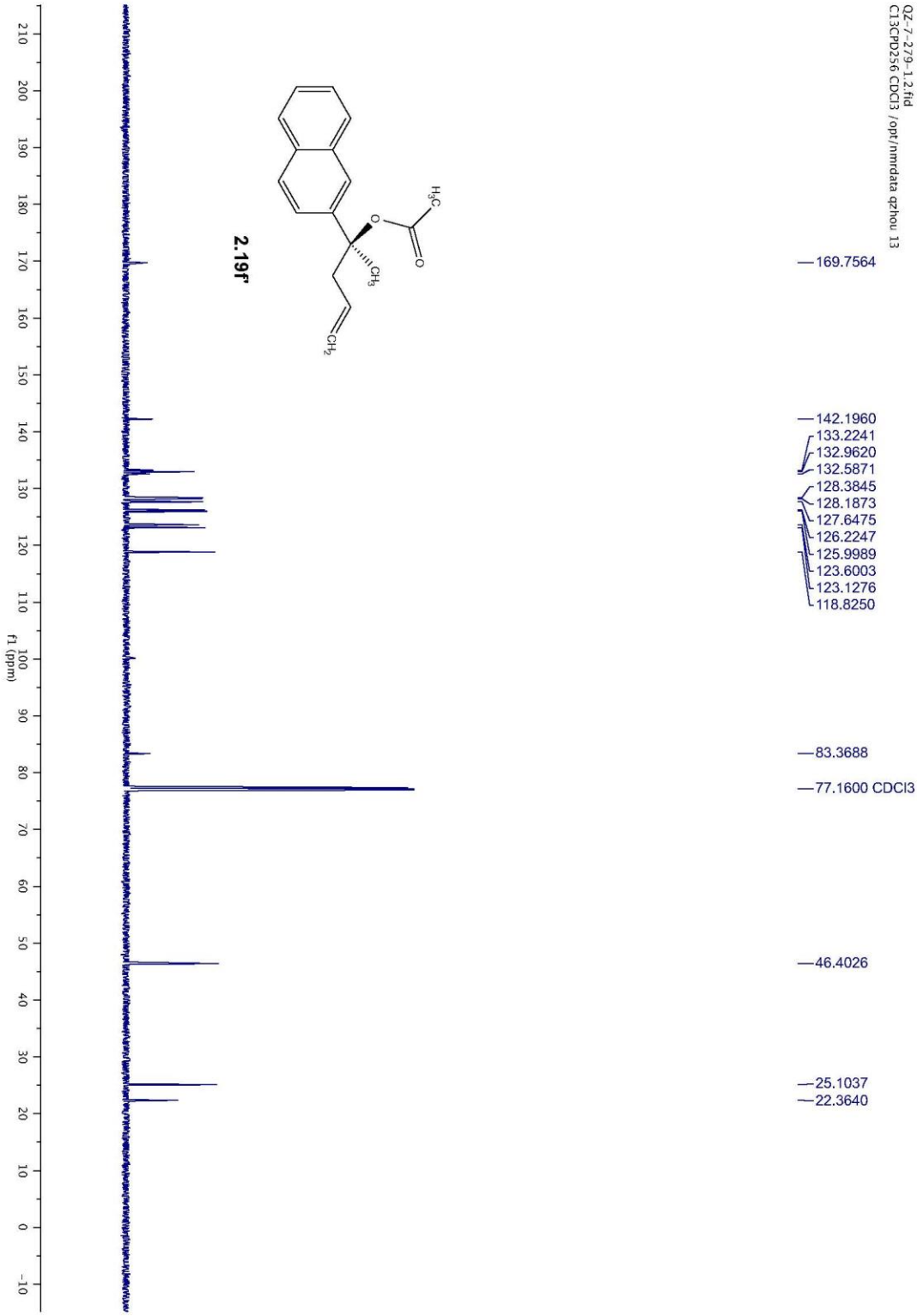
QZ-7-279-1.2.fid
C13CPD256 CDCl3 /opt/nmrdata qzhou 13
2.19f
169.7564
142.1960
133.2241
132.9620
132.5871
128.3845
128.1873
127.6475
126.2247
125.9989
123.6003
123.1276
118.8250
83.3688
77.1600 CDCl3
46.4026
25.1037
22.3640
f1 (ppm)

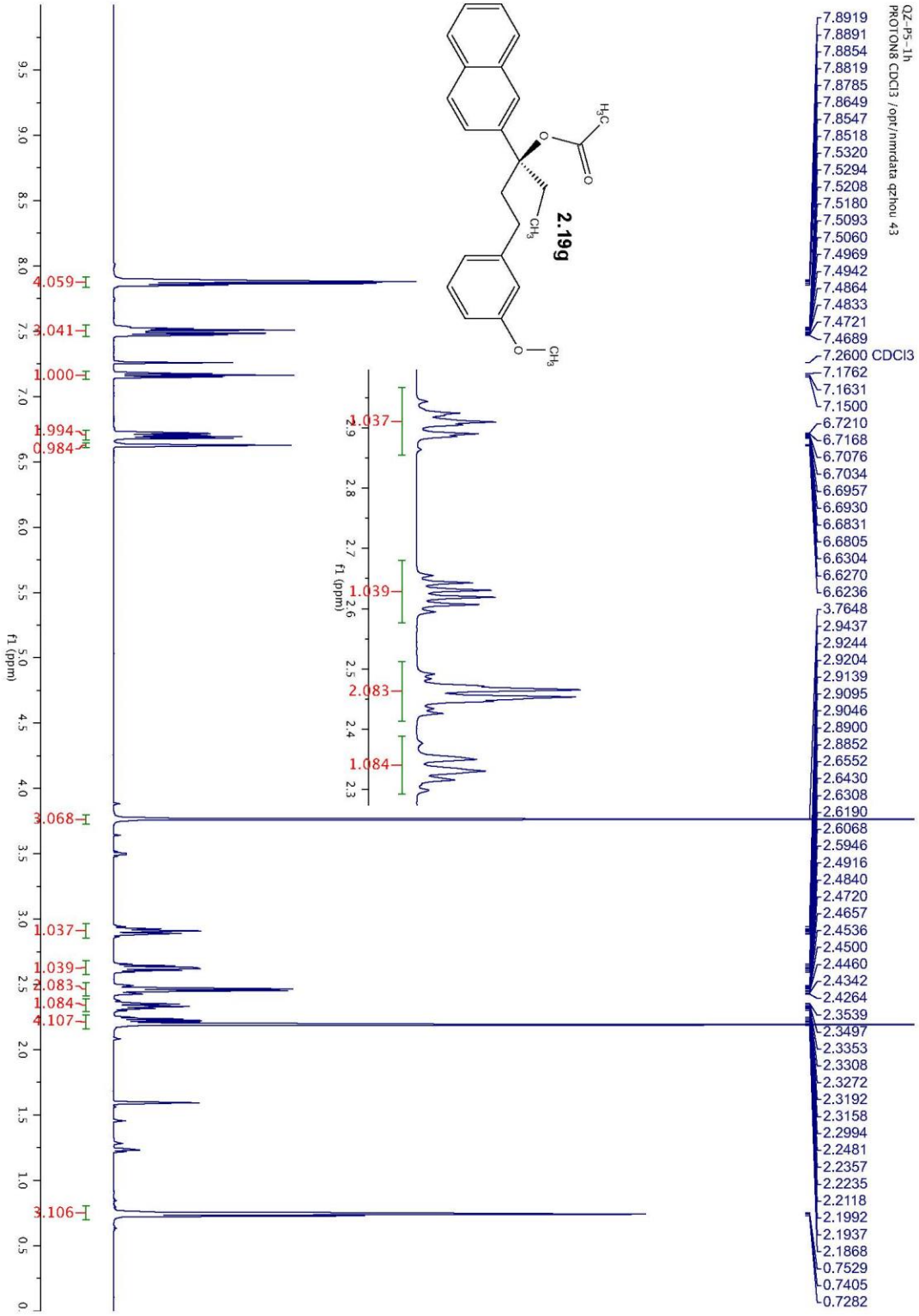
2.19g
QZ-P5-1h
PROTON6 CDCl3 /opt/nmrdata qzhou 43
7.8919
7.8891
7.8854
7.8819
7.8785
7.8649
7.8547
7.8518
7.5320
7.5294
7.5208
7.5180
7.5093
7.5060
7.4969
7.4942
7.4864
7.4833
7.4721
7.4689
7.2600 CDCl3
7.1762
7.1631
7.1500
6.7210
6.7168
6.7076
6.7034
6.6957
6.6930
6.6831
6.6805
6.6304
6.6270
6.6236
3.7648
2.9437
2.9244
2.9204
2.9139
2.9095
2.9046
2.8900
2.8852
2.6552
2.6430
2.6308
2.6190
2.6068
2.5946
2.4916
2.4840
2.4720
2.4657
2.4536
2.4500
2.4460
2.4342
2.4264
2.3539
2.3497
2.3353
2.3308
2.3272
2.3192
2.3158
2.2994
2.2481
2.2357
2.2235
2.2118
2.1992
2.1937
2.1868
0.7529
0.7405
0.7282
4.059
3.041
1.000
1.994
0.984
3.068
1.037
1.039
2.083
1.084
4.107
3.106
1.037
1.039
2.083
1.084
f1 (ppm)

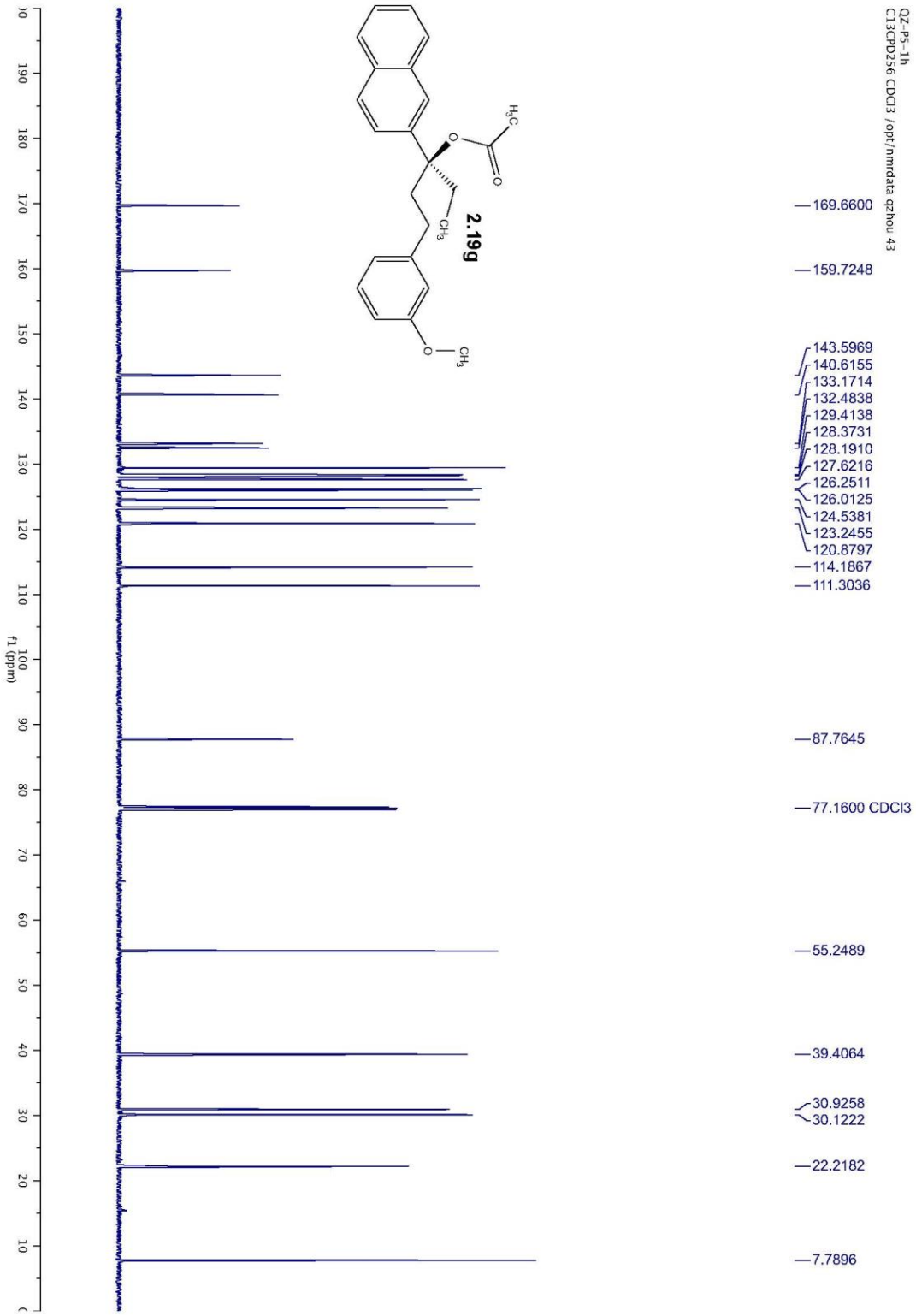
QZ-P5-1h
C13CPD256 CDCl3 /opt/nmrdata qzhou 43
2.19g
f1 (ppm)
169.6600
159.7248
143.5969
140.6155
133.1714
132.4838
129.4138
128.3731
128.1910
127.6216
126.2511
126.0125
124.5381
123.2455
120.8797
114.1867
111.3036
87.7645
77.1600 CDCl3
55.2489
39.4064
30.9258
30.1222
22.2182
7.7896

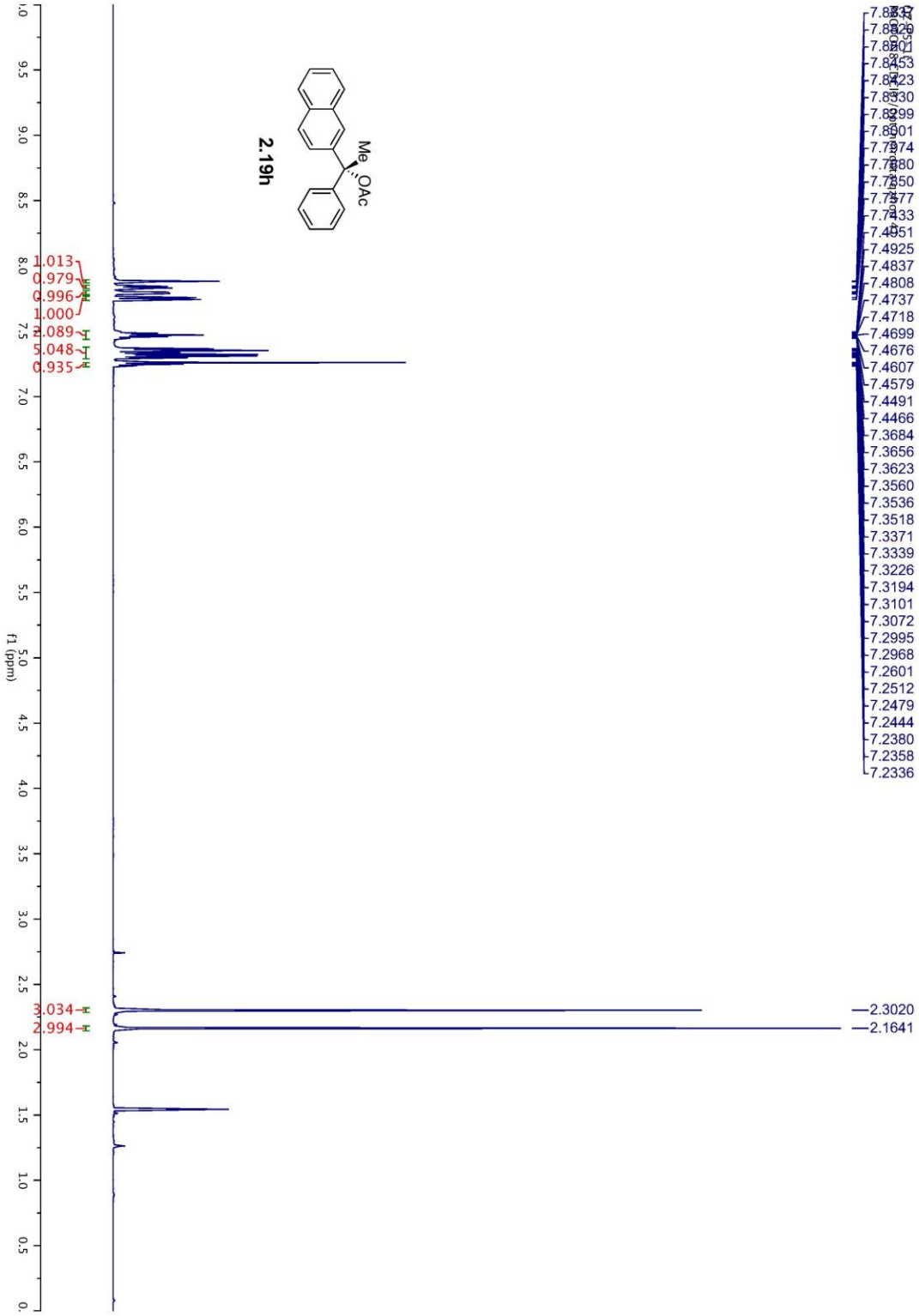
2.19h
Me
OAc
1.013
0.979
0.996
1.000
2.089
5.048
0.935
3.034
2.994
2.3020
2.1641
f1 (ppm)

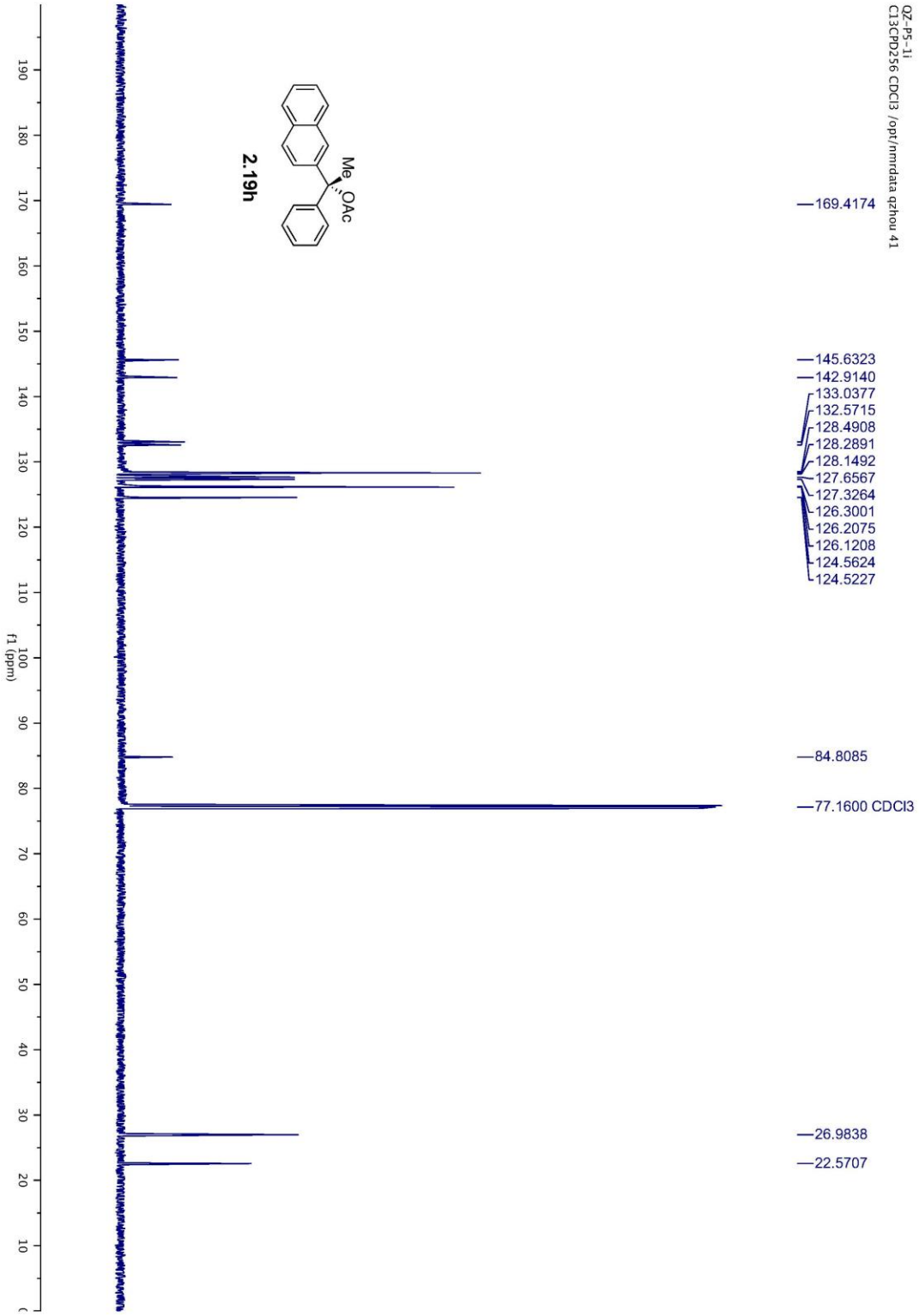
QZ-PS-1i
C13CPD256 CDCl3 /opt/nmrdata qzhou 41
2.19h
Me
OAc
169.4174
145.6323
142.9140
133.0377
132.5715
128.4908
128.2891
128.1492
127.6567
127.3264
126.3001
126.2075
126.1208
124.5624
124.5227
84.8085
77.1600 CDCl3
26.9838
22.5707
f1 (ppm)

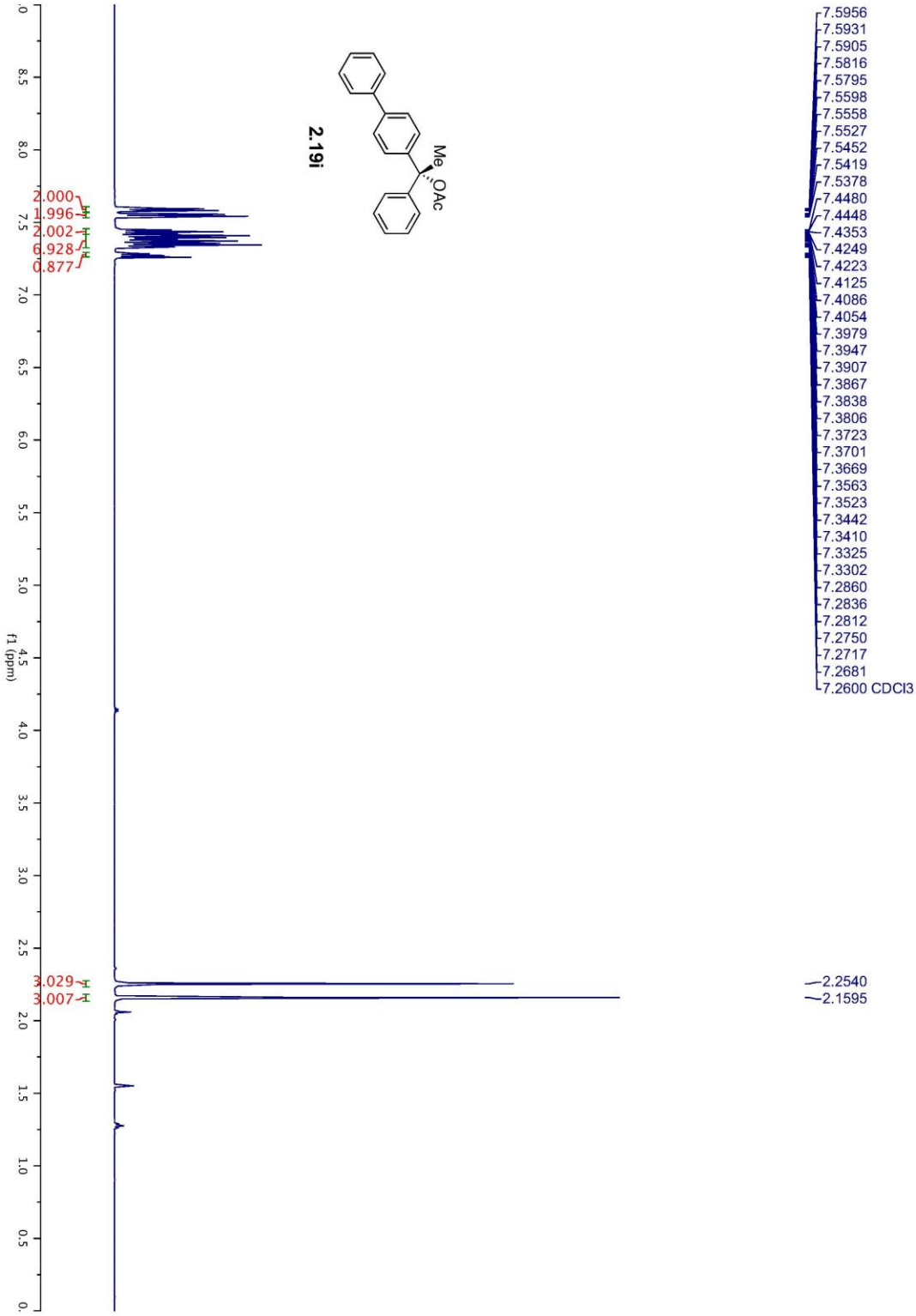
2.19i
Me
OAc
2.000
1.996
2.002
6.928
0.877
3.029
3.007
7.5956
7.5931
7.5905
7.5816
7.5795
7.5598
7.5558
7.5527
7.5452
7.5419
7.5378
7.4480
7.4448
7.4353
7.4249
7.4223
7.4125
7.4086
7.4054
7.3979
7.3947
7.3907
7.3867
7.3838
7.3806
7.3723
7.3701
7.3669
7.3563
7.3523
7.3442
7.3410
7.3325
7.3302
7.2860
7.2836
7.2812
7.2750
7.2717
7.2681
7.2600 CDCl3
2.2540
2.1595
f1 (ppm)

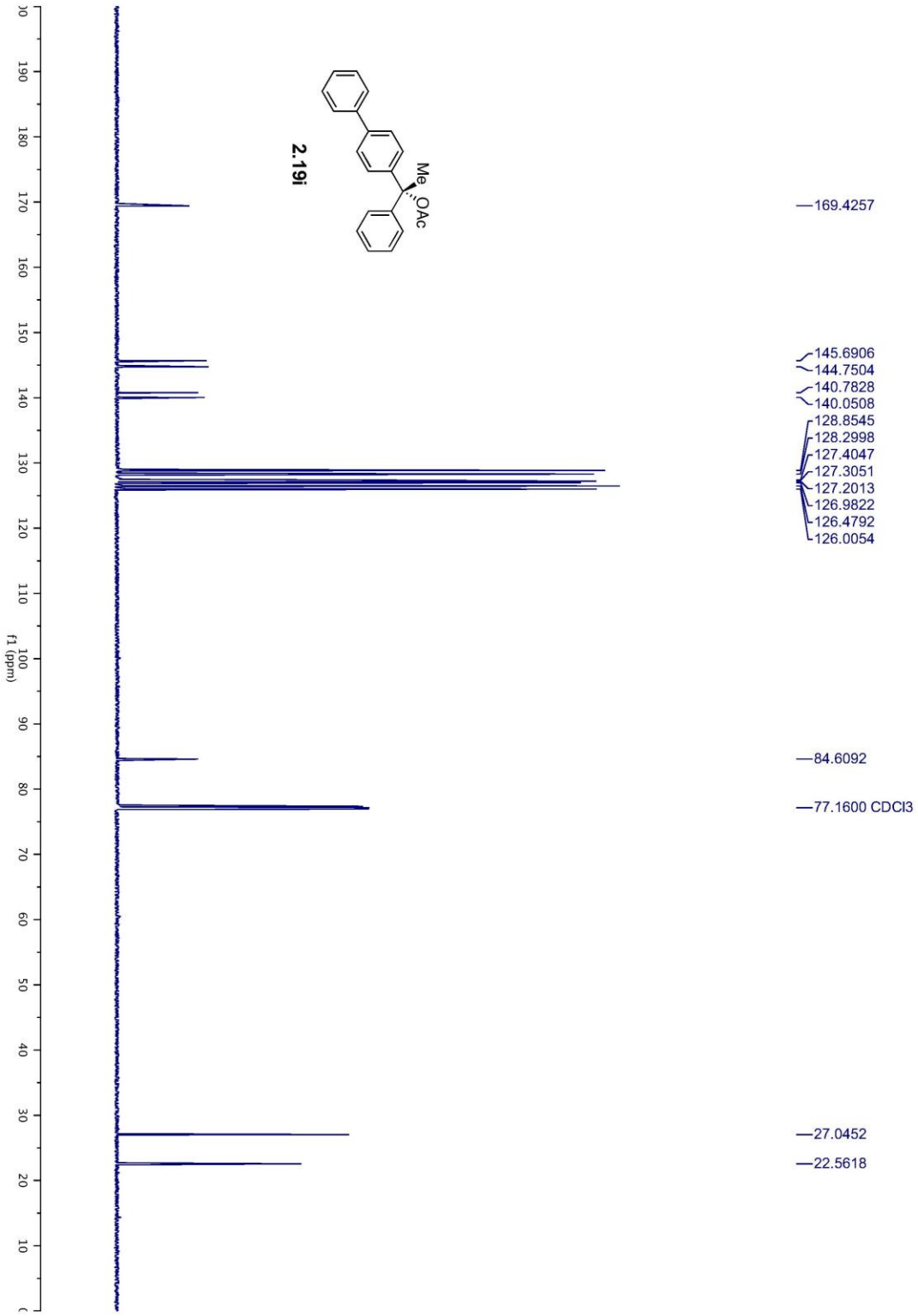
2.19i
Me
OAc
169.4257
145.6906
144.7504
140.7828
140.0508
128.8545
128.2998
127.4047
127.3051
127.2013
126.9822
126.4792
126.0054
84.6092
77.1600 CDCl3
27.0452
22.5618
f1 (ppm)

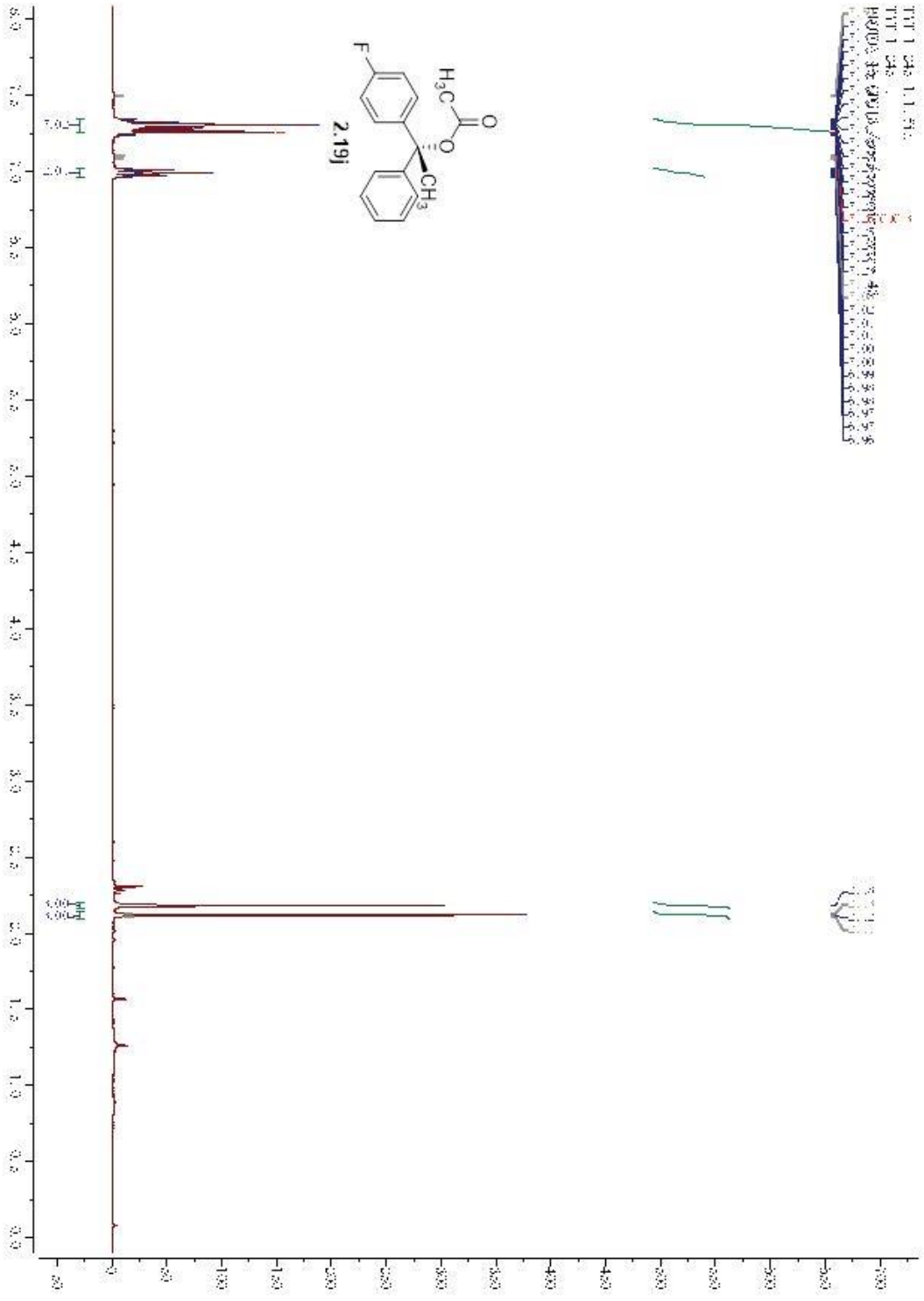
F
O
O
CH3
2.19j

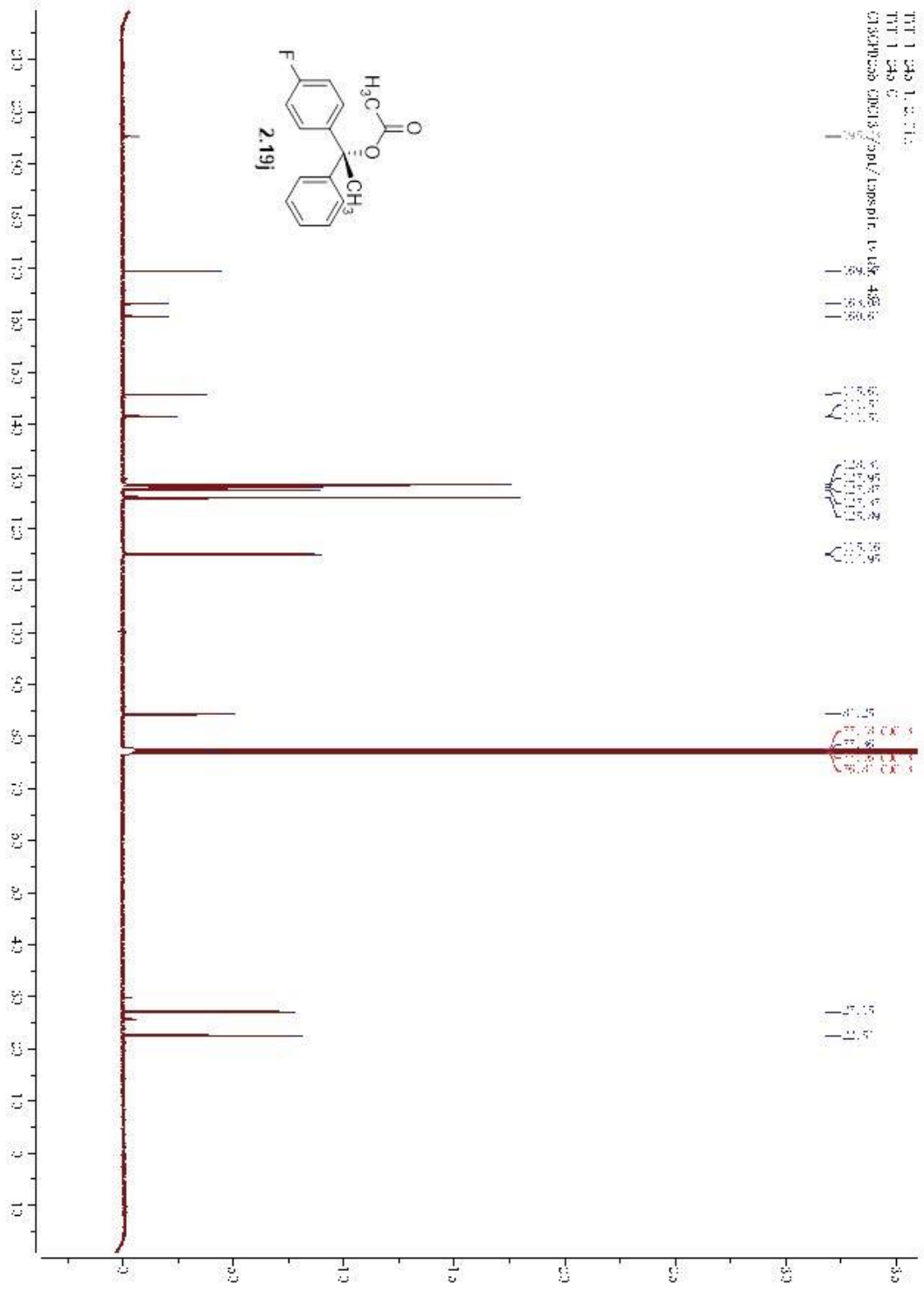
F
H3C
O
O
CH3
2.19j

F
O
O
CH3
2.19j

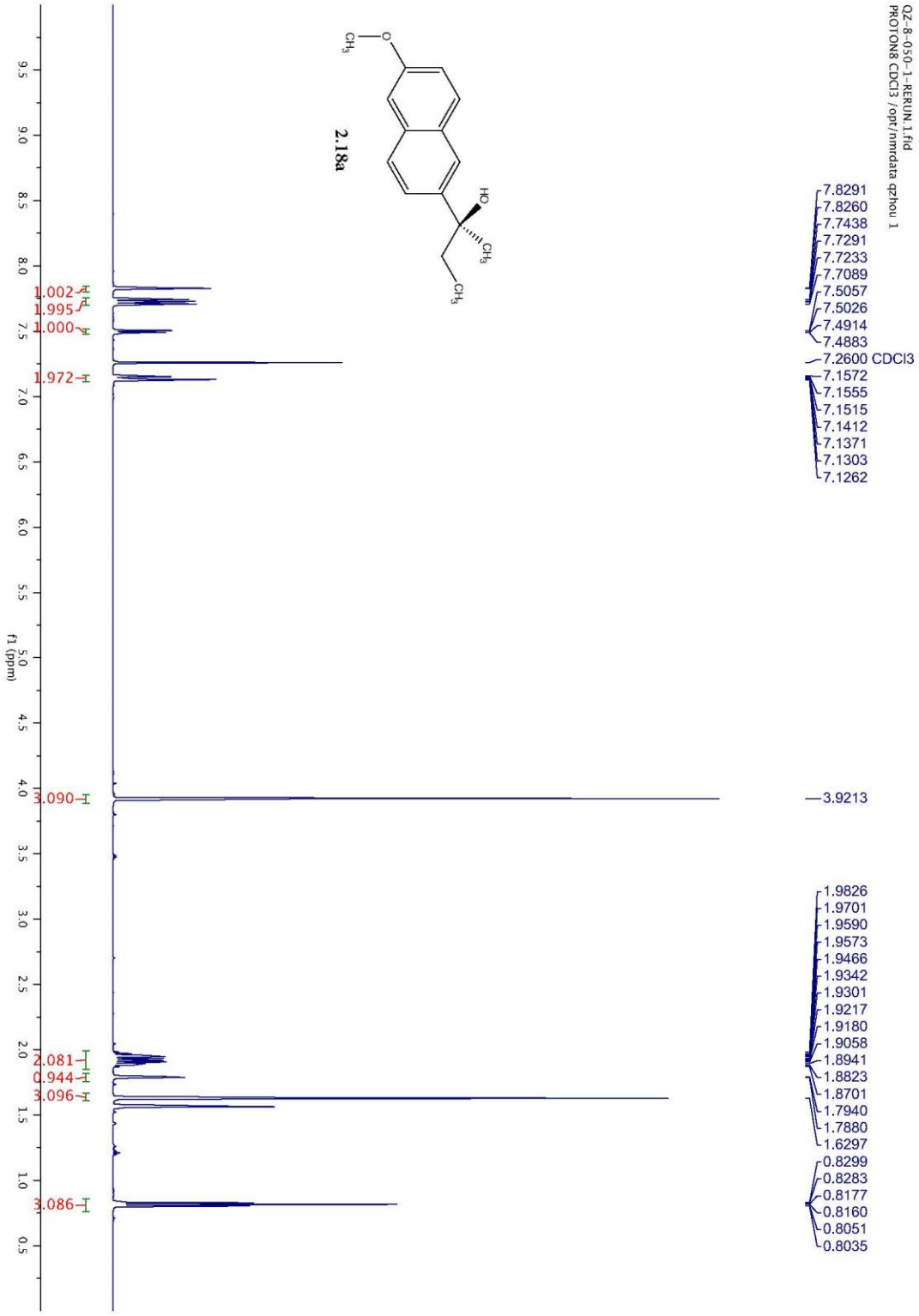
QZ-8-050-1-RERUN.1.fid
PROTON8 CDCl3 /opt/nmrdata qzhou 1
2.18a
f1 (ppm)
1.002
1.995
1.000
1.972
3.090
2.081
0.944
3.096
3.086
7.8291
7.8260
7.7438
7.7291
7.7233
7.7089
7.5057
7.5026
7.4914
7.4883
7.2600 CDCl3
7.1572
7.1555
7.1515
7.1412
7.1371
7.1303
7.1262
3.9213
1.9826
1.9701
1.9590
1.9573
1.9466
1.9342
1.9301
1.9217
1.9180
1.9058
1.8941
1.8823
1.8701
1.7940
1.7880
1.6297
0.8299
0.8283
0.8177
0.8160
0.8051
0.8035

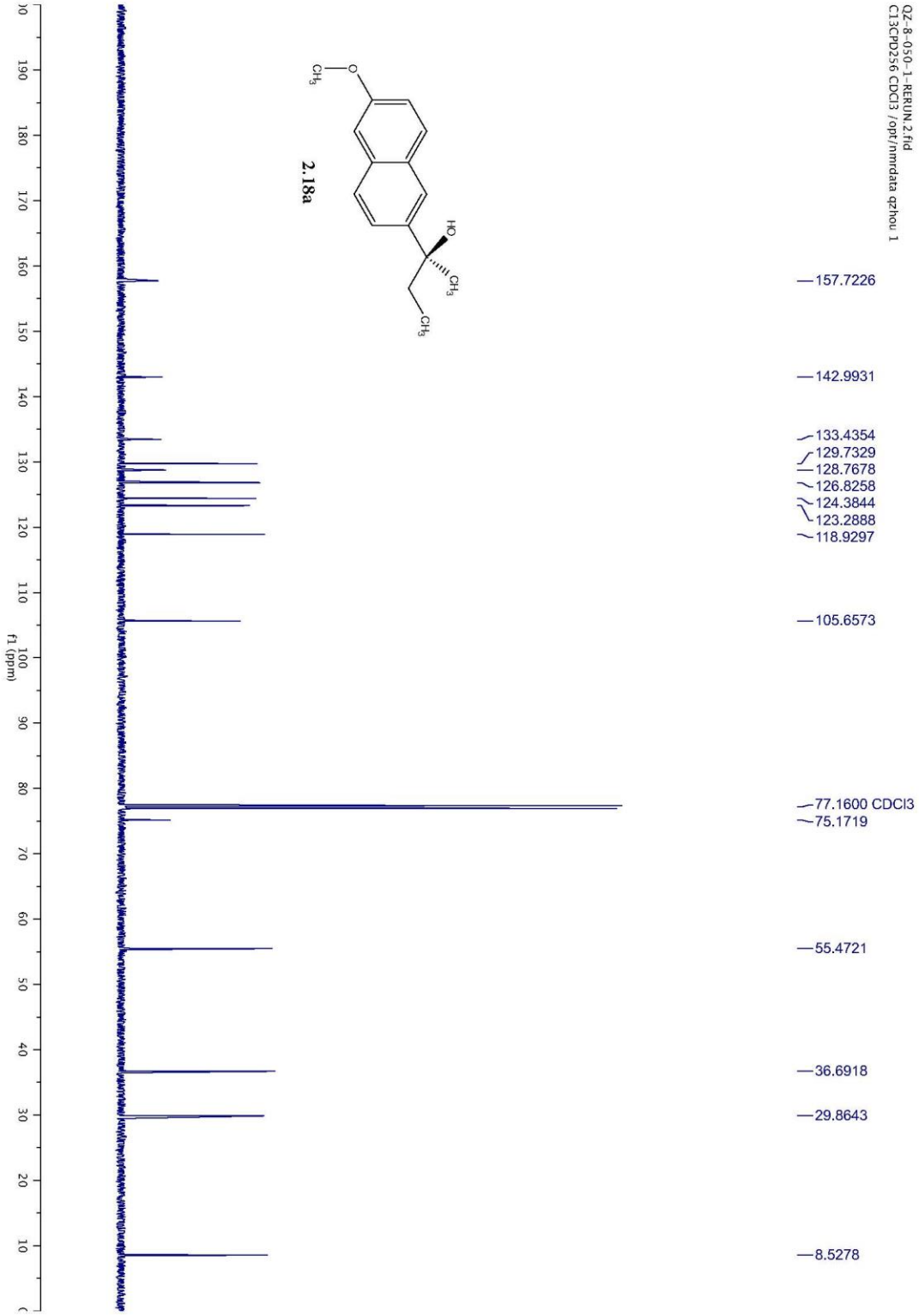
QZ-8-050-1-RERUN.2.fid
C13CPD256 CDCl3 /opt/nmrdata qzhou 1
2.18a
157.7226
142.9931
133.4354
129.7329
128.7678
126.8258
124.3844
123.2888
118.9297
105.6573
77.1600 CDCl3
75.1719
55.4721
36.6918
29.8643
8.5278
f1 (ppm)

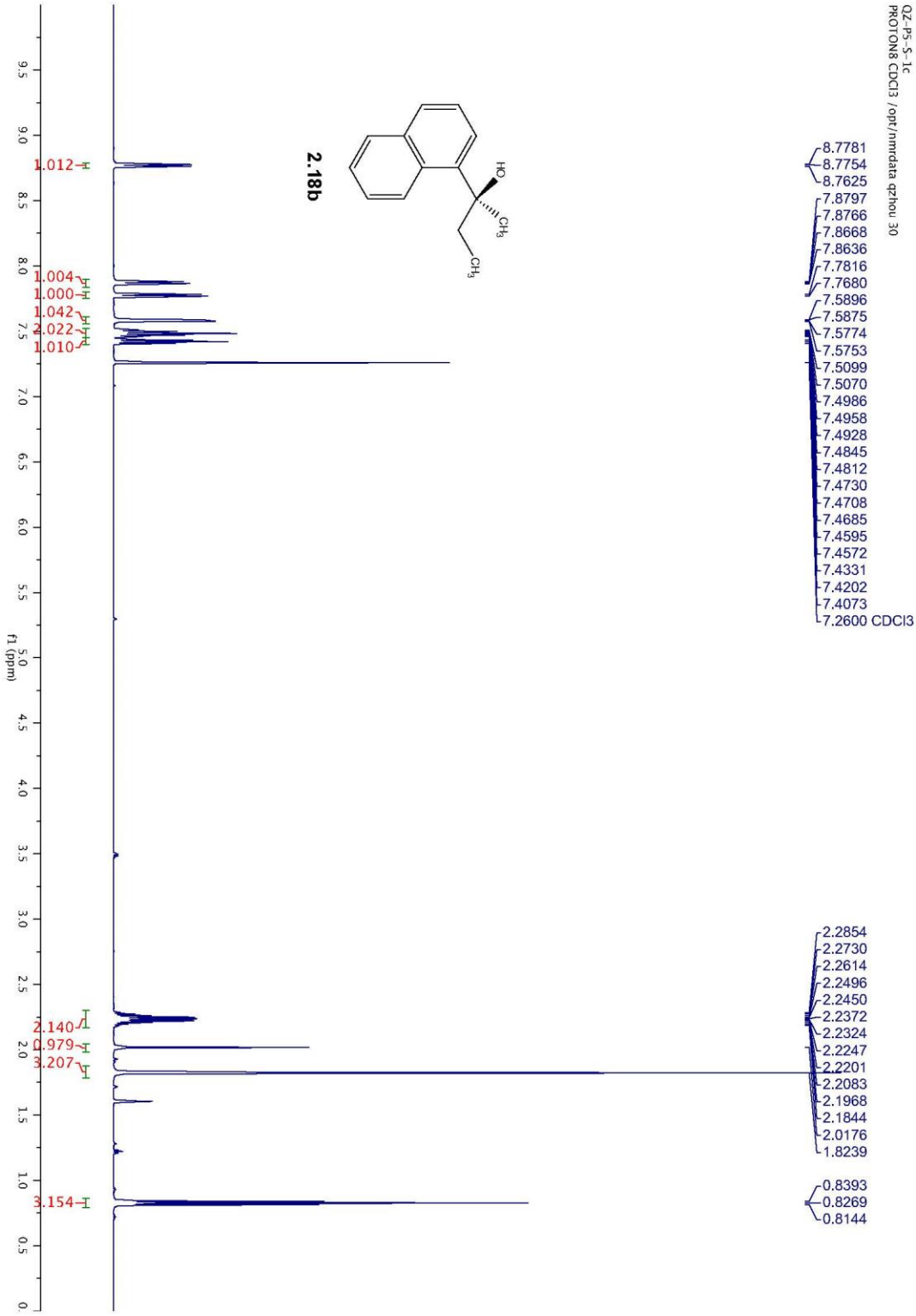
QZ-P5-S-1C
PROTON8 CDCl3 /opt/nmrdata qzhou 30
2.18b
HO
CH3
CH3
f1 (ppm)
1.012
1.004
1.000
1.042
2.022
1.010
2.140
0.979
3.207
3.154
8.7781
8.7754
8.7625
7.8797
7.8766
7.8668
7.8636
7.7816
7.7680
7.5896
7.5875
7.5774
7.5753
7.5099
7.5070
7.4986
7.4958
7.4928
7.4845
7.4812
7.4730
7.4708
7.4685
7.4595
7.4572
7.4331
7.4202
7.4073
7.2600 CDCl3
2.2854
2.2730
2.2614
2.2496
2.2450
2.2372
2.2324
2.2247
2.2201
2.2083
2.1968
2.1844
2.0176
1.8239
0.8393
0.8269
0.8144

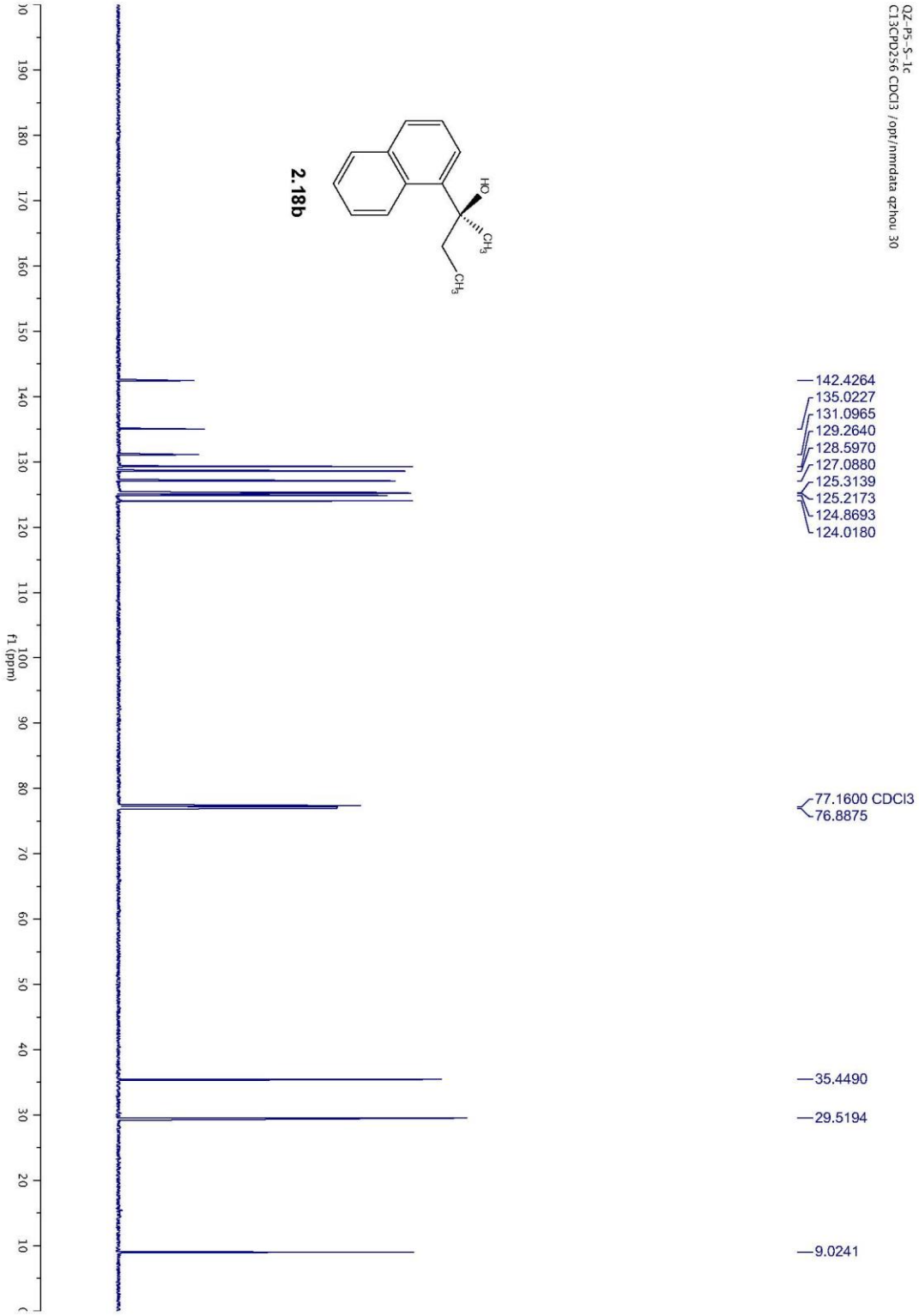
QZ-P5-S-1c
C13CPD256 CDCl3 /opt/nmrdata qzhou 30
2.18b
HO
CH3
CH3
142.4264
135.0227
131.0965
129.2640
128.5970
127.0880
125.3139
125.2173
124.8693
124.0180
77.1600 CDCl3
76.8875
35.4490
29.5194
9.0241
f1 (ppm)

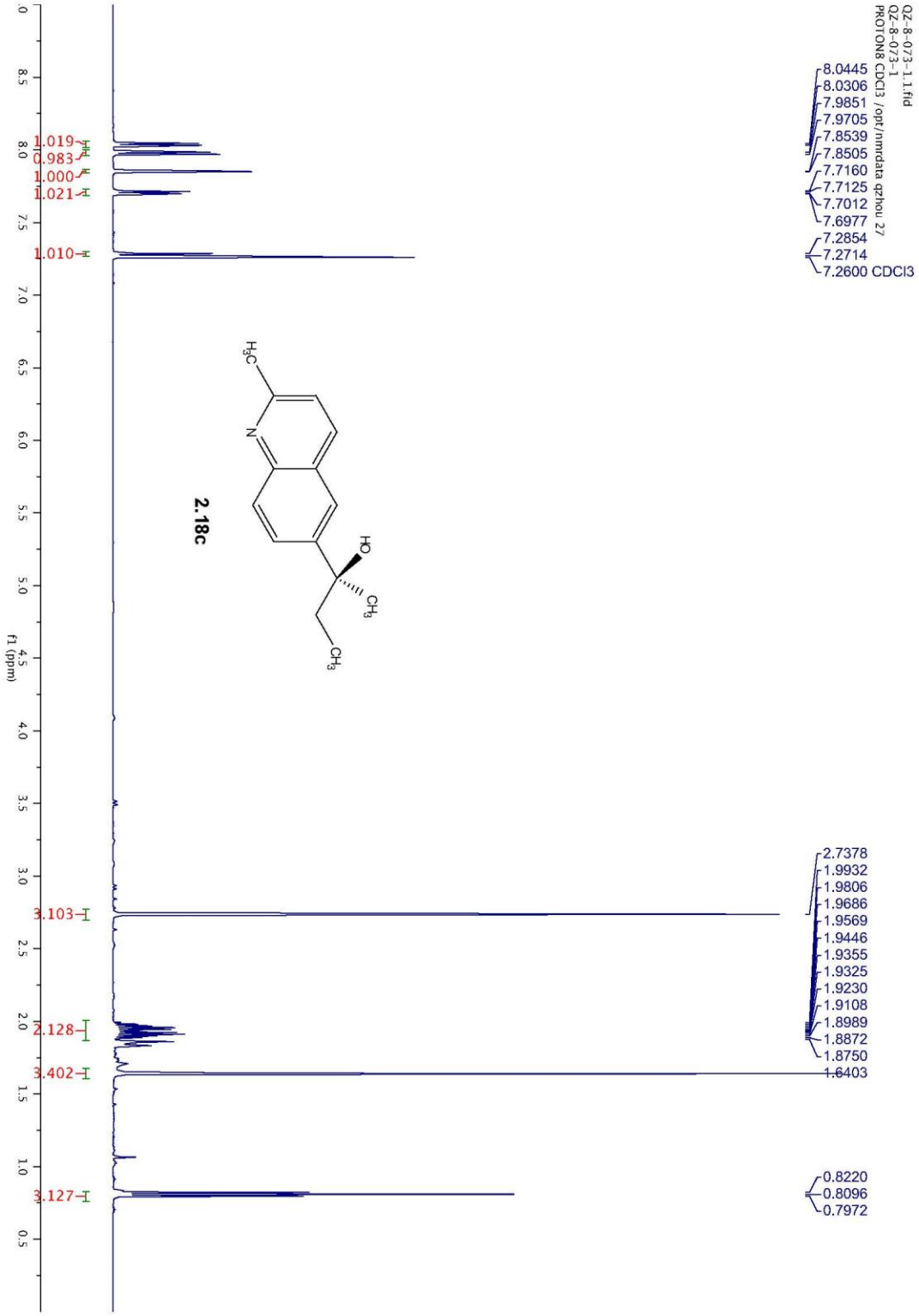
QZ-8-073-1.1.fid
QZ-8-073-1
PROTON8 CDCl3 /opt/nmrdata qzhou 27
8.0445
8.0306
7.9851
7.9705
7.8539
7.8505
7.7160
7.7125
7.7012
7.6977
7.2854
7.2714
7.2600 CDCl3
2.7378
1.9932
1.9806
1.9686
1.9569
1.9446
1.9355
1.9325
1.9230
1.9108
1.8989
1.8872
1.8750
1.6403
0.8220
0.8096
0.7972
1.019
0.983
1.000
1.021
1.010
3.103
2.128
3.402
3.127
f1 (ppm)
2.18c
H3C
N
OH
CH3
CH3

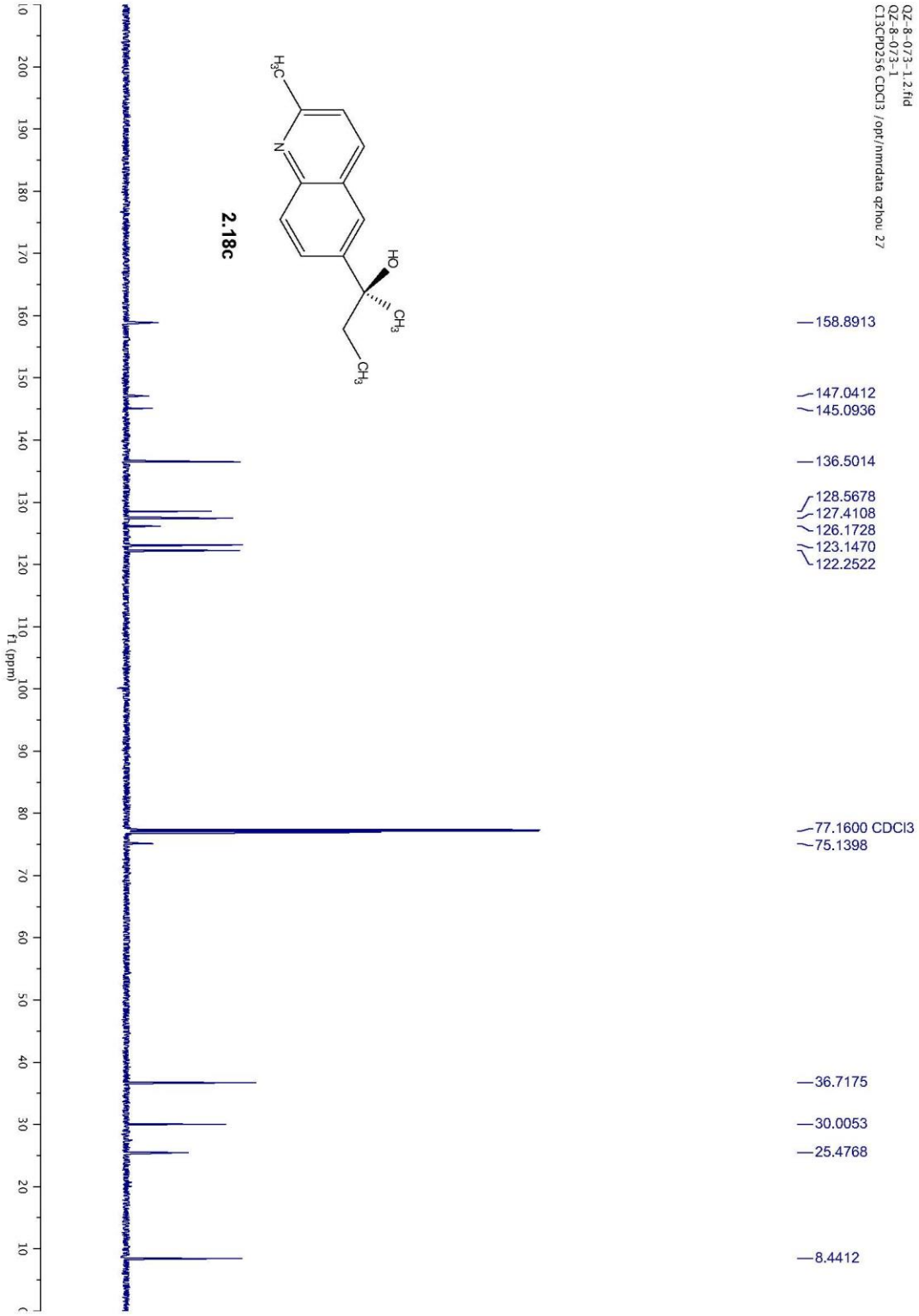
QZ-8-073-1.2.fid
QZ-8-073-1
C13CPD256 CDCl3 /opt/nmrdata qzhou 27
2.18c
158.8913
147.0412
145.0936
136.5014
128.5678
127.4108
126.1728
123.1470
122.2522
77.1600 CDCl3
75.1398
36.7175
30.0053
25.4768
8.4412
f1 (ppm)

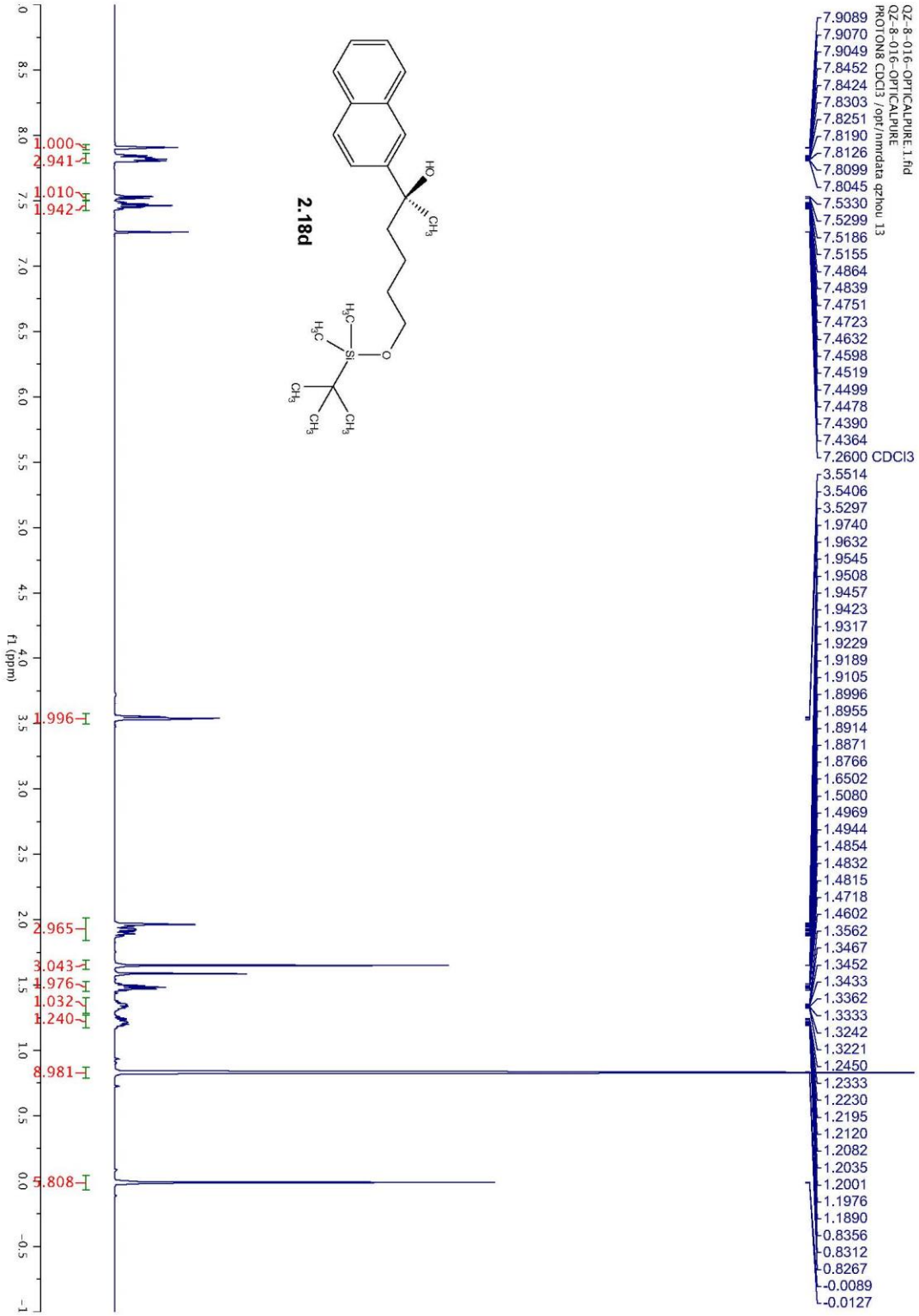
2.18d
f1 (ppm)
1.000
2.941
1.010
1.942
1.996
2.965
3.043
1.976
1.032
1.240
8.981
5.808
QZ-8-016-OPTICALPURE.1.fid
QZ-8-016-OPTICALPURE
PROTON8 CDCl3 /opt/nmrdata qzhou 13
7.9089
7.9070
7.9049
7.8452
7.8424
7.8303
7.8251
7.8190
7.8126
7.8099
7.8045
7.5330
7.5299
7.5186
7.5155
7.4864
7.4839
7.4751
7.4723
7.4632
7.4598
7.4519
7.4499
7.4478
7.4390
7.4364
7.2600 CDCl3
3.5514
3.5406
3.5297
1.9740
1.9632
1.9545
1.9508
1.9457
1.9423
1.9317
1.9229
1.9189
1.9105
1.8996
1.8955
1.8914
1.8871
1.8766
1.6502
1.5080
1.4969
1.4944
1.4854
1.4832
1.4815
1.4718
1.4602
1.3562
1.3467
1.3452
1.3433
1.3362
1.3333
1.3242
1.3221
1.2450
1.2333
1.2230
1.2195
1.2120
1.2082
1.2035
1.2001
1.1976
1.1890
0.8356
0.8312
0.8267
-0.0089
-0.0127

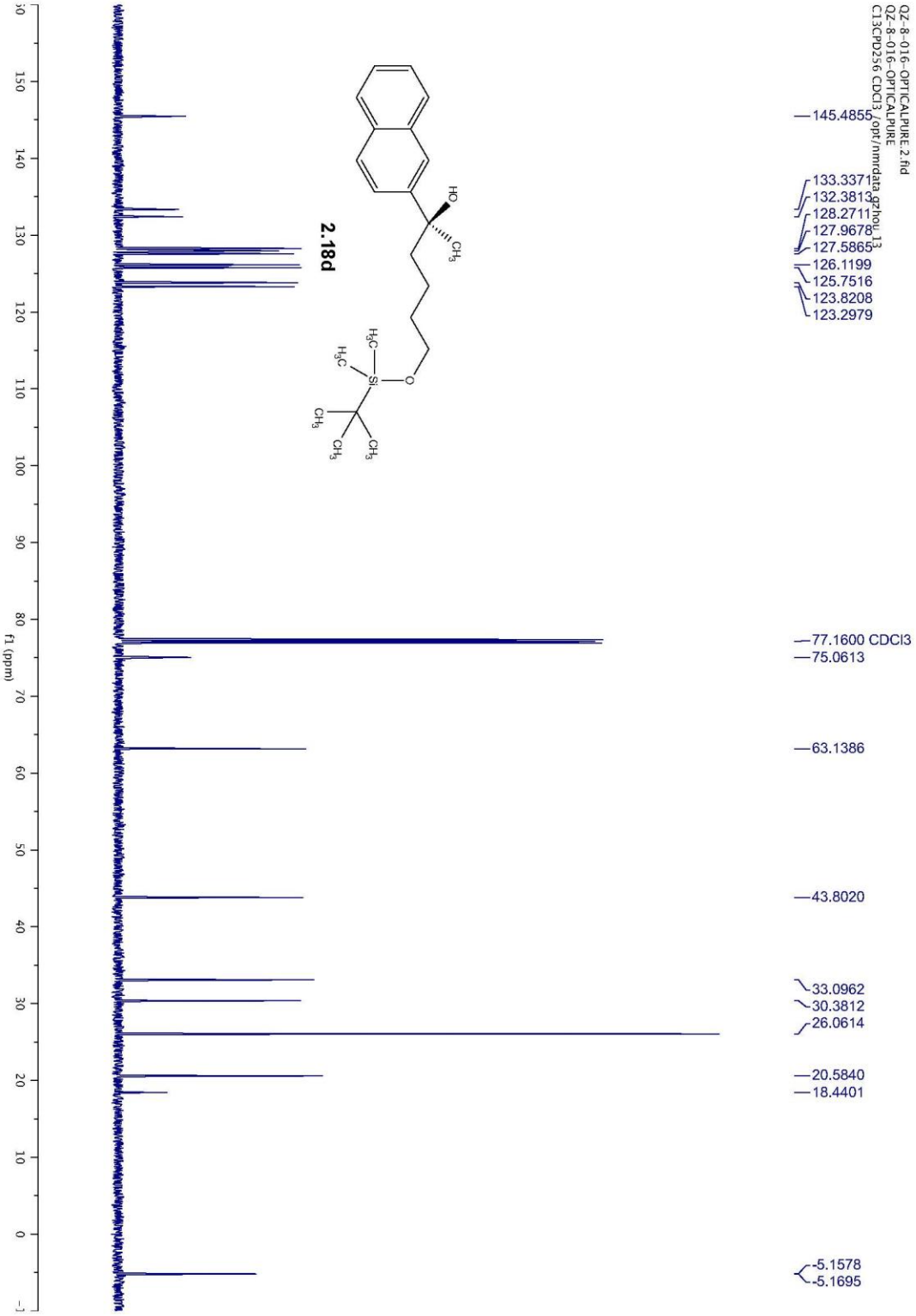
QZ-8-016-OPTICALPURE.2.fid
QZ-8-016-OPTICALPURE
C13CPD256 CDCl3 /opt/nmrdata.gzhou 13
145.4855
133.3371
132.3813
128.2711
127.9678
127.5865
126.1199
125.7516
123.8208
123.2979
77.1600 CDCl3
75.0613
63.1386
43.8020
33.0962
30.3812
26.0614
20.5840
18.4401
-5.1578
-5.1695
2.18d
HO
CH3
H3C
Si
O
CH3
CH3
CH3
f1 (ppm)

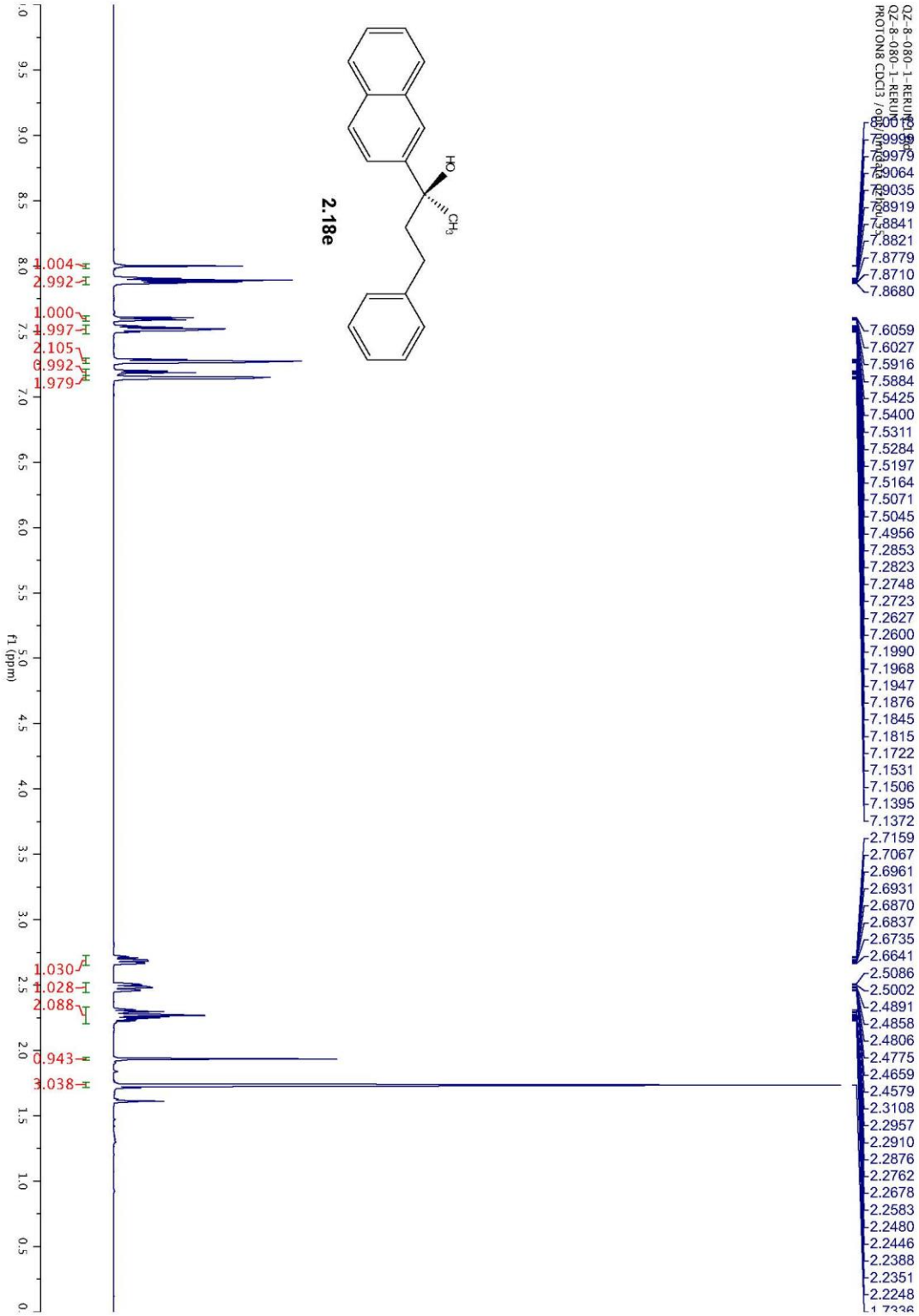
2.18e
OH
CH3
f1 (ppm)
1.004
2.992
1.000
1.997
2.105
0.992
1.979
1.030
1.028
2.088
0.943
3.038
7.8680
7.8710
7.8779
7.8821
7.8841
7.6059
7.6027
7.5916
7.5884
7.5425
7.5400
7.5311
7.5284
7.5197
7.5164
7.5071
7.5045
7.4956
7.2853
7.2823
7.2748
7.2723
7.2627
7.2600
7.1990
7.1968
7.1947
7.1876
7.1845
7.1815
7.1722
7.1531
7.1506
7.1395
7.1372
2.7159
2.7067
2.6961
2.6931
2.6870
2.6837
2.6735
2.6641
2.5086
2.5002
2.4891
2.4858
2.4806
2.4775
2.4659
2.4579
2.3108
2.2957
2.2910
2.2876
2.2762
2.2678
2.2583
2.2480
2.2446
2.2388
2.2351
2.2248

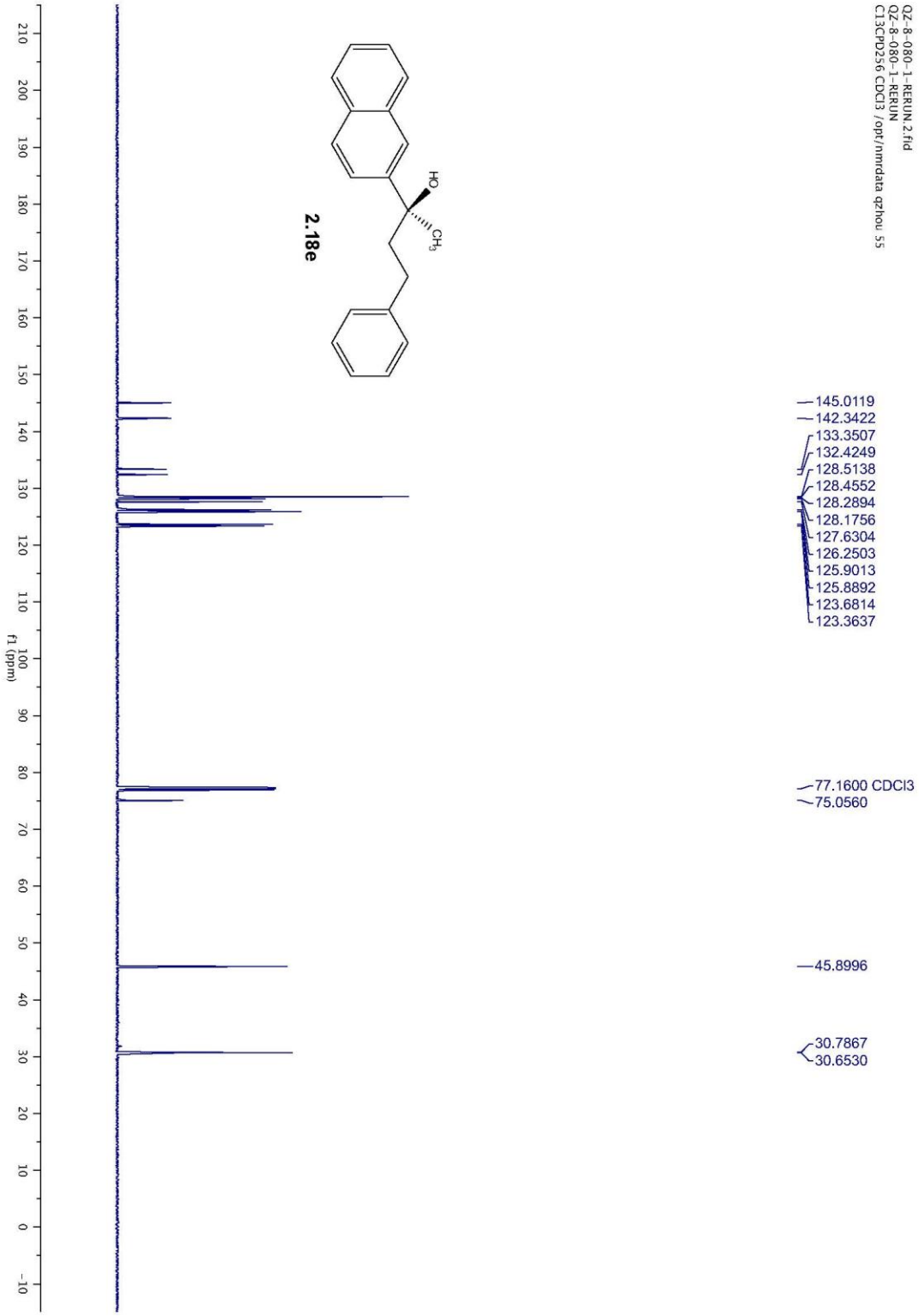
QZ-8-080-1-RERUN.2.fid
QZ-8-080-1-RERUN
C13CPD256 CDCl3 /opt/nmrdata qzhou 55
2.18e
HO
CH3
145.0119
142.3422
133.3507
132.4249
128.5138
128.4552
128.2894
128.1756
127.6304
126.2503
125.9013
125.8892
123.6814
123.3637
77.1600 CDCl3
75.0560
45.8996
30.7867
30.6530
f1 (ppm)

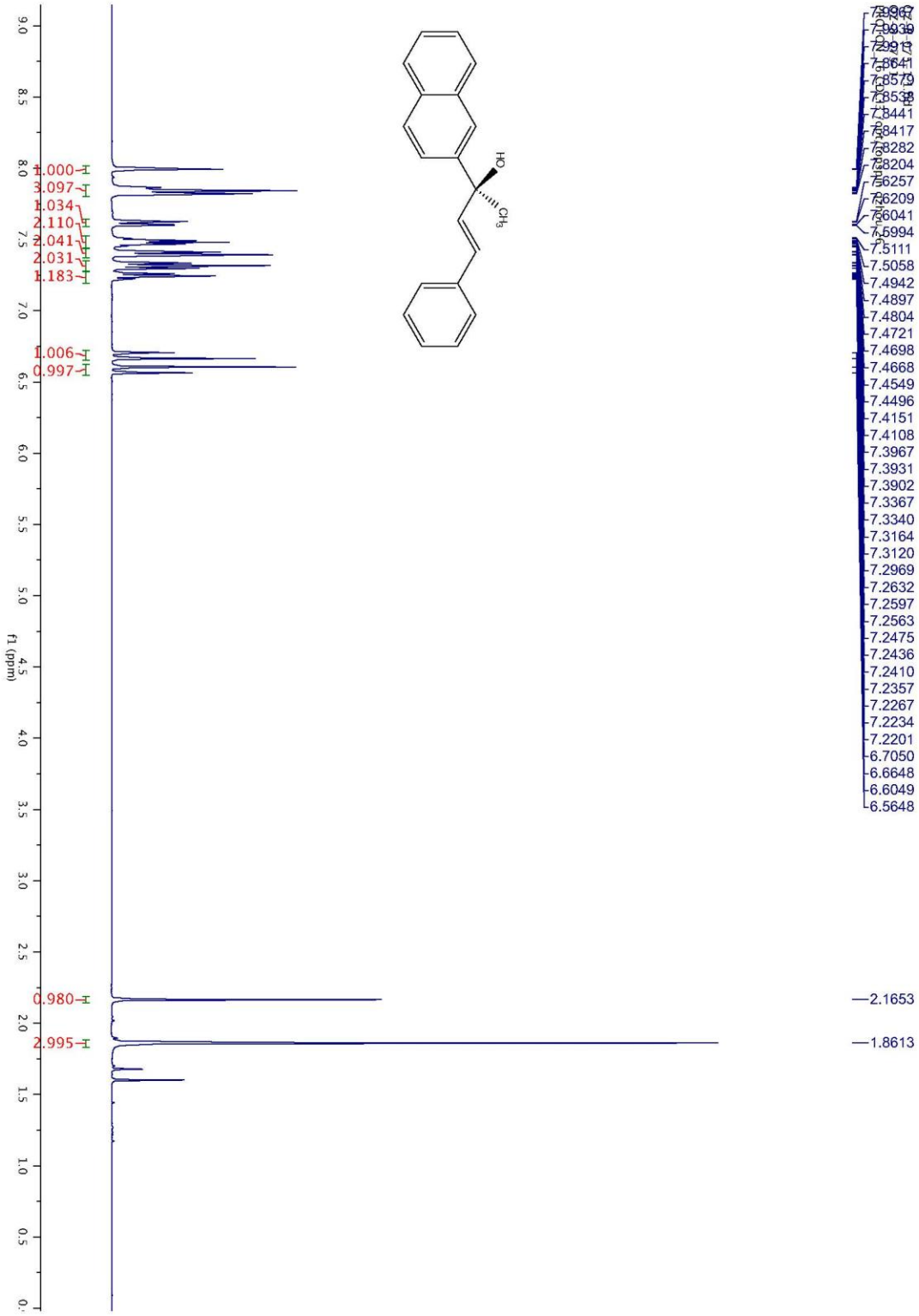
1.000
3.097
1.034
2.110
2.041
2.031
1.183
1.006
0.997
0.980
2.995
f1 (ppm)
OH
CH3
7.5111
7.5058
7.4942
7.4897
7.4804
7.4721
7.4698
7.4668
7.4549
7.4496
7.4151
7.4108
7.3967
7.3931
7.3902
7.3367
7.3340
7.3164
7.3120
7.2969
7.2632
7.2597
7.2563
7.2475
7.2436
7.2410
7.2357
7.2267
7.2234
7.2201
6.7050
6.6648
6.6049
6.5648
2.1653
1.8613

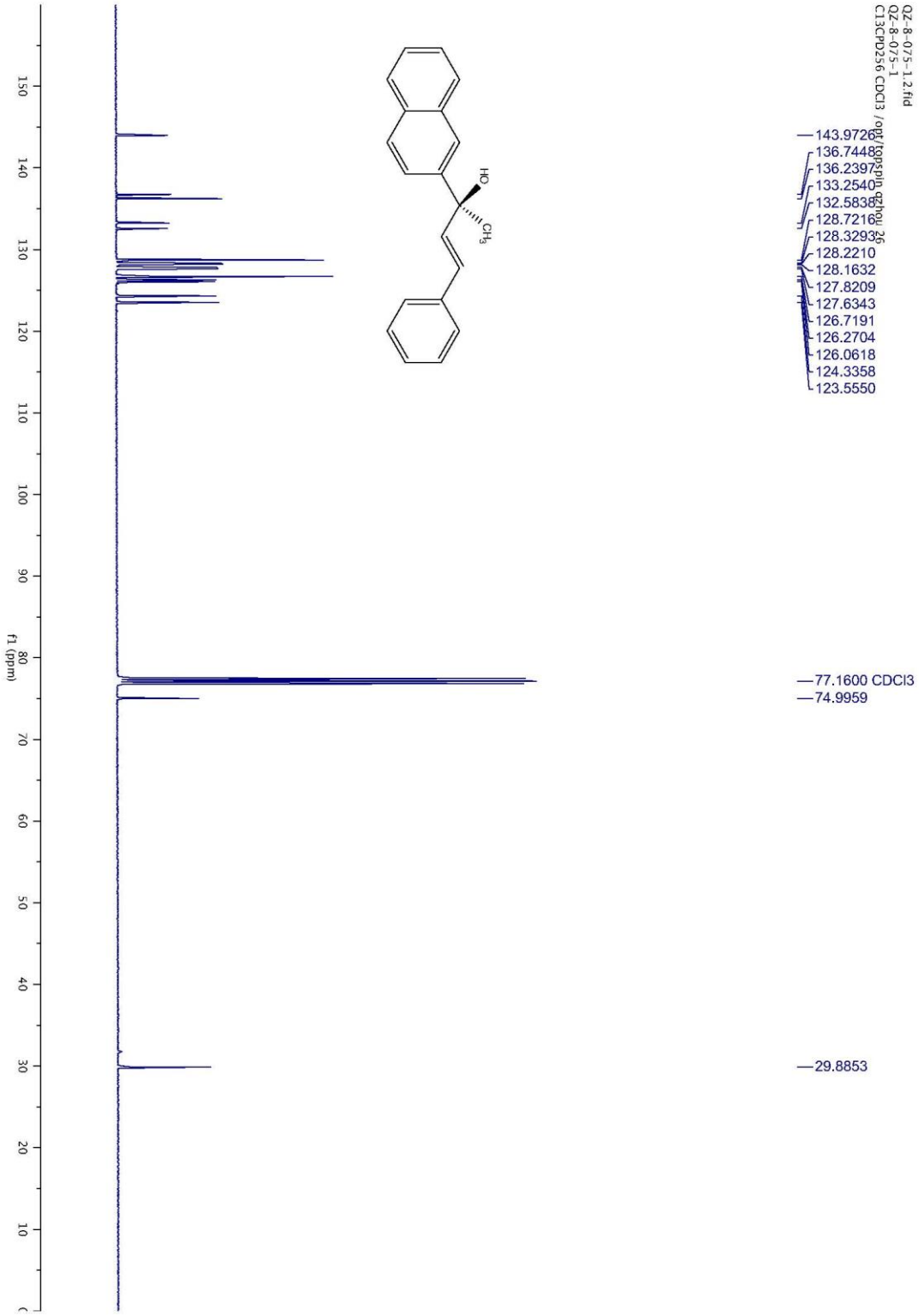
QZ-8-075-1.2.fid
QZ-8-075-1
C13CPD256 CDCl3 /opt/topspin qzhou 26
143.9726
136.7448
136.2397
133.2540
132.5838
128.7216
128.3293
128.2210
128.1632
127.8209
127.6343
126.7191
126.2704
126.0618
124.3358
123.5550
77.1600 CDCl3
74.9959
29.8853
HO
CH3
f1 (ppm)

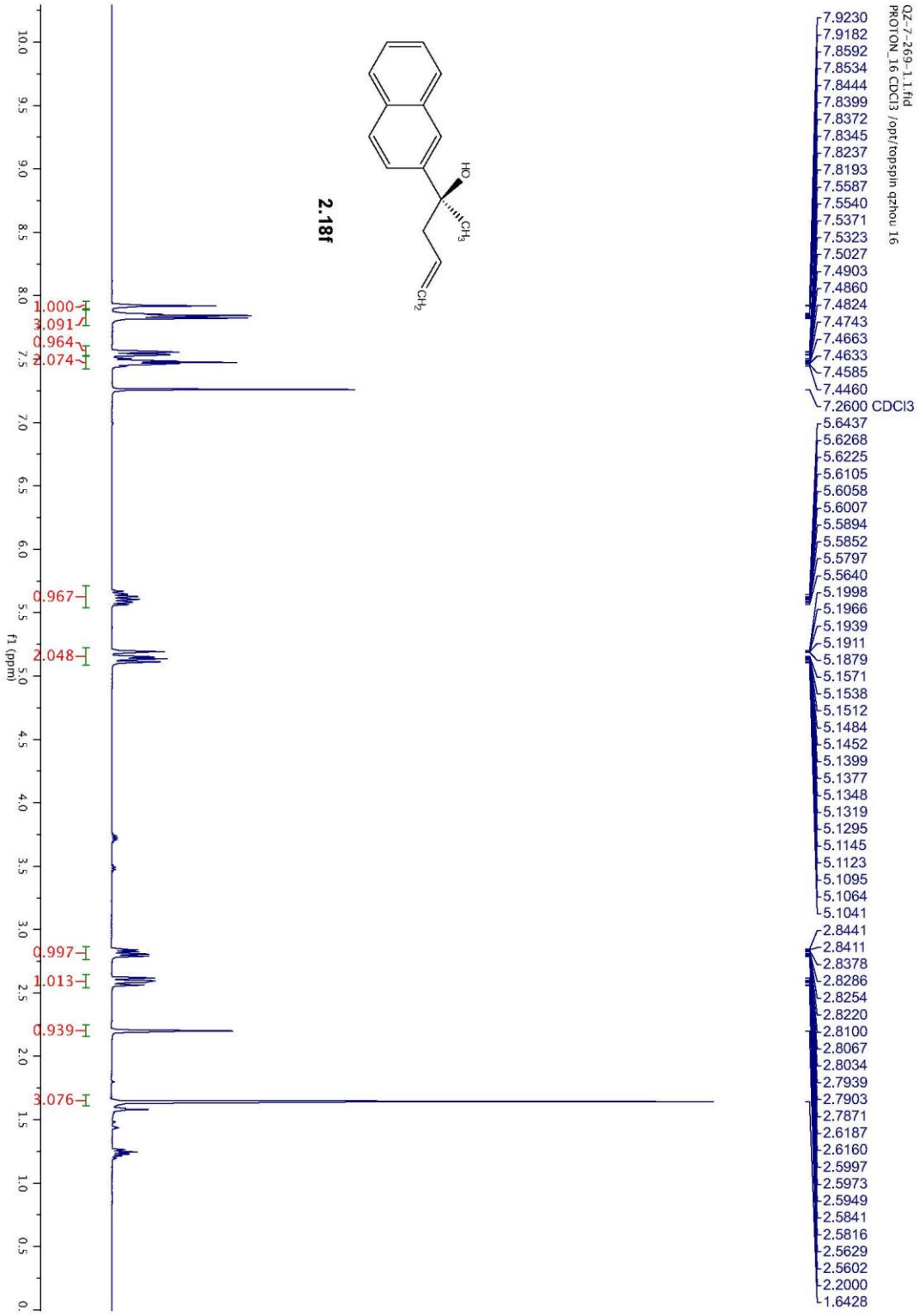
2.18f
HO
CH3
CH2
1.000
3.091
0.964
2.074
0.967
2.048
0.997
1.013
0.939
3.076
f1 (ppm)
QZ-7-269-1.1.fid
PROTON_16 CDCl3 /opt/topspin qzhou 16
7.9230
7.9182
7.8592
7.8534
7.8444
7.8399
7.8372
7.8345
7.8237
7.8193
7.5587
7.5540
7.5371
7.5323
7.5027
7.4903
7.4860
7.4824
7.4743
7.4663
7.4633
7.4585
7.4460
7.2600 CDCl3
5.6437
5.6268
5.6225
5.6105
5.6058
5.6007
5.5894
5.5852
5.5797
5.5640
5.1998
5.1966
5.1939
5.1911
5.1879
5.1571
5.1538
5.1512
5.1484
5.1452
5.1399
5.1377
5.1348
5.1319
5.1295
5.1145
5.1123
5.1095
5.1064
5.1041
2.8441
2.8411
2.8378
2.8286
2.8254
2.8220
2.8100
2.8067
2.8034
2.7939
2.7903
2.7871
2.6187
2.6160
2.5997
2.5973
2.5949
2.5841
2.5816
2.5629
2.5602
2.2000
1.6428

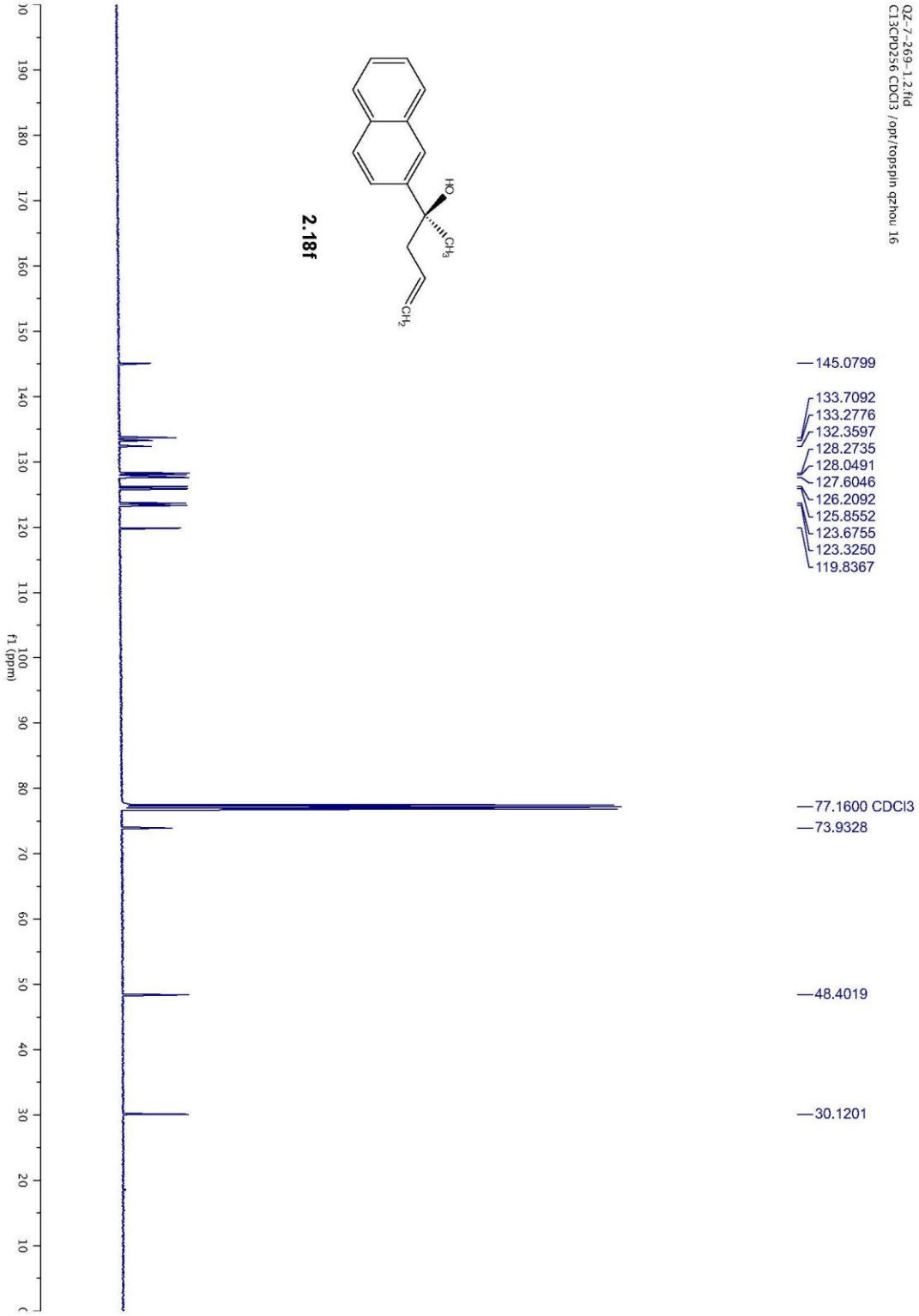
QZ-7-269-1.2.fid
C13CPD256 CDCl3 /opt/topspin qzhou 16
2.18f
HO
CH3
CH2
f1 (ppm)
145.0799
133.7092
133.2776
132.3597
128.2735
128.0491
127.6046
126.2092
125.8552
123.6755
123.3250
119.8367
77.1600 CDCl3
73.9328
48.4019
30.1201

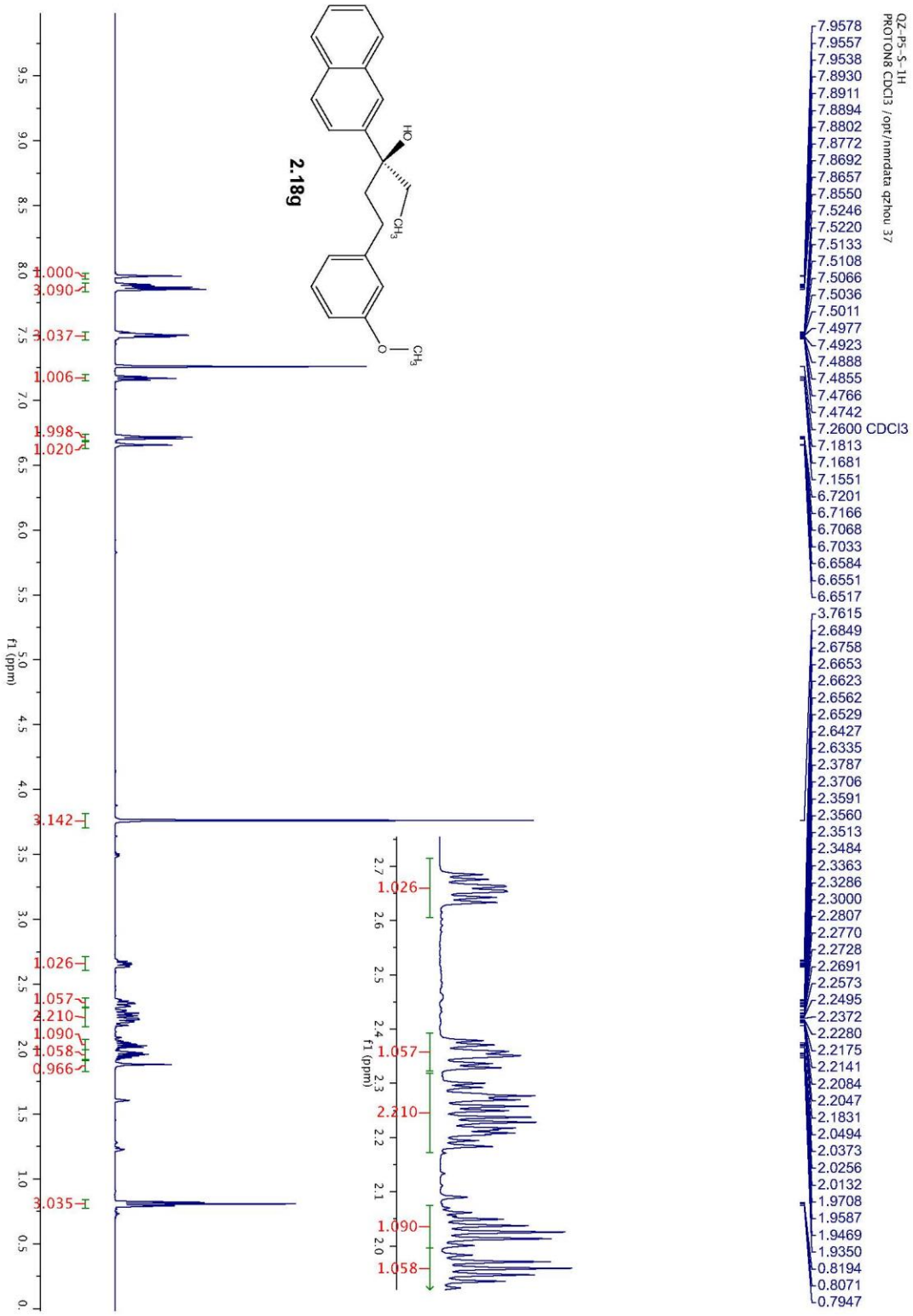
2.18g
HO
CH3
O
CH3
1.000
3.090
3.037
1.006
1.998
1.020
3.142
1.026
1.057
2.210
1.090
1.058
0.966
3.035
f1 (ppm)
1.026
1.057
2.210
1.090
1.058
QZ-P5--S--1H
PROTON8 CDCl3 /opt/nmrdata qzhou 37
7.9578
7.9557
7.9538
7.8930
7.8911
7.8894
7.8802
7.8772
7.8692
7.8657
7.8550
7.5246
7.5220
7.5133
7.5108
7.5066
7.5036
7.5011
7.4977
7.4923
7.4888
7.4855
7.4766
7.4742
7.2600 CDCl3
7.1813
7.1681
7.1551
6.7201
6.7166
6.7068
6.7033
6.6584
6.6551
6.6517
3.7615
2.6849
2.6758
2.6653
2.6623
2.6562
2.6529
2.6427
2.6335
2.3787
2.3706
2.3591
2.3560
2.3513
2.3484
2.3363
2.3286
2.3000
2.2807
2.2770
2.2728
2.2691
2.2573
2.2495
2.2372
2.2280
2.2175
2.2141
2.2084
2.2047
2.1831
2.0494
2.0373
2.0256
2.0132
1.9708
1.9587
1.9469
1.9350
0.8194
0.8071
0.7947

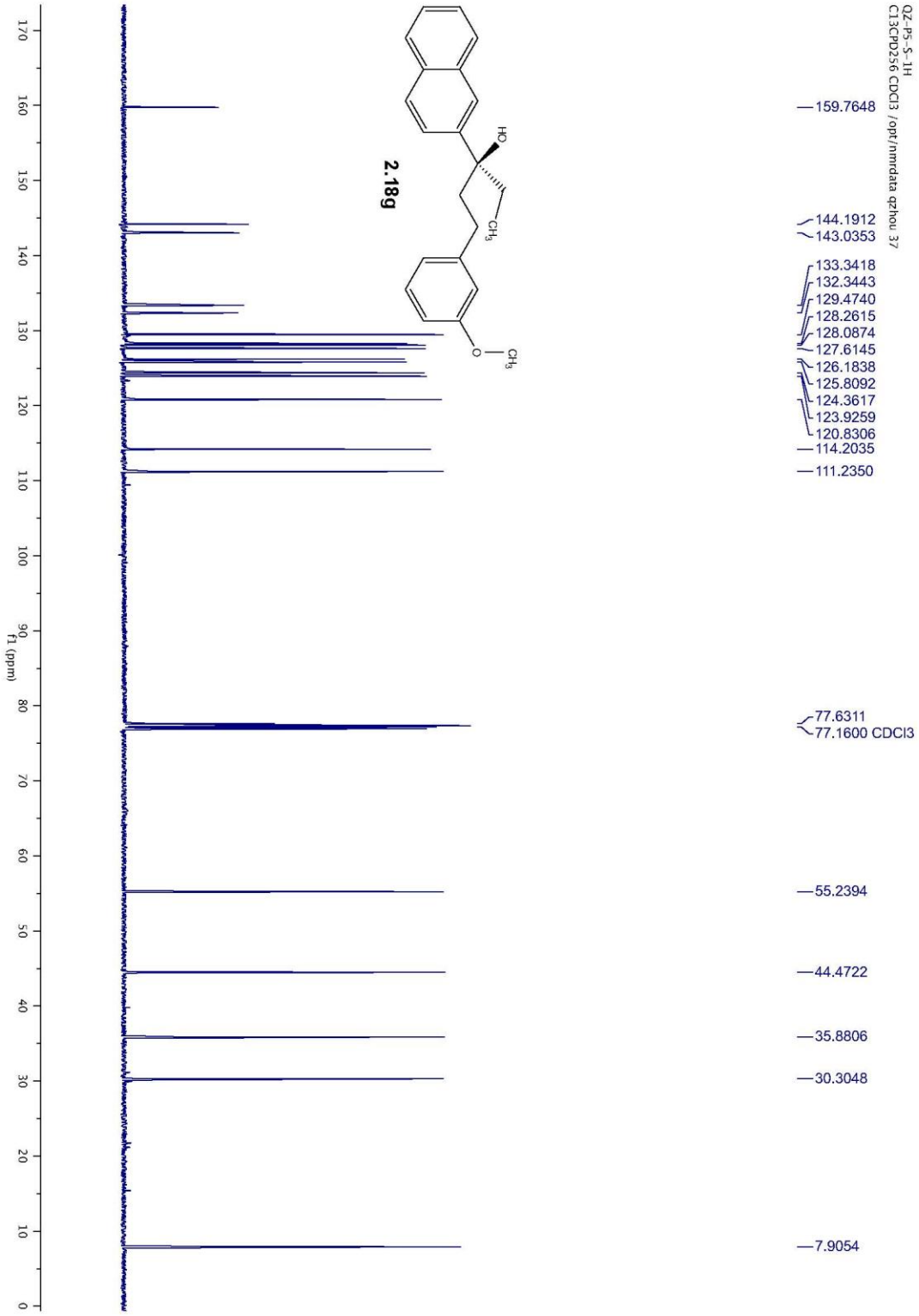
QZ-P5-S-1H
C13CPD256 CDCl3 /opt/nmrdata qzhou 37
2.18g
HO
CH3
O
CH3
159.7648
144.1912
143.0353
133.3418
132.3443
129.4740
128.2615
128.0874
127.6145
126.1838
125.8092
124.3617
123.9259
120.8306
114.2035
111.2350
77.6311
77.1600 CDCl3
55.2394
44.4722
35.8806
30.3048
7.9054
f1 (ppm)

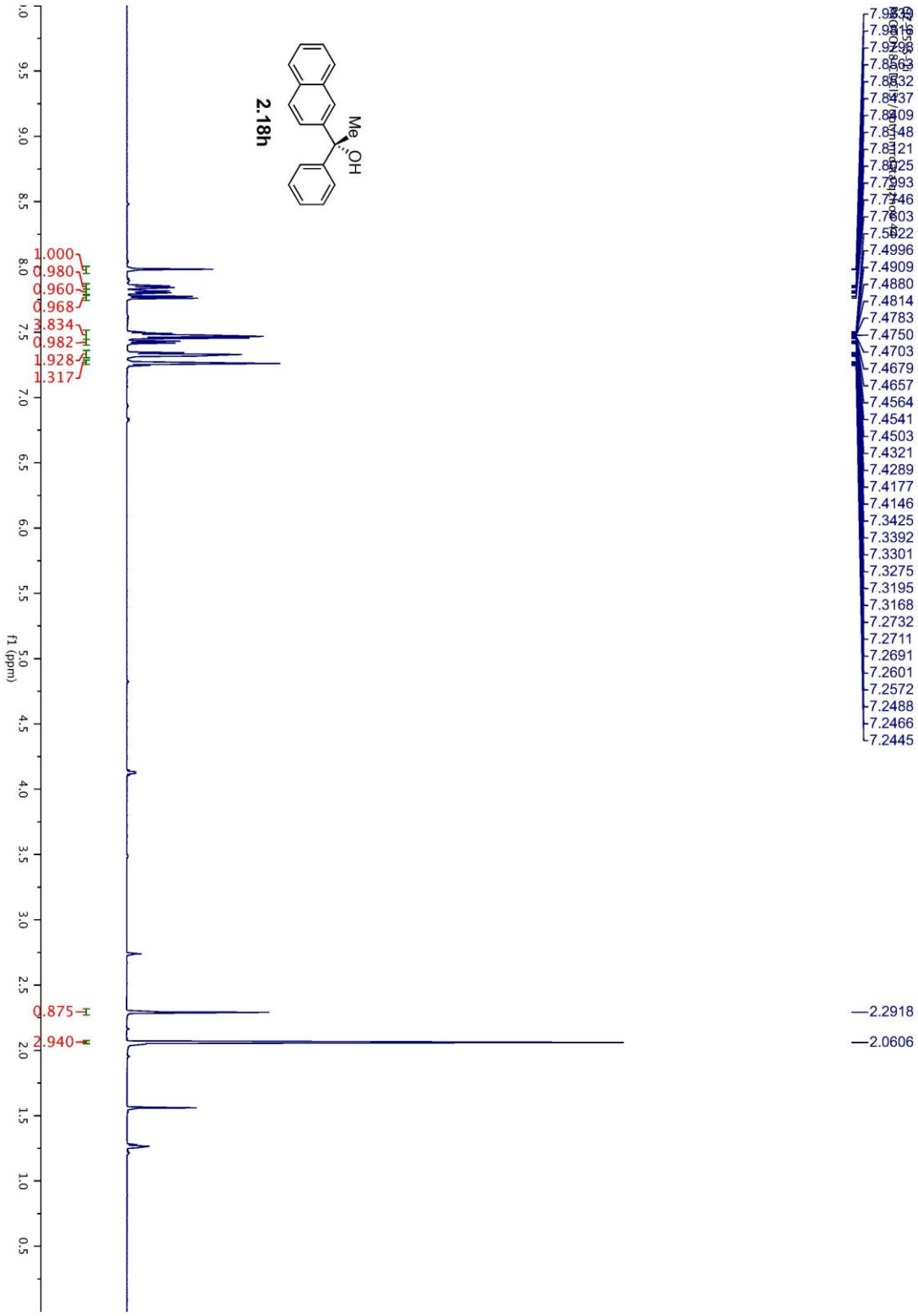
2.18h
Me
OH
1.000
0.980
0.960
0.968
3.834
0.982
1.928
1.317
0.875
2.940
2.2918
2.0606
f1 (ppm)

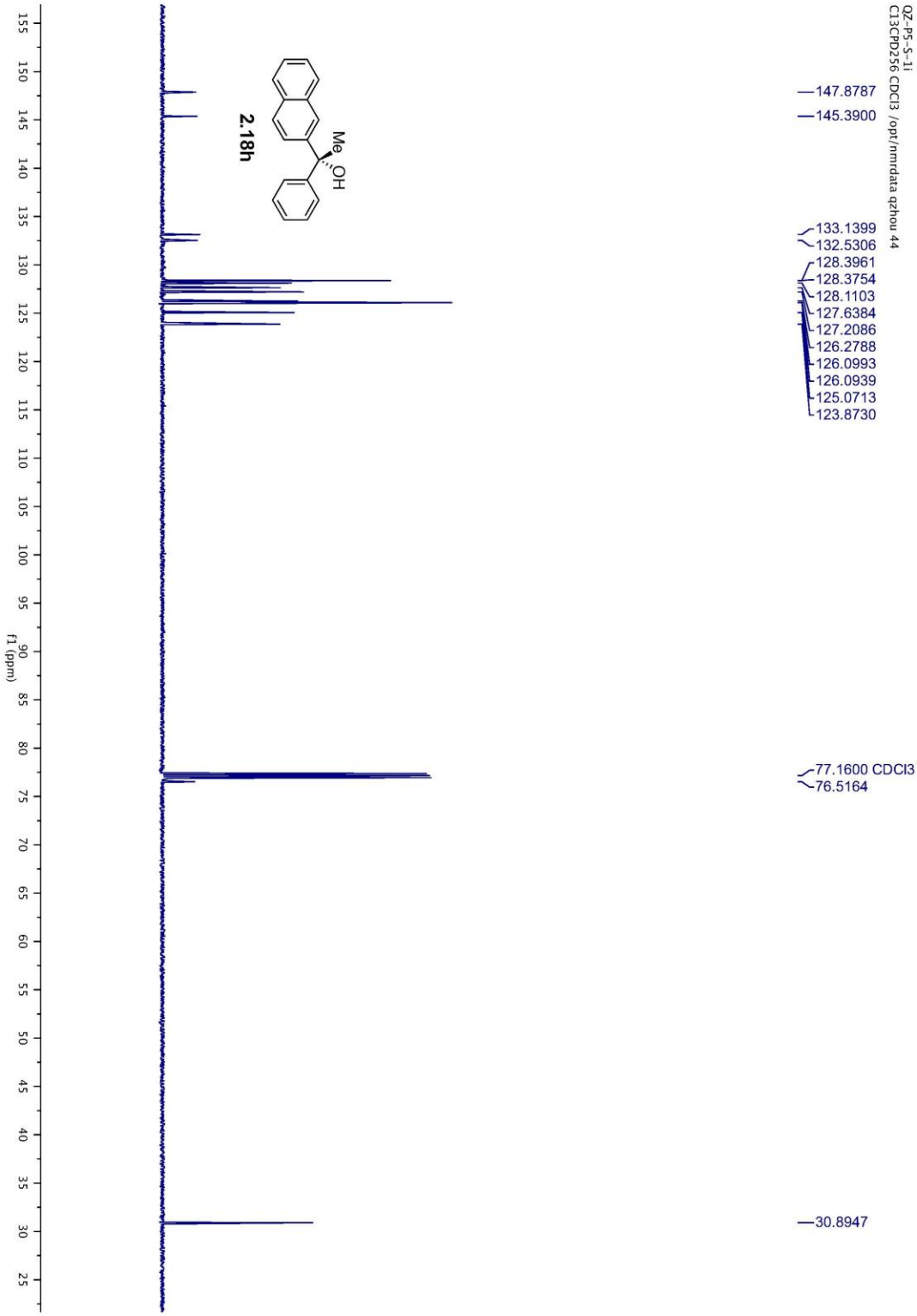
QZ-P5-S-1i
C13CPD256 CDCl3 /opt/nmrdata qzhou 44
147.8787
145.3900
133.1399
132.5306
128.3961
128.3754
128.1103
127.6384
127.2086
126.2788
126.0993
126.0939
125.0713
123.8730
77.1600 CDCl3
76.5164
30.8947
2.18h
Me
OH
f1 (ppm)

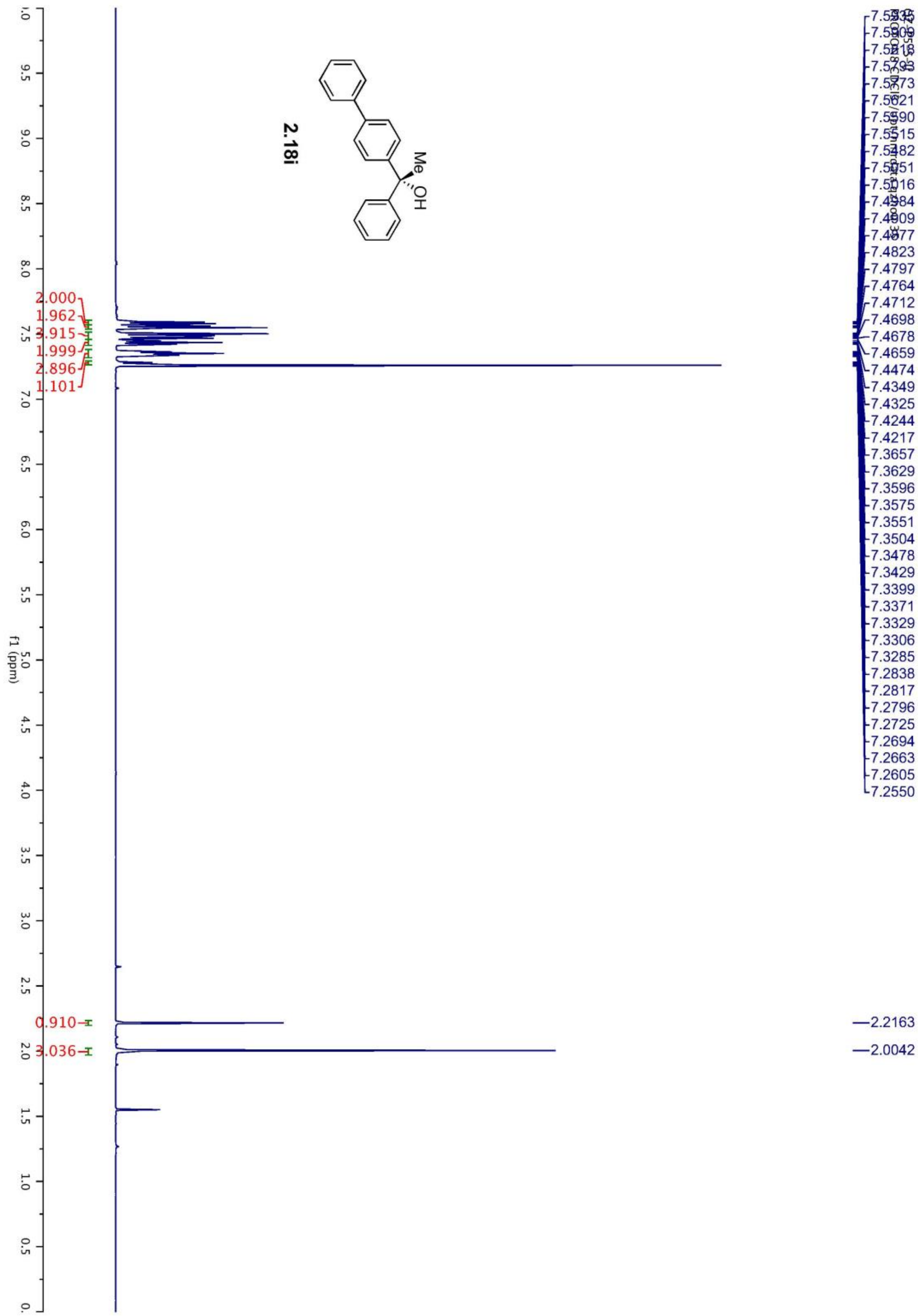

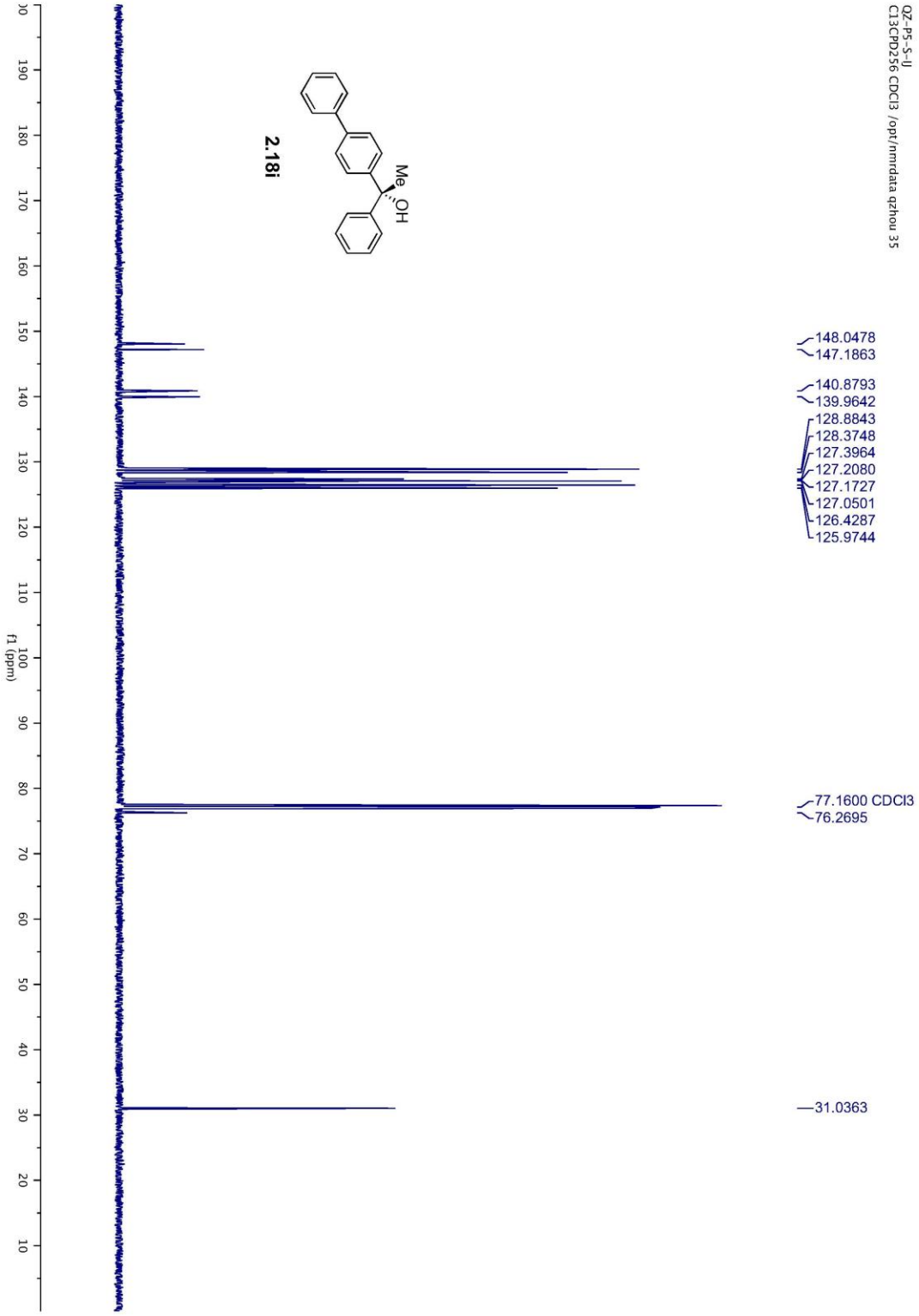
QZ-PS-S-IJ
C13CPD256 CDCl3 /opt/nmrdata qzhou 35
2.18i
Me
OH
148.0478
147.1863
140.8793
139.9642
128.8843
128.3748
127.3964
127.2080
127.1727
127.0501
126.4287
125.9744
77.1600 CDCl3
76.2695
31.0363
f1 (ppm)

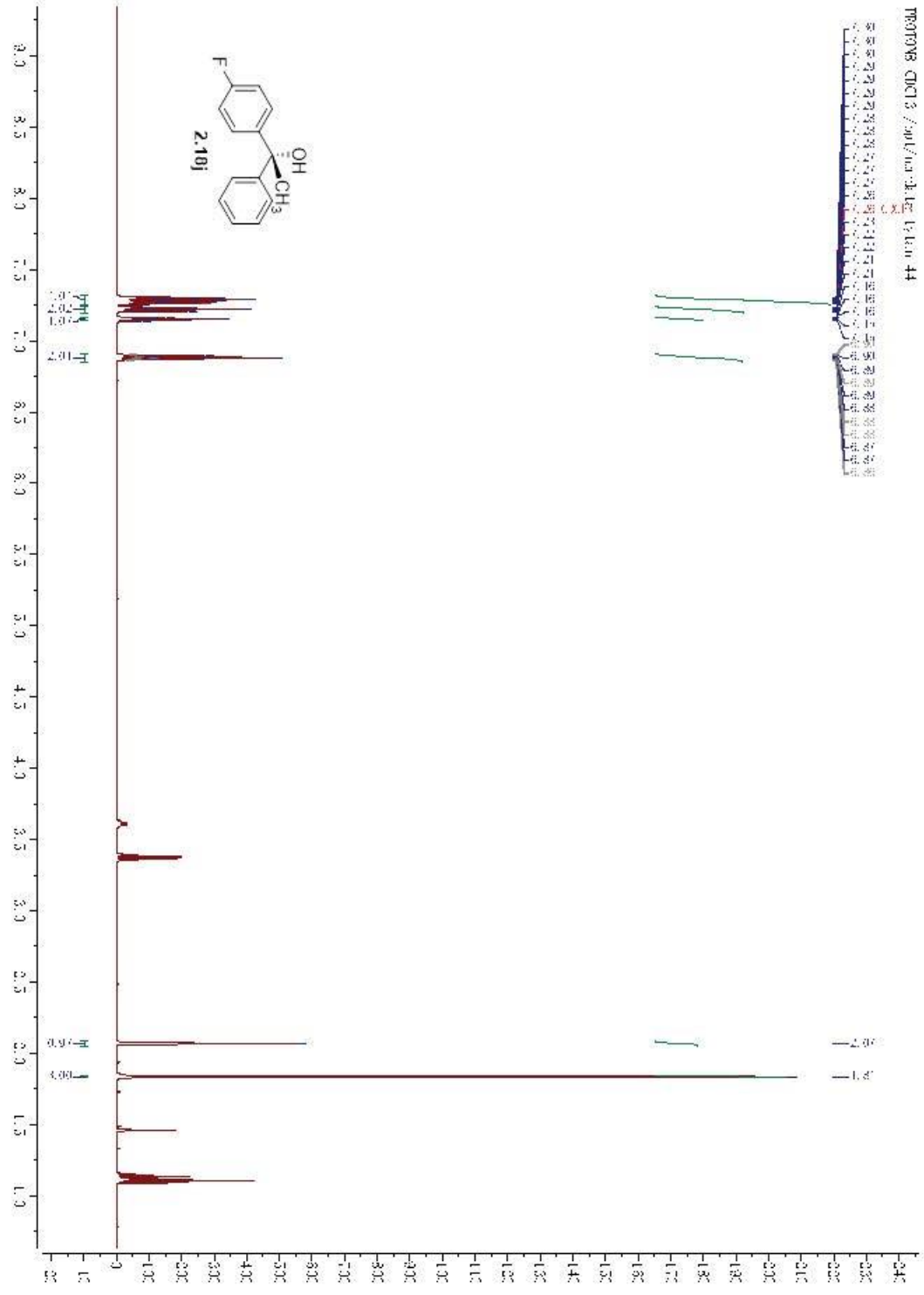
F
OH
CH3
2.10j

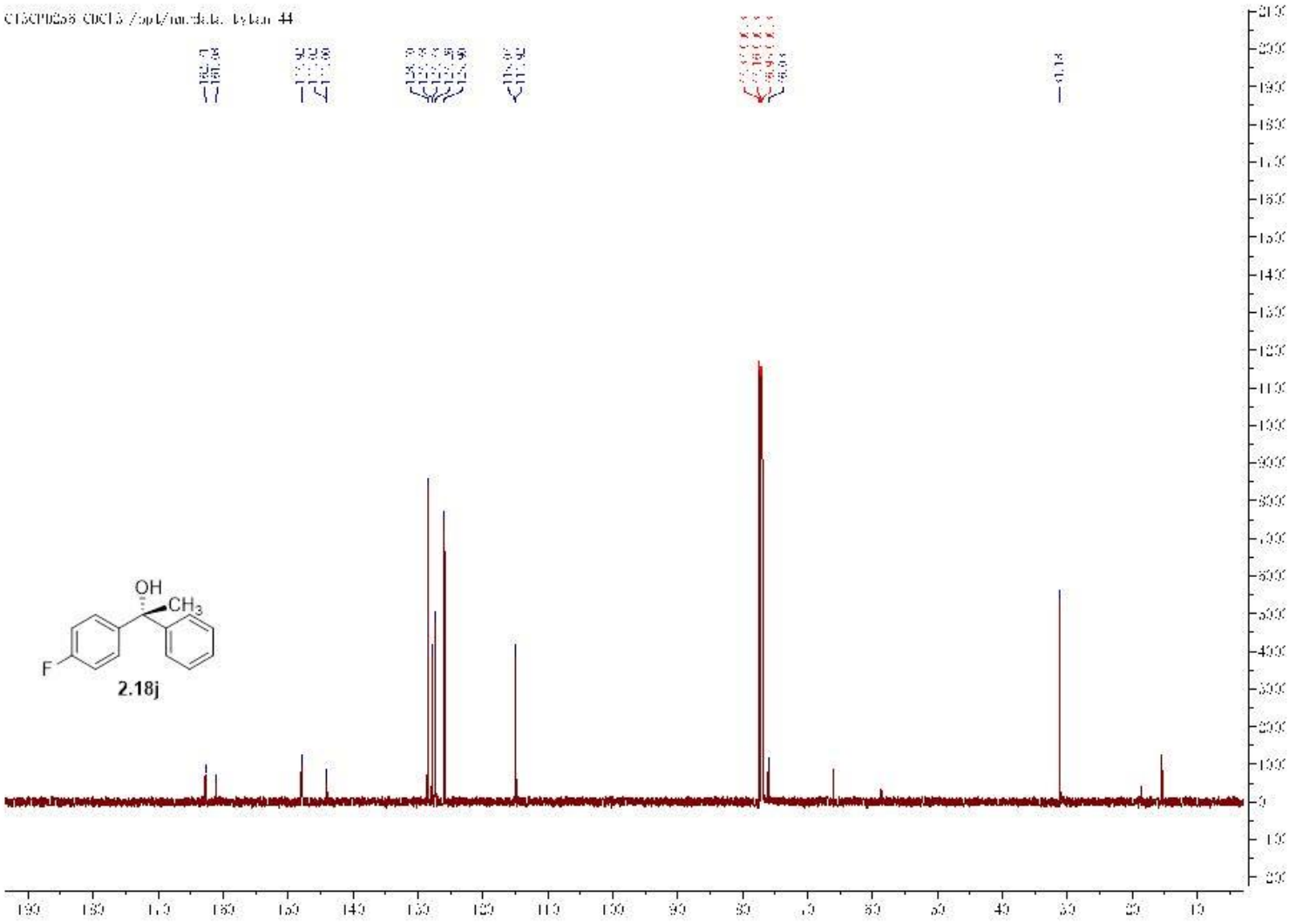
OH
CH3
F
2.18j

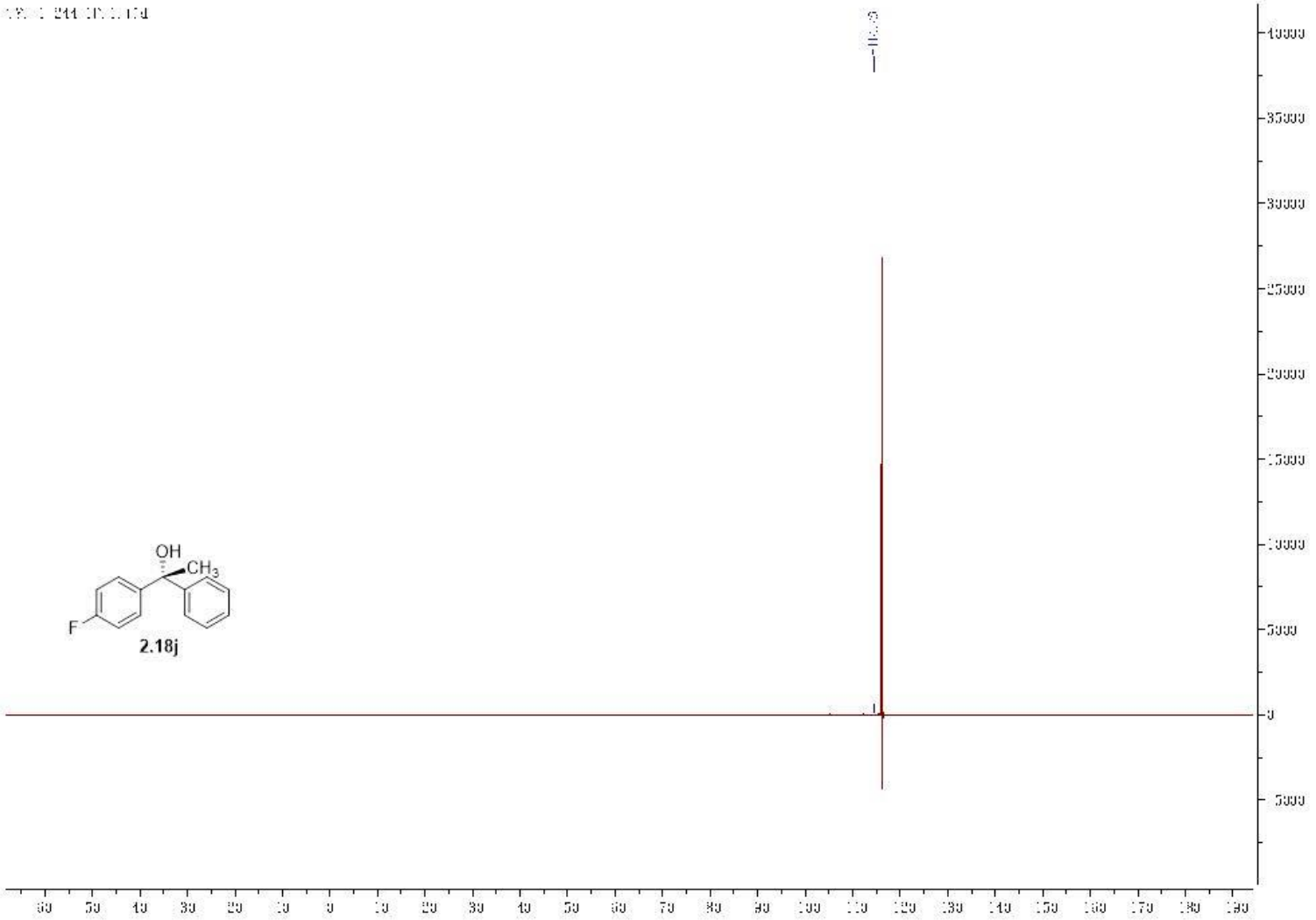
OH
CH3
F
2.18j

Racemic **2.22**

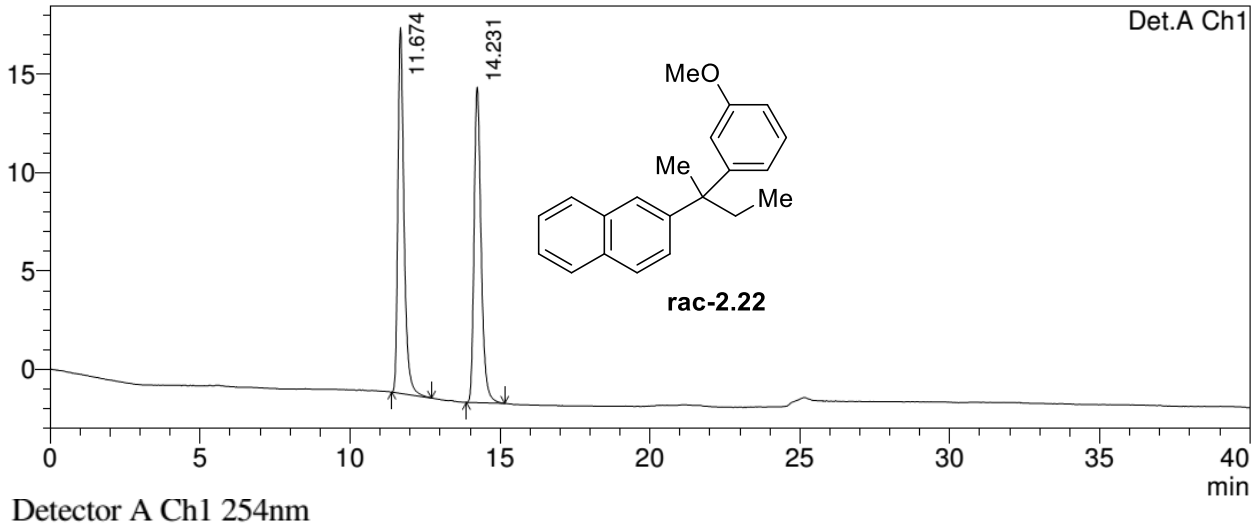

Detector A Ch1 254nm

Peak#	Ret. Time	Area	Height	Area %	Height %
1	11.674	264030	18609	50.155	53.657
2	14.231	262397	16073	49.845	46.343
Total		526427	34682	100.000	100.000

Enantioenriched **2.22**, 93% ee

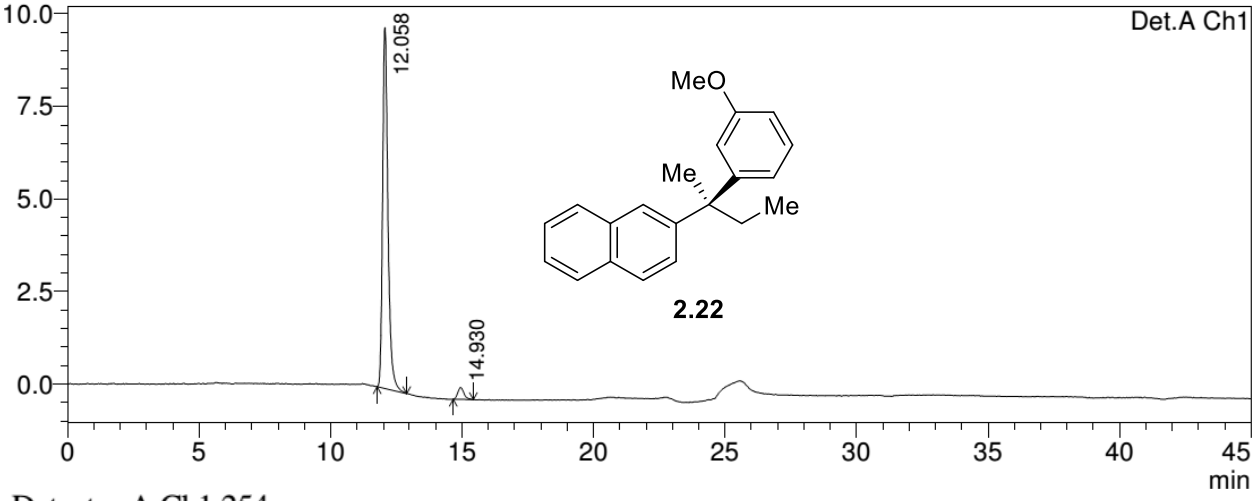

Detector A Ch1 254nm

Peak#	Ret. Time	Area	Height	Area %	Height %
1	12.058	138560	9748	96.319	96.759
2	14.930	5295	326	3.681	3.241
Total		143855	10075	100.000	100.000

Racemic **2.24**

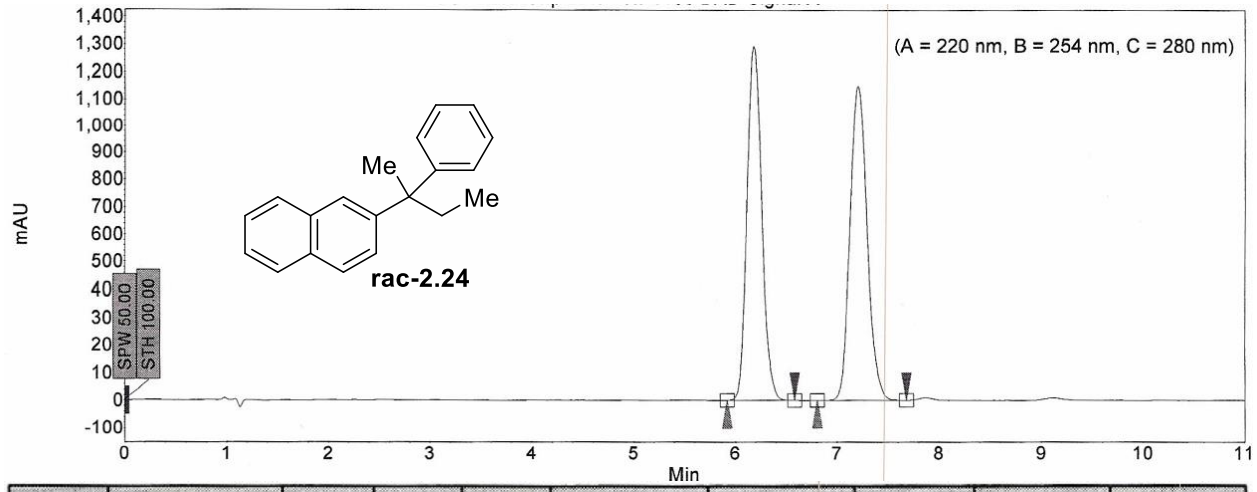

Index	Name	Start	Time	End	RT Offset	Quantity	Height	Area	Area
		[Min]	[Min]	[Min]	[Min]	[% Area]	[µV]	[µV.Min]	[%]
1	UNKNOWN	5.92	6.18	6.58	0.00	49.41	1292.6	217.5	49.413
2	UNKNOWN	6.81	7.21	7.68	0.00	50.59	1148.9	222.7	50.587
Total						100.00	2441.5	440.2	100.000

Enantioenriched **2.24**, 95% ee

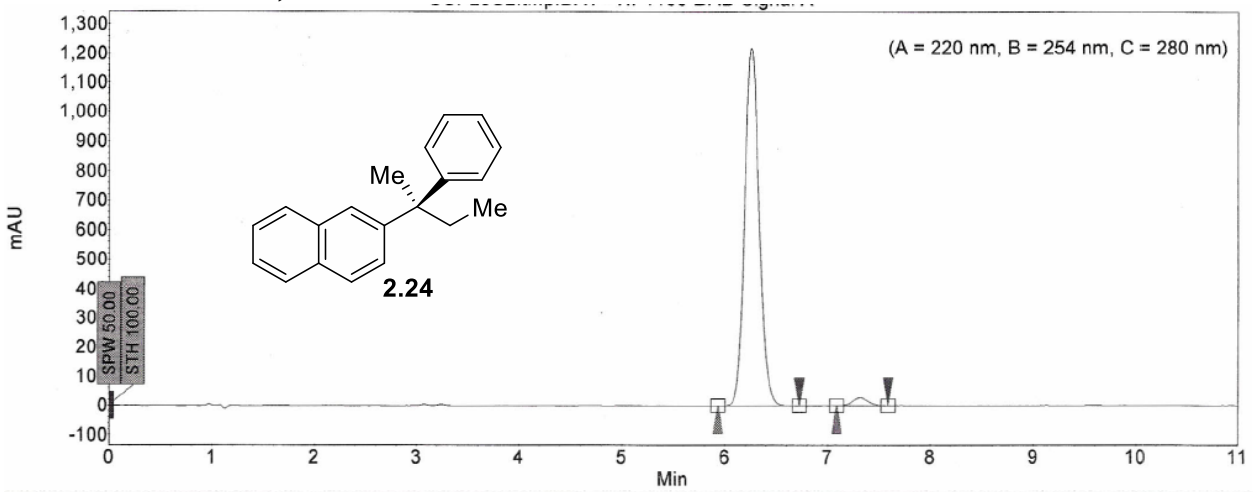

Index	Name	Start	Time	End	RT Offset	Quantity	Height	Area	Area
		[Min]	[Min]	[Min]	[Min]	[% Area]	[µV]	[µV.Min]	[%]
2	UNKNOWN	5.93	6.25	6.73	0.00	97.62	1220.1	202.1	97.625
1	UNKNOWN	7.09	7.32	7.59	0.00	2.38	27.5	4.9	2.375
Total						100.00	1247.6	207.0	100.000

Racemic **2.25**

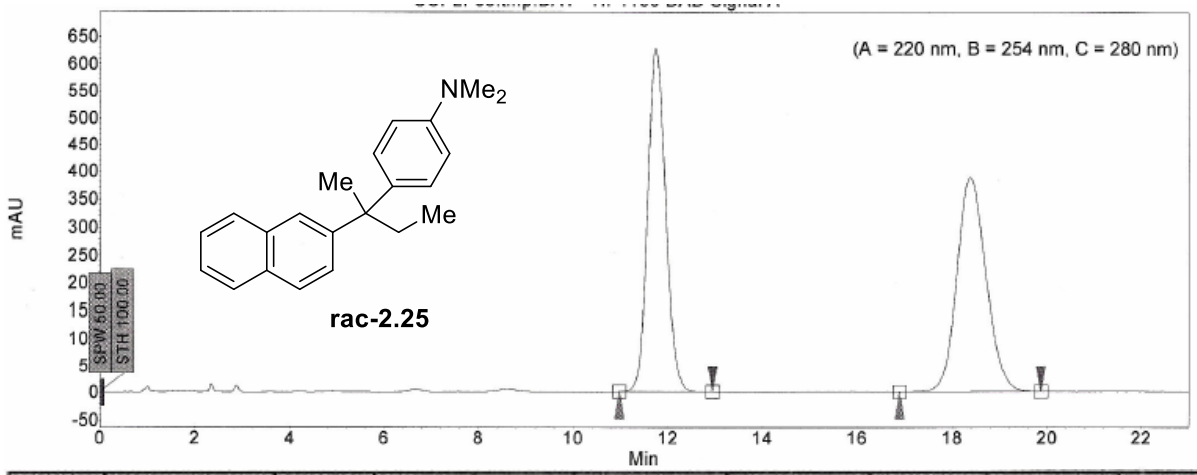

Index	Name	Start	Time	End	RT Offset	Quantity	Height	Area	Area
		[Min]	[Min]	[Min]	[Min]	[% Area]	[µV]	[µV.Min]	[%]
1	UNKNOWN	10.97	11.74	12.94	0.00	49.90	627.8	276.5	49.904
2	UNKNOWN	16.89	18.37	19.87	0.00	50.10	387.5	277.5	50.096
Total						100.00	1015.2	554.0	100.000

Enantioenriched **2.25**, 96% ee

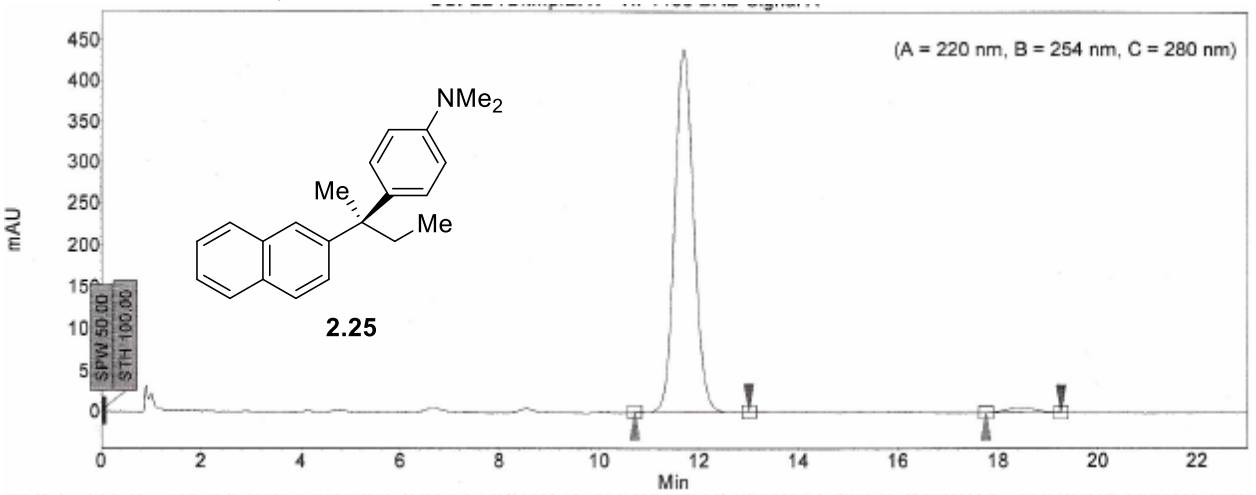

Index	Name	Start	Time	End	RT Offset	Quantity	Height	Area	Area
		[Min]	[Min]	[Min]	[Min]	[% Area]	[µV]	[µV.Min]	[%]
1	UNKNOWN	10.71	11.68	13.00	0.00	97.91	439.2	193.4	97.908
2	UNKNOWN	17.76	18.49	19.25	0.00	2.09	6.1	4.1	2.092
Total						100.00	445.4	197.5	100.000

Racemic **2.26**

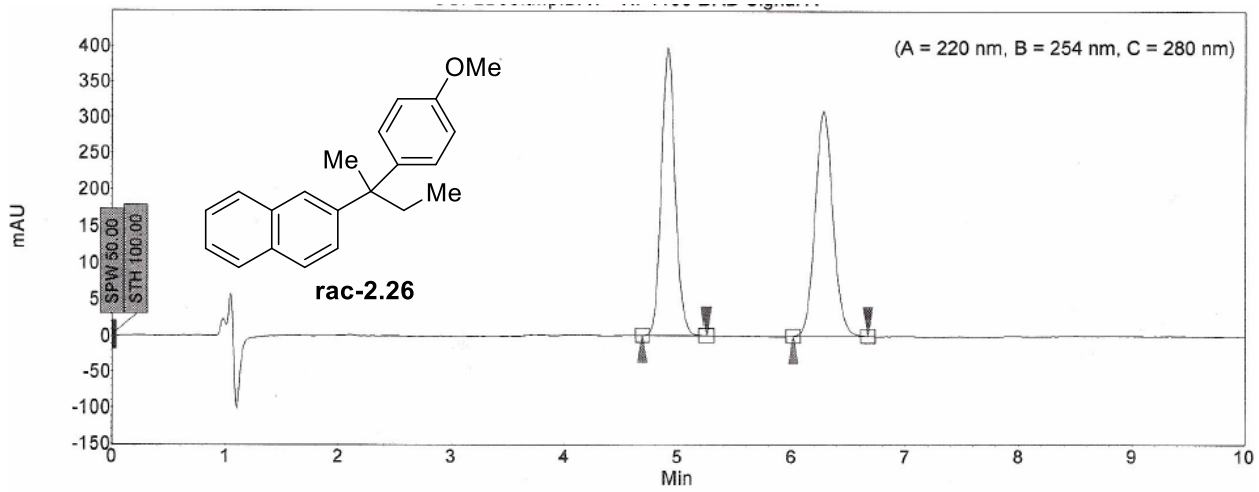

Index	Name	Start	Time	End	RT Offset	Quantity	Height	Area	Area
		[Min]	[Min]	[Min]	[Min]	[% Area]	[µV]	[µV.Min]	[%]
1	UNKNOWN	4.69	4.91	5.25	0.00	49.78	396.5	55.7	49.783
2	UNKNOWN	6.01	6.28	6.67	0.00	50.22	308.1	56.2	50.217
Total						100.00	704.6	112.0	100.000

Enantioenriched **2.26**, 96% ee

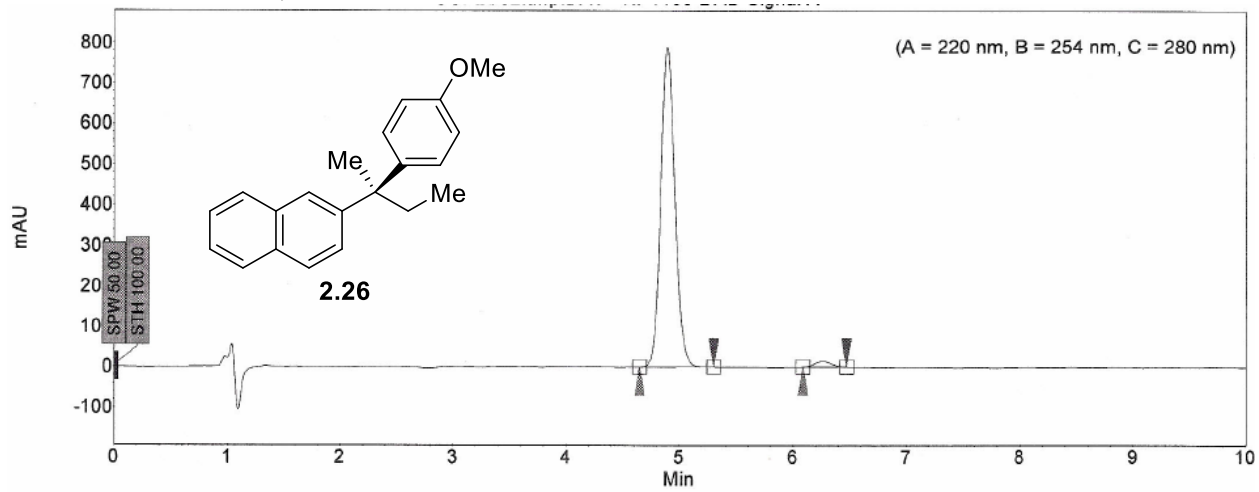

Index	Name	Start	Time	End	RT Offset	Quantity	Height	Area	Area
		[Min]	[Min]	[Min]	[Min]	[% Area]	[µV]	[µV.Min]	[%]
2	UNKNOWN	4.65	4.89	5.30	0.00	98.05	790.5	114.5	98.051
1	UNKNOWN	6.09	6.27	6.47	0.00	1.95	13.5	2.3	1.949
Total						100.00	804.0	116.8	100.000

Racemic **2.27**

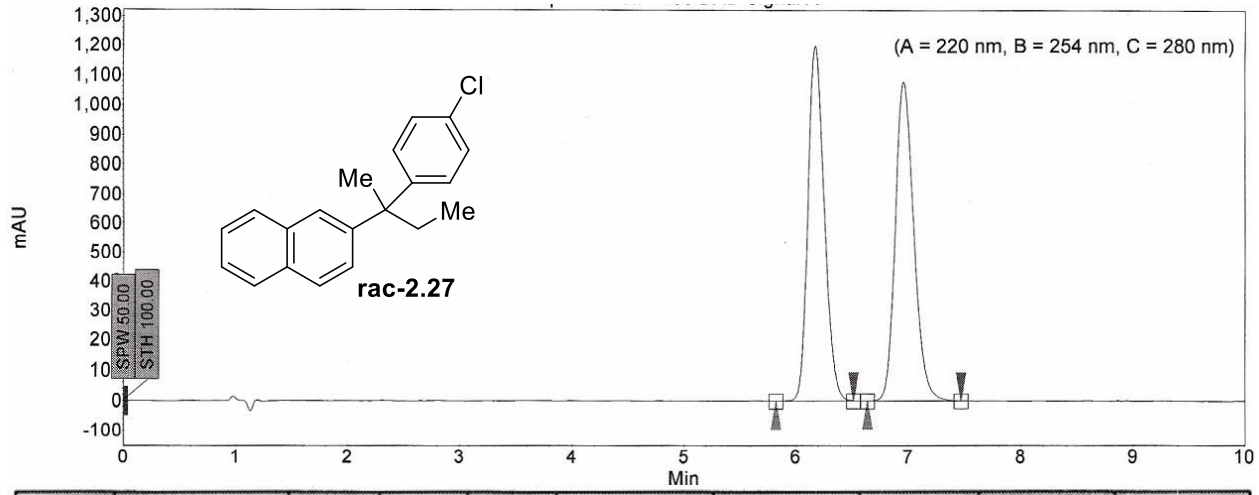

Index	Name	Start	Time	End	RT Offset	Quantity	Height	Area	Area
		[Min]	[Min]	[Min]	[Min]	[% Area]	[µV]	[µV.Min]	[%]
1	UNKNOWN	5.82	6.17	6.52	0.00	49.58	1197.4	201.8	49.580
2	UNKNOWN	6.64	6.96	7.47	0.00	50.42	1078.7	205.2	50.420
Total						100.00	2276.1	407.0	100.000

Enantioenriched **2.27**, 92% ee

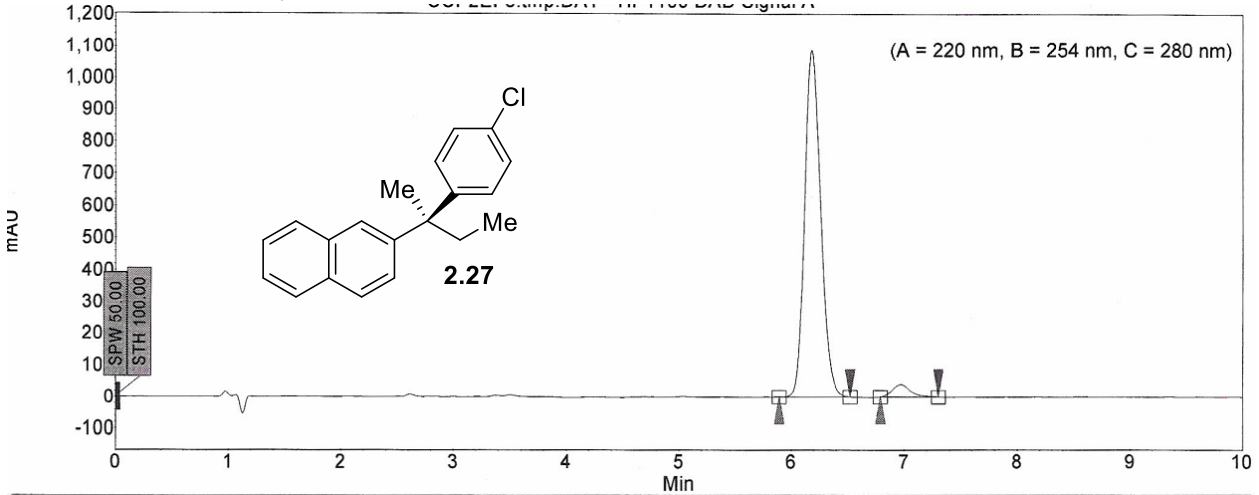

Index	Name	Start	Time	End	RT Offset	Quantity	Height	Area	Area
		[Min]	[Min]	[Min]	[Min]	[% Area]	[µV]	[µV.Min]	[%]
1	UNKNOWN	5.89	6.18	6.52	0.00	96.01	1087.1	180.0	96.009
2	UNKNOWN	6.79	6.97	7.30	0.00	3.99	41.2	7.5	3.991
Total						100.00	1128.3	187.4	100.000

Racemic **2.28**

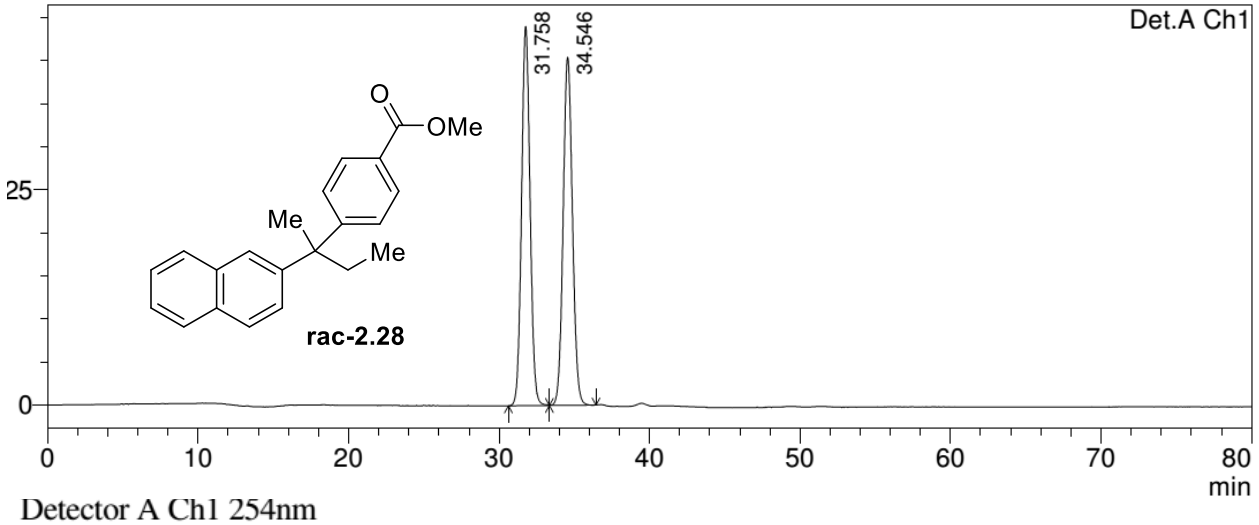

Detector A Ch1 254nm

Peak#	Ret. Time	Area	Height	Area %	Height %
1	31.758	1728236	44032	49.845	52.134
2	34.546	1738977	40427	50.155	47.866
Total		3467213	84459	100.000	100.000

Enantioenriched **2.28**, 96% ee

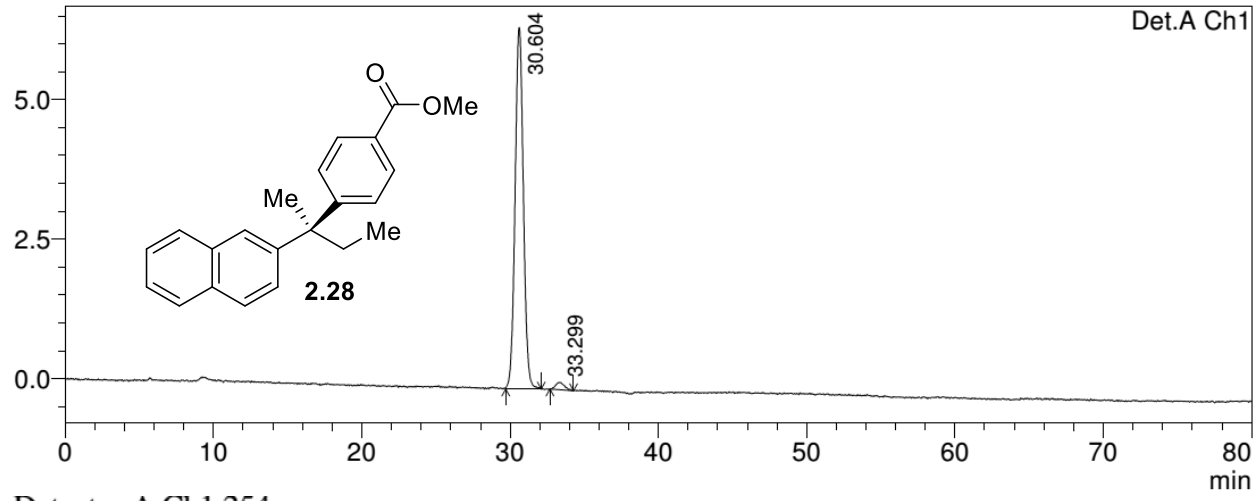

Detector A Ch1 254nm

Peak#	Ret. Time	Area	Height	Area %	Height %
1	30.604	251321	6477	97.885	98.017
2	33.299	5430	131	2.115	1.983
Total		256751	6608	100.000	100.000

Racemic **2.29**

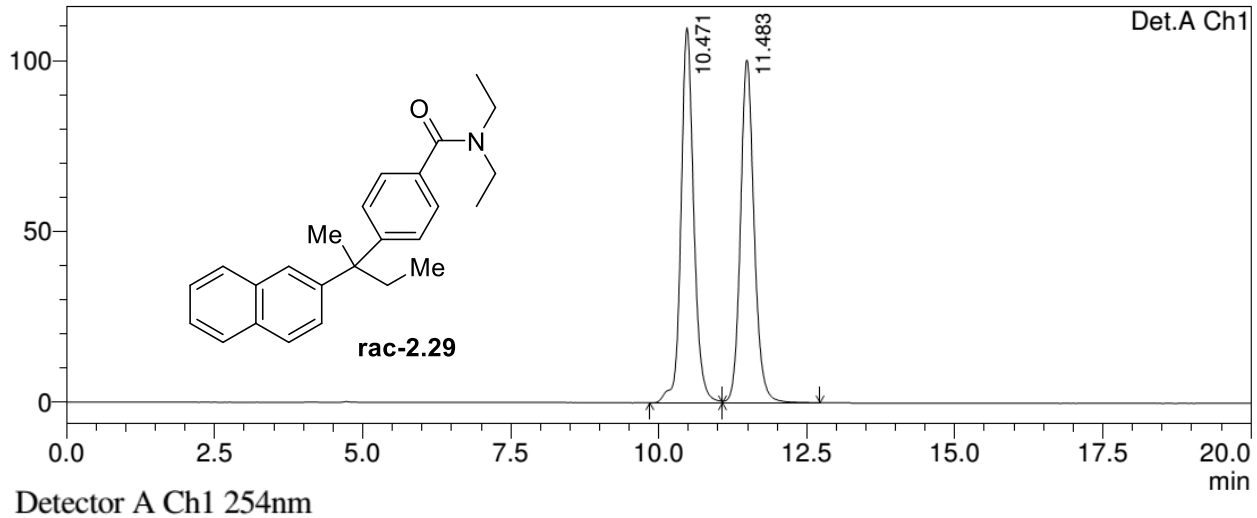

Detector A Ch1 254nm

Peak#	Ret. Time	Area	Height	Area %	Height %
1	10.471	1653101	109872	50.507	52.247
2	11.483	1619926	100424	49.493	47.753
Total		3273026	210296	100.000	100.000

Enantioenriched **2.29**, 94% ee

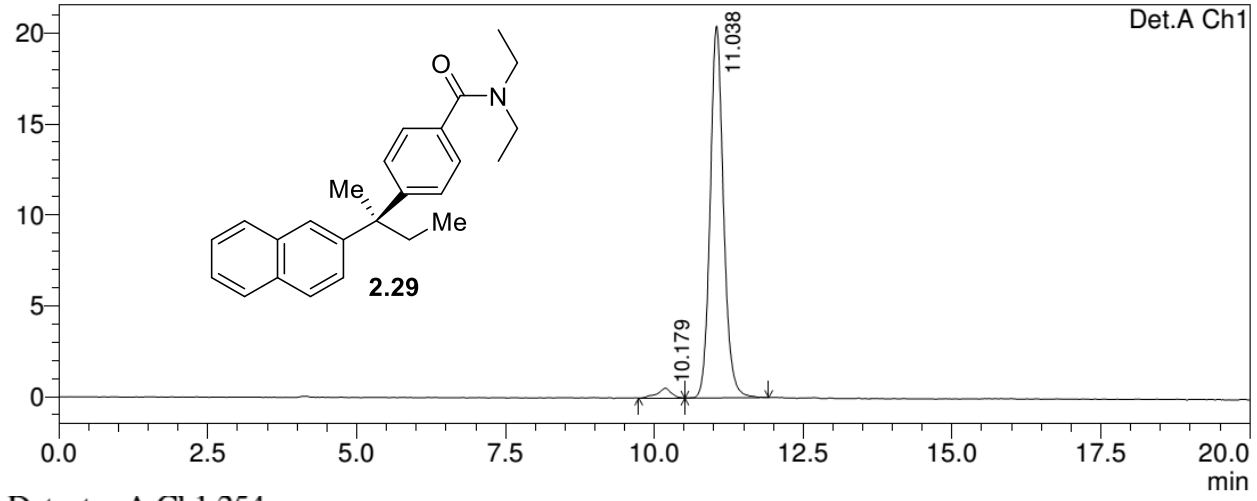

Detector A Ch1 254nm

Peak#	Ret. Time	Area	Height	Area %	Height %
1	10.179	9333	548	2.832	2.609
2	11.038	320214	20472	97.168	97.391
Total		329548	21021	100.000	100.000

Enantioenriched (*R*)-**2.29**, 96% ee (crystal used for X-ray diffraction analysis)

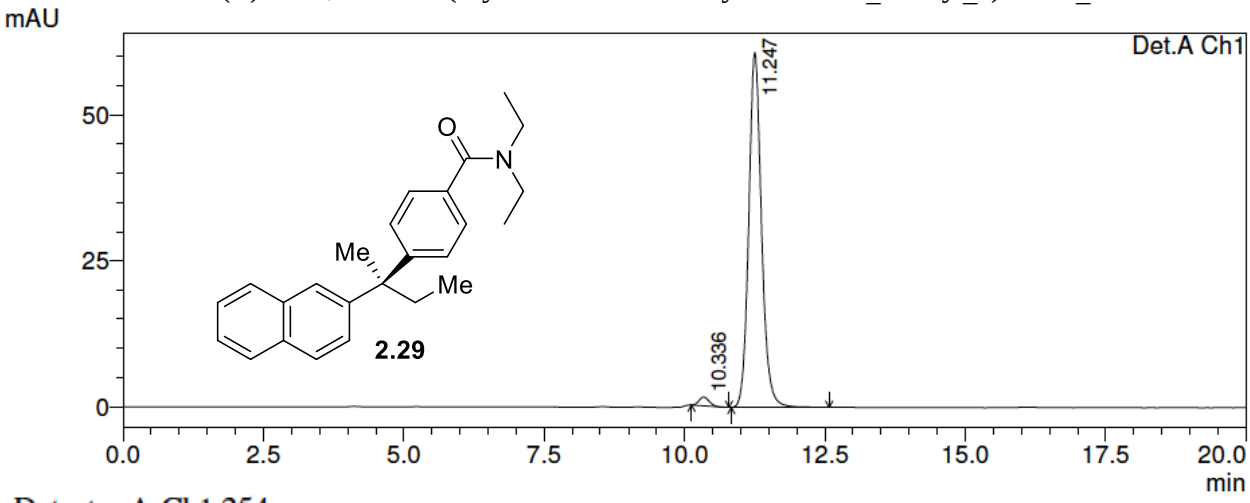

Detector A Ch1 254nm

Peak#	Ret. Time	Area	Height	Area %	Height %
1	10.336	17968	1480	1.829	2.376
2	11.247	964530	60841	98.171	97.624
Total		982498	62321	100.000	100.000

Racemic **2.30**

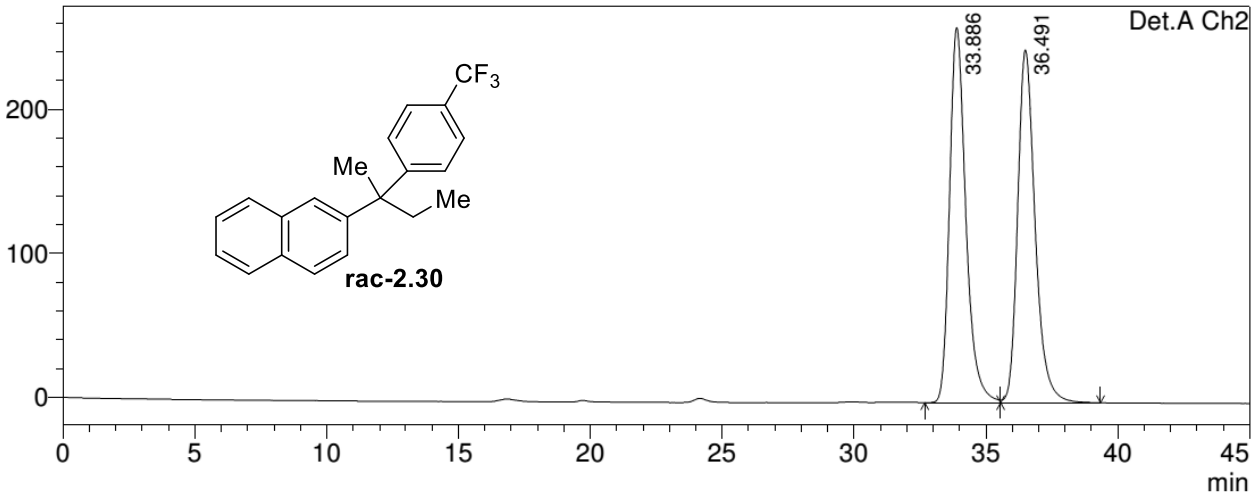

Detector A Ch1 254nm

Peak#	Ret. Time	Area	Height	Area %	Height %
1	33.885	1587788	36919	49.856	51.534
2	36.489	1596950	34721	50.144	48.466
Total		3184738	71640	100.000	100.000

Enantioenriched **2.30**, 96% ee

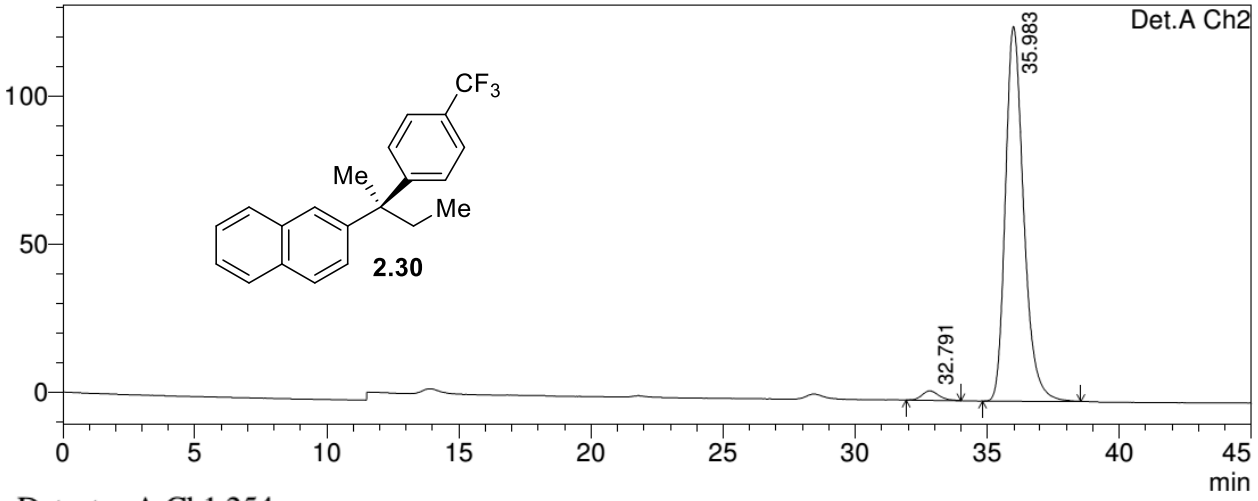

Detector A Ch1 254nm

Peak#	Ret. Time	Area	Height	Area %	Height %
1	35.980	18779	442	2.148	2.424
2	39.173	855635	17798	97.852	97.576
Total		874414	18241	100.000	100.000

Racemic **2.31**

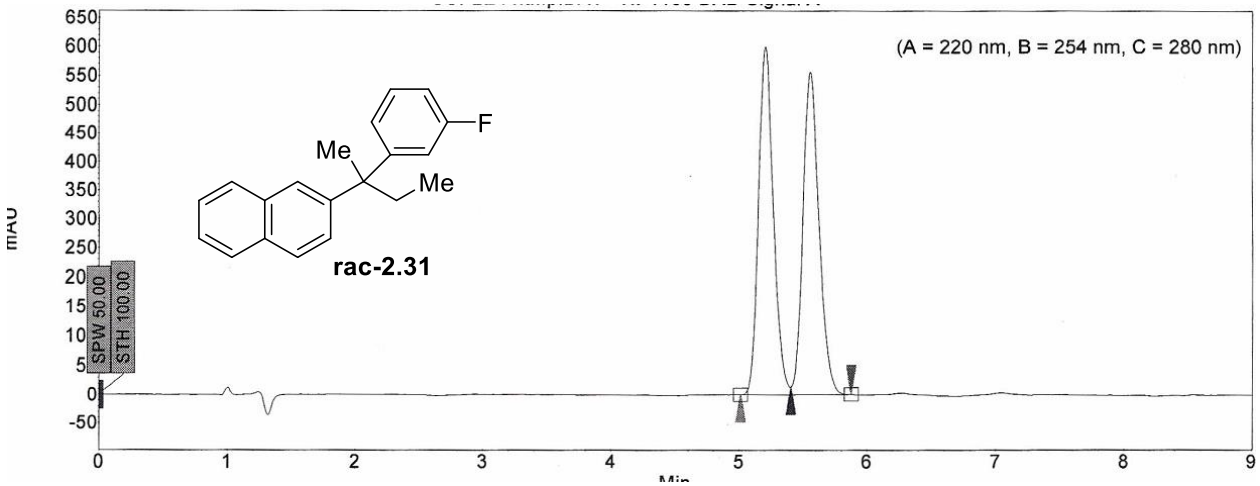

Index	Name	Start	Time	End	RT Offset	Quantity	Height	Area	Area
		[Min]	[Min]	[Min]	[Min]	[% Area]	[µV]	[µV.Min]	[%]
1	UNKNOWN	5.01	5.21	5.41	0.00	49.95	599.1	80.3	49.946
2	UNKNOWN	5.41	5.55	5.88	0.00	50.05	555.9	80.5	50.054
Total						100.00	1155.0	160.8	100.000

Enantioenriched **2.31**, 94% ee

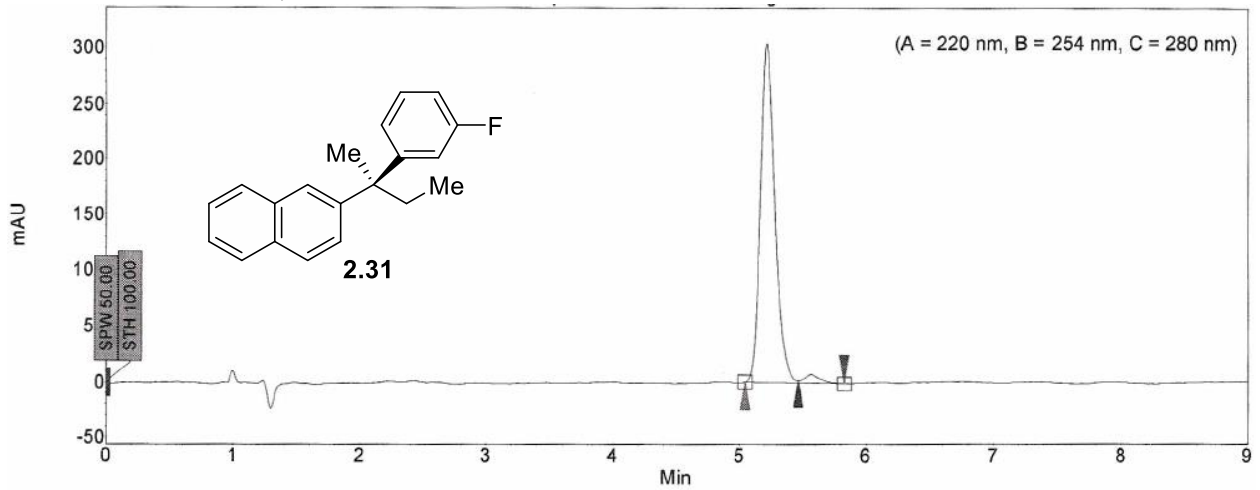

Index	Name	Start	Time	End	RT Offset	Quantity	Height	Area	Area
		[Min]	[Min]	[Min]	[Min]	[% Area]	[µV]	[µV.Min]	[%]
1	UNKNOWN	5.05	5.22	5.47	0.00	97.13	303.5	40.2	97.132
2	UNKNOWN	5.47	5.57	5.83	0.00	2.87	7.8	1.2	2.868
Total						100.00	311.3	41.4	100.000

Racemic **2.32**

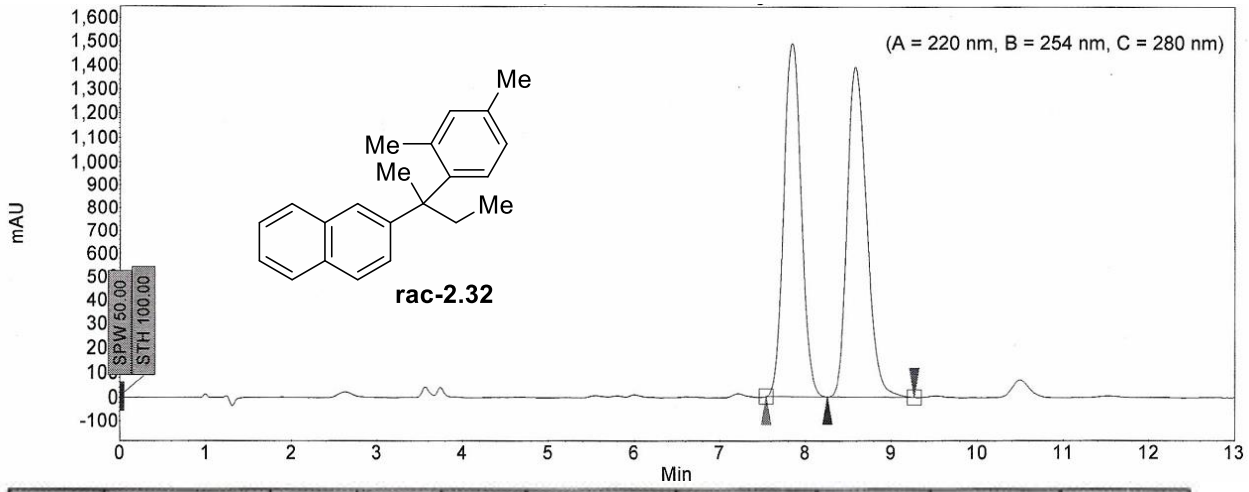

Index	Name	Start	Time	End	RT Offset	Quantity	Height	Area	Area
		[Min]	[Min]	[Min]	[Min]	[% Area]	[µV]	[µV.Min]	[%]
1	UNKNOWN	7.55	7.85	8.26	0.00	49.14	1491.2	352.2	49.145
2	UNKNOWN	8.26	8.59	9.27	0.00	50.86	1391.4	364.5	50.855
Total						100.00	2882.6	716.8	100.000

Enantioenriched **2.32**, 95% ee

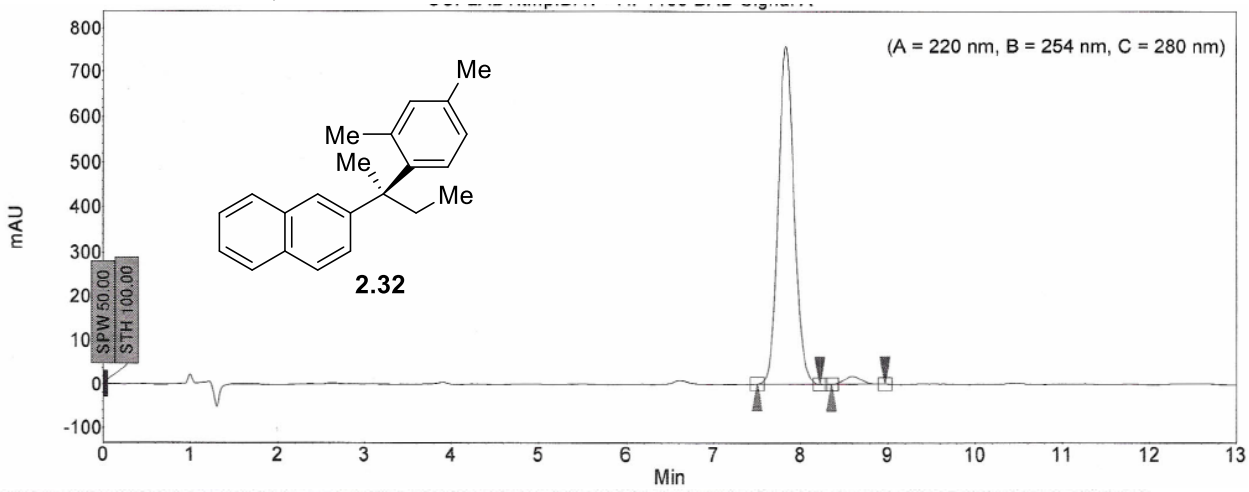

Index	Name	Start	Time	End	RT Offset	Quantity	Height	Area	Area
		[Min]	[Min]	[Min]	[Min]	[% Area]	[µV]	[µV.Min]	[%]
1	UNKNOWN	7.50	7.83	8.22	0.00	97.52	758.0	161.1	97.517
2	UNKNOWN	8.36	8.59	8.97	0.00	2.48	18.4	4.1	2.483
Total						100.00	776.4	165.2	100.000

Racemic **2.33**

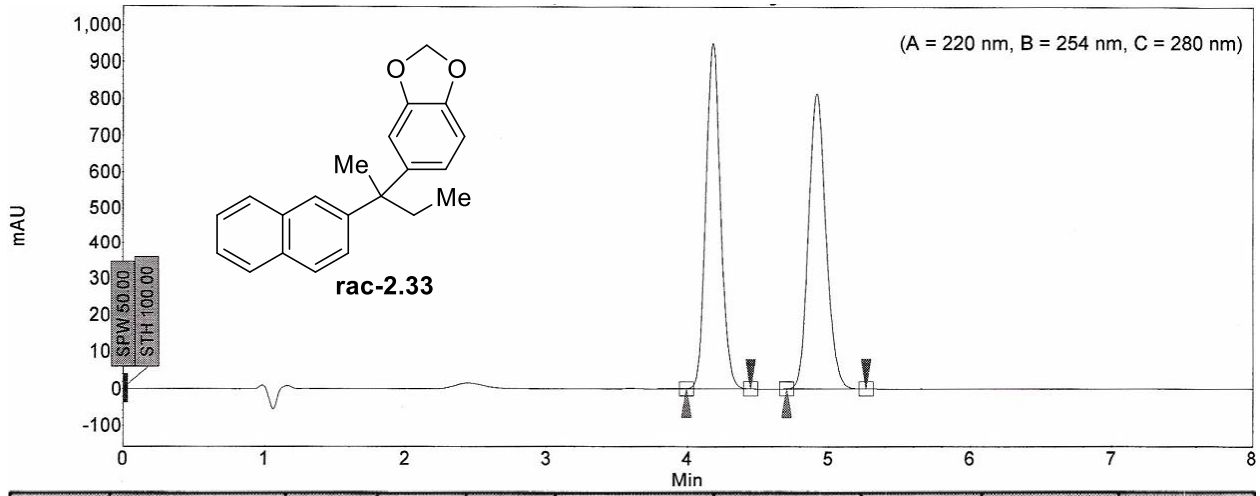

Index	Name	Start	Time	End	RT Offset	Quantity	Height	Area	Area
		[Min]	[Min]	[Min]	[Min]	[% Area]	[µV]	[µV.Min]	[%]
1	UNKNOWN	3.99	4.18	4.45	0.00	49.67	950.2	114.9	49.670
2	UNKNOWN	4.70	4.91	5.27	0.00	50.33	814.4	116.4	50.330
Total						100.00	1764.6	231.2	100.000

Enantioenriched **2.33**, 92% ee

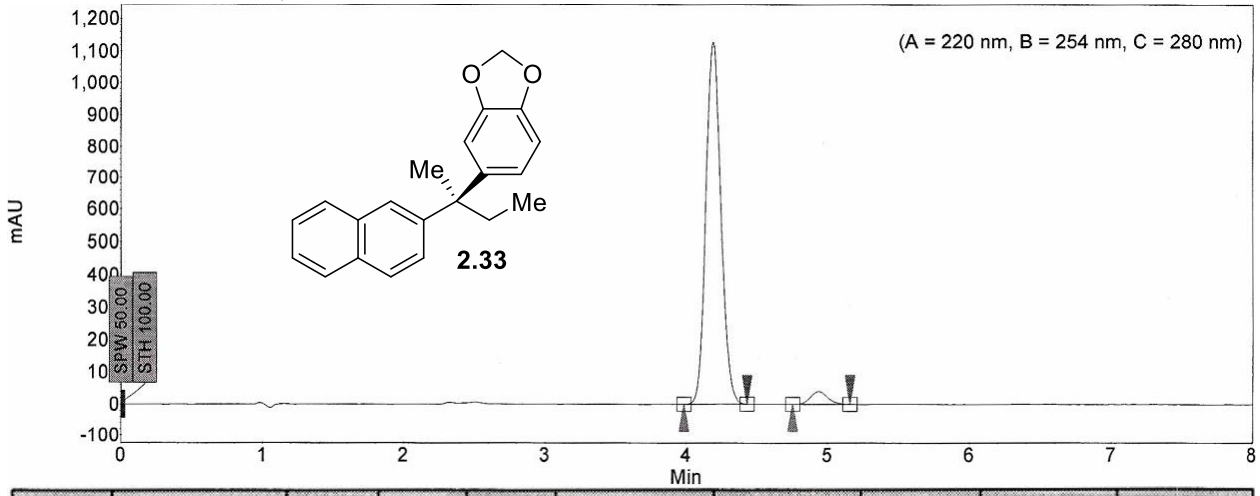

Index	Name	Start	Time	End	RT Offset	Quantity	Height	Area	Area
		[Min]	[Min]	[Min]	[Min]	[% Area]	[µV]	[µV.Min]	[%]
1	UNKNOWN	3.98	4.19	4.43	0.00	96.07	1130.0	139.5	96.066
2	UNKNOWN	4.75	4.93	5.16	0.00	3.93	41.1	5.7	3.934
Total						100.00	1171.2	145.2	100.000

Racemic **2.34**

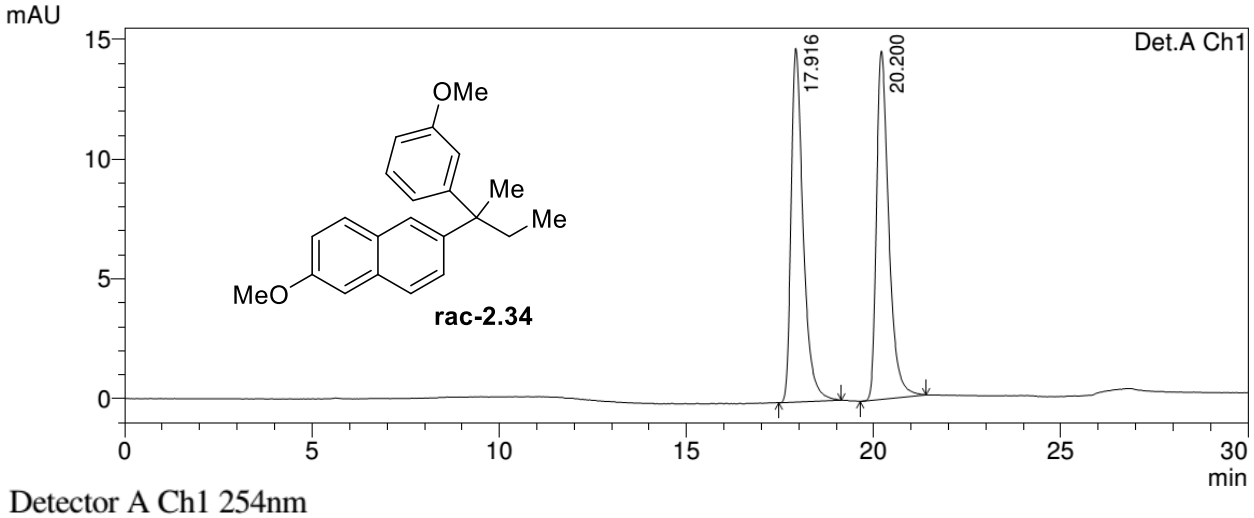

Detector A Ch1 254nm

Peak#	Ret. Time	Area	Height	Area %	Height %
1	17.916	330741	14782	49.859	50.395
2	20.200	332617	14550	50.141	49.605
Total		663357	29332	100.000	100.000

Enantioenriched **2.34**, 90% ee

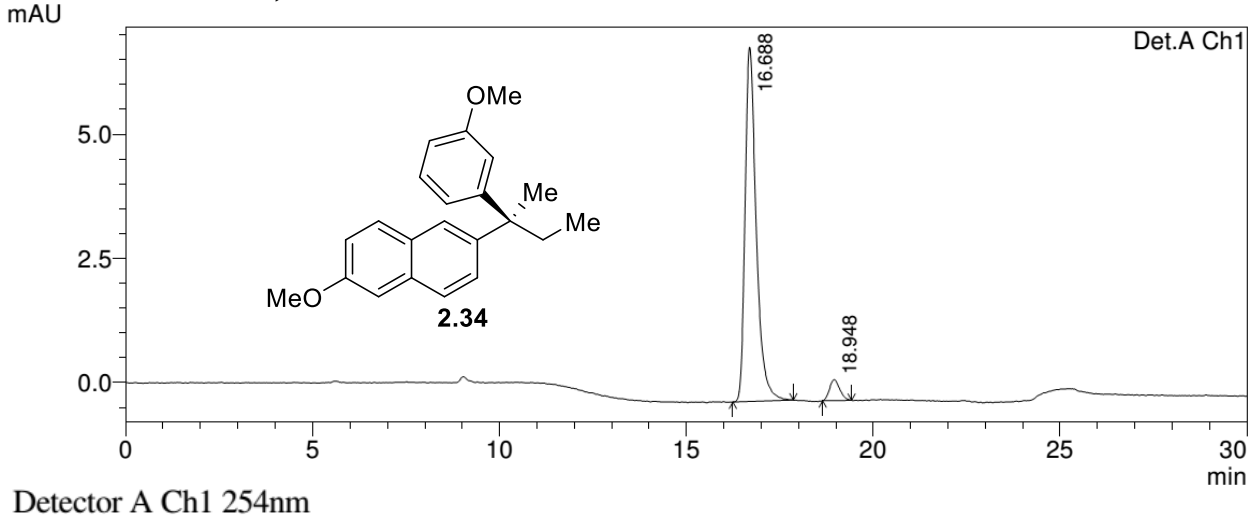

Detector A Ch1 254nm

Peak#	Ret. Time	Area	Height	Area %	Height %
1	16.688	147777	7132	94.789	94.386
2	18.948	8124	424	5.211	5.614
Total		155901	7556	100.000	100.000

Racemic **2.35**

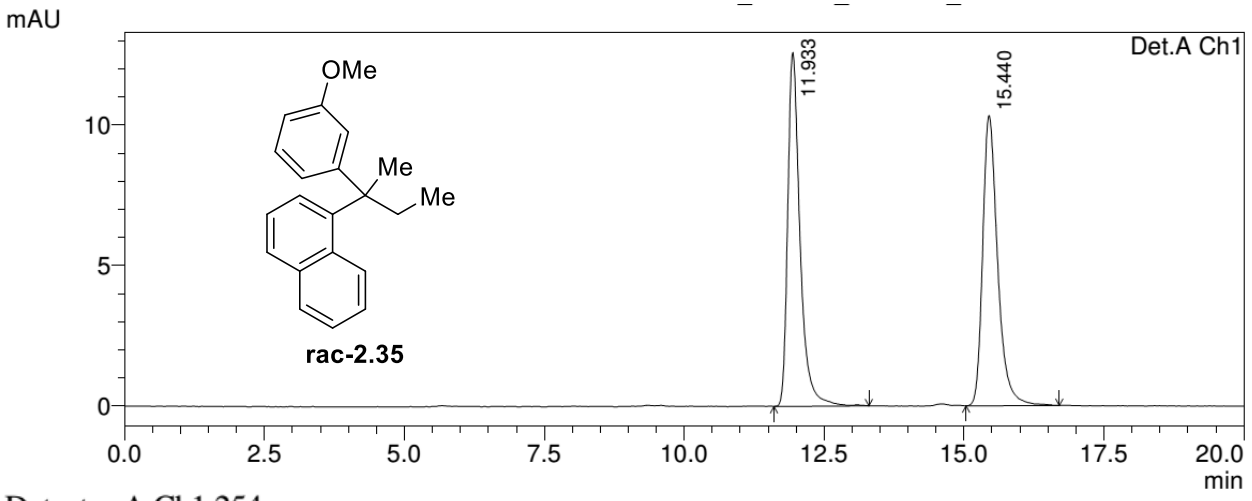

Detector A Ch1 254nm

Peak#	Ret. Time	Area	Height	Area %	Height %
1	11.933	192477	12599	50.018	54.934
2	15.440	192342	10336	49.982	45.066
Total		384819	22934	100.000	100.000

Enantioenriched **2.35**, 88% ee

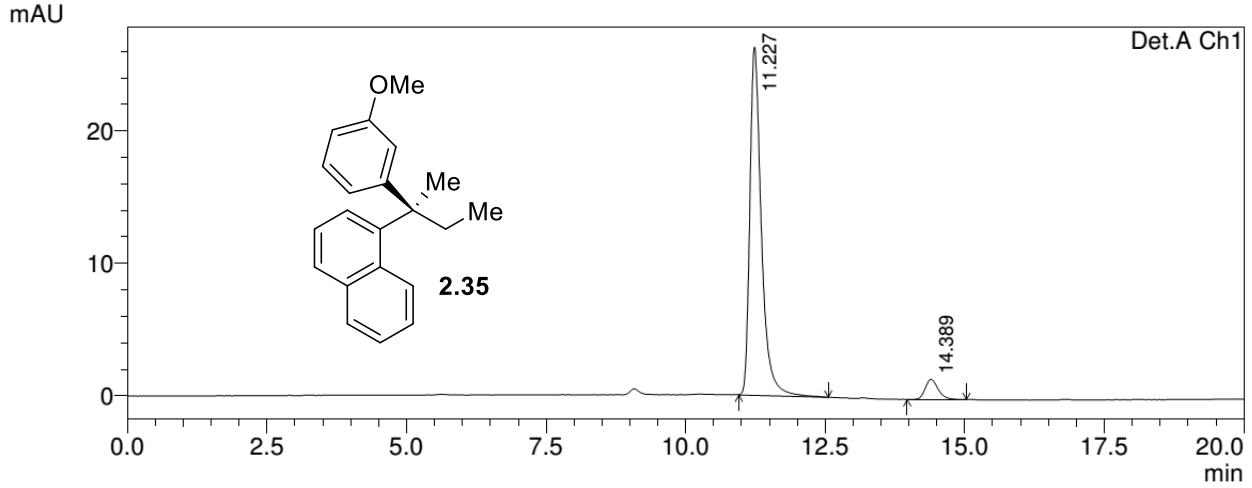

Detector A Ch1 254nm

Peak#	Ret. Time	Area	Height	Area %	Height %
1	11.227	378067	26292	93.832	94.517
2	14.389	24853	1525	6.168	5.483
Total		402920	27817	100.000	100.000

Racemic **2.36**

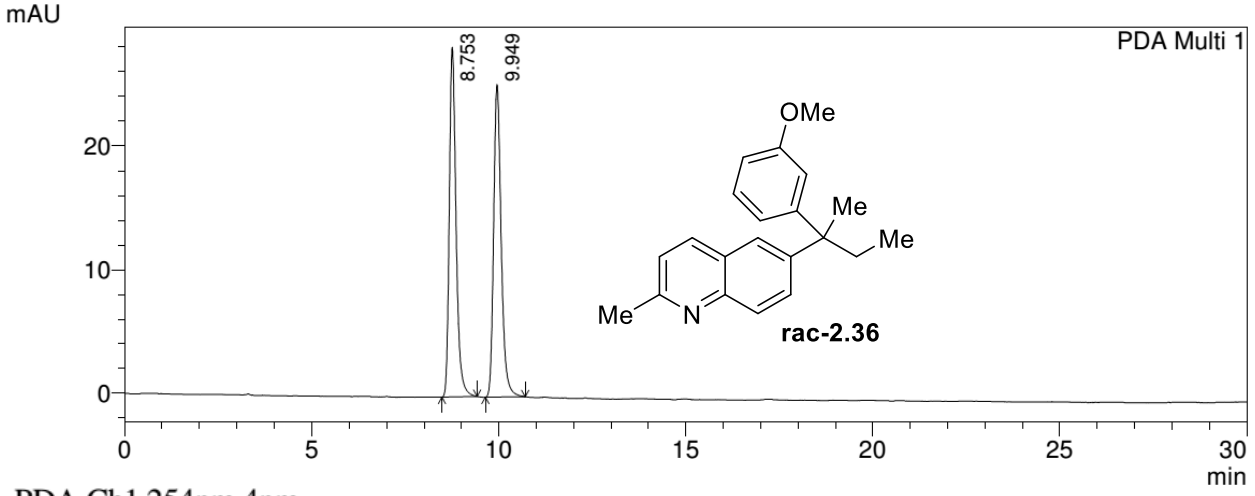

PDA Ch1 254nm 4nm

Peak#	Ret. Time	Area	Height	Area %	Height %
1	8.753	355326	28276	50.038	52.795
2	9.949	354785	25282	49.962	47.205
Total		710111	53557	100.000	100.000

Enantioenriched **2.36**, 97% ee

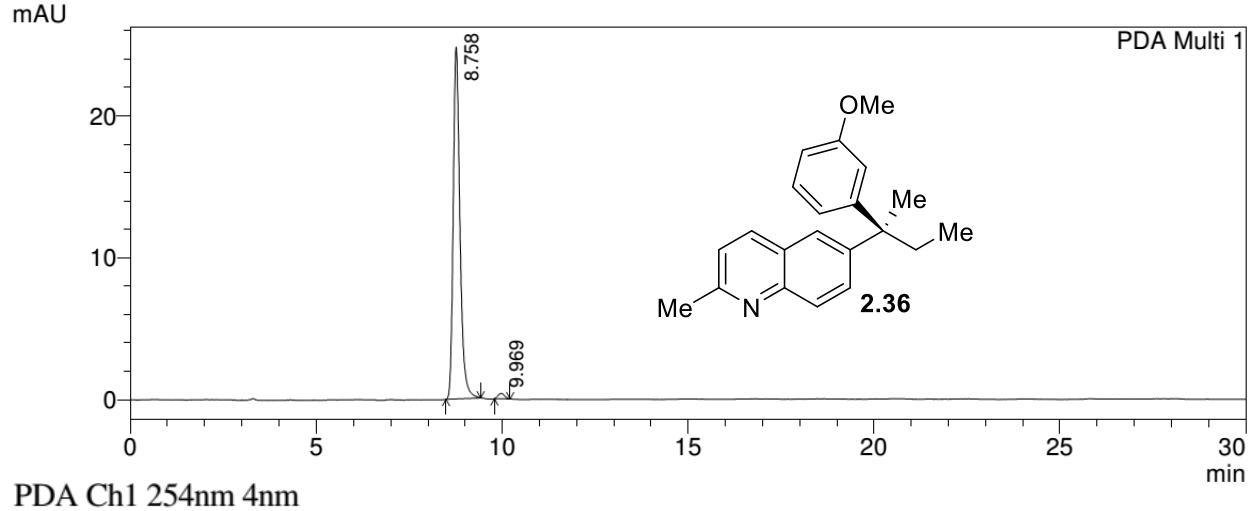

PDA Ch1 254nm 4nm

Peak#	Ret. Time	Area	Height	Area %	Height %
1	8.758	310956	24796	98.496	98.455
2	9.969	4747	389	1.504	1.545
Total		315703	25185	100.000	100.000

Racemic **2.37**

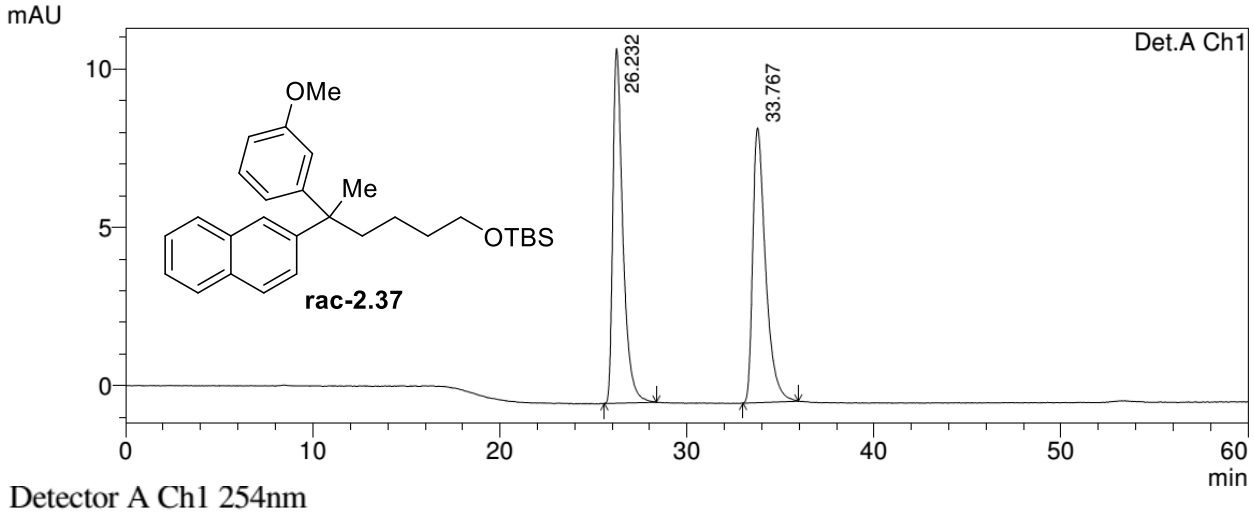

Detector A Ch1 254nm

Peak#	Ret. Time	Area	Height	Area %	Height %
1	26.232	416026	11202	50.139	56.329
2	33.767	413712	8684	49.861	43.671
Total		829738	19886	100.000	100.000

Enantioenriched **2.37**, 99% ee

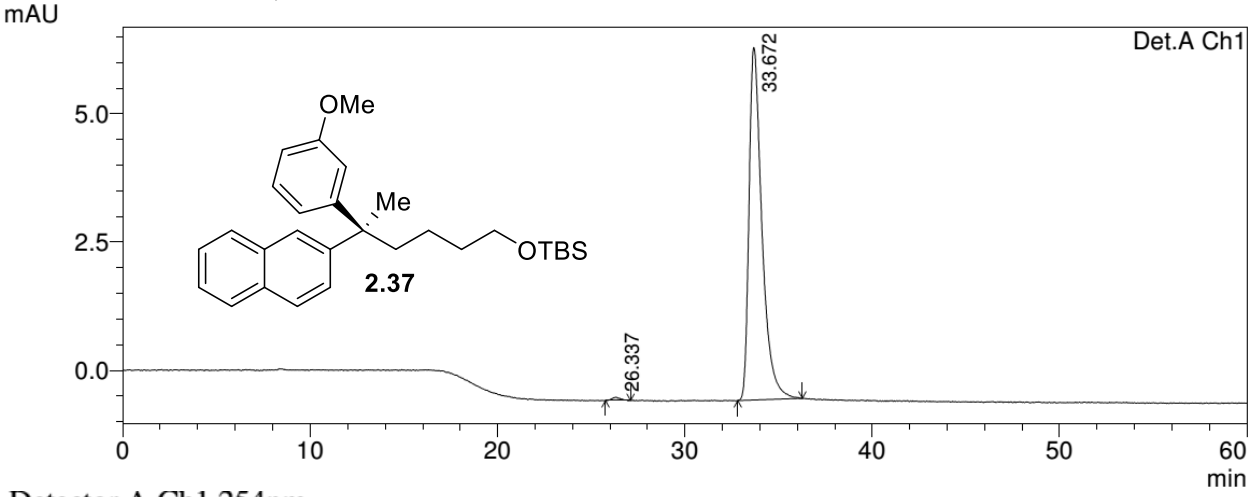

Detector A Ch1 254nm

Peak#	Ret. Time	Area	Height	Area %	Height %
1	26.337	2073	64	0.625	0.925
2	33.672	329423	6878	99.375	99.075
Total		331496	6942	100.000	100.000

Racemic **2.38**

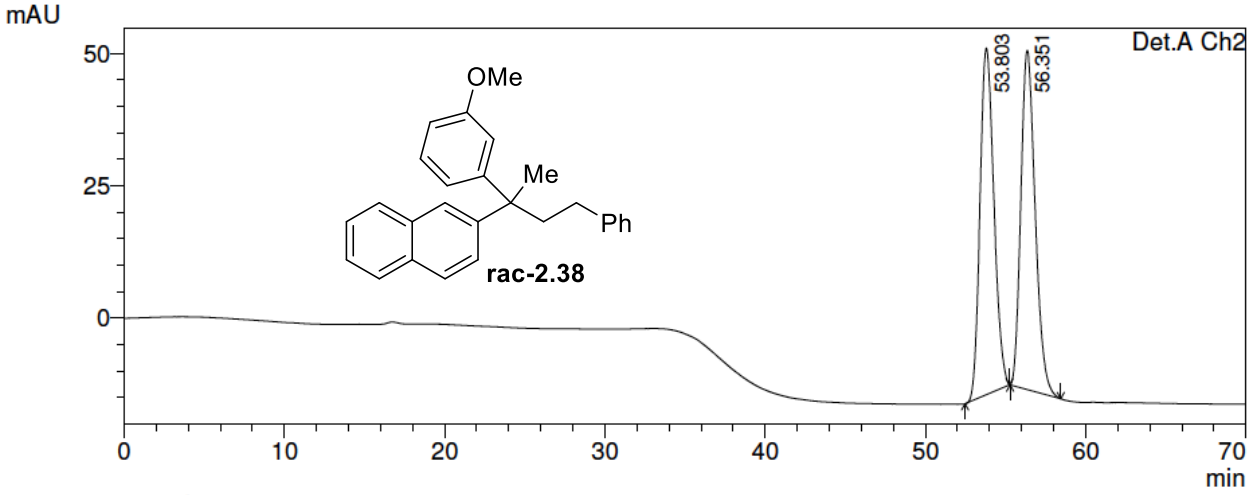

Detector A Ch2 220nm

Peak#	Ret. Time	Area	Height	Area %	Height %
1	53.803	3938543	65377	49.786	50.537
2	56.351	3972469	63987	50.214	49.463
Total		7911011	129364	100.000	100.000

Enantioenriched **2.38**, 94% ee

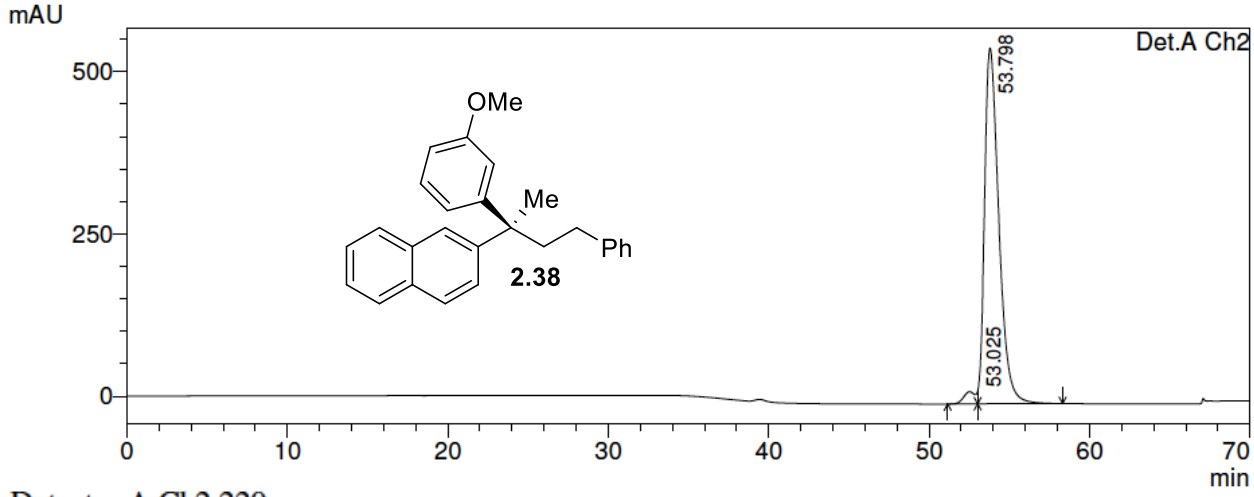

Detector A Ch2 220nm

Peak#	Ret. Time	Area	Height	Area %	Height %
1	53.025	977426	19027	2.811	3.355
2	53.798	33790474	548101	97.189	96.645
Total		34767901	567128	100.000	100.000

Racemic **2.39**

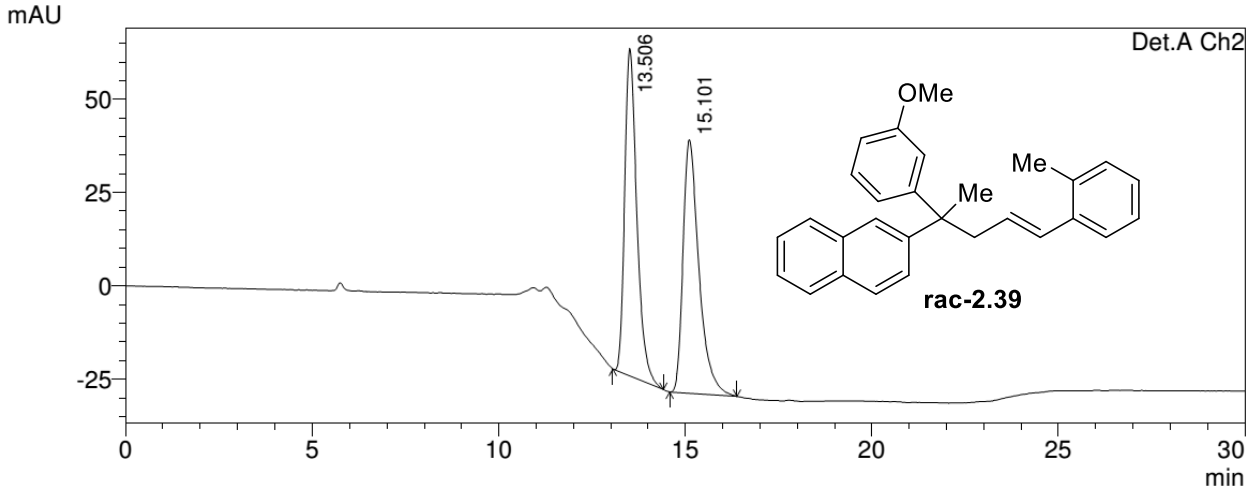

Peak#	Ret. Time	Area	Height	Area %	Height %
1	13.506	1981293	87791	49.645	56.359
2	15.101	2009656	67980	50.355	43.641
Total		3990949	155771	100.000	100.000

Enantioenriched **2.39**, 94% ee

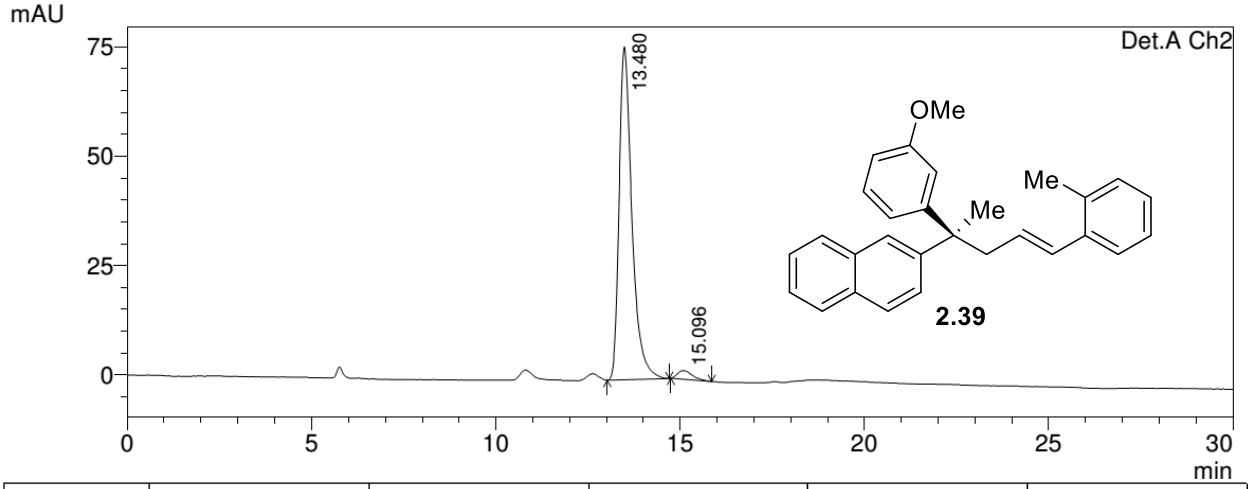

Peak#	Ret. Time	Area	Height	Area %	Height %
1	13.480	1845100	76078	97.047	97.444
2	15.096	56141	1996	2.953	2.556
Total		1901241	78073	100.000	100.000

Racemic **2.40**

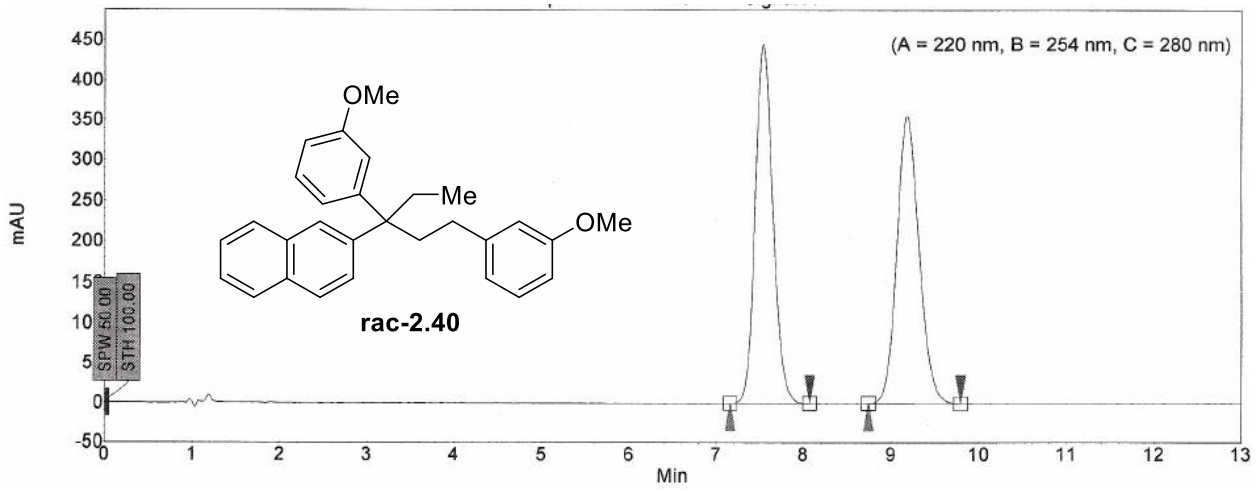

Index	Name	Start	Time	End	RT Offset	Quantity	Height	Area	Area
		[Min]	[Min]	[Min]	[Min]	[% Area]	[µV]	[µV.Min]	[%]
1	UNKNOWN	7.16	7.54	8.07	0.00	49.93	445.3	104.9	49.926
2	UNKNOWN	8.74	9.18	9.79	0.00	50.07	356.0	105.2	50.074
Total						100.00	801.3	210.1	100.000

Enantioenriched **2.40**, 87% ee

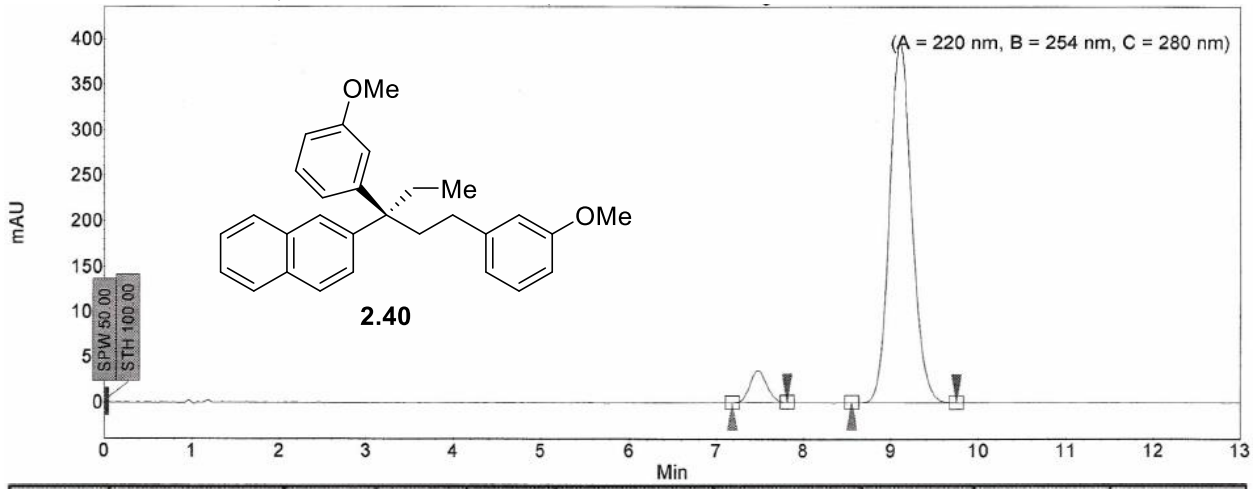

Index	Name	Start	Time	End	RT Offset	Quantity	Height	Area	Area
		[Min]	[Min]	[Min]	[Min]	[% Area]	[µV]	[µV.Min]	[%]
1	UNKNOWN	7.18	7.48	7.81	0.00	6.28	34.8	7.8	6.282
2	UNKNOWN	8.55	9.10	9.75	0.00	93.72	396.5	116.7	93.718
Total						100.00	431.3	124.6	100.000

Racemic **2.41**

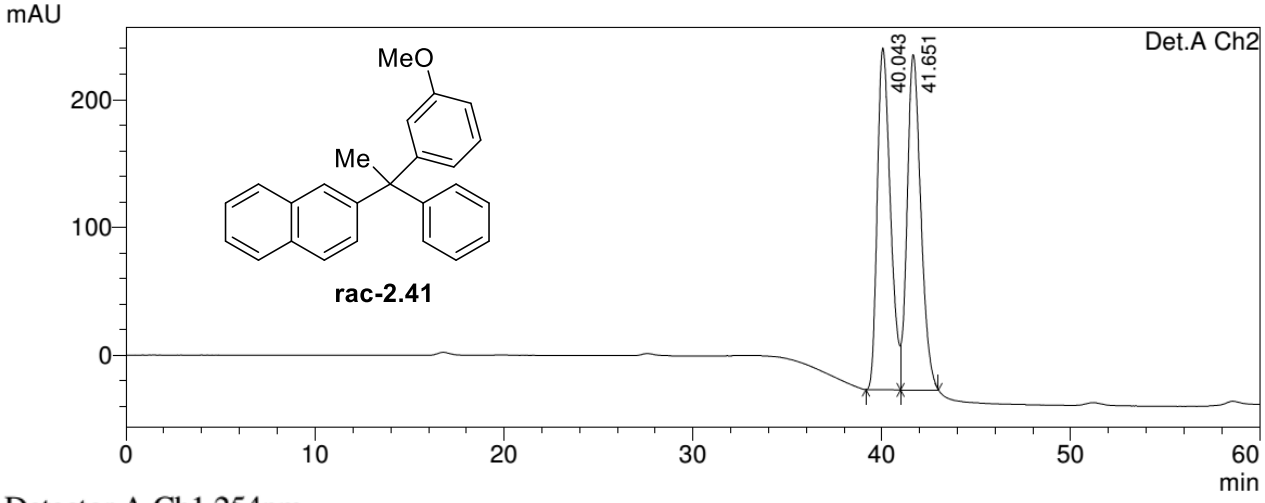

Detector A Ch1 254nm

Peak#	Ret. Time	Area	Height	Area %	Height %
1	40.045	1348999	27748	49.573	50.539
2	41.650	1372253	27157	50.427	49.461
Total		2721252	54905	100.000	100.000

Enantioenriched **2.41,** 94% ee

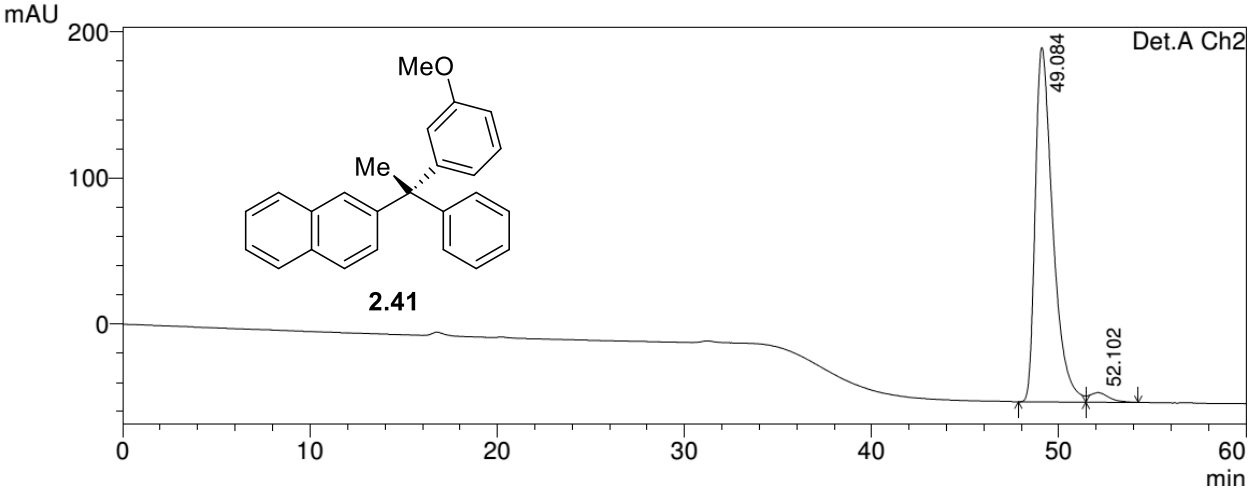

Detector A Ch2 210nm

Peak#	Ret. Time	Area	Height	Area %	Height %
1	49.084	15876695	242733	97.073	97.378
2	52.102	478750	6535	2.927	2.622
Total		16355444	249267	100.000	100.000

Racemic **2.42**

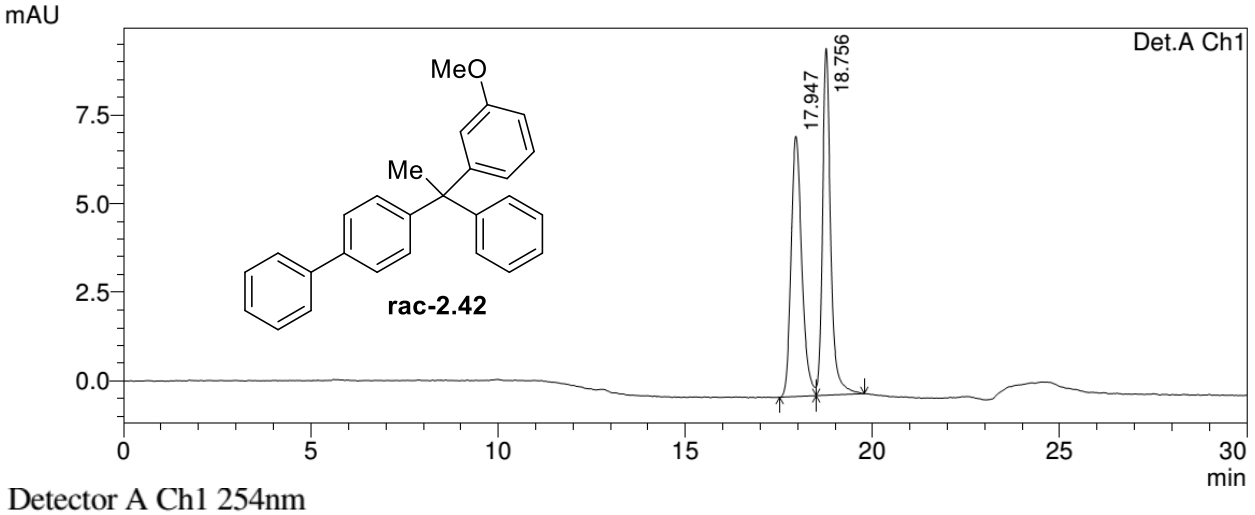

Detector A Ch1 254nm

Peak#	Ret. Time	Area	Height	Area %	Height %
1	17.947	146239	7340	49.779	42.872
2	18.756	147539	9781	50.221	57.128
Total		293778	17120	100.000	100.000

Enantioenriched **2.42**, 91% ee

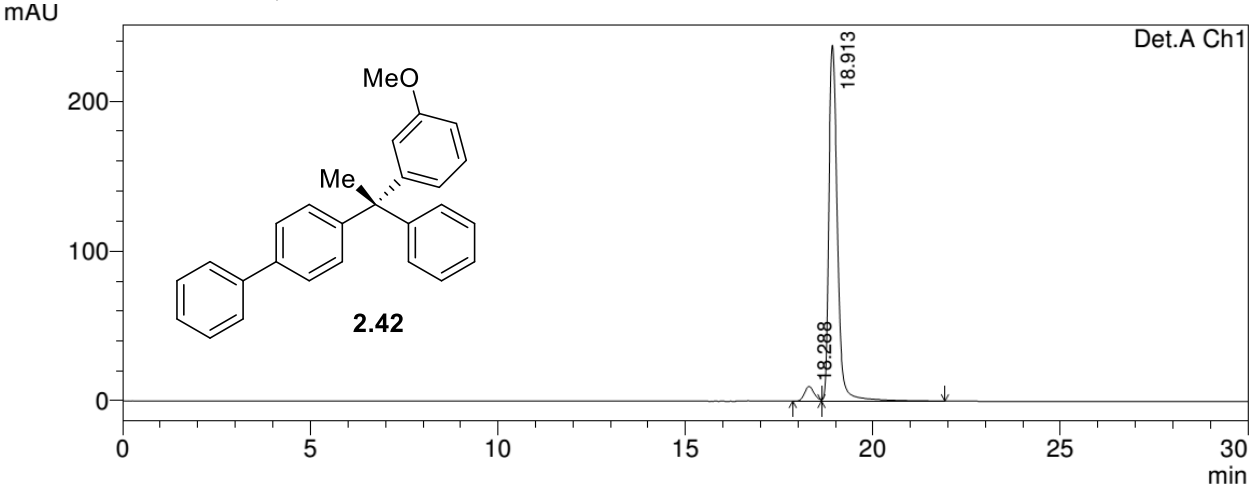

Detector A Ch1 254nm

Peak#	Ret. Time	Area	Height	Area %	Height %
1	18.288	179299	9861	4.531	3.984
2	18.913	3777644	237657	95.469	96.016
Total		3956943	247518	100.000	100.000

Racemic **2.46**

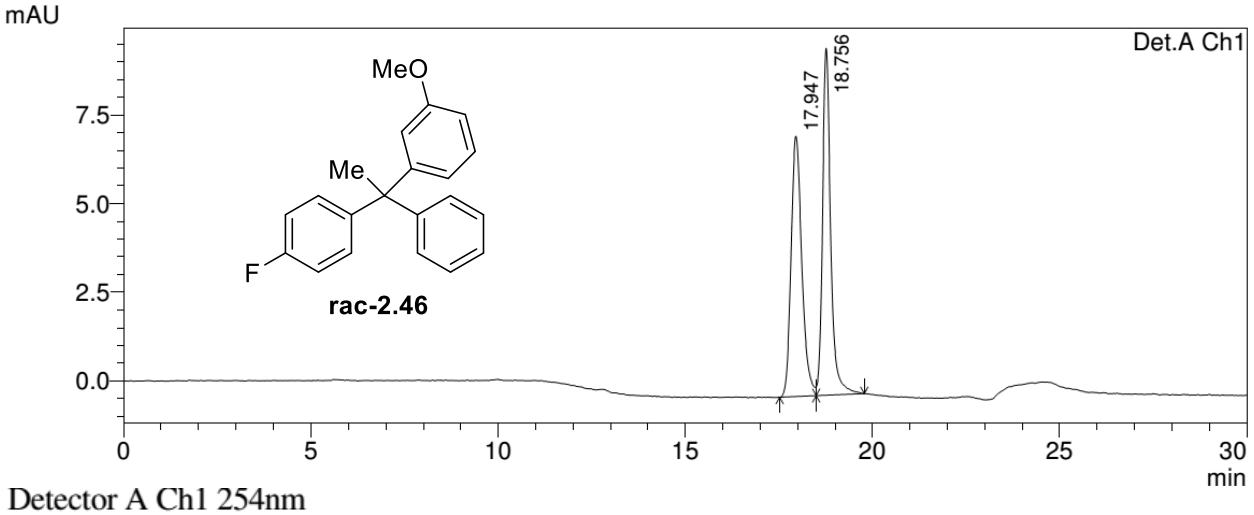

Detector A Ch1 254nm

Peak#	Ret. Time	Area	Height	Area %	Height %
1	17.947	146239	7340	49.779	42.872
2	18.756	147539	9781	50.221	57.128
Total		293778	17120	100.000	100.000

Enantioenriched **2.46**, 76% ee

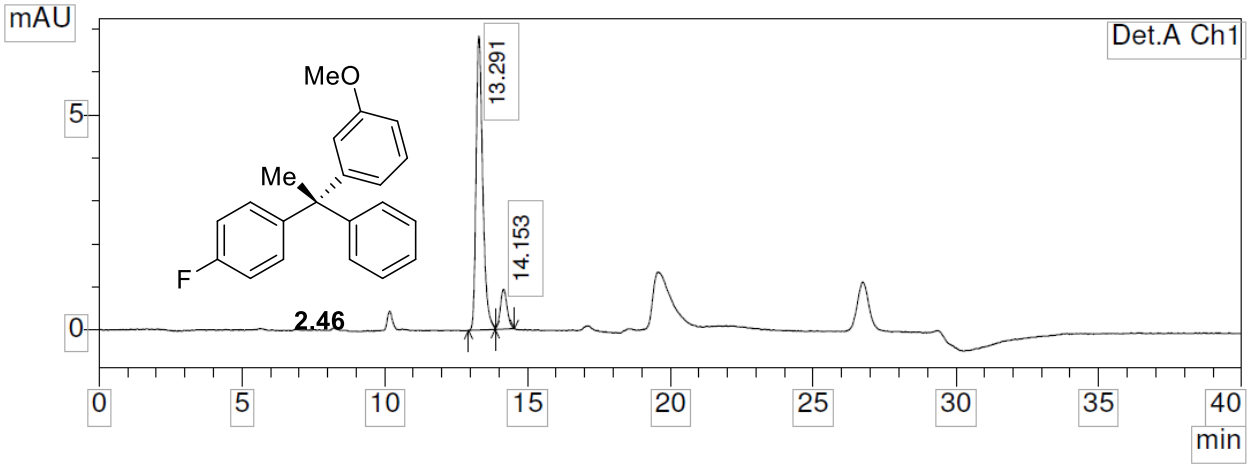

Detector A Ch1 254nm

Peak#	Ret. Time	Area	Height	Area %	Height %
1	13.291	111446	6859	87.882	88.091
2	14.153	15367	927	12.118	11.909
Total		126813	7787	100.000	100.000

Racemic **2.19**

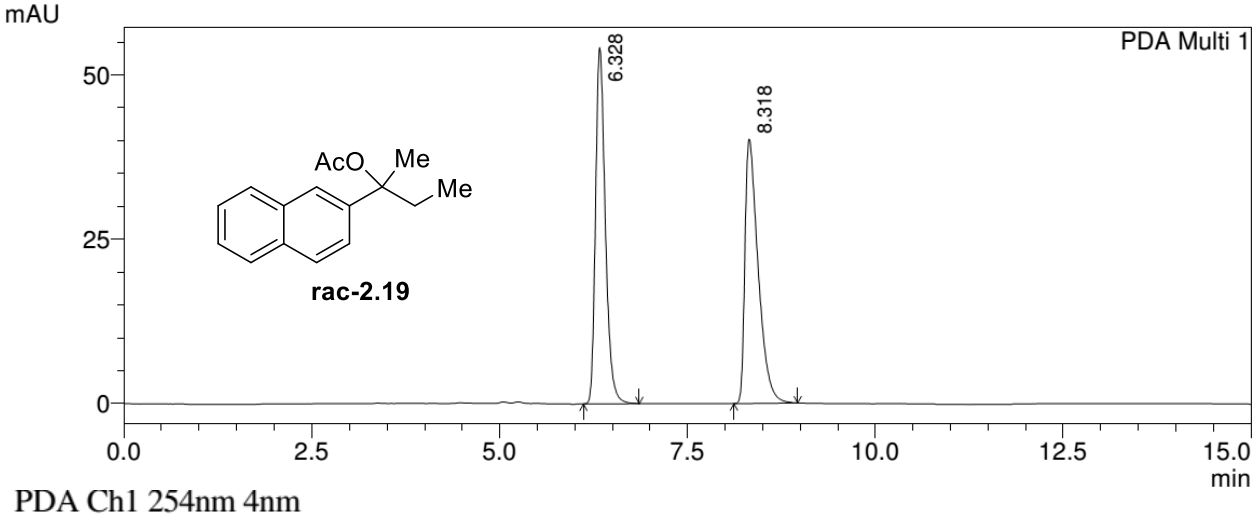

PDA Ch1 254nm 4nm

Peak#	Ret. Time	Area	Height	Area %	Height %
1	6.328	491674	54209	49.939	57.391
2	8.318	492882	40246	50.061	42.609
Total		984556	94456	100.000	100.000

Enantioenriched **2.19,** 96% ee

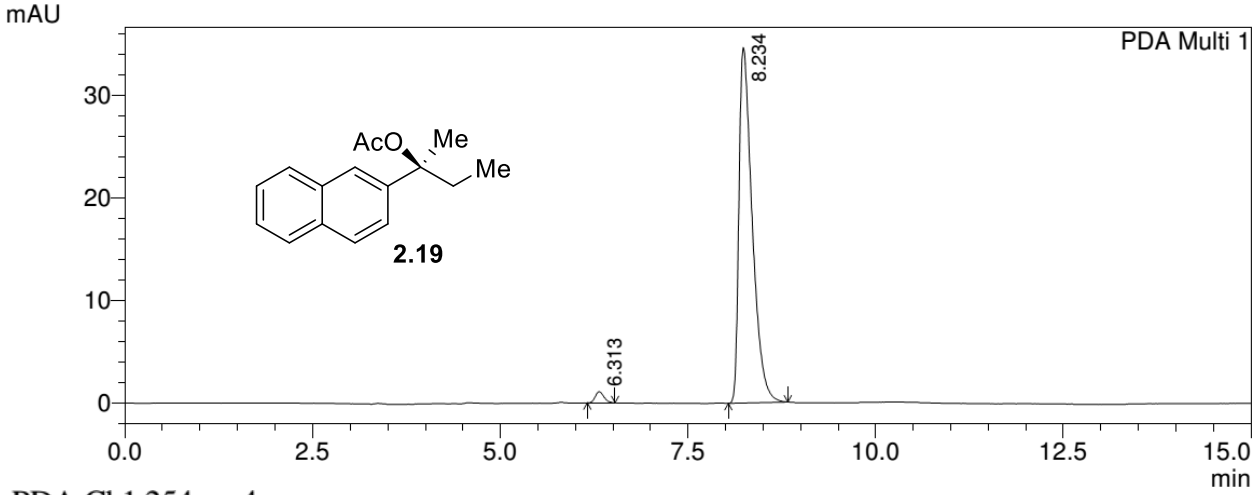

PDA Ch1 254nm 4nm

Peak#	Ret. Time	Area	Height	Area %	Height %
1	6.313	8728	1084	2.011	3.036
2	8.234	425380	34633	97.989	96.964
Total		434108	35717	100.000	100.000

Racemic **2.19b**

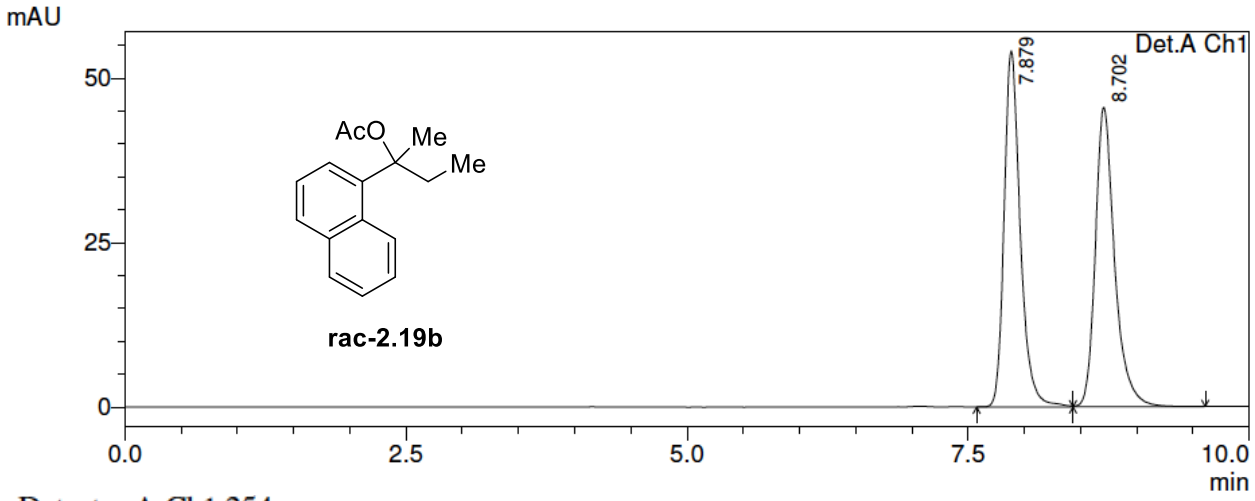

Detector A Ch1 254nm

Peak#	Ret. Time	Area	Height	Area %	Height %
1	7.879	542497	54132	49.894	54.318
2	8.702	544812	45525	50.106	45.682
Total		1087309	99658	100.000	100.000

Enantioenriched **2.19b,** 90% ee

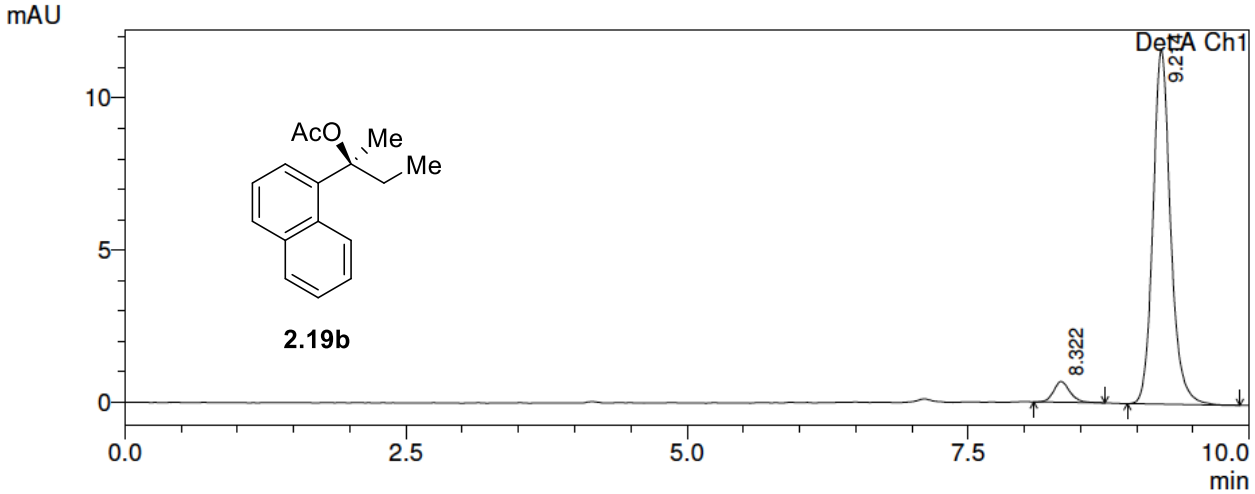

Detector A Ch1 254nm

Peak#	Ret. Time	Area	Height	Area %	Height %
1	8.322	6955	681	5.184	5.523
2	9.214	127204	11657	94.816	94.477
Total		134159	12338	100.000	100.000

Racemic **2.19c**

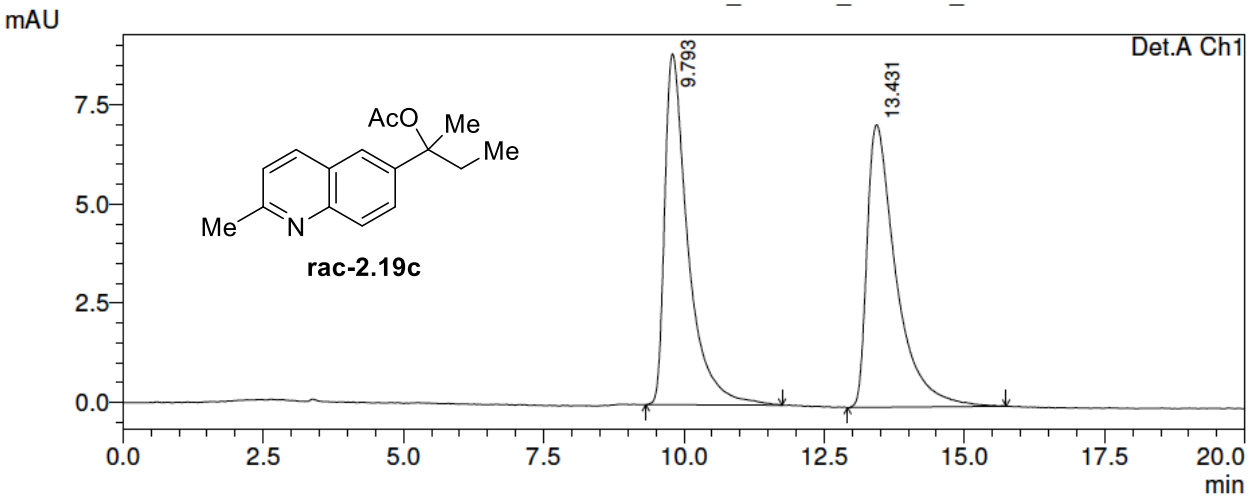

Detector A Ch1 254nm

Peak#	Ret. Time	Area	Height	Area %	Height %
1	9.793	255341	8840	49.841	55.369
2	13.431	256972	7126	50.159	44.631
Total		512313	15966	100.000	100.000

Enantioenriched **2.19c,** 99% ee

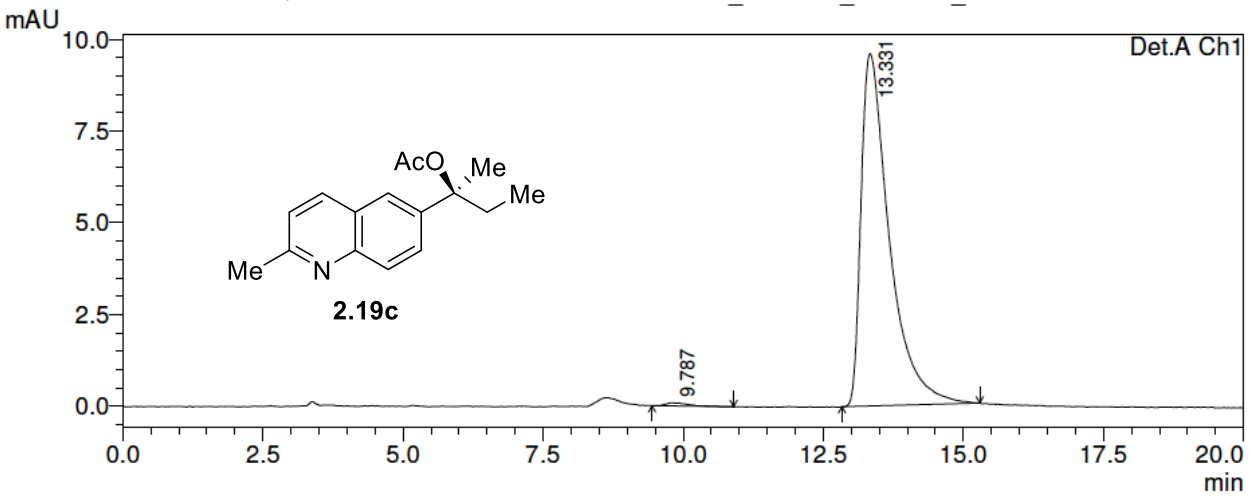

Detector A Ch1 254nm

Peak#	Ret. Time	Area	Height	Area %	Height %
1	9.787	2432	82	0.716	0.847
2	13.331	337293	9599	99.284	99.153
Total		339725	9681	100.000	100.000

Racemic **2.19d**

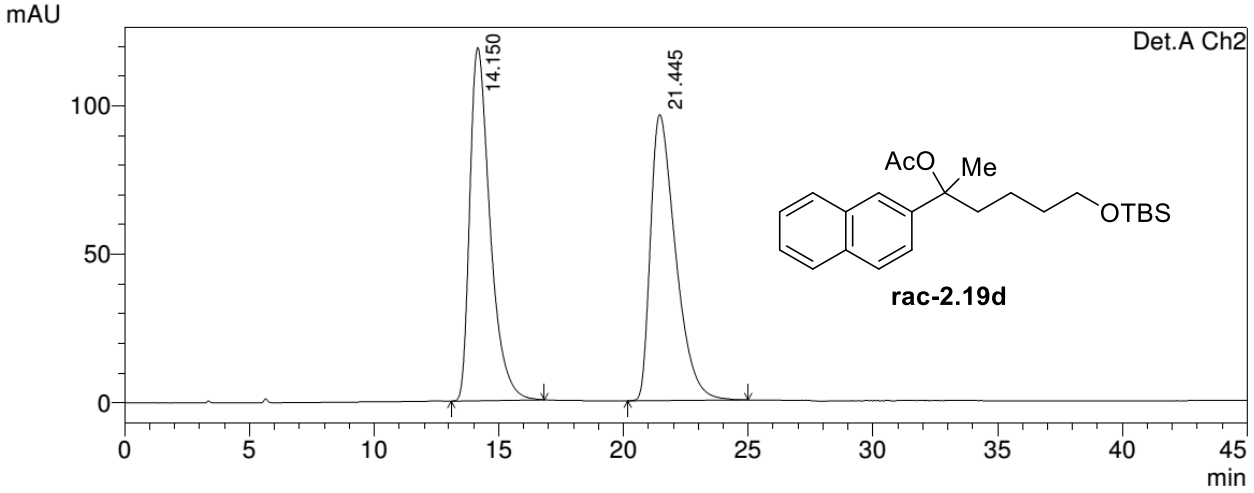

Detector A Ch2 220nm

Peak#	Ret. Time	Area	Height	Area %	Height %
1	14.150	6717068	118892	49.889	55.245
2	21.445	6746910	96316	50.111	44.755
Total		13463978	215209	100.000	100.000

Enantioenriched **2.19d,** 99% ee

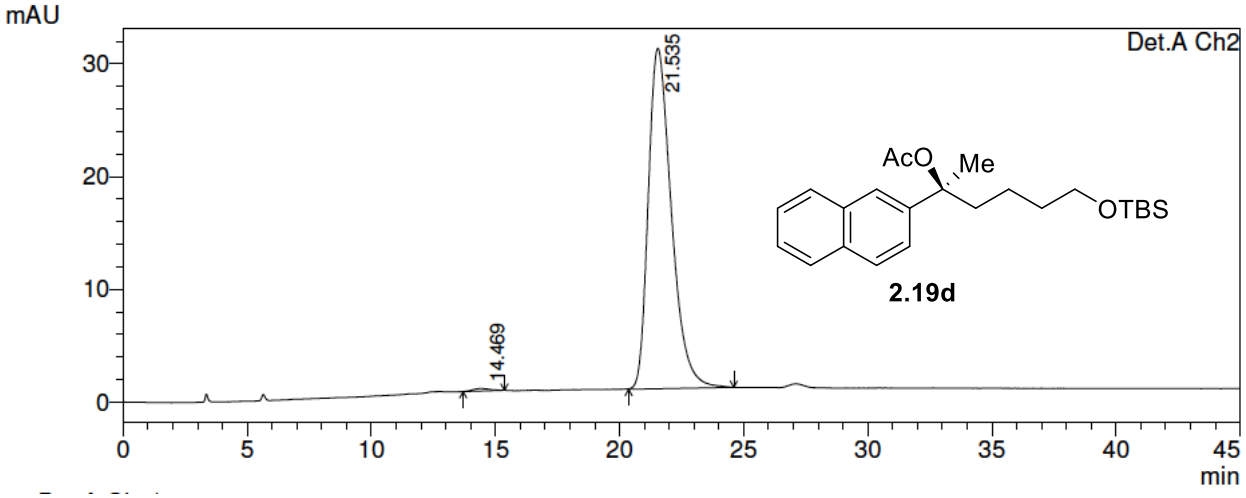

Detector A Ch2 220nm

Peak#	Ret. Time	Area	Height	Area %	Height %
1	14.469	10257	216	0.521	0.711
2	21.535	1957089	30206	99.479	99.289
Total		1967346	30422	100.000	100.000

Racemic **2.19e**

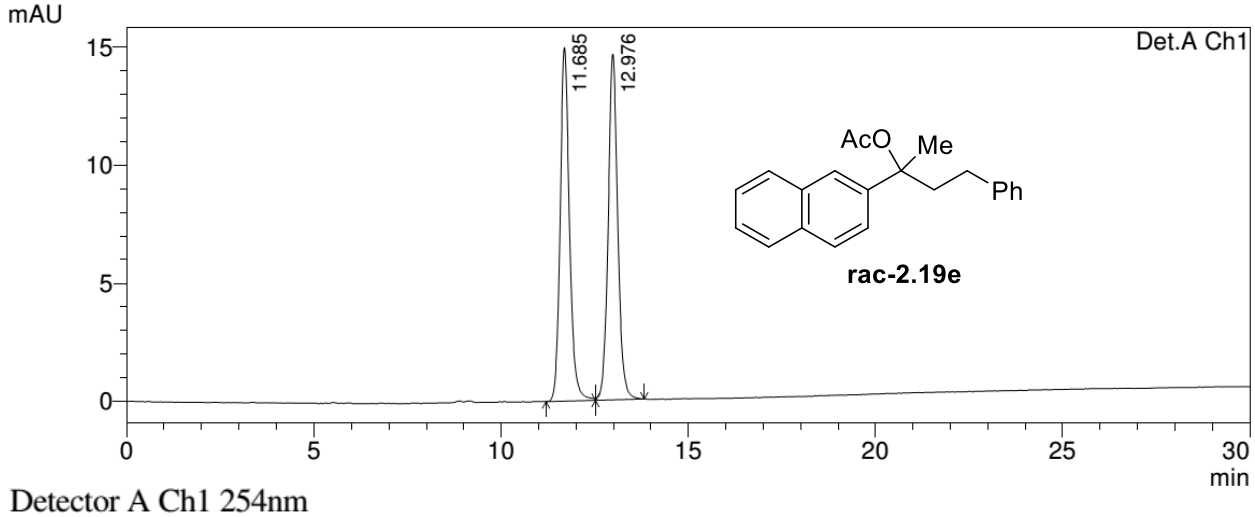

Detector A Ch1 254nm

Peak#	Ret. Time	Area	Height	Area %	Height %
1	11.685	259259	14975	49.898	50.568
2	12.976	260324	14639	50.102	49.432
Total		519583	29614	100.000	100.000

Enantioenriched **2.19e,** 94% ee

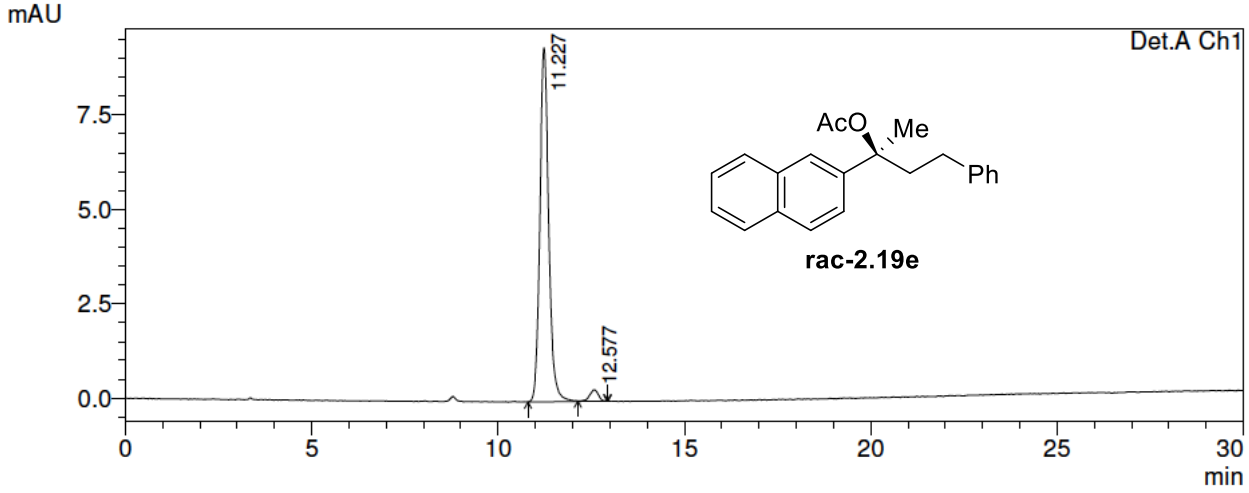

Detector A Ch1 254nm

Peak#	Ret. Time	Area	Height	Area %	Height %
1	11.227	154894	9370	97.078	96.964
2	12.577	4663	293	2.922	3.036
Total		159557	9664	100.000	100.000

Racemic **2.19f**

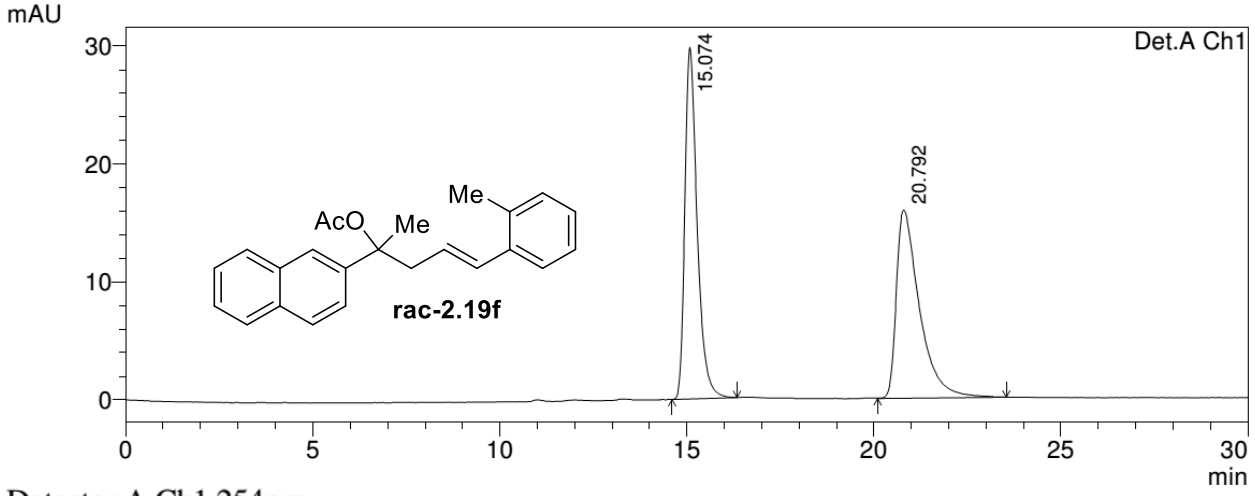

Detector A Ch1 254nm

Peak#	Ret. Time	Area	Height	Area %	Height %
1	15.074	682100	29840	49.883	65.138
2	20.792	685307	15970	50.117	34.862
Total		1367408	45811	100.000	100.000

Enantioenriched **2.19f,** 96% ee

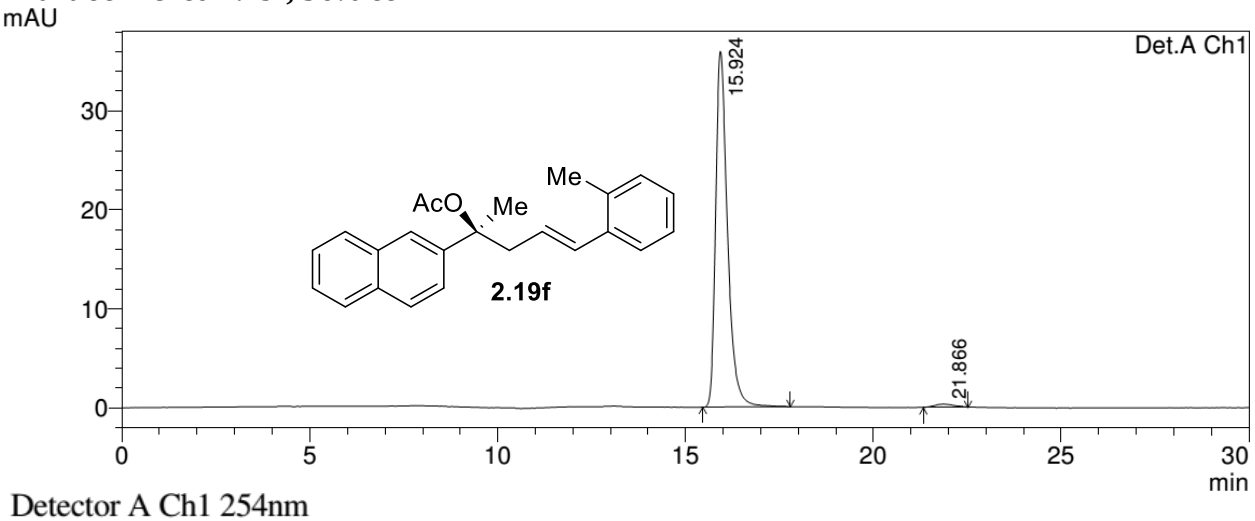

Detector A Ch1 254nm

Peak#	Ret. Time	Area	Height	Area %	Height %
1	15.924	789682	35965	98.270	99.044
2	21.866	13905	347	1.730	0.956
Total		803587	36312	100.000	100.000

Racemic **2.19h**

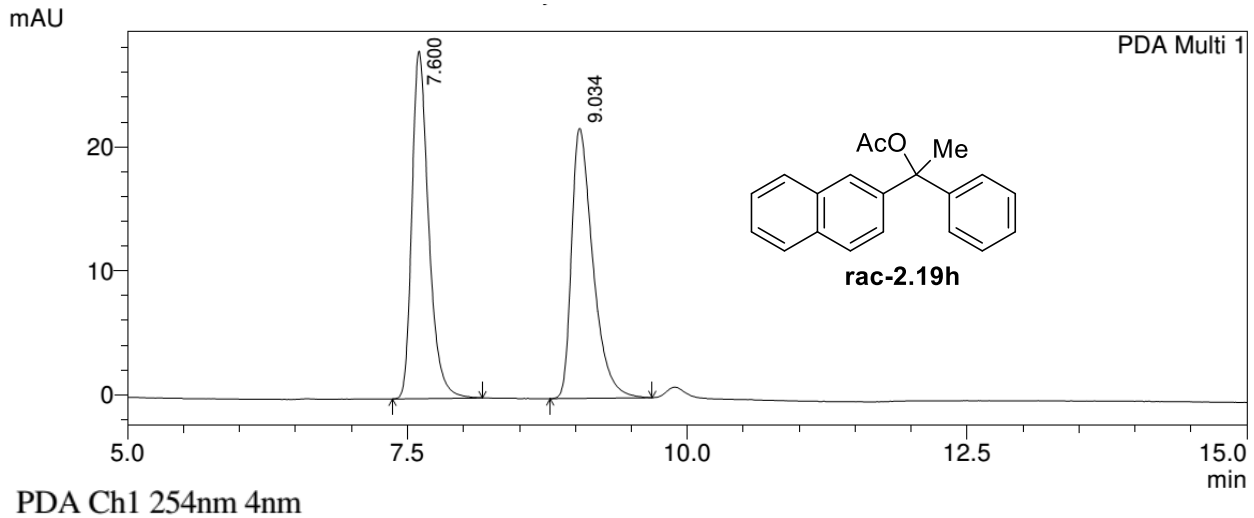

PDA Ch1 254nm 4nm

Peak#	Ret. Time	Area	Height	Area %	Height %
1	7.600	291470	28014	50.165	56.265
2	9.034	289554	21776	49.835	43.735
Total		581024	49790	100.000	100.000

Enantioenriched **2.19h,** 96% ee

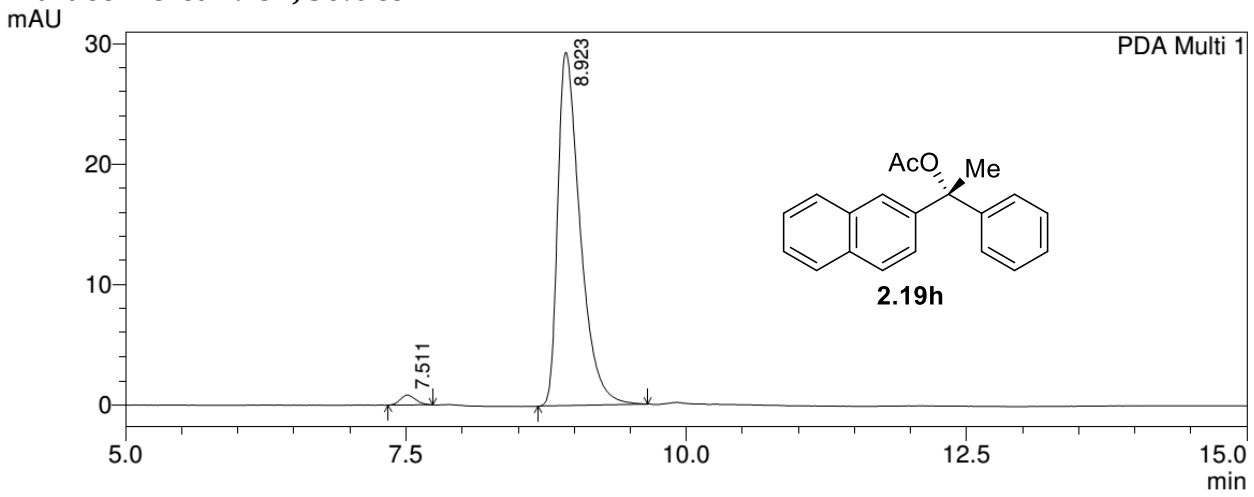

PDA Ch1 254nm 4nm

Peak#	Ret. Time	Area	Height	Area %	Height %
1	7.511	7964	824	1.915	2.731
2	8.923	407977	29359	98.085	97.269
Total		415942	30183	100.000	100.000

Racemic **2.18**

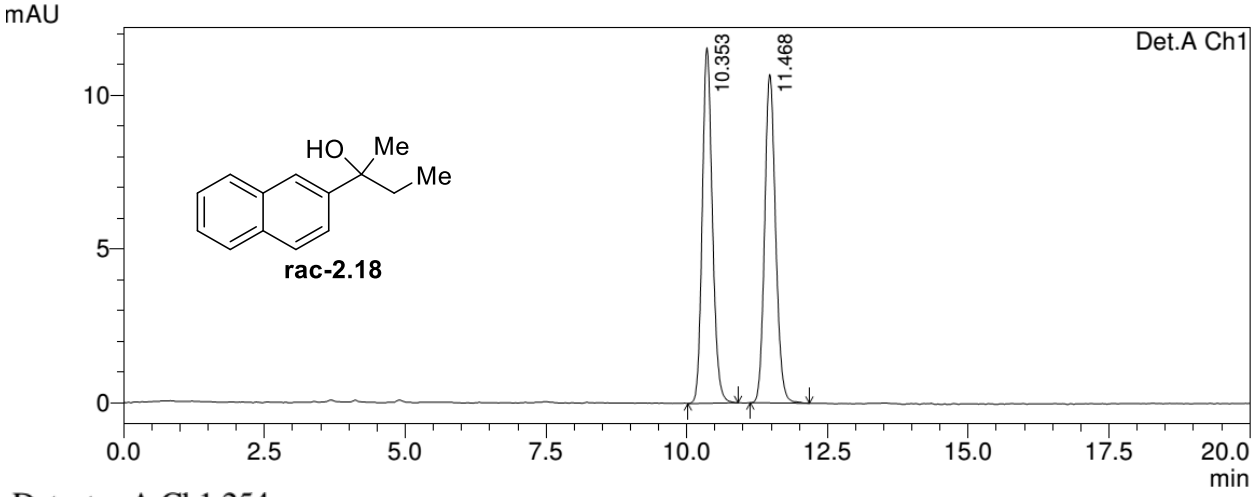

Detector A Ch1 254nm

Peak#	Ret. Time	Area	Height	Area %	Height %
1	10.353	144648	11554	49.962	51.955
2	11.468	144869	10684	50.038	48.045
Total		289518	22238	100.000	100.000

Enantioenriched **2.18,** 96% ee

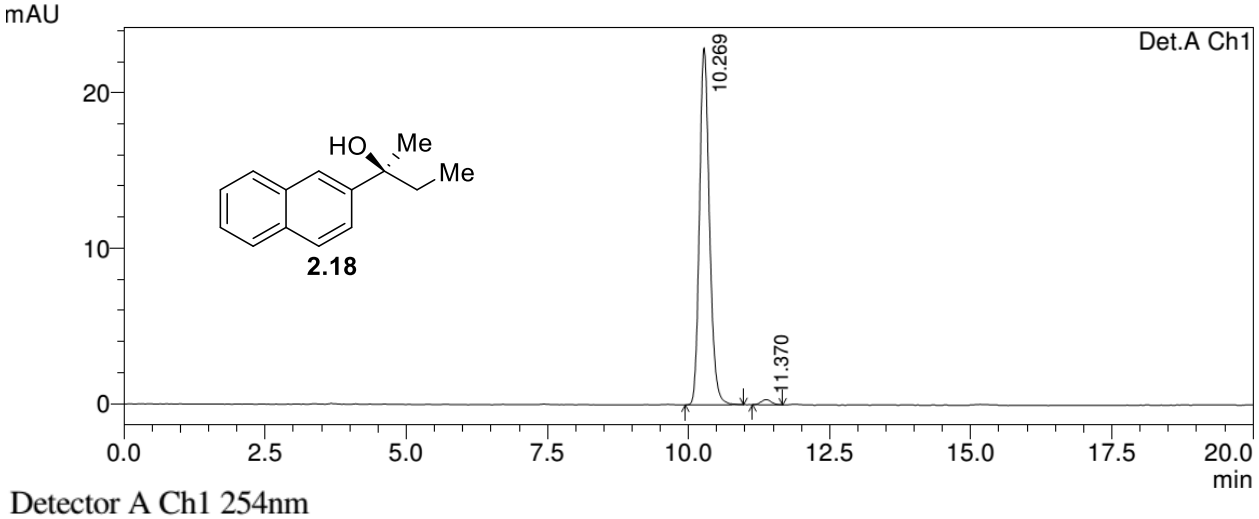

Detector A Ch1 254nm

Peak#	Ret. Time	Area	Height	Area %	Height %
1	10.269	283433	22977	98.493	98.537
2	11.370	4338	341	1.507	1.463
Total		287771	23318	100.000	100.000

Racemic **2.18a**

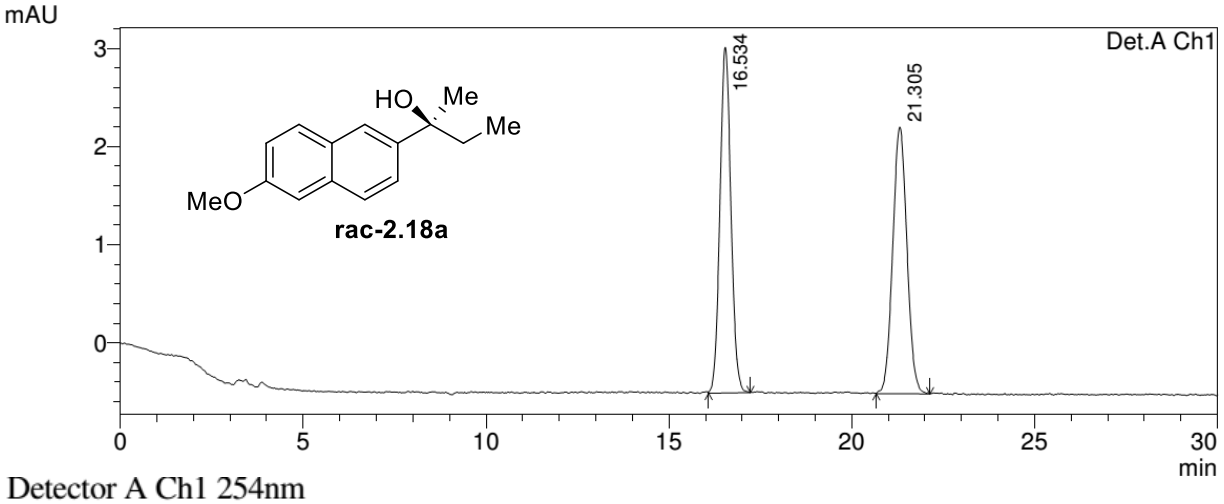

Detector A Ch1 254nm

Peak#	Ret. Time	Area	Height	Area %	Height %
1	16.534	73547	3522	50.022	56.460
2	21.305	73483	2716	49.978	43.540
Total		147031	6238	100.000	100.000

Enantioenriched **2.18a,** 91% ee

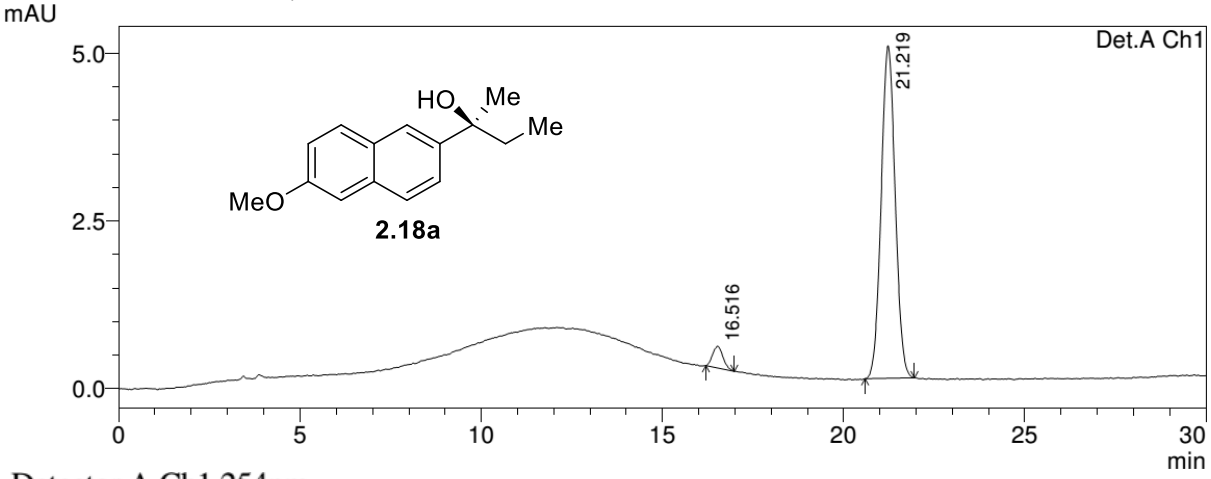

Detector A Ch1 254nm

Peak#	Ret. Time	Area	Height	Area %	Height %
1	16.516	6536	328	4.672	6.201
2	21.219	133384	4962	95.328	93.799
Total		139920	5291	100.000	100.000

Racemic **2.18b**

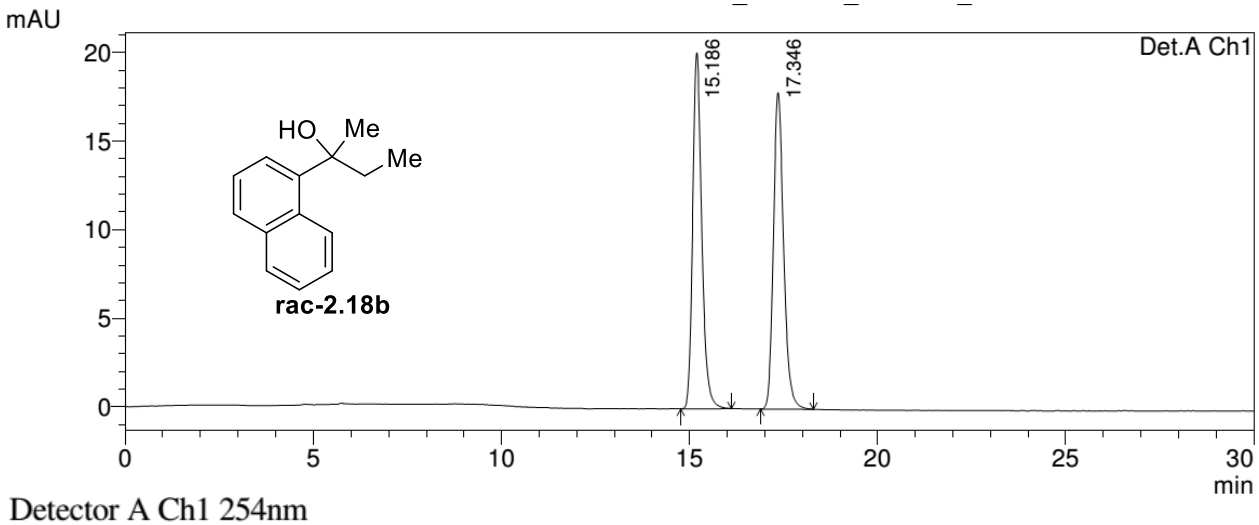

Detector A Ch1 254nm

Peak#	Ret. Time	Area	Height	Area %	Height %
1	15.186	337510	20102	49.967	52.913
2	17.346	337952	17889	50.033	47.087
Total		675461	37991	100.000	100.000

Enantioenriched **2.18b,** 90% ee

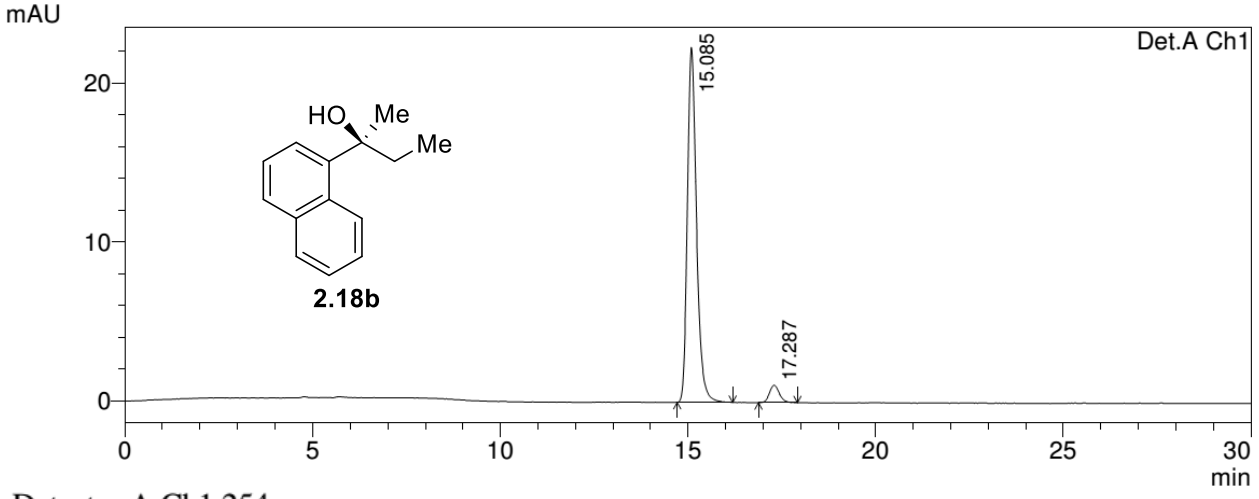

Detector A Ch1 254nm

Peak#	Ret. Time	Area	Height	Area %	Height %
1	15.085	379069	22316	94.789	95.245
2	17.287	20837	1114	5.211	4.755
Total		399906	23430	100.000	100.000

Racemic **2.18c**

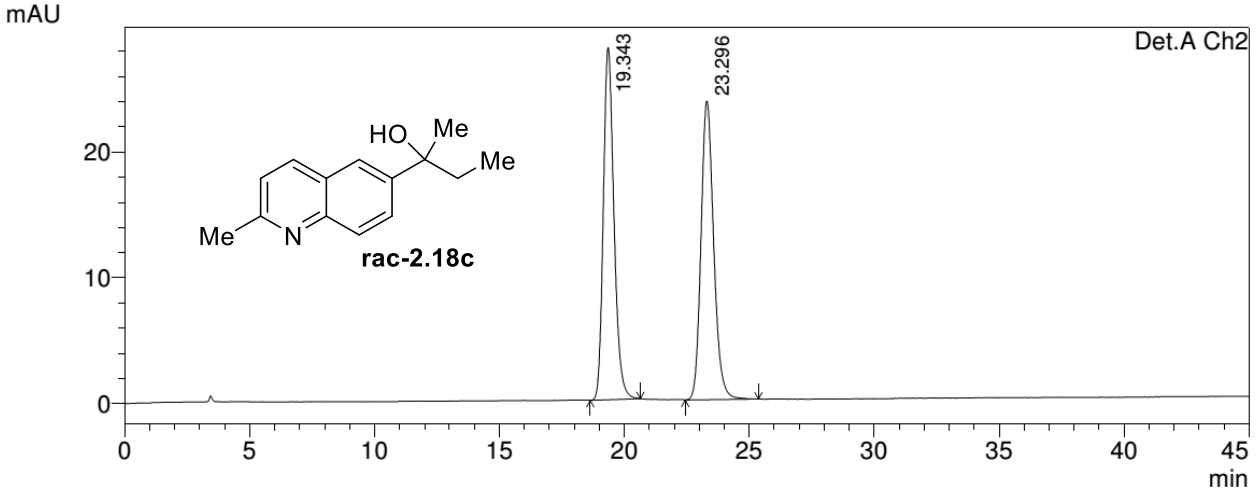

Detector A Ch2 230nm

Peak#	Ret. Time	Area	Height	Area %	Height %
1	19.343	830508	27995	49.756	54.100
2	23.296	838670	23752	50.244	45.900
Total		1669178	51747	100.000	100.000

Enantioenriched **2.18c,** 99% ee

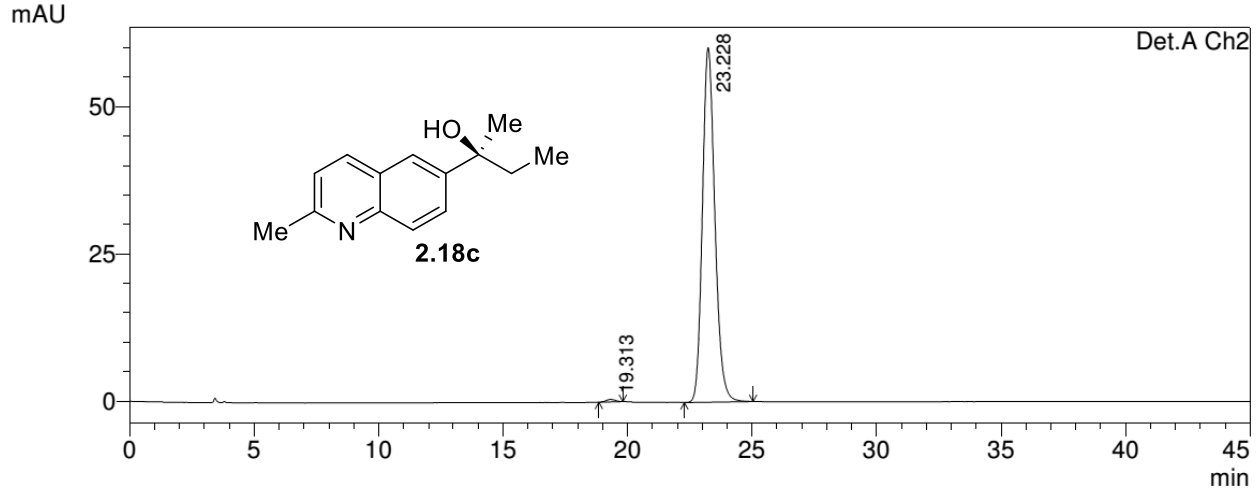

Detector A Ch2 230nm

Peak#	Ret. Time	Area	Height	Area %	Height %
1	19.313	10754	429	0.510	0.708
2	23.228	2099723	60224	99.490	99.292
Total		2110477	60653	100.000	100.000

Racemic **2.18d**

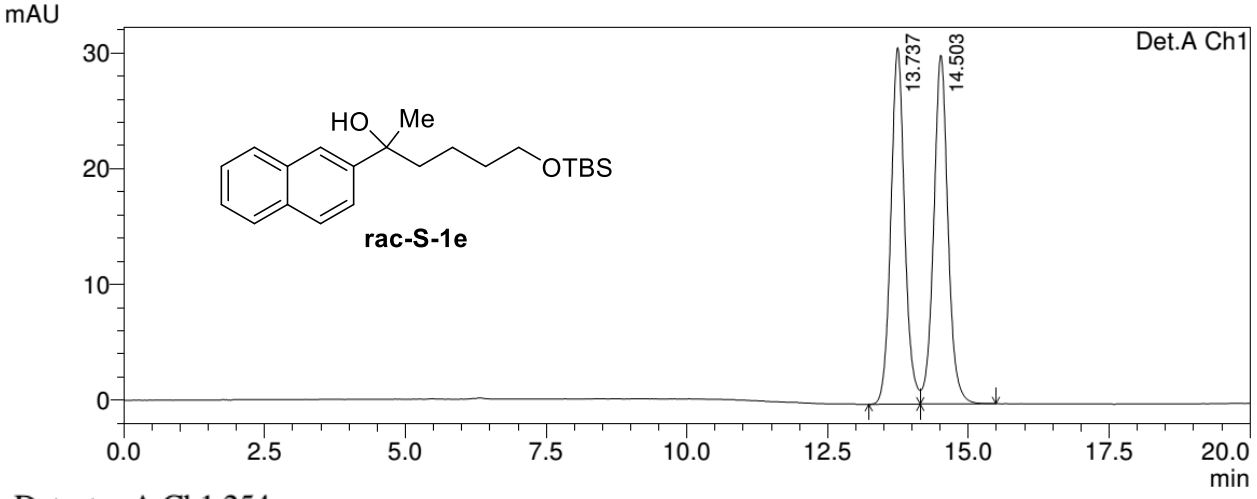

Detector A Ch1 254nm

Peak#	Ret. Time	Area	Height	Area %	Height %
1	13.737	525563	30811	49.594	50.552
2	14.503	534166	30139	50.406	49.448
Total		1059729	60950	100.000	100.000

Enantioenriched **2.18d,** 99% ee

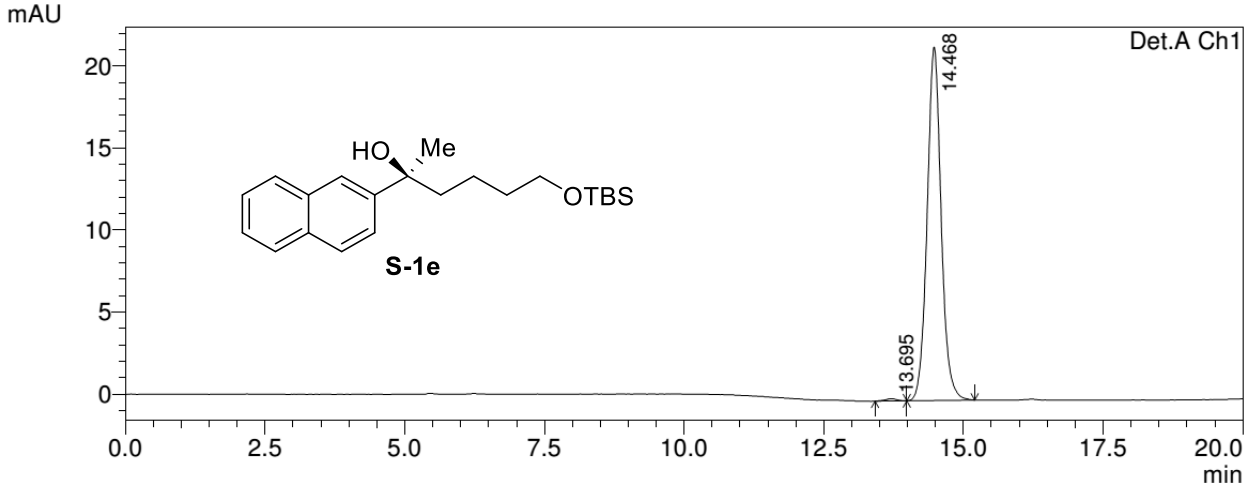

Detector A Ch1 254nm

Peak#	Ret. Time	Area	Height	Area %	Height %
1	13.695	2096	141	0.553	0.651
2	14.468	376900	21525	99.447	99.349
Total		378996	21666	100.000	100.000

Racemic 2-(Naphthalen-2-yl)pent-4-en-2-ol (**2.18f**)

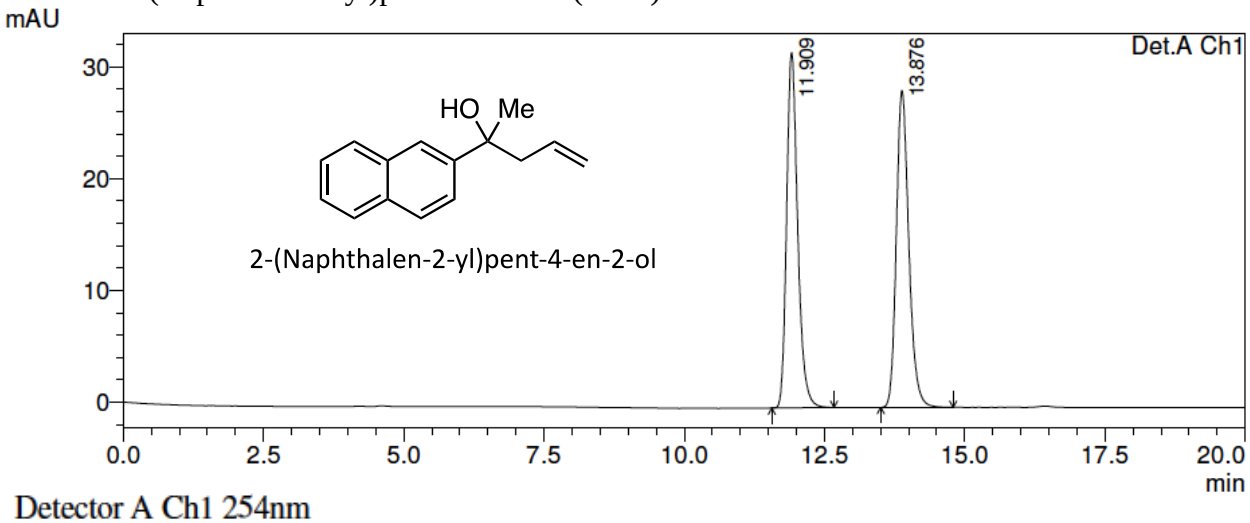

Detector A Ch1 254nm

Peak#	Ret. Time	Area	Height	Area %	Height %
1	11.909	435852	31788	49.790	52.848
2	13.876	439530	28362	50.210	47.152
Total		875382	60150	100.000	100.000

Enantioenriched 2-(Naphthalen-2-yl)pent-4-en-2-ol (**2.18f**)**,** 96% ee

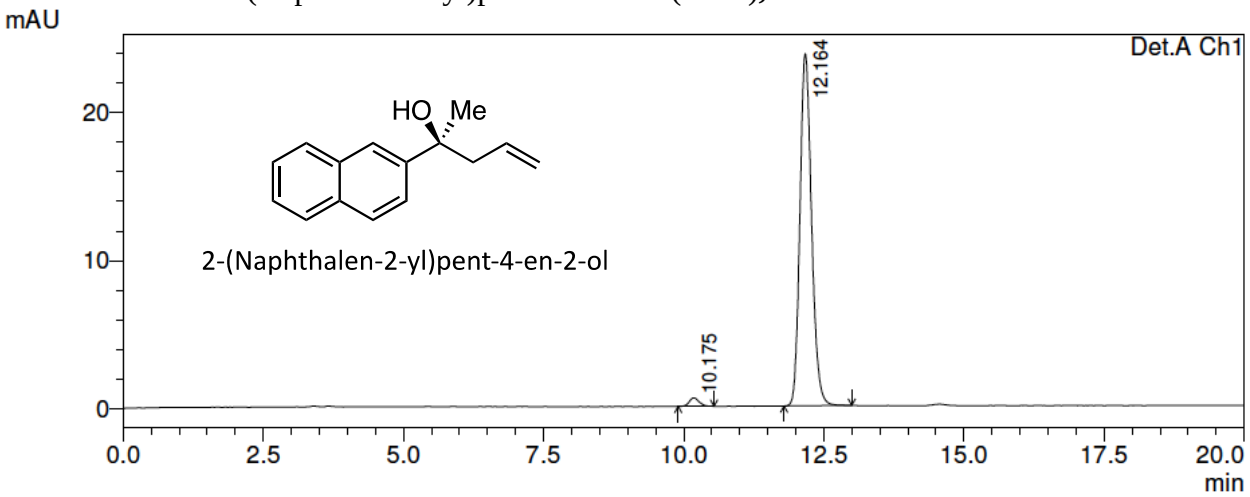

Detector A Ch1 254nm

Peak#	Ret. Time	Area	Height	Area %	Height %
1	10.175	7104	570	2.024	2.336
2	12.164	343811	23822	97.976	97.664
Total		350915	24392	100.000	100.000

Racemic **2.18g**

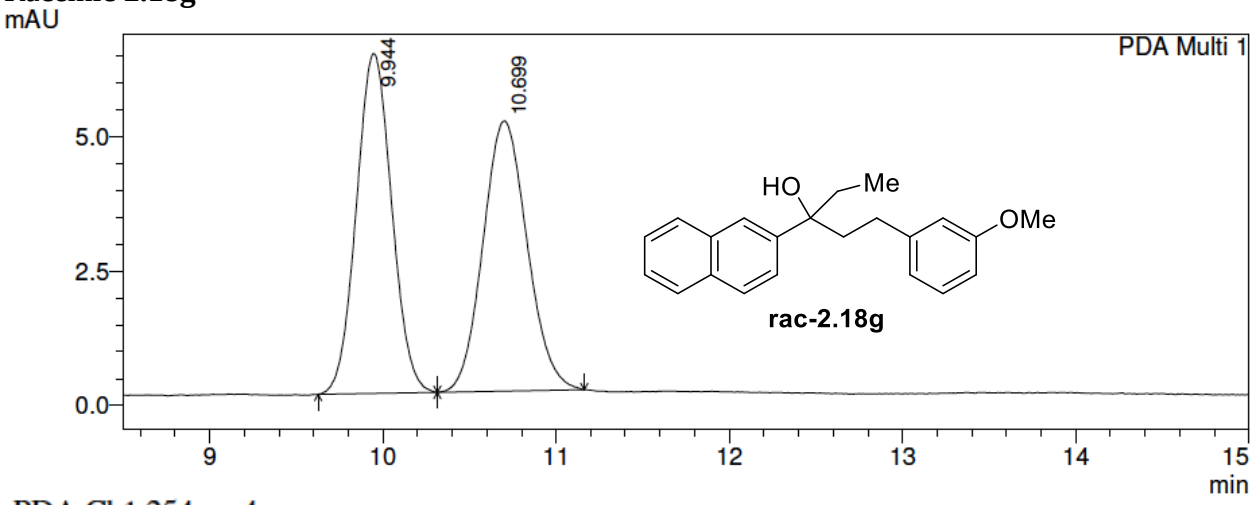

PDA Ch1 254nm 4nm

Peak#	Ret. Time	Area	Height	Area %	Height %
1	9.944	89648	6313	50.174	55.701
2	10.699	89026	5021	49.826	44.299
Total		178674	11333	100.000	100.000

Enantioenriched **2.18g,** 89% ee

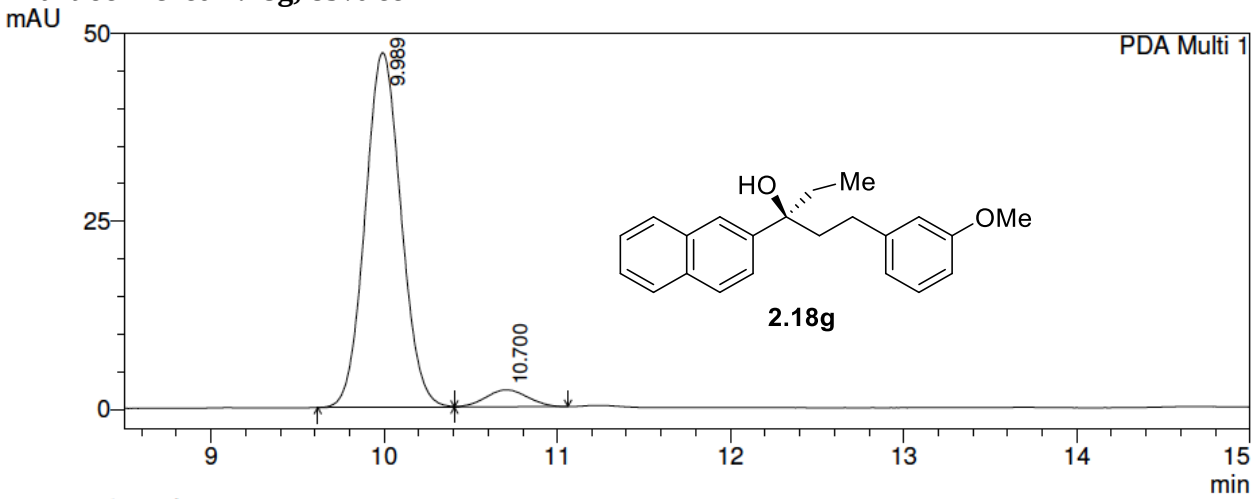

PDA Ch1 254nm 4nm

Peak#	Ret. Time	Area	Height	Area %	Height %
1	9.989	678937	47129	94.701	95.414
2	10.700	37992	2265	5.299	4.586
Total		716930	49394	100.000	100.000

Racemic **2.18h**

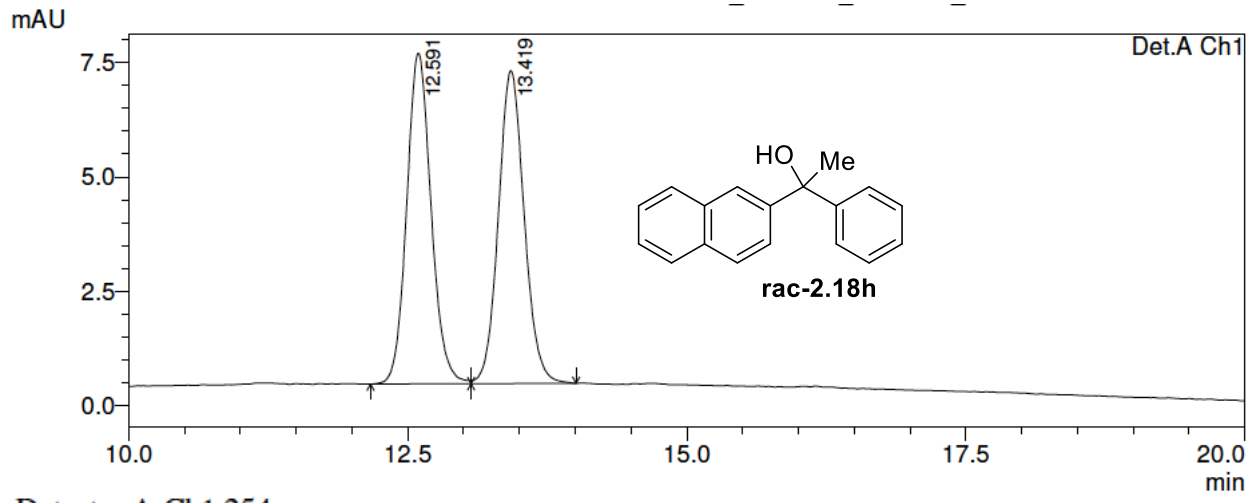

Detector A Ch1 254nm

Peak#	Ret. Time	Area	Height	Area %	Height %
1	12.591	110150	7219	50.024	51.378
2	13.419	110043	6832	49.976	48.622
Total		220194	14051	100.000	100.000

Enantioenriched **2.18h,** 96% ee

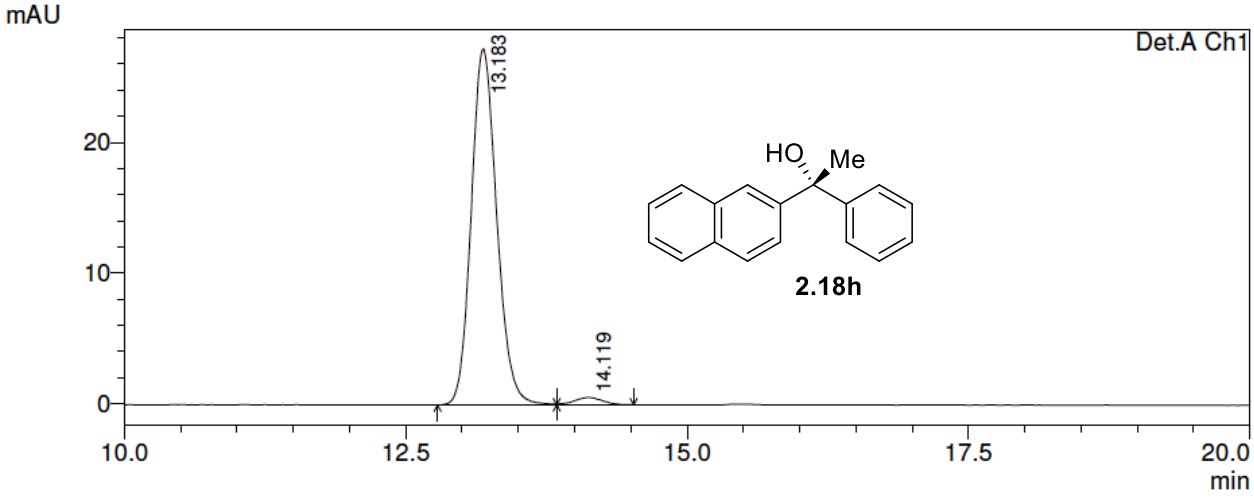

Detector A Ch1 254nm

Peak#	Ret. Time	Area	Height	Area %	Height %
1	13.183	429320	27232	97.819	98.017
2	14.119	9571	551	2.181	1.983
Total		438890	27783	100.000	100.000

Racemic **2.18i**

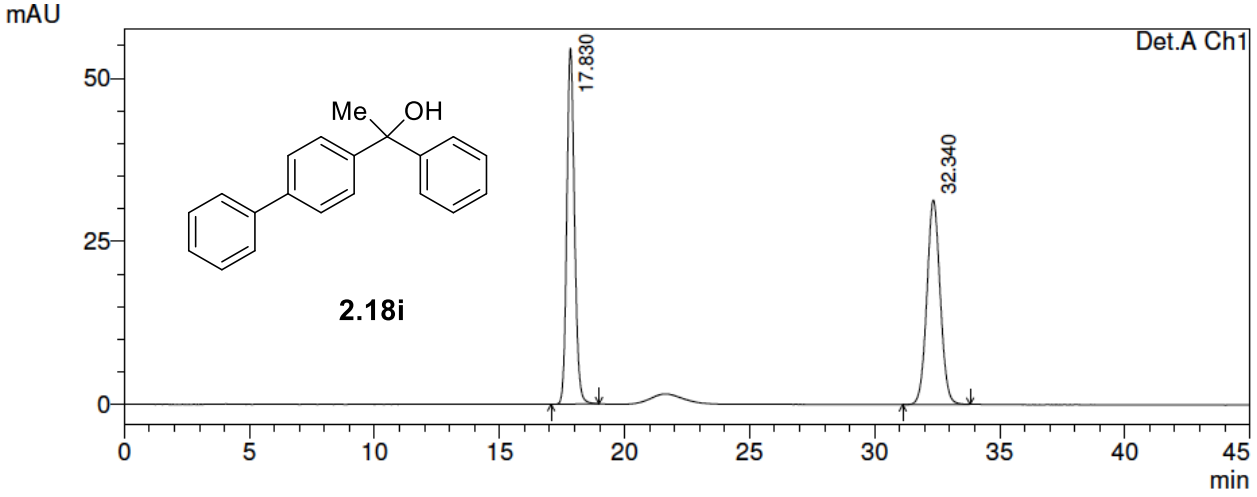

Detector A Ch1 254nm

Peak#	Ret. Time	Area	Height	Area %	Height %
1	17.830	1163647	54572	49.994	63.499
2	32.340	1163916	31370	50.006	36.501
Total		2327563	85942	100.000	100.000

Enantioenriched **2.18i,** 91% ee

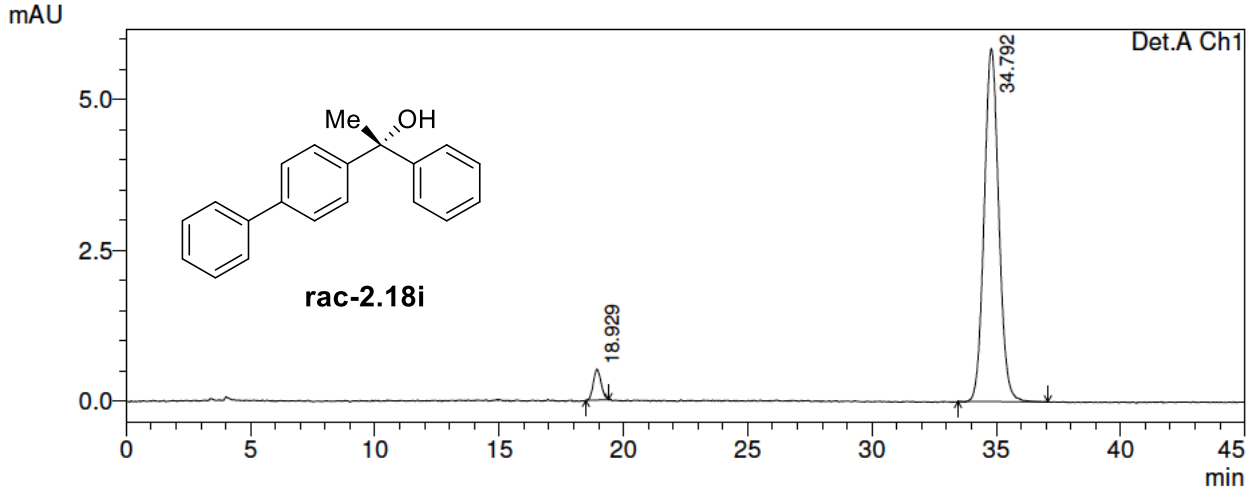

Detector A Ch1 254nm

Peak#	Ret. Time	Area	Height	Area %	Height %
1	18.929	11129	512	4.454	8.053
2	34.792	238760	5845	95.546	91.947
Total		249889	6357	100.000	100.000

Racemic **2.18j**

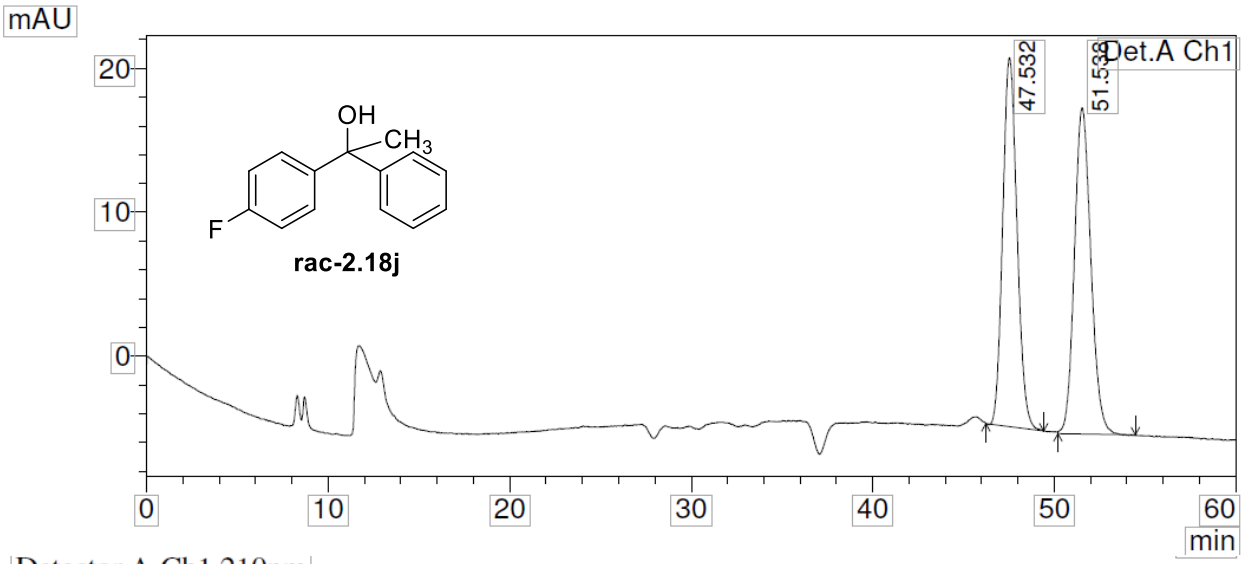

Detector A Ch1 210nm

Peak#	Ret. Time	Area	Height	Area %	Height %
1	47.532	1402602	25630	49.626	53.076
2	51.538	1423738	22659	50.374	46.924
Total		2826340	48289	100.000	100.000

Enantioenriched **2.18j,** 90% ee

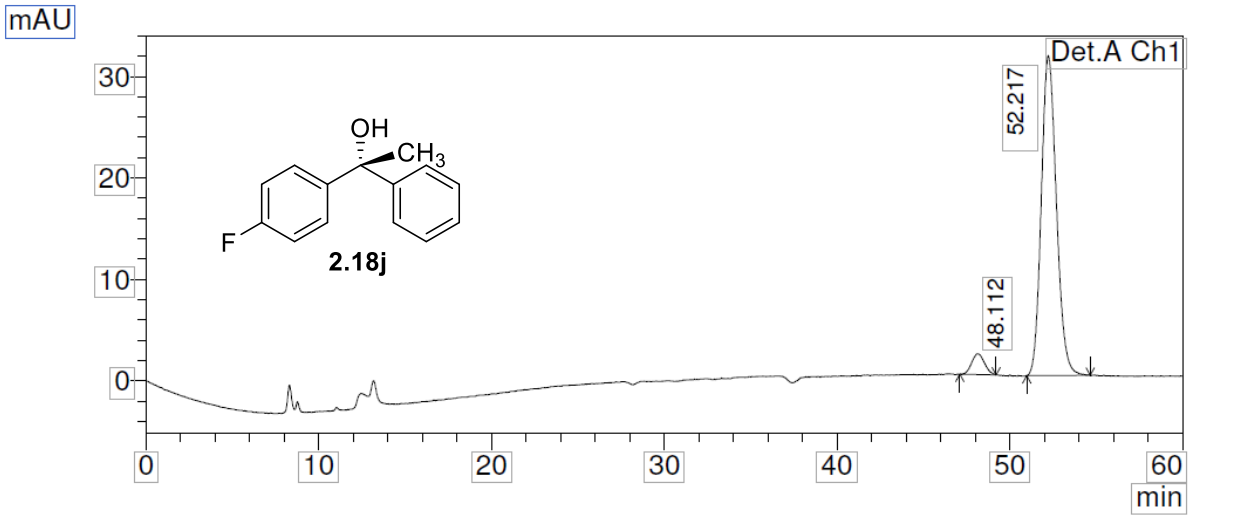

Detector A Ch1 210nm

Peak#	Ret. Time	Area	Height	Area %	Height %
1	48.112	105584	2056	5.216	6.123
2	52.217	1918457	31520	94.784	93.877
Total		2024041	33576	100.000	100.000

Appendix B

PERMISSION LETTER